

➤ **BOOK OF PROCEEDINGS**



With the support of the
French Car Industry



International Conference, Demo Cars and Exhibition

SIA VISION 2022

Vehicle and Infrastructure Safety
Improvement in Adverse Conditions

SIA
2022 **VISION** 

**19-20 OCTOBRE
2022**

**CITÉ DES SCIENCES ET DE
L'INDUSTRIE, PARIS - FRANCE**



Make Ideas Shine



Visit us at
Booth S201

Lumileds.com



Hector Fratty,
Conference Chairman,
Driving Vision News

WE ARE MORE THAN READY FOR THE NEXT EDITION OF OUR GREAT EVENT

We are on tracks for the 2022 SIA VISION Congress which will be held in Paris on 19 and 20 October during the PARIS AUTOMOTIVE WEEK at La Cité des Sciences de la Villette, a place totally dedicated to technologies, a strong example for the vehicle Lighting & ADAS/AD community.

The event will bring together more than 600 worldwide participants involved in lighting and ADAS, directors, managers, and experts following the 34 lectures, visiting the 30 exhibition booths, and networking during breaks, lunches and dinner.

Contributions are confirmed from car makers Audi, BMW, Hyundai, Mercedes-Benz, Renault, Stellantis, Volvo, their main worldwide lighting/ ADAS suppliers, the regulators and universities, all which will highlight the recent innovations on safety, design, and trends in marketing and in regulations.

One discussion panel will host fruitful exchanges between 6 masters experts and drives/expo demo-cars carrying groups of participants to show off the real-world function of the latest innovations in lighting, and ADAS.

« Once again, we are expecting the most relevant worldwide experts in the LIGHTING and ADAS fields to address key topics for vision and road safety. We look forward to welcoming you "In Real Life" in October 2022. »

COMMITTEES

Conference Chair

Hector FRATTY, DRIVING VISION NEWS

Steering Committee

Frédéric CHARON, SIA
Gabriel CLEMENT, ZF GROUP
Mathieu COLLOT, STELLANTIS
Matthieu DABEK, STELLANTIS
Benjamin DONETTE, RENAULT GROUP
Jean-François DACQUAY, RENAULT GROUP
Cécric GESNOUIN, PLASTICOMNIUM
Whilk GONCALVES, STELLANTIS
Antoine LAFAY, VALEO
Gilles LE CALVEZ, VALEO
Christophe LE LIGNE, VALEO
Sébastien LEFRANC, CONTINENTAL
Paul-Henri MATHA, VOLVO CARS
Clément NOUVEL, VALEO
Martin PIERRELEE, SIA
Jean-Paul RAVIER, DRIVING VISION NEWS
Christian TAFFIN, RENAULT GROUP
Gérard YAHIAOUI, NEXYAD

Scientific Committee Lighting

François BEDU, RENAULT GROUP
John BULLOUGH, RENSSELAER
Jean-Paul CHARRET, JPCONSULTING
Hector FRATTY, DRIVING VISION NEWS
Whilk GONCALVES, VALEO
Wolfgang HUHNS, DRIVING VISION NEWS
Tran Quoc KHANH, TUD
Michael KLEINKES, HELLA
Motohiro KOMATSU, KOITO
Paul-Henri MATHA, VOLVO CARS
Rainer NEUMANN, VARROC
Benoit REISS, VALEO
Ernst-Olaf ROSENHAHN, MARELLI AL
Ralf SCHAEFER, RS CONSULT
Ingolf SCHNEIDER, ADAM OPEL
Dirk VANDERHAEGHEN, LUMILEDS

Scientific Committee ADAS

Benazouz BRADAÏ, VALEO
Matthieu DABEK, STELLANTIS
Hector FRATTY, DRIVING VISION NEWS
Gil GONCALVES, MICHELIN
Jan-Erik KALLHAMMER, VEONEER
Gilles LE CALVEZ, VALEO
Sébastien LEFRANC, CONTINENTAL
Heiko LEPPIN, CONTINENTAL
Gaël MONFRONT, ROBERT BOSCH
Marc PAJON, RENAULT GROUP
Mohamed RAHAL, VEDECOM
Caroline ROBERT-LANDRY, ZF



LIGHTING EXPERTISE CENTER

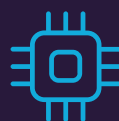
Best-in-class technology and engineers for the lighting of the future in the automotive industry.



**Mechanical
integration**



Optics



Electronics



Visualization

Capgemini Engineering's Lighting Expertise Center is located in Barcelona, in the facilities of the Automotive Technological Center. It has the best professionals and technologies to provide unique solutions for manufacturers in an environment where innovation is the main constant.

Check out our solutions video:



Capgemini  engineering

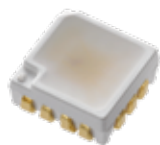
www.capgemini-engineering.com

PROGRAMME 19 OCTOBER, 2022

07:30	>	ATTENDEES REGISTRATION & COFFEE IN THE EXHIBITION
08:20	>	Welcome Introduction by SIA Chief Executive
08:30	>	Opening address by the Conference Chairman Hector FRATTY, SIA VISION Conference Chairman
08:40	>	KEYNOTE SPEECH: Nicolas MOREL, Deputy Chief Engineering Officer – STELLANTIS
		INNOVATIVE LIGHTING SYSTEMS // Chairman: Benjamin DONETTE, RENAULT
09:00	>	New styling trend and new functionalities in latest Renault lighting systems François BEDU, RENAULT
09:20	>	Detection of the road lighting using a conventional camera system David DHUME, HELLA
09:40	>	Slim & Dual Function Optical system for next generation of headlamps Hyun Soo LEE, HYUNDAI
10:00	>	The perfect micro-optical headlight Christopher BREMER, SUSS
10:20	>	Q & A
10:40	>	COFFEE BREAK IN THE EXHIBITION
		NEW TRENDS IN LIGHTING DESIGN // Chairman: Jean-Paul RAVIER
11:20	>	Ultra thin solutions for front lighting Arnaud PERROTIN, VALEO
11:40	>	New Light Styling Approach in Headlamps – Challenges and Possibilities Gerald BOEHM, ZKW
12:00	>	Light emphasized sensor integration - the issue of seeing and being seen Christian BUCHBERGER, MARELLI
12:20	>	Q & A
12:40	>	LUNCH BREAK IN THE EXHIBITION
		IMPROVED SENSOR PERFORMANCE // Chairwoman: Sophie DE LAMBERT, VALEO
14:20	>	Overview of emerging visual sensors for autonomous driving Julien MOREAU, UTC
14:40	>	The Automotive Night & All-Weather Camera and Its Critical Role in the Automotive Sensor Suite David OFER, BRIGHTWAY
15:00	>	Investigation of the influence of camera parameters on data quality for highly automated vehicles David HOFFMAN, TU DARMSTADT
15:20	>	Q & A
		ROAD PROJECTION STAKES // Chairman: Ingolf SCHNEIDER, STELLANTIS
15:30	>	Digital Projections: Distraction Potential for Other Traffic Participants Michel HAMM, AUDI
15:50	>	Review of user's evaluation and the needs for road projections around a vehicle Alexander STUCKERT, BMW & Julien MULLER, ANSYS
16:10	>	Digital Projections: The next level of freedom and customization in vehicle design Michael ROSENAUER, OSRAM
16:30	>	Q & A
16:40	>	COFFEE BREAK IN THE EXHIBITION
		VALIDATION AND ADVERSE WEATHER CONDITIONS // Chairman: Gilles LE CALVEZ, VALEO
17:20	>	Simulation of Adverse Weather as an Enabler for the Development and Validation of Automated Driving Systems in All Challenging Conditions Werner RITTER, MERCEDEZ
17:40	>	Comparing Vehicle Safety Systems in Adverse Condition Splash and Spray between Road and Test Site Jan-Erik KÄLLHAMMER, VEONEER
18:00	>	Use and development of the PAVIN fog and rain platform in the framework of the H2020 AWARD project Pierre DUTHON, CEREMA
18:20	>	Q & A
18:30	>	ROUND TABLE - UNECE REGULATION FOR LIGHTING AND ADAS: STATUS, FUTURE AND STAKES
19:30	>	DINNER COCKTAIL IN THE EXHIBITION & TEST DRIVES
22:00	>	FIN JOUR 1



Everlight Highlight SIA VISION 2022



Product Name		EL 3534-RGBISE03911L-AM
Package Size (mm)		3.5 x 3.4 x 1.3
Luminous intensity (@Typ. I _F)	Red	400 mcd
	Green	900 mcd
	Blue	100 mcd
	White	1400 mcd
Typ. Current		R: 13.5mA, G: 13.5mA, B: 11mA, W: 38mA
Max. T _j		125°C
Operating Temp.		-40~+105°C
Qualification		AEC-Q100/AEC-Q102 RevA
Sulfur Robustness class[1]		Class A

VCSEL : VS-FI3535



Product Name	VS-FI3535-D110-85/L2-W0940/TR8-AM VS-FI3535-D44-36/T2-W0940/TR8-AM
Package Size (mm)	3.5 x 3.5x 1.6
If	4A
Power @4A(Max)	3.2W
Peak Wavelength	940nm
Spectral Bandwidth(Max)	4nm
Wavelength Shift over Temperature (Typ)	0.06nm/K
V _f @4A (Max)	2.4V
Thermal Resistance	4K/W
Operating Temperature	-40°C~+105°C
Qualification	AEC-Q102 Rev A/ IEC 60825
Sulfur Robustness class[1]	Class A
Different viewing angle options(110°x 85°/ 44° x 36°)	

[1]Sulfur Robustness defined following Corrosion Class guidance from AEC-Q102 Rev A

GERMANY, KARLSRUHE
EVERLIGHT ELECTRONICS EUROPE GMBH
Siemensallee 84, Building 7302, 5F
76187 Karlsruhe, Germany
TEL: +49-721-82447-3
FAX: +49-721-82447-40
EMAIL: info@everlight-eu.de

MICHIGAN USA
EVERLIGHT AMERICAS INC.
28345 Beck Road, Suite 109
Wixom, MI, 48393
TEL: +1-734-224-9880 Ext:102
FAX: +1-734-224-9922
EMAIL: salesmarketing@everlightamericas.com

EVERLIGHT
AUTOMOTIVE

PROGRAMME 20 OCTOBER, 2022

07:30	>	ACCUEIL DES PARTICIPANTS CAFÉ
08:00	>	KEYNOTE SPEECH: Nikolai SETZER, CEO - CONTINENTAL
08:15	>	KEYNOTE SPEECH: Laurent FAVRE, CEO - PLASTIC OMNIUM
ADB TECHNOLOGIES AND COMMUNICATIONS // Chairman: Whilk GONCALVES, VALEO		
08:30	>	The transition for ADB in the US market and lighting strategy Valérie MOLTO, STELLANTIS
08:45	>	Communication with Exterior Lighting through High Definition Front & Rear Signaling functions Antoine DE LAMBERTERIE, VALEO
09:00	>	Low Profile ADB Headlamp System with Efficient Light Guide Technology and Improved Safety Standard (HSPR) Rainer NEUMANN, VARROC
09:15	>	Q & A
09:40	>	COFFEE BREAK IN THE EXHIBITION
ADVANCED LIGHT SOURCES // Chairman: Wolfgang HUHN, DVN		
10:20	>	Highest luminance color LEDs for a next level of visual safety experience around the car Benno SPINGER, LUMILEDS
10:35	>	Exploring the challenges in micro-LED pixelated light source, μ PLS, for high-resolution headlamps Menno SCHAKEL, NICHIA
10:50	>	Advancing OLED Lighting Technology for Automotive Applications Soeren HARTMANN, OLED WORKS
11:05	>	Q & A
LIGHTING AND SUSTAINABILITY // Chairman: Christophe LE LIGNE, VALEO		
11:15	>	Exterior lighting function and better understanding about their usage Paul-Henri MATHA, VOLVO
11:30	>	Analysis of Energy Consumption of modern Headlamp Systems and Options for Energy Consumption Reduction Ernst-Olaf ROSENHAHN, MARELLI
11:45	>	Efficiency enhancement opportunities for automotive lighting systems by traffic situation analysis Anil ERKAN, TUD
12:00	>	Q & A
12:10	>	LUNCH BREAK IN THE EXHIBITION
INNOVATIVE CONCEPTS AND COMPLEMENTARY FEATURES // Chairman: Matthieu DABEK, STELLANTIS		
13:30	>	Challenges for DRIVER ASSISTANCE PROJECTIONS Philipp ROECKL, STELLANTIS
13:45	>	Intelligent Speed Assist for EU GSR: New cloud-based approach and key findings Alexandre GARNAULT, VALEO
14:00	>	Reconstruction and mapping of the road profile from sensors embedded in vehicle Ramon GURIDIS, STELLANTIS
14:15	>	Pave the way for a safe automated driving at level crossings Richard DENIS, VALEO
14:30	>	Q & A
ASSESSMENT FOR SAFETY IMPROVMENT // Chairman: Rainer NEUMANN, VARROC		
14:40	>	Investigation of effectiveness and conflict of a road projection lamp for cyclists, using a VR system Kohei MURATA, KOITO
14:55	>	Where does the driver want light? International survey for a customer-oriented assessment of headlights Christian HINTERWÄLDER, AUDI
15:10	>	Ambitious front lighting ratings and latest updates of regulations world wide: The perfect match? Armin AUSTERSCHULTE, MARELLI
15:35	>	Q & A
SIMULATION FOR ADAS DEVELOPMENT // Chairman: Antoine LAFAY, VALEO		
15:50	>	Computer graphics to challenge the physical process and mockup of the lighting and front camera design Benoît DESCHAMPS, RENAULT GROUP
16:05	>	Evaluation of decision-making and planning of autonomous vehicle by simulation Mohammed TAHA BOUDALI, IRT SYSTEM X
16:20	>	Virtual modeling of an ADAS radar Vanessa PALMIER, IRT SYSTEM X
16:35	>	Q & A
16:45	>	CLOSING REMARKS
17:00	>	CLOSING



SUSS MicroOptics

ENABLING THE REVOLUTION IN AUTOMOTIVE LIGHTING

SUSS MicroOptics is a global leader in micro-optics technology and manufacturingwide offering a wide range of applications for imprinted microlens arrays (MLAs) in automotive projections systems.

SUSS MicroOptics SA
Phone: +41 32 566 44 44
sales.smo@suss.com
www.suss-microoptics.com

- + **Next Generation Headlamps**
- + **Road Communication**
- + **Design Projections**
- + **Interior Lighting**

Open your mind to new design ideas with microlens array-based lighting solutions for the automotive industry!



INNOVATIVE LIGHTING SYSTEMS	P.11
NEW TRENDS IN LIGHTING DESIGN	P.33
IMPROVED SENSOR PERFORMANCE	P.49
ROAD PROJECTION STAKES	P.68
VALIDATION AND ADVERSE WEATHER CONDITIONS	P.95
ADB TECHNOLOGIES AND COMMUNICATIONS	P.116
ADVANCED LIGHT SOURCES	P.133
LIGHTING AND SUSTAINIBILITY	P.148
INNOVATIVE CONCEPTS AND COMPLEMENTARY FEATURES	P.167
ASSESSMENT FOR SFETY IMPROVEMENT	P.191
SIMULATION FOR ADAS DEVELOPMENT	P.211



Sensing in a new light

Advancing optical solutions
in automotive and mobility

ams-osram.com

Sensing is life

am **OSRAM**

INNOVATIVE LIGHTING SYSTEMS



DRIVING A NEW GENERATION OF MOBILITY

We are looking forward to meet you at booth S210.

www.plasticomnium.com

New Styling trend and new functionalities in latest Renault Lighting systems

F. BEDU¹, S. GOBIER¹, C. DREYER¹, V. CALAIS¹, P. VIGNERON¹, N. VENOT¹

1: RENAULT Group, Technocentre, 1 avenue du Golf, 78280 Guyancourt, France

Abstract: 2022 is an important year for RENAULT with 2 major launches in Europe based on 2 platforms shared in the Alliance:

- Megane E-Tech on CMF-EV
- Austral on CMF-CD3

These platforms have in their DNA a new EE architecture that integrates a lot of new functionalities for exterior and interior lighting systems.

In the meantime, Renault proposes a new styling approach with an evolution of the signatures at the front with very narrow headlamps but also at the rear of the vehicle with a “moiré” effect.

Thanks to the EE architecture, these headlamps are smarter and propose full AFS and ADB to improve visibility in all conditions.

In addition, a dynamic mode of the interior ambient lighting system has been introduced based on circadian cycle.

Keywords: Light signature, advanced front lighting technologies, ambient lighting

1. Introduction

New vehicle platform with a large evolution of EE architecture is an opportunity which is not available for each new vehicle.



Figure 1: New Megane E-Tech and new Austral

For the launch of Megane E-Tech and Austral, 2 platforms shared in the Alliance are Renault's first application. With these platforms, a large evolution of EE architecture has been pushed in parallel that gives the possibility to introduce new EE concept and to propose new functions for our customers. 2 major topics can be highlighted from system point of view:

- a new smart LDM called L4 connected in LIN to USM gives the possibility to propose full AFS functionalities and more complex welcome and goodbye scenarios.
- A third generation of ALU (Ambient Lighting Unit) with new communication interface adapted to the ambient light system gives more freedom to shape ambient lighting and allows to generate new scenarios like the dynamic mood light called “Living mode”.

In parallel, designers have pushed engineers to find smart solutions to create narrow headlamps to fit with upper grill dimension and propose modernity on the front end with new proportions.

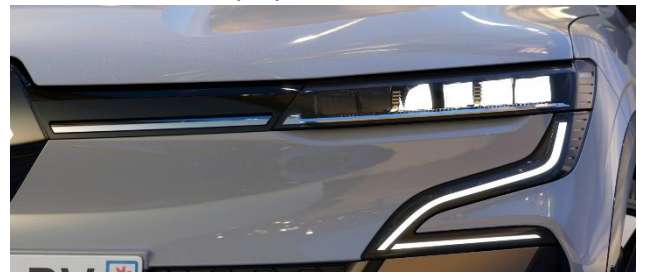


Figure 2: Compact headlamp on Megane E-Tech

In the meantime, a new concept called “moiré effect” has been developed in the rear lamps to offer originality and a high tech feeling in the appearance of the vehicles.



Figure 3: Moiré effect on Austral rear lamp

2. New styling intentions

2.1 Narrow headlamps

At the beginning of Megane and Austral projects, 2 challenges were addressed to Engineering team. First was the strong wish of styling to decrease height of headlamps compared to full LED headlamps under development or already on the market [1], [2]. Second objective was to propose an efficient AFS system and ADB as these vehicles addressed C-segment market.

These requests were placed under economical pressure.

Different investigations were made internally and have led to a multi-reflector type headlamps in order to have the possibility to manage different light distribution realized by one source placed in one reflector. Size of the cavity was the main challenge with styling.

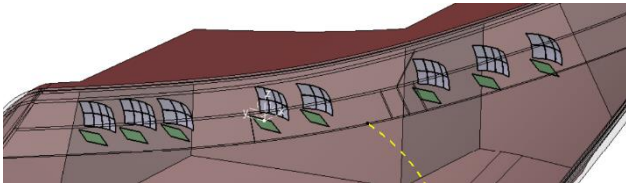


Figure 4: Headlamp concept with reflectors 20x20mm

Internal evaluation began with 20x20mm reflector size requested by styling with poor efficiency. After multiple loops, agreement was found for a dimension of 35x40mm reflector size with an average efficiency of 36% for LB and 41% for Matrix Beam.

Another important challenge with this concept is link to the alignment of multiple reflectors to obtain the final photometry and the precision of LED positioning with a small focal length.

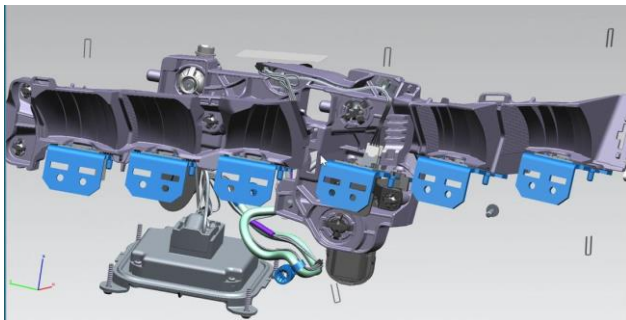


Figure 5: Optical system with 6 LSUs and LDM L4 of Megane E-Tech

As the cut-off line is spread between 2 cavities ACoL and SCoL generating a symmetrical horizontal cut-off and an asymmetrical cut-off, a micro adjustment mechanism was required on one of them to achieve performance, quality of cut-off and conformity of the photometry.

2.2 Moiré effect

In 2016, Styling department presented the concept-car TreZor. In the rear lamp, numerous fibre optics were installed, and a motor was twisting the lines to change aspect and give the impression of a living element.



Figure 6: TreZor concept-car rearlamp

This was the starting point of the collaboration with styling who transforms this request with moiré effect pictures.

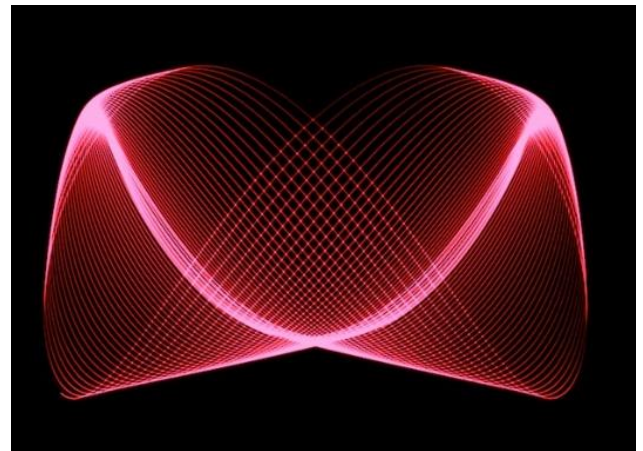


Figure 7: Moiré effect on lit lines

To realize it, the idea was to generate thin lines placed on different layers to give this impression of a living rear lamp when you turn around it.

For the thin lines, different solutions were studied with Tier1 suppliers: micro prisms positive or negative, laser graining, painting, ... Lit aspects were quite similar except in very close distance where differences were noticeable.

Optical concept was fixed, styling had to define the pattern on the 2 surfaces, not an easy task when you explore a new approach.

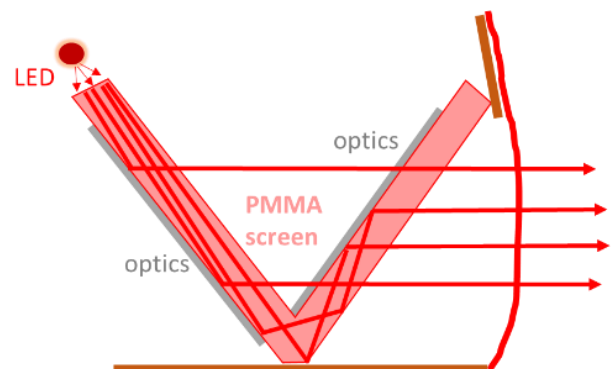


Figure 8: Optical principle of Moiré effect

3. New functionalities

3.1 AFS

With the new EE architecture, an exterior lighting LIN network was created. The LDM L4 connected to the LIN was designed with the possibility to have 8 independent outputs for LowBeam and HighBeam.

Many features were integrated in the different components and especially a full AFS system.

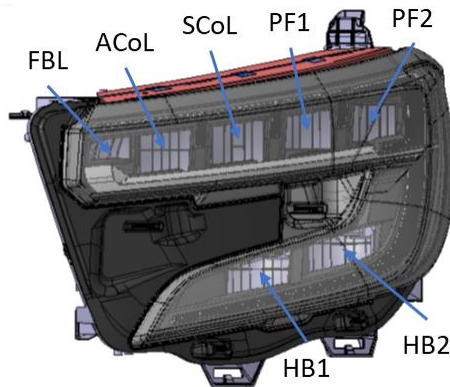


Figure 9: Austral AFS headlamps with 7 cavities

As it was possible to drive light sources independently, it was possible to shape light beams by a management of their level of power. In USM, new logics were implemented to generate up to 24 light distributions.

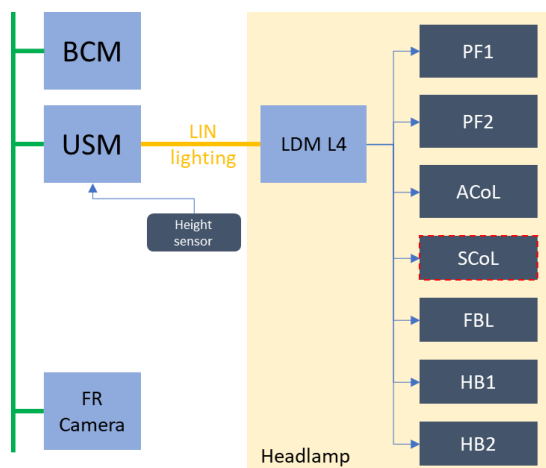


Figure 10: Global EE architecture of AFS system.

For Megane and Austral, only 18 were implemented. To the conventional City, Country, Motorway and Rainy modes, a tourist mode and 2 HB modes one for low speed and the other one for all speed were added.

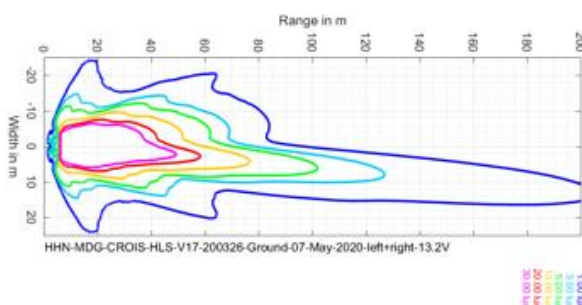


Figure 11: AFS LowBeam Country Light distribution

A manual activation of an All-Weather mode is also possible, equivalent to a fog function. This manual

activation in an AFS system that shall be fully automatic was a tricky point for homologation. This manual mode was considered as the neutral mode of the system.

Renault wasn't authorized to implement this All-Weather light distribution for non AFS system. An evolution of the regulation should be useful to allow such feature that can replace fog lamps for non AFS system.

A turning version of all these light distributions was also implemented.

From system point of view, different information are required to manage it: vehicle speed, wiper status, manual control for driver with combi switch or central panel, front camera info for road's type and steering wheel angle.

3.2 ADB

ADB headlamps were developed only for Austral vehicle. This version is an upgrade of the AFS headlamp with a more sophisticated dynamic Turn indicator and new light sources and reflectors for the 2 cavities dedicated to high beam illumination.

All the features deployed for AFS version are present and are running with the same behaviour.

From electronic architecture point of view, ADB is managed like an add-on. A specific ECU, the LCU is connected to the CAN network of the vehicle to access to front camera information but also other information available on the network. LCU defines with its algorithm the shadow on vehicles or the dimming on traffic sign to generate in term of size and localization but also, the switch OFF in urban area the activation of specific light distribution on highway and the launch of some animations. These data are transferred to an 2nd LDM, the ADB driver with a private CAN network.

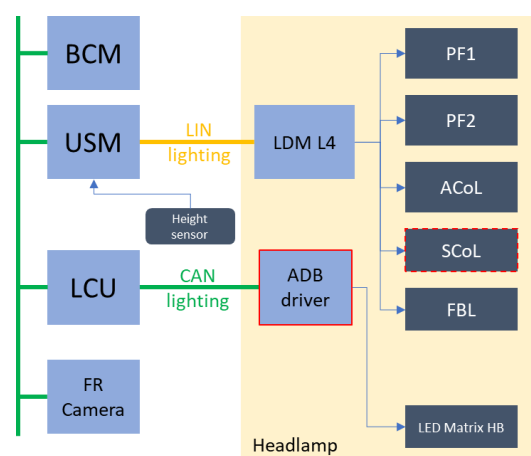


Figure 12: Global EE architecture of ADB system

With this new EE architecture, a new front camera is available with a better resolution and an improved detection rate.

3.3 Welcome/Goodbye

For Welcome or Goodbye sequence, it is possible to store different scenarios in the LDM. The use of the different cavities but also of the DRL outputs allows designers to create smart effect on the vehicle.

3.4 Living light mode

An evolution of the ambient lighting system has been done with this new EE architecture. To offer more flexibility in the settings, LIN messages have been modified and a third generation of ALU family has been designed for this system.

8 colours are available for the customers which fit with colour themes of displays. The newness is mainly based on the Living Light mode feature. To create an extension of the environment inside the vehicle, colours automatically changed each 30 minutes to follow sunrise, zenith, sunset, or night.



Figure 13: Evolution of the sun position in the sky

To create this effect a specific palette of 48 colours has been defined to fit with circadian cycle. Display themes are following ambient light with their 8 colours.

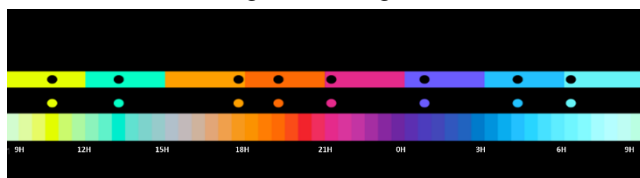


Figure 14: Colours palette for Living Light mode

4. Perspectives

With the 2nd step of Renaultion, the strategic plan of Renault Group, these 2 new vehicles show new styling orientation and more technological oriented systems.

In the future, lighting systems will be enriched with the future software-defined vehicles platform. Features for comfort, safety and pleasure will be available.

In parallel, miniaturisation of optical systems will continue thanks to brighter light sources, improvement of process but also with the improvement of optical system efficacy.

In the same time, stylists will request light signatures with animation, light decoration on front and rear bodies of the vehicle.

This will open new topics and new challenges for Lighting engineers.

5. Conclusion

After the revolution of the electronics in the lighting that has been done in a very short term with the replacement of xenon and halogen headlamps with LED headlamps, the software revolution opens a new era. The integration of more intelligence in the lighting system gives an access to a new field of creativity, to the interconnexion with other embedded systems of the vehicle that enrich information and propose new possibilities for safety.

In the same time, stylists will request more complex and qualitative signatures with less space for Low Beam and High beam optical systems. Pressure on carbon footprint will be more present in the decade and it will require from optical engineers to continue to work on compacity and efficacy of the optical systems at a reasonable price.

Safety improvement and neutral carbon footprint are 2 of the 3 pillars of Renault Group environmental and societal strategy.

6. Acknowledgement

This new generation of vehicles is the success of a large team with the contribution of engineers and technicians in charge of lighting parts but also of lighting systems. This is also the success of Tier1 and Tier2 suppliers that have accepted to work in the frame defined by Renault and have transformed our concept into industrial reality for the comfort and safety of our final customers.

7. References

- [1] MATHA Paul-Henri, "Full LED Headlamp Gen. 3: How Renault continues to reduce cost and increase performance", VISION, Paris, 2018.
- [2] BEDU François, "Renault LED Front Lighting for economic vehicles", VISION, Paris, 2020

8. Glossary

ACoL: Asymmetrical Cut-off line light distribution

ALU: Ambient Lighting Unit

CMF: Common Modular Family

FBL: Fixed Bending Light distribution

LCU: Light Control Unit, ECU dedicated to ADB function computation

LSU: Light Source Unit composed of LED, PCB, heatsink, connector and Rbin

LDM: LED Driver Module, with or without intelligence inside

PF1/PF2: Prefield light distribution

SCoL: Symmetrical Cut-off line light distribution

USM: Under-hood Switching Module, a multi feature ECU of the vehicle.

Re.Inventing.Product.Headlamp

D. Duhme¹

1: HELLA GmbH & Co. KGaA, Rixbecker Straße 75, 59552 Lippstadt / Germany

Abstract: The headlamp as we know it today will disappear. This is obvious by considering latest concept cars. We see light sculptures perfectly integrated into the overall design concept. And the part we call “outer lens” today does not exist. It’s all about glowing signatures, large areas for communication and ultra slim surfaces for main light functions. The boundaries between headlamps, car body lighting products and rear combination lamps are gone. And this is refreshing, because it’s different from everything we have done so far as a producer of lighting equipment. On the other hand, this evolution of automotive lighting inevitably leads to the question:

What is our future product?

This paper is intended to provide a retrospective and one possible answer on the previous question. A high-level system architecture with respect to mechanics, electronics and software/function will be sketched.

Keywords: headlamp, architecture, sustainability

1. Introduction

To start with the same understanding, a definition of the word “headlamp” is helpful:

A headlamp is the device, attached to the front of a vehicle, that produces and distributes a beam of light, called headlight, that illuminates the road ahead. [1] The headlight itself is very well discussed and regulated. But what about the mechanical device headlamp? Looking backwards we can define at least three categories:

1. The headlamp is attached to the vehicle as a stand-alone device.
2. The headlamp is part of the vehicle’s design.
3. The headlamp is hidden inside the vehicle’s body.

If these categories are still fitting to new challenges like Sustainability or if a new category must be invented, will be discussed on the next pages.

2. Retrospective

As one reference for younger car history the quartet “Edel-Flitzer” from 1996 gives an overview about different premium cars. 10 out of 32 have pop-up headlamps or very narrow cover lenses. Figure 1 shows the corresponding cars. Regarding the pop-up headlamp the Ferrari F40, Ferrari Testarossa, Lamborghini Diablo, Lister Storm, Spectre R42, BMW 850i and Ford Probe are to be mentioned. The signal functions of those cars are separated in an additional component with a slim signature. In contrast to that, the headlamp signatures of the Alfa Romeo GTV, Aston Martin Lagonda and especially the Opel Calibra are reduced to a minimum size, including main beam, with respect to the available technologies back then. Accordingly, we can define two main mechanical strategies: Hiding and reducing. Both strategies are based on the still existing motivation of clean and exiting design. Considering some of the latest concepts like BMW iVision Circular [3], Audi Skysphere [4] or Mercedes-Benz Vision EQS Concept [5] these cars are chasing the same dream of hiding and reducing. The Lucid Air with its benchmarking cover lens height is one of the latest milestones in series production.



Figure 1: Top Ass: Edel-Flitzer (1996) [2]

3. Seamless Frontend – Plug and Play Backend

A car is art - emotion - the expression of feelings. At first glance this is far away from engineering but on the second, it's worth to look out for the connection. Figure 2 shows the cycle of creativity by Neri Oxman. She describes the cycle as followed:

“Usually art is for expression, science is for exploration, engineering is for invention and design is for communication. Why can't we take these four squares and create a cycle out of them, where you constantly shifting from one domain to another? The Input from one domain becomes the output from another. Science converts information into knowledge. Engineering converts knowledge into utility. Design converts utility into cultural behavior and context. Art is taking that cultural behavior and questions our perception of the world.” [6]

The cycle can be used as a tool to analyze the interdependence of the different domains and to reach the bird's eye perspective on our daily business.

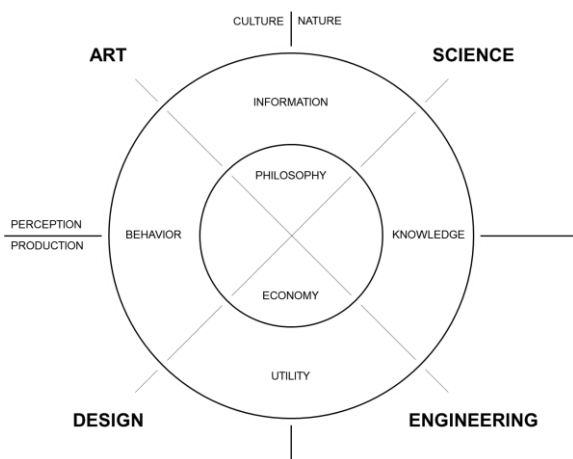


Figure 2: The Cycle of Creativity [7]

In the past decade we had two main drivers for the development of headlamps. Figure 3 expresses the today's status where the combination of Design and Lighting Technology is resulting in high-end products. The product headlamp has become a complex and fully integrated system, facing the never-ending challenge to find a good compromise between latest lighting technology and extraordinary design. And this challenge starts again and again for every product cycle. Until now we have reached a level of engineering excellence which is hard to exceed. Headlights made by matrix pattern, laser light sources, digital mirror devices and the upcoming pixelated solid state light sources are just a few examples.

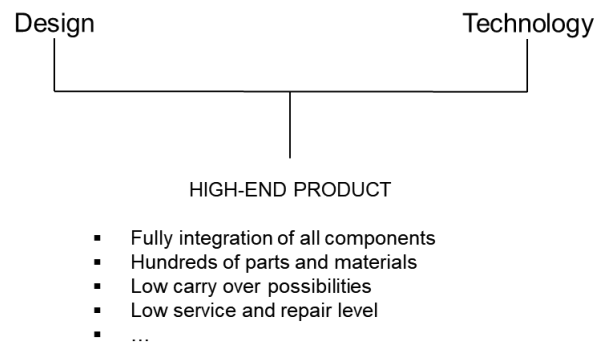


Figure 3: Status today

Considering Sustainability in the context of Oxman's cycle we are facing an additional dimension with respect to the next decade which is ahead of us. To find the right location for Sustainability inside the cycle is challenging. The center of the cycle seems best fitting, based on an understanding of Sustainability as the right balance of culture and nature defined by our knowledge and behavior. In addition, the balance of information and utility should lead to the right production strategies compared to our perception of the specific product. This complex definition might be one reason why Sustainability often seems like an unspecific buzzword without the corresponding context. To make it more specific, Figure 4 shows one possible consequence by considering Design, Technology and Sustainability for the upcoming decade of headlight development. The product headlamp must become simple again by not losing the reached level of lighting functionality and aesthetic aspiration.

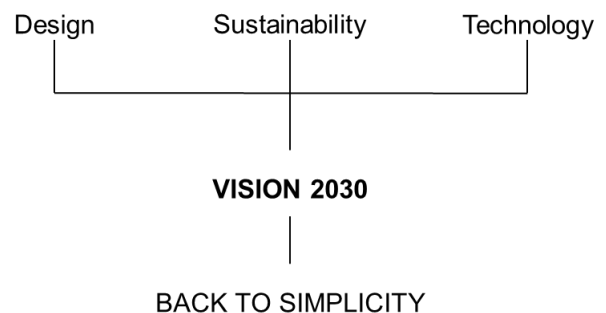


Figure 4: Vision 2030

Why simple again? Figure 5 gives a sketchy overview of different steps in vehicle architecture for different car types. In 2000 we had **Internal Combustion Engine Vehicles (ICEV)** with a surveyable number of components for the headlight system. Serviceability of the light source was naturally possible. In 2020 we had **Plug-in Hybrid Electric Vehicles (PHEV)** with a super complex car architecture. The headlight system is based on hundreds of LEDs. A cascade of ECUs is necessary to bring the latest lighting functions onto the street [8]. In 2030 we will have **Battery Electric Vehicles (BEV)**, **Fuel Cell Electric Vehicles (FCEV)** and **Autonomous Vehicles (AV)** with new components like Lidars or Displays. The **Advanced Driver-Assistance Systems (ADAS)** architecture, including sensors and actors like headlight modules, should be simplified to a status of 2000. The specific requirements are accessibility and easy coupling.

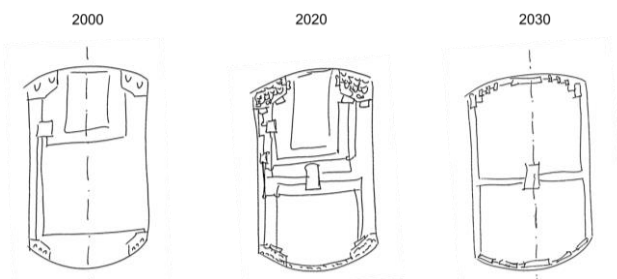


Figure 5: Back to Simplicity

Figure 6 shows a proposal for an enabling architecture called “Seamless Frontend – Plug and Play Backend”. To combine Design, Technology and Sustainability the Design should be separated from the necessary hardware for headlights or sensing as much as possible. The exterior design elements should be reduced to the outer skin of the car with a minimum number of parts which can be easily removed. The today's cover lens area should be reduced to the necessary light emitting surface including safety margins for adjustment and leveling (Figure 7). Highly decorative polymer bezels can be reduced to a minimum by that approach. Behind this design layer the hardware layer could be positioned. Main components of the hardware layer are the carrier frame directly attached to the inner structure of the car platform and the ADAS components including headlight modules. By reducing the visible part of the headlight modules to their light emitting surface a high reuse capability finally could be achieved.

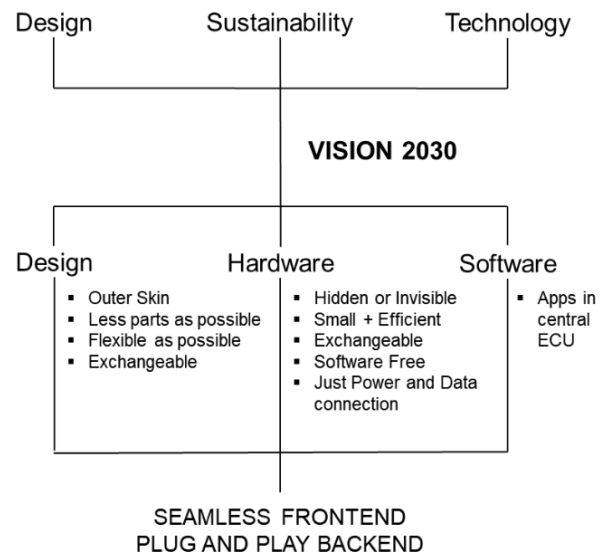


Figure 6: Seamless Frontend – Plug and Play Backend

We could understand the headlight components and sensors as intrinsic parts of the car platform and not as part of the exterior anymore. The product headlamp would disappear and the product headlight system would shift from a single component to multiple subcomponents directly attached to the platform. By doing so, we open up the possibility of reuse, serviceability, hardware upgrades and a new design opportunities.

Figure 7 shows the building blocks of the architecture: 1- Structure of car platform / 2 – Headlight carrier frame / 3 - Encapsulated SSL I X or CLA subcomponents / 4 - Headlight emitting surface + cylindrical lens arrays or smart glass / 5 - Bezel / 6 - Transparent part in outer skin / 7 - Outer skin. Potential technologies for some of the building blocks will be discussed in the following chapter.



Figure 7: Building Blocks

4. Enabling technologies

Necessary technologies for the concept “Seamless Frontend – Plug and Play Backend” can be clustered in Coupling, Subcomponents and Hiding:

4.1 Coupling

All subcomponents should be connected as simple as possible. Looking to the non-automotive world USB-C is becoming the standard interface for different types of mobile devices [9]. Data and Power supply via one connector is the main aspect. An equal electrical automotive interface for all types of subcomponents would be mandatory. The mechanical part of this required interface must fulfill additional functions compared to an USB-C connector. The precise and simple attachment of all subcomponents to the carrier frame is the main aspect. Additional tuning in production and corresponding in the repair shop is a No-Go. The carrier frame, including a combined and harmonized interface for power, data and mechanical coupling becomes the main development part for a new car. Each subcomponent should have its own DC/DC converter and IC for communication. Once those stand-alone subcomponents are equipped with the previous described interface, the market opens up to serviceability, re-use, retrofit and hardware upgrade solutions available from various suppliers. Delivering electrical power and data from a central ECU would be the key aspect for OEMs.

4.2 Subcomponents

To reduce the transparent area in the outer skin, the subcomponents should have a minimum light emission surface. HELLA's latest CLA technology, which is already on the road, enables a narrow light emission down to 10mm. In addition, the CLA technology is capable of horizontal, vertical or any other shaped signatures. With respect to the plug and play potential, the construction depth and tolerance-insensitivity between collimator and cylindrical lens array are the biggest advantages. Technologies like the multirow SSL|100 or high-res SSL|HD have the potential to become stand-alone modules for several use cases like matrix beam and ADAS projections. To lower the visibility in off-state, hiding can be considered. In combination CLA and SSL|X subcomponents are capable to reach state of the art headlight performance.

4.3 Hiding

The topic of hiding can be separated in passive and active hiding. Passive hiding is already established in modern cars by simply splitting the signal functions from the main beam functions.

The design footprint of the main beam function is typically reduced by using dark colors and low mounting positions. This approach increases the overall number of components or ends up in very large headlamps with two clear components in the cover lens. Active hiding has been done before by mechanical movement, as discussed in chapter 3. A modern interpretation is Volvos Concept Re-charge [13]. Motivated by the goal of reducing the overall material effort for the active hiding function, smart glass solutions are promising. Latest developments enable electrical switching from dark to transparent state or from colored to transparent state. To enable maximum design flexibility with respect to 2.5D and 3D surfaces, HELLA is developing polymer-based guest-host display solutions for frontend integration.

Figure 8 shows the system diagram of the described concept from Figure 7. In comparison to today's headlamp systems, you will find some crucial differences:

1. The outer skin, including the transparent part for the headlight beam, can be removed
2. The carrier frame, including the leveling system, is not attached to a weak polymer housing than to the stiff car platform
3. The mechanical and electrical interface, including the reference system and bolting, to enable an easy exchange to the frontside

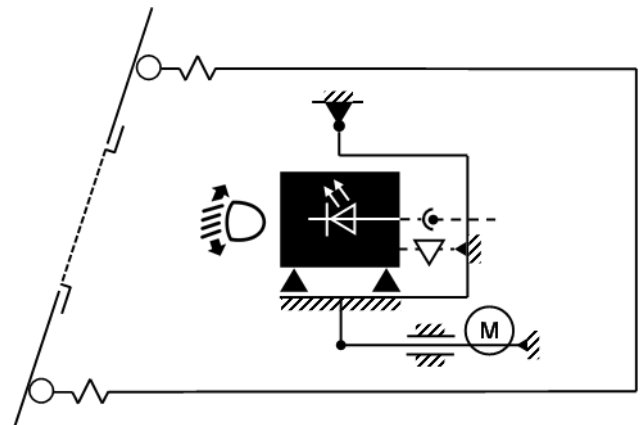


Figure 8: System Diagram

5. Summary and Outlook

The following conclusion will finally try to answer the initial question:

What is our future product?

First, we must separate the product categories headlight and headlamp. The product headlight will stay the same as long as existing regulations will stay the same. For the product headlamp, things look different. Coming from three historical types of headlamps (see Chapter 1), which ended up in various interpretations with lasting dreams of hiding and reducing (see Chapter 2), we are now facing the new big thing: Sustainability.

By using headlamp specifications based on the era of halogen bulbs and ICEVs we will make insignificant steps towards a better balance between culture and nature. In the proposed concept of "Seamless Frontend – Plug and Play Backend" today's product headlamp does not exist anymore. Instead, we would have subcomponents from various suppliers to enable reuse, serviceability, retrofit and hardware upgrades (see Chapter 3).

The product headlight will be enabled by the categories: Coupling, Subcomponents and Hiding and their related technologies (see Chapter 4).

The common definition of a combined and harmonized interface for all kind of ADAS subcomponents, including headlight modules required by the BEVs, FCEVs and AVs in 2030 and beyond, could be a starting point.

7. References

- [1] Wikipedia: "*Headlamp*", <https://en.wikipedia.org/wiki/Headlamp>, visited 2022-09-22
- [2] Augsburger und Stralsunder Spielkarten-Fabriken: "*Edel-Flitzer*", Top Ass, 1996
- [3] BMW AG: "*DER BMW iVISION CIRCULAR*", <https://www.bmw.de/de/topics/faszination-bmw/bmw-concept-cars/bmw-i-vision-circular-ueberblick.html>, visited 2022-09-22
- [4] Audi AG: "*Audi skysphere concept*", <https://www.progress.audi/progress/en/concept-cars/audi-skysphere-concept.html>, visited 2022-09-22
- [5] Mercedes-Benz AG: "*VISION EQS show car*", <https://www.mercedes-benz.com/en/vehicles/passenger-cars/concept-cars/vision-eqs/>, visited 2022-09-22
- [6] Neri Oxman: "*Bio-Architecture*", Abstract: The Art of Design (Season 2, Episode 2), Netflix, 2019
- [7] Neri Oxman: "*Age of Entanglement*", <https://iods.mitpress.mit.edu/pub/ageofentanglement/release/1>, visited 2022-09-22
- [8] Wartzek, Saure, Wilks: "*Making Future Complexity in Lighting Electronics Manageable*", ATZelectronics worldwide 15 (44-47), 2020
- [9] European Commission: "*One common charging solution for all*", https://ec.europa.eu/growth/sectors/electrical-and-electronic-engineering-industries-eei/radio-equipment-directive-red/one-common-charging-solution-all_en, visited 2022-09-22
- [10] Volvo Car Corporation: "*The Volvo Concept Recharge is a manifesto for Volvo Cars' pure electric future*", <https://www.media.volvocars.com/global/en-gb/media/pressreleases/283548/the-volvo-concept-recharge-is-a-manifesto-for-volvo-cars-pure-electric-future>, visited 2022-09-22

SLIM & DUAL OPTICAL SYSTEM FOR NEXT HENERATION OF HEADLAMPS

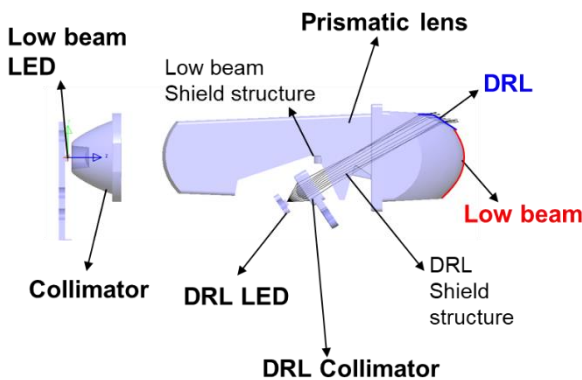
Hyunsoo Lee¹, Gilwon Han¹, Donghwa Kang¹

1: Hyundai Mobis, 17-2 Mabuk-Ro 240 Beongil, Yongin-Si, Gyeonggi-Do, Korea

Abstract : When a new car is released on the market, we can see easily an image of a lit area on a new car with dark background. It shows a signature image of a new car directly. Because a lot of car makers wants to show their design identity as lighting images. And also they would like to keep a same image during day and night. To realize it, low beam optical module should work for DRL function too. But it is quite difficult because light distribution area is quite different each other. Low beam has horizontal cut off line. But DRL is more like high beam which is without cut off line.

Here we have an idea to operate both functions properly by using the Prism Optical Module which is for Bi-Function. POM (prism optical module) has 2 light sources for low beam and DRL. Each light sources turn on and off for day and night! It gives a same design identity all days. It is real signature for the next generation headlamp.

POM consists of 2 light sources, collimator lenses, Prism lens which is for light guide with projection lens. It can be seen as below photo.



<Fig 1. Prismatic Optical Module>

Keywords: Prismatic, collimator, LED, Lens, Low beam, DRL

1. Introduction

1.1 Design Trend & Brand signature

When a new car is released, we can easily see the image of the illuminated part of the new car with a dark background. It shows the signature image of the new car directly. This is when many automakers want to show their design identity through lighting images. They also want to keep the same image day

and night. To realize this, the low-beam optical module must also work with the DRL function. However, it is quite difficult because the light distribution area is quite different. The low beam has a horizontal cut line. However, DRL is more like a high beam with no blocking line. Therefore, most finished cars have made signatures using the DRL & TRUN function.



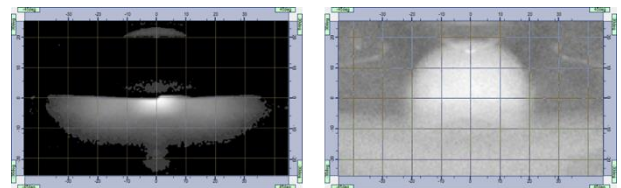
<Fig 2. Examples of new models launching with lighting^[1~4]>

If so, how can the future of vehicle design change if low beam, DRL, and TURN signals can be implemented in one image? I can't give you a specific answer, but it's clear that new ideas can create new images. In this paper, we will discuss this essential solution.

1.2 Day & Night time lit images of headlight

As mentioned, low beam and DRL have different light distribution areas. Low beam has cut-off as shown in the figure below, and DRL does not have cut-off, so there are two types in one lens optical system.




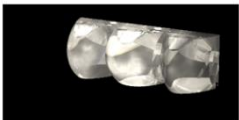
It is difficult to implement functions together.



<Fig 3. different light distribution and intensity>

Therefore, many vehicles released so far used an additional light source in a low beam for the same

image day and night, and used only the lighting image for the design of the light during the DRL function. In this way, the function that satisfies the actual regulations is implemented in a separate DRL module, and the low beam only implements the lit image using Sub LED. Therefore, the difference between low beam and DRL images occurs.

Function	Up 15deg	Up 15deg, R 30deg
Low		
DRL		

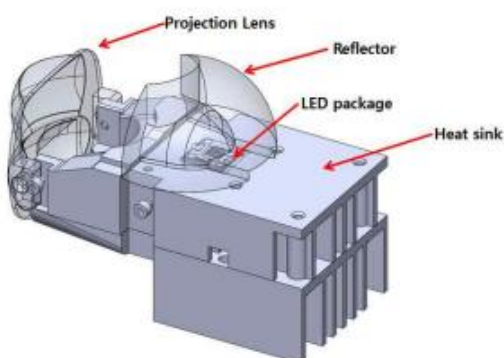
<Table 1. Different lit images of 2 functions>

2. Development the system

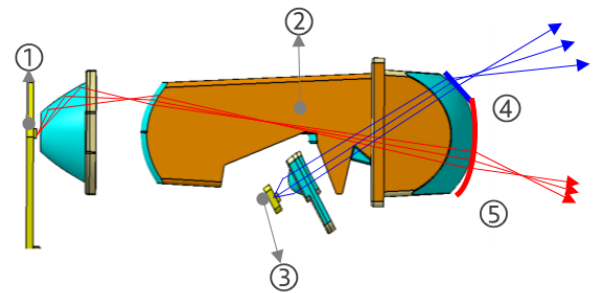
2.1 Optical system

Let's look at the optical design concept for a new optical system to implement two functions with different light distribution areas using one module.

Looking at the structure of the low beam, it can be divided into a light source part, a projection part (lens), and a beam shaping part as shown in Figure 4 below. At this time, it can be seen that an empty space exists from the end of the beam shaping part (the focal area of the projection part) to the lower part. An optical system as shown in Figure 5 was devised with a focus on how to implement the DRL function using this space.



<Fig 4. Projection optical system>



No.	Detail part	Role	Comparing
①	Low input	Focusing on a focal point of low output lens	Reflector
②	Cut off structure	cut off a low beam	Shield
③	DRL input	guiding lights to DRL output	-
④	DRL output	DRL beam projection	-
⑤	LOW output	LOW beam projection	Aspherical lens

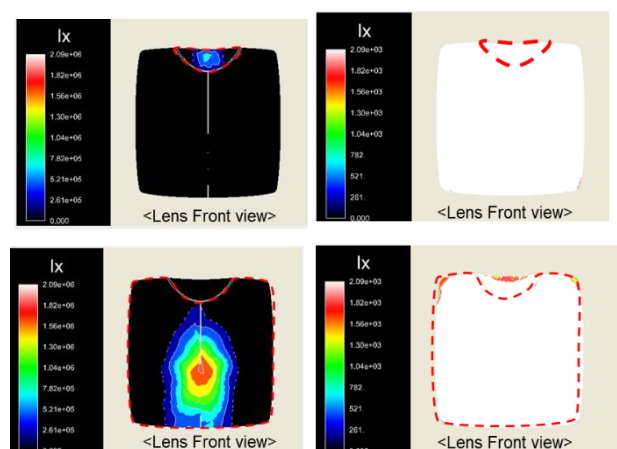
<Fig 5. Schema of Prismatic module for DRL & Low beam>

As can be seen in Figure 5, the path of the light from Low LED and the path of light from DRL go to the final exit lens. More precisely, the upper part of the exit lens is a lens in charge of the DRL light distribution area, and the lower part is a lens in charge of the LOW light distribution area.

Looking at each area, No. 1 is an LED light source for low beam, and No. 3 is an LED light source for DRL.

Light from each light source is incident on the Prismatic lens (No. 5) through each collimator. The incident light implements a function through the light distribution area arranged at the upper and lower parts.

Two lenses for different functions are attached together and look like one lens, but if you look at the actual optical density, they are separated as follows.



<Fig 6. Optical Density_ High resolution for left photo,
Low resolution for right photo>

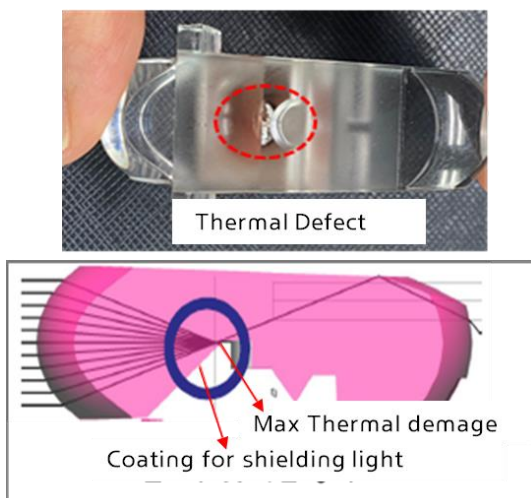
As two different beams use one channel, inter-channel interference may occur. However, in the case of the low beam, as shown in the figure below, the upper part of the lens is rarely used, so it does not have a significant effect on the overall beam pattern. A separate structure should be added so that the DRL does not go to the lower part of the exit lens.(See Fig.1 shield structure)

2.2 Design considerations

The considerations in the detailed design are minimization of heat damage and chromatic aberration. Let's take a look at each.

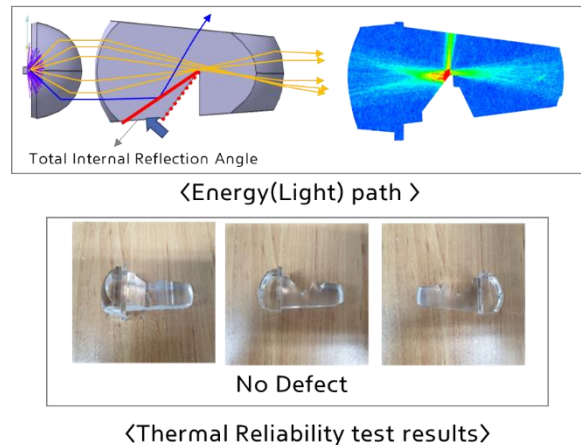
Other configurations of the optical system are general, but it is necessary to focus on the Low Beam Shield Structure area, which is the section that shapes the beam. Low beam can be divided into a hot zone area for long distance and a wide zone for near brightness and wide range. Due to the principle of the projection optical system, the beam for the hot zone is inevitably gathered in the Kink area of the shield structure. Therefore, the light is concentrated in the corresponding area and the heat concentration is increased.

Also, certain areas may need surface treatment for clear cut-off lines. In fact, when surface treatment (evaporation, surface coating, etc.) is performed on the relevant area for clear cut-off, carbonization occurs as shown in the figure below. In order to cut light in the relevant area, it is necessary to find a way to minimize light absorption and prevent light transmission.



<Fig 7. Thermal Defect of prismatic lens>

Therefore, it is necessary to surface-treat the high heat-resistant material or to reduce light absorption. Of the two methods, the method of reducing light absorption would be reasonable in terms of product price. Therefore, it is a clear specification that can minimize light absorption, so that the proceeding light can be total reflection to minimize light transmission. Through this, both PC and PMMA, which are common optical materials, can be used. In terms of chromatic aberration due to light injection, PMMA material is more suitable for Prismatic lenses.



<Fig 8. Energy Path and Test result>

Hyundai Mobis Rest...


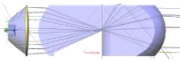

If the collimator is used in a way that directs light in a general form, color separation occurs severely as shown in Figure 10 below. This is a phenomenon that occurs as the aberration that occurs primarily in the collimator is projected as it is without mixing. There are two ways to overcome this.

	Previous design
Simulation Image	
Concept	
Detail	<p>. Chromatic aberration occurs at the outer part of the lens</p> <p>. There is no ray mixing before projection</p>

<Table 2. Color aberration from previous design>

The first is mixing using the guide surface of the prismatic lens, and the second is mixing by changing

The collimator to the TIR structure. In terms of PKG implementation, it is possible to miniaturize the type to which the TIR structure is applied. Therefore, the method of Beam Shaping after mixing in TIR as shown in Figure 11 below would be more suitable.

	Improvement plan 1	Improvement plan 2
Simulation Image		
Concept		
Detail	<ul style="list-style-type: none"> TIR type collimator has suppressed chromatic aberration. Rays which have different wavelengths are mixed up by TIR collimator possible. 	<ul style="list-style-type: none"> Upper light guide of prismatic lens should work for reflector. There is ray mixing before projection.

<Table 3. Improved design for color aberration>

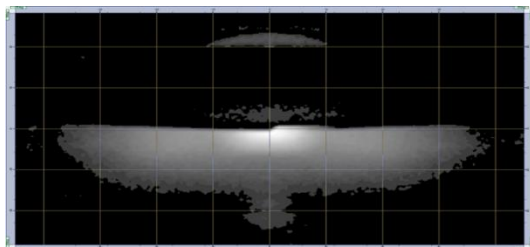
3. Result

So far, we have had improved result as follow from those above studies

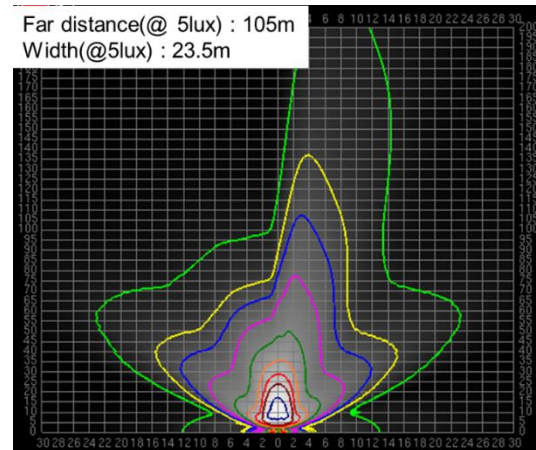
Of course, 2 regulations are meet which are R. 123 for Low beam and R 87 for DRL. And there are some brief performance below;

It can be suitable performance for luxury segments

Hyundai Mobis Restricted



Unit	Result
Max intensity	34,560 cd
Beam width	± 35 deg
Total Flux	770 lm



<Fig 9. Performance of the system>

In terms of design aspects, we do not need any dedicated module for DRL. See below images.
Lit images of 2 functions are almost coincidence.



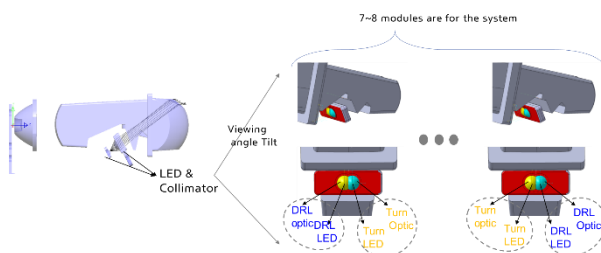
<Fig 10. Lit image of each function in direction of 30 degrees upside>

4. Conclusion and Forecast

Through this study, low beam and DRL were implemented as one optical system to realize the same day/night image. As mentioned in the introduction, signatures have been implemented using DRL and Turn in common. If so, what happens if we implement the Turn Indicator function as well

as Low beam and DRL through the corresponding optical system?

As shown in 13 below, by changing the DRL LAM and DRL Optic, it can be confirmed by simulation that three functions (Low beam, DRL, Turn) can be implemented. However, about 3 times more current than the previous DRL is required. This uses the same power used as the low beam, and there is no thermal problem because it shares the heat dissipation system with the low beam in structure, but there is a disadvantage that the power used can be relatively excessive.



<Fig 11. Tri-Functions schema>

In conclusion, as three functions can be implemented with one optical module, various attempts will be made possible to design a headlamp that shows signature images only with DRL and TURN as well as day and night images.

Hyundai Mobis Restricted

But, in terms of safety, we should consider deeply about this tri-function. Because it has only 1 module for 3 functions. DRL/ Low beam is beta function. And DRL/ Turn also work for properly by regulation. How about Low beam / Turn indicator! We will have some argument with that function by using at same module. Some body need dedicated module for Turn improving safety.

Function	Upside view	Front view	Downside view
Low beam			
TURN / DRL			
LOW beam ON with TURN / DRL			

<Fig 12. Tri-function Images>

The package size of this optical system is shown in the table below. Dot image can be implemented with

12mm high module, and line image can be implemented with 25mm high module.

	Line image (1 module size : 25 x 25mm)	Dot image (1 module size : 12 x 12mm)
Image		
Module composition	8ea	7ea
Module size (LxHxT)	230 * 70 * 188 mm	280 * 85 * 140 mm
Number of LEDs	1chip x 8EA (Low) 1chip x 8EA (DRL)	1chip x 7EA (Low) 1chip x 7EA (DRL)
Power consumption	40W(Low)/ 10W(DRL)	35W(Low)/ 10W(DRL)
Total flux	760lm	770lm

<Table 4. 2 kinds of design possibilities>

The brand identity or vehicle signature image, which was implemented with DRL and TURN, can be reduced by placing a system consisting of at least 7 modules with a height of 12 mm in various designs or implementing a line image with one module with a height of 25 mm. By extending it to beam, we can expect new possibilities.

5. Reference

[1] [Automobilesport.com/first-teaser-future-renault-concept-car---234336.html](https://www.automobilesport.com/first-teaser-future-renault-concept-car---234336.html)

[2] [Gearpartrol.com/cars/a39451938/bmw-io7-april-2022/](https://www.gearpartrol.com/cars/a39451938/bmw-io7-april-2022/)

[3] [Autoevolution.com/news/2019-mercedes-benz-gle-shows-off-full-led-headlights-in-video=teaser-128462.html#agal_1](https://www.autoevolution.com/news/2019-mercedes-benz-gle-shows-off-full-led-headlights-in-video=teaser-128462.html#agal_1)

[4] [carexpert.com/au/car-news/2023-bmw-m4-csl-teased-may-20-reveal-confirmed#gallery-2](https://www.carexpert.com/au/car-news/2023-bmw-m4-csl-teased-may-20-reveal-confirmed#gallery-2)

Landscape of Microlens- Array Headlamps

C. Bremer¹, P. Heissler¹, W. Noell¹, R. Völkel¹

1: SUSS MicroOptics, Rouges-Terres 61, 2068 Hauterive, Switzerland

Abstract: This post details the benefits of MLA technology with a focus on current trends.

In addition, the production process is examined in more detail and an overview of the most important patents in the field of MLA headlights is shown. In the last part, an overview of design guidelines is given within reasonable boundary conditions from manufacturing as well as optical perspective.

Keywords: MLA, MLA Headlamp, Production, Imprint

1. Advantages of MLA Headlamps

1.1 Design

New technologies open a manifold of possibilities for new designs. Micro Lens Arrays (MLAs), for example, enable several design features while maintaining high efficiencies, like one of the main trends in automotive lighting: ultra slim headlamps [1].



Figure 1: Examples for "Ultra Slim Headlamps"
Source: DVN Report [1].

Since the lighting function is built in each micro channel different forms and variations of forms are possible. The arrangement of the channels in a straight horizontal line as shown in Figure 1 (GAC Time Concept) as well as the arrangement in vertical lines (Figure 2) can be implemented easily.



Figure 2: Arrangement of lighting modules in vertical lines, Source: DVN-Report [1].

Another trend are extended, 2D or even 3D illuminated surfaces. The lenses within the MLA have a diameter around 1mm and an observer is not resolving each single lens from a certain distance. This leads to the perception of the light emitting area as a homogenous, illuminated surface. This means that new lighting concepts without the approach of using traditional lenses become possible. Concepts (so far mainly for DRL-functions) are shown in Figure 3. Since the lighting function is defined within each unit cell it is possible to produce complex geometry like shown below or even more complex shapes.



Figure 3: Different concepts for lighting Left side and right side show illuminated surfaces, Source: DVN-Report [1].

The MLAs can also enable "invisible headlights". The side of the aperture, which is directed to the street, can be coated with different metals or colors. Therefore, the headlight module disappears when seen from the front.

1.2 Volume and Weight

Another advantage of the MLA-Technology is that it allows a reduction of volume and size of the optical system. Compared to conventional technologies, MLA systems are able to reduce the overall weight are shorter in integration depth and smaller in height [2].

1.3 Integration and functionality

With wafer level technology higher integration levels are possible. Currently, Condenser lens, aperture and projections are combined to a single element. In the future it will also be possible to include collimation optics or even LED-Matrices with wafer stacking technology. Due to the multichannel approach an outstanding homogenization as well as complex gray

scaling and manipulation of the beam are possible. Sharp or blurry edges can be generated by the superposition of the illumination from different channels. The first models using these advantages are the Hyundai Genesis G90 and the Lucid Air (see **Erreur ! Source du renvoi introuvable.**).



Figure 4: Top: Slim headlight from Genesis G90 enabled with MLAs; Bottom: Lucid Air: First car on the market with MLA Technology.

2. Production

2.1 Imprint

The wafer level process allows upscaling and high integration of complex optical systems. The process is shown in Figure 5.

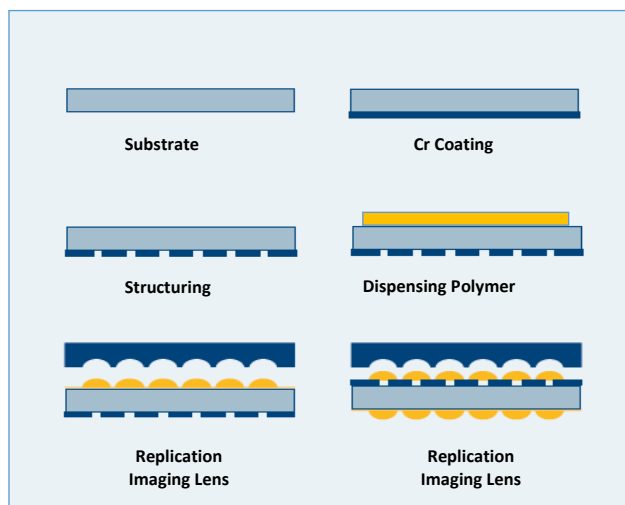


Figure 5: Imprint process for light carpets

Substrate: Different glass materials with different thicknesses can be chosen.

Cr-coating: Chromium can be replaced by other metals/ materials with different coating. It is also possible to have different coatings on each side. Highly reflective or absorbing coatings can be used.

Lithography: Each microchannel is structured by lithography with a resolution of a few micrometers.

Replication imaging lens: different methods are possible to generate the stamp masters to fulfill requirements on shape and form. The stamp is used to imprint the shape of the lenses into the polymer. The same is done on the opposite side of the module. With these tools, it is possible to generate different modules, like shown in Figure 6. For light carpet applications, the design “Lens Array + Cr-Layer” is used. For Headlight application, a wafer stacking of the elements is typically used.

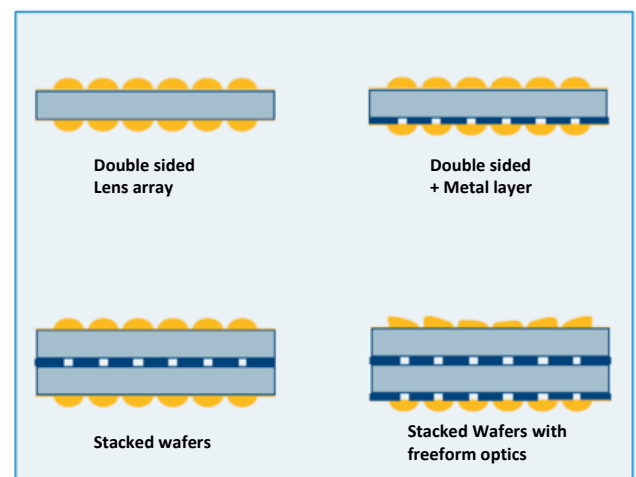


Figure 6: Possible MLA configurations.

2.2 Singulation

Newly developed singulation technologies are not only more efficient but also enable freeform MLA geometries. Rounded corners or even round MLAs are the most obvious implementation. Slanted edges allow the MLA headlights to follow the 3-dimensional contour of the car by a stacking approach. With full 2D freeform dicing, MLAs in the shape of logos, letters or other objects, like diamonds or horses, can be realized. This opens up a new design toolbox for automotive front design.

2.3 Cost and scale

The described MLAs are manufactured on state of the art semiconductor technology. On a semiconductor scale, volumes of these “dies” are still rather low today. With increasing demand, the full economies of scale of semiconductor manufacturing will drive costs

down significantly. The most obvious example is the wafer size. Currently most of the manufacturing of these MLAs is still running on 200mm wafers. The move to 300mm technology will directly result in a 2.25 increase surface area of each wafer, enabling a much higher number of MALs to be manufactured in a single step.

3. IP Landscape

3.1 Overview

As Figure 7 shows, the number of patent applications for microstructures in headlights is increasing over the past ten years. The drop seen in 2020 could be caused by the reduced activities due to the COVID pandemic.

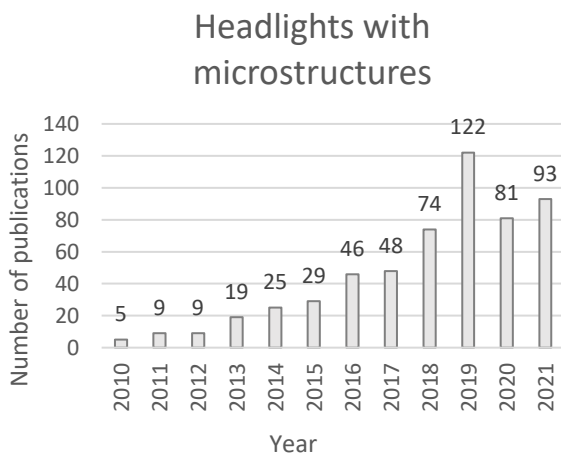


Figure 7: The number of publications for IP-Class: F21S in combination with microlens and variations of that wording.

3.2 Patents from various companies

The requirements for MLA technology can be seen from the vehicles on the road as well as from the patents filed by various manufacturers.

ZKW has a big portfolio of patents. Patent AT514967B1 [3] describes an optical system that includes an entrance lens array, an aperture as well as an exit lens array (see Figure 8). In a special case of the application, the exit optics can be designed as free-form lenses. As already shown in Figure 6, this can be realized very well with imprint technology.

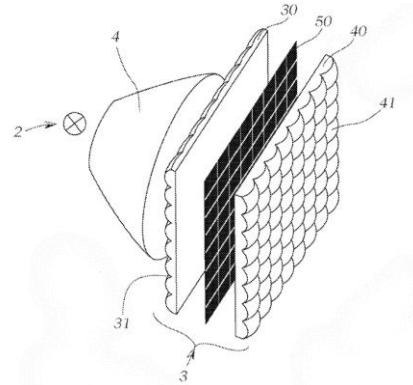


Figure 8: light module as described in AT514967B1 [3].

Lucid's Air is the first vehicle to put MLAs on the road. A variety of technological ideas for MLA technology can be found in patent specification US10232763 B1. A multitude of LED groups enables digital beamsteering. The different groups illuminate different areas of the intermediate image plane and thus enable a shift of the hotspot depending on the requirements.

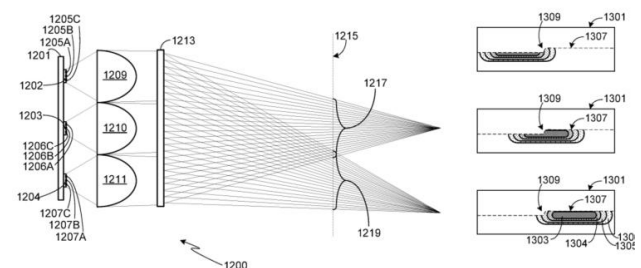


Figure 9: Adaptive headlight functionality. For further explanation see [4].

In this patent, a hexagonal arrangement of the channels is preferred, since this reduces the crosstalk and thus the intensity of the ghost images.

Likewise, it is described that this can be done efficiently by a displacement between input aperture and output aperture. The shift can be less than 25% (compare Figure 10).

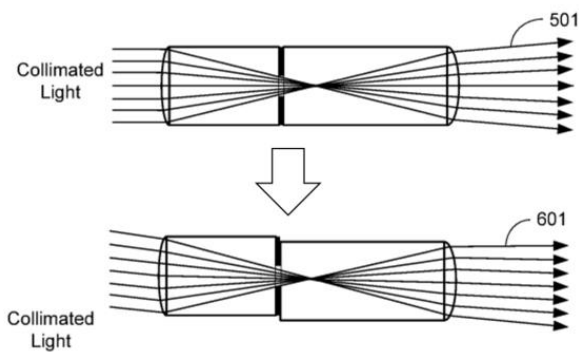


Figure 10: Proposed displacement to enable high-efficiency low beam functions [4].

This displacement between entrance and exit aperture can be realized very easily with the help of the imprint process. The input aperture can be slightly offset from the chrome layer during the manufacturing process.

The disclosure document DE102019213502A1 describes an MLA light module that follows the contour of the vehicle by tilting the elements (Figure 11).

This results in slanted edges (compare Figure 12) of the MLAs in the design. This can be realized by an in-house developed dicing technology at SUSS MicroOptics, which also enables round edges or more advanced freeform designs.

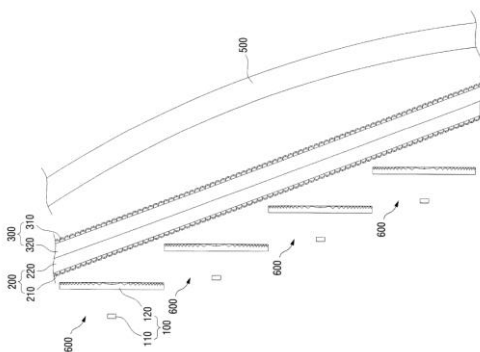


Figure 11: MLAs arranged at an angle, which follows the vehicle contour [5].

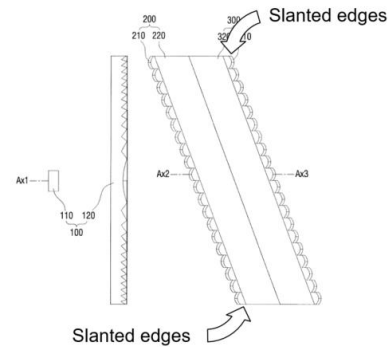


Figure 12: Single element with slanted edges [5].

4. Best solutions from manufacturing perspective

The ideas presented above are largely detached from a defined parameter space. In the following, a practicable parameter space will be presented, which, from the point of view of imprint technology, enables the best results in terms of performance and yield.

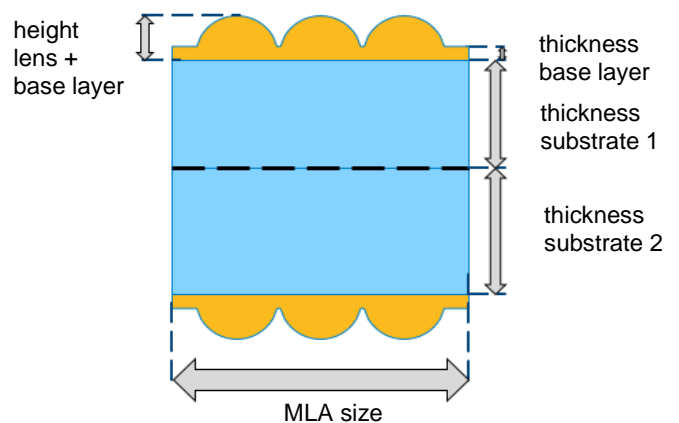


Figure 13: Description of an MLA

4.1 Geometry

The smallest size of the single MLA chip is limited by the etendue of the LED.

The larger the chips, the more difficult it is to achieve a high yield in production. Large chips, up to 50 mm edge length and beyond are well within the capability of the manufacturing technology. Reduced chip sizes around 20 x 20 mm² and smaller will increase manufacturing performance. This trade-off between chip manufacturing, subsequent packaging complexity and design aspects needs to be resolved during the design to manufacture process.

Due to the increasing challenges for dicing thicker layers, the thickness of the wafer package should remain below 6 mm if possible. Different materials such as Borofloat or D263 can be used for the substrates.

4.2 Optics

The optical parameters also result in part from the framework conditions given by the technology. The thickness of the baselayer is best controlled in a range from 50 μm to 150 μm . To enable the optimal base layer thickness, the thickness of the substrates can be adjusted during the optical design. The lens SAG should be less than 350 μm (base layer + lens SAG < 500 μm). The conic constant can be adapted to the design. For imaging systems, this is usually in the range of -0.45.

Ideally, the RoC of the lens is larger in the range > 0.8 mm.

Parameter	Min Value	Max Value
MLA Chip	Etendue limit	
Element thickness	2 mm	6 mm
Base layer	30 μm	150 μm
Base layer + SAG	50 μm	500 μm
RoC	\approx 0.8 mm	

5. Conclusion & Outlook

The most important trends such as ultra slim headlamps or illuminated surfaces are very well met by MLA based headlamp systems.

The imprint process can guarantee the approaches of the different patents such as a precise orientation of the chromium layer to the projection optics, a displacement between the input and output lens as well as sloping edges of MLA chips. With optical designs within the parameters given in this article, stable and highly efficient MLA headlight systems can be built. In the future, by expanding production to 300 mm technology, costs will continue to drop significantly and competitive MLAs for headlights will be produced.

6. Acknowledgement

The authors acknowledge the contribution of their colleagues to this work.

7. References

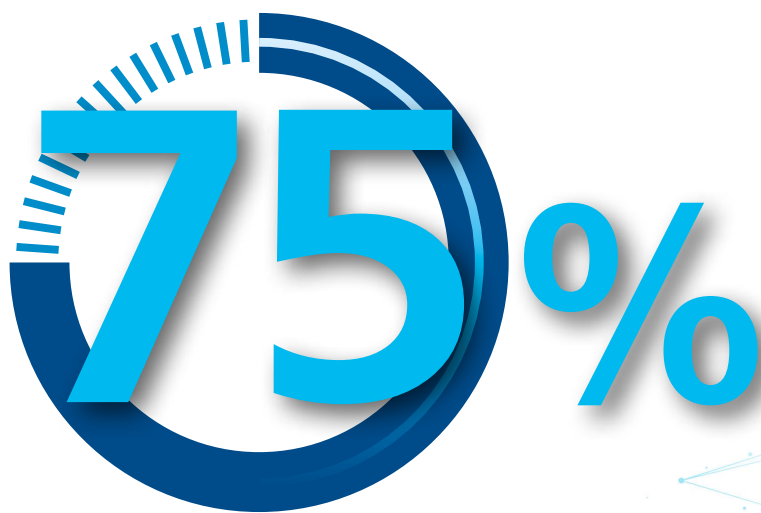
- [1] DVN, "DVN Report on last Concept and Production Vehicles", 2022
- [2] Hans-Christoph Eckstein and Lingxuan Zhu, "MLA application in headlamp and advantages" US DVN Workshop, (Rochester, MI, USA), 2022
- [3] ZKW, "AT514967B1 – Mikroprojektionslichtmodul für einen Kraftfahrzeugscheinwerfer", Friedrich Bauer and Gerald Boehm, , Patent, 2013.
- [4] Atieva (now: Lucid), "US10232763 – Solid State adaptive headlight", Wiebke und Hans-Christoph Eckstein, Eric Bach, Patent, 2018.
- [5] SL Corp. "DE102019213502A1 – Fahrzeugleuchte", Nak Jung Choi, Gyeongsan-si, Jong Woon Kim, 2019

8. Glossary

MLA: Micro lens array

RoC: Radius of Curvature

NEW TRENDS IN LIGHTING DESIGN



75%

less assembly time and costs

ARNOLD TriPress® is a triangular quick fastening system that can be clinched into plastic, light metals and steel. Two components can be joined quickly and economically by pressing in the TriPress® fastener.

- no assembly errors
- very secure
against unscrewing by itself
- uses more economical
operating materials and tools

www.arnold-fastening.com



ARNOLD®
BlueFastening Systems

MEMBER OF THE WÜRTH  GROUP

New Approach for functional Styling Challenges and Possibilities Crystal Lighting

Gerald Boehm¹, Alexander Buck²

1: ZKW, Rottenhauser Strasse 8, Wieselburg, Austria

2: BMW AG, Knorrstr. 147, 80788 Munich, Germany

Abstract: Today we find headlights in most vehicles, which almost always combine all lighting functions. These often represent a compromise in terms of styling and functionality. High functional demands usually require main light modules with a corresponding size and limited styling options. Daytime running lights and direction indicators usually allow for a styling-driven concept. These two issues often interfere with each other. One possible way out is to distribute the light functions across several housings. This opens a new spectrum of possibilities in terms of design and functional implementation.

A completely new approach was chosen for the BMW 7 Series. The presentation would like to present this new concept, show the possibilities, discuss the new central styling elements - the crystals - and finally also deal with the challenges in the series implementation. Daytime running lights and direction indicators are supported by a new concept of optical elements - crystals.

Keywords: Crystals, head light, styling,

1. Introduction

Crystals have been used in optics for many centuries. Even before lenses or reflectors were used, crystals were used as the first optical aids - ice crystals, crystalline minerals and much more.

The main optical properties of crystalline transparent materials are reflection, refraction and absorption.

The crystal as a defining element stands for luxury in many ways. BMW has already successfully implemented this design element in many equipment details in the past, especially in the interior. It was now the goal of BMW, together with ZKW, to place this crystal element in the headlight accordingly and create headlights with a unique appearance for the new BMW i7.

The focus was on the crystal as a free-standing element. This should be integrated as a central element in the headlight - standing in the foreground in the off state when only being passively illuminated

by sunlight and even more so in the actively illuminated state. The iconic character of the crystal had to be supported and implemented as a new design element – “BMW Iconic Glow”.

Tom Binder, Head of Exterior Light Design at BMW, speaks of a step that no one has taken before: “Up to now, you have only seen homogeneous light strips on the road – the crystal headlights are the complete opposite of that. The dazzling, vibrant light image is a world apart from the familiar accurate light graphic. The precision is in the glass material, though, which can be machined much more finely and precisely than plastic.” [1]

ZKW also pursued the topic of crystal independently of BMW and developed its own solutions. The priority here was to find a solution based on plastic and to build on the experience gained in the BMW project. The glass crystal concept in the BMW headlight was the yardstick and goal, with the ZKW solution being about a more cost-effective solution that can also find its way below the luxury segment. The result comes close to the target solution, but does not achieve the brilliant and clear appearance - which is acceptable for the target segment.

As a further approach, ZKW is pursuing a solution with which light functions such as DRL or DI can be implemented directly. For this purpose, further optical and lighting algorithms have been developed and already implemented.

The topic of crystal and crystal optics will be an exciting topic for the near future in the automotive lighting sector.

2. BMW 7 Series Head Lamp Concept

The new face of the BMW 7 series is defined partly by the luminous kidney contour, but above all by the headlights, which are each separated into two, one above the other. The lower ones incorporate the main light modules with low beam and high beam and are very discreet and unlit during daytime operation. The crystals, two pairs each, are displayed in the upper headlights as the main design elements sparkling in

the sunlight. Individually controlled LEDs and special chaotic optics behind the crystals create an irregular, lively glow during nighttime and constitute daytime running light, indicator light, and unique welcome and goodbye functions.



Figure 1: BMW 7 Headlights © BMW



Figure 2: BMW 7 Light Animation © BMW

2.1. Challenge of Integration

A long series of challenges were overcome as part of the integration of the crystals into the lamps. Never have such large crystals made of glass been installed in a vehicle lamp with a premium claim. The requirements specifically for design and functionality - animation of the crystals as a defining element - were very high. The mechanical and optical integration into an automotive lighting concept was challenging. Many technological solutions were necessary, several of them are described as examples within the next paragraphs.



Figure 3: BMW 7 Crystals - Signalling Lamp © BMW

The crystals should also glow/sparkle with light functions. To do this, it was necessary to include the crystals in the light calculation – more on that later.

A very demanding challenge was the mounting of the crystals due to the large weight. A mechanically robust mounting was required, which should not interfere with the free standing appearance of the crystals. As a second challenge, the fixation could not get in the way of the lighting technology. The result was a combination of clip and glue. The crystals are clipped from the rear top and are held against the bezel on the lower side of the crystal. The clip connection is stabilized with a glue connection.



Figure 4: BMW 7 Free standing Crystals

This was necessary because the crystal made of glass and the holder made of a metal-plastic combination have different thermal expansion coefficients and the connection also had to withstand mechanical shocks without damaging the crystal itself. The visibility of the connection was prevented in the lower part by a metallic coating on the crystal. This coating is also used optically as described in paragraph 2.3

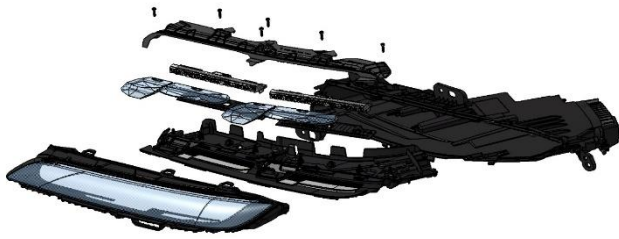


Figure 5: BMW 7 Construction of the Lamp

2.2. Challenges for the off-state appearance

To achieve the best appearance, the daytime running light and thus the crystals were placed at a position where they cannot only be seen from the front but also from the top when approaching the car. The crystals are seen from various positions and sunlight is striking the surfaces from as many angles as possible.

The crystals themselves come from the Swarovski company – a world famous manufacturer of jewelry and crystal products and a partner of BMW for high-premium car line equipment concepts. The crystals were designed according to BMW's styling and geometric specifications and the individual surfaces follow the teachings of jeweler manufacture in order to achieve the best possible crystal effect.

The angles of all facets are optimized and all the surfaces are polished to maximize the sparkling effect and to see the typical rainbow sparkle when seeing the lamp in bright sunlight.



Figure 6: BMW 7 Crystal Shape © BMW

2.3 Challenges of the lighting technology

The crystals themselves should glow/sparkle with the light functions DRL, POL and DI. The challenge was to design the lighting technology for illuminating the crystals in such a way that the legal light values for the lighting functions and BMW requirements are observed. The crystals should "sparkle" - to achieve this, peak light values are necessary in some narrow angle areas, but these should not be set too brightly

in order not to exceed the maximum permitted light values, but the requirements of BMW for the effect should be achieved. Furthermore, the sparkle should look random.

These requirements were achieved by means of thick-wall optics placed behind the crystals, which are used like light guides (fig. 7). The decoupling surface of the thick-wall optics was given seemingly randomly arranged decoupling elements. These elements were calculated with a random tool, whereby the requirements for the light distribution through the crystal were considered as a limit variable in the calculation. That is, the complex front of the crystals with the many facets was also included in the light calculation values.

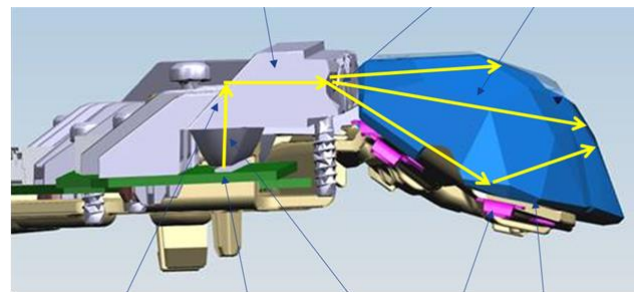


Figure 7: BMW 7 Crystal Light Path

As already mentioned, the metallic coating of the crystals on the bottom side was used to hide the mounting, but also to improve the 3D effect of the crystals and to support the sparkling effect. This also had to be included in the light design and calculation of the decoupling structure of the thick-wall optics behind.

2.4. Challenges for the welcome and goodbye functions

The sparkling effect should be shown by the welcome and goodbye animation sequence. To this end, the LEDs used for the static operation in daytime running light are switched on and off in a targeted manner. Control of each individual LED is achieved by the software in the headlight ECU. Programming each LED with an individual curve for the brightness creates the dynamic sparkling effect.

This use case also had to be included in the design of the decoupling structure of the thick-wall optics. The crosstalk of the individual LEDs on neighboring areas should not destroy the effect of the dynamic twinkling.

**The new BMW 7 Head Lamp Concept
A new "crystal" in the Headlamp Sky was born.**

3. New ZKW Approaches

3.1 Other possible Solutions - large Crystals

Large glass crystals such as those in the BMW 7 are certainly the most sophisticated and visually appealing solutions of the highest quality. The next step for ZKW was to look for a solution that in principle takes over the requirements, but also implements this adequately for the lower vehicle classes. Glass crystals are in a class of their own when it comes to clarity and play of colour/sparkle. How can this behavior be pursued with cost-effective approaches? ZKW has now developed a process and material selection that allows crystals with similar behavior to be produced from plastic. The choice of material simplifies the integration here without fundamentally influencing the optical crystal and light-technical effect.

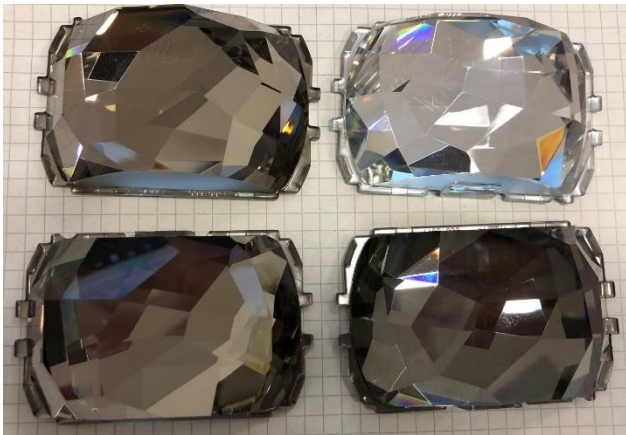


Figure 8: ZKW Crystals

The concept of the coated floor area has also been expanded. With a colored coating, the crystals can be used for a range of additional optical effects. A combination of different color effects can be taken to simulate ruby, emerald and sapphire as well.

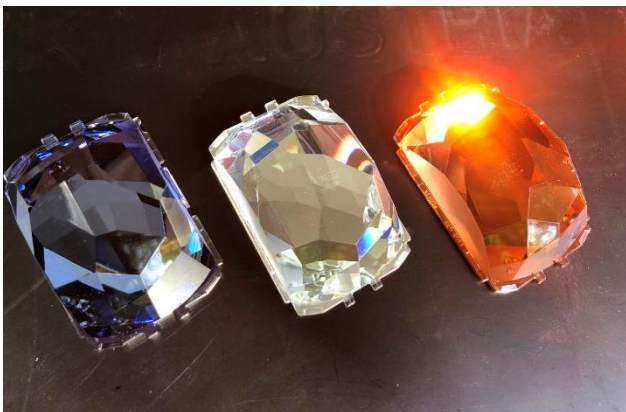


Figure 9: ZKW coloured Crystals

3.2. What comes after homogeneous Light Guides - Crystal Light Guides

Many years ago, the first DRL solutions and direction indicators based on LED technology started. By lining up the LEDs, many different contours for DRL and DI were implemented in many headlights. This was a big and successful step towards styling-oriented lighting functions. As the next technological step, the homogeneous contour was required. Today we try to increase this homogeneity and drive it to an optimum through ever newer technological approaches - but what comes next.

ZKW has developed a technology with which randomly or defined designed crystal-like structures can be integrated into a light guide. In addition, however, this light guide should also fulfill lighting functions such as DRL, POL and/or DI. We have now developed a process which puts these requirements into practice. A light guide with a crystal structure that can be used to implement signal light functions. This approach is also possible for rear lights.



Figure 10: ZKW Crystal-Lightguide

A very flexible solution that enables a new design language and can draw on proven technologies.



Figure 10: ZKW Crystal-Headlamp Concept

NOW
Crystal is the new Chrome!!!

4. References

- [1] BMW Marketing – BMW Homepage
<https://www.bmw.com/en/magazine/design/swarovski-crystal-headlights-in-BMW-i7.html>

Light Emphasized Sensor Integration – the Issue of Seeing and Being Seen

C. Buchberger¹, D. Baccarin¹, M. Gebauer¹, C. Frank¹, M. Licht¹, S. Döhler¹, M. Antonipieri¹

1: Marelli Automotive Lighting Reutlingen (Germany) GmbH
Tübinger Str. 123
72762 Reutlingen
Germany

Abstract: Advanced Driver Assistance Systems (ADAS) and autonomous vehicles (AD) rely on powerful sensors to “see” and connect with the surrounding environment. Camera, RADAR and LiDAR sensors are key enablers to future mobility – they work together to support all five levels of automated driving.

In a recent AD level 3 vehicle more than 20 sensors are used for driving assistance and with the rising numbers all possible mounting positions (e.g., front end, grill, windshield) must be considered. For all these sensors the positions must be optimized, and the challenge is to find the best location for every sensor to ensure optimized function and perfect styling.

When integrating the sensors into a modern vehicle car maker often try to hide the sensors as much as possible to maintain the well know styling. On the other hand, sensor integration into head lights, rear lamps and illuminated front grills raise new challenges which cause to brake with the common rules: the optimization of the cover, assembly, and all conditions for the sensor functions.

By integrating sensor functions into head light, rear lamps and grills the step to emphasize these functions with light is as obvious as challenging cause it brings new specifications and constraints.

Keywords: ADAS, Autonomous Driving, Sensor Integration, Light Animation, Front Lamp, Rear Lamp, Grill

1. Introduction

Autonomous Driving in an advanced, high ADAS level need a precise and detailed digital copy of the environment. Different kind of sensing systems are the enabler to bring more intelligence inside the vehicle and make driving smarter. LiDAR, RADAR, visual camera systems and ultrasonic devices are the most familiar key technologies to get closer to the autonomous driving level 5 vision and brings us closer

into the driving world of the future. After first technique demonstrators which shows a lot of sensors mounted on top of the roof and side of the vehicle there are a lot of arguments for a smarter and even more aesthetical integration [1,2].

If we look to the levels of autonomous driving, we find key technologies which empower to enter the next level and two things become obvious (Table 1):

- the number of sensors increases by a factor of 6. In fact, the Audi etron 2020 for examples is equipped with 20 sensors.
- to enter ADAS level 5 a 360° field of view is recommended [3,4,5]

ADAS LEVEL	DESCRIPTION	KEY ENABLER	NUMBER OF SENSORS
0	MOMENTARY DRIVING ASSISTANCE		
1	DRIVER ASSISTANCE	OBJECT DETECTION	6
2	ADDITIONAL AUTOMATION	OBJECT DETECTION	13
3	CONDITIONAL AUTOMATITION	HIGH RESOLUTION TARGET SEPARATION	24
4	HIGH AUTOMATION	3D DETECTION	38
5	FULL AUTOMATION	360° OBJECT RECOGNITION	35

Table 1: ADAS LEVELS and Key Features and Enabler

Beside a lot of challenges that occurs when facing sensor integration into a vehicle we will focus on the following on how to find a balance between sensor function, which will be the benefits and how we are able to support and emphasize sensor functions in combination with vehicle exterior lighting.

The Smart Corner Concept (Figure 1, 2) describes the idea to offer head lamp, rear lamps, centre high



Figure 1: Smart Corner Prototype - Head Light with integrated LiDAR Module

mounted stop lamps, grills and other lighting devices that already are prominent located in or on the edges of the car as a host for sensor functions and take synergies and advantages herewith.



Figure 2: Smart Corner Prototype - Rear Lamp with integrated RADAR Module

2. Sensor, Potential and Field of View

2.1 Field of View and the Benefit of Smart Corner Integration

As described in the introduction a blind spotless 360° field of view will be the key enabler of ADAS level 5. Anyhow – in case there will be no significant chances in vehicle exterior not a single mounting position will fulfil this request. Integrating sensors in the corners of a vehicle gives some advantages compared. The location in the corner brings for example a better view when approaching a crossing and an early detection of an obstacle otherwise covered by oncoming or preceding traffic. Other studies concluded that the time benefit for recognizing an obstacle is up to 1sec

which may be a distance of approximately 30 m where you are able to recognize objects earlier [6].

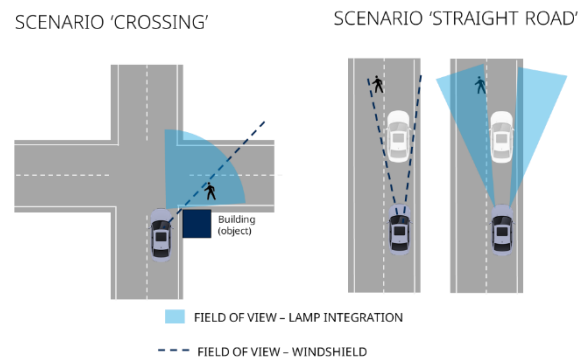


Figure 3: Schematic Bird Eye View : Head Light Mount vs. Windshield

Anyhow even if you place the sensors on the edges of the car you will not cover 360° field of view but blind spots on the side, front and rear of the vehicle will remain even if you push them to a minimum by using sensors with wide horizontal field of view angles (Figure 3). But with the Smart Corner location and the low mounting height of head lights and rear lamps especially the area close to the front and the rear of a vehicle, which is essential for level 5 slow motion movements e.g., for starting and parking, can be captured much better and with less sensors. But to say it totally clear: 360° field of view without excepting blind spots will not be feasible only with sensors mounted in the head light or rear lamps and other mounting places like vehicle grill must be considered.

For all types of sensors head light and rear lamp mounting bring some common advantages:

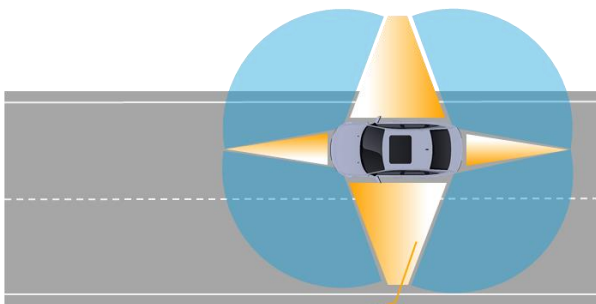
- environmental protection: vehicle lamps are known to last environmental conditions like sun, rain, snow, or other weather conditions and give a secure host for high end mechanical or electronical equipment mounted inside.
- cleaning system: head light cleaning systems are established on the head light market since the introduction of HID lamps and can s



Figure 4: FOV Rendering - Head Lights (left) vs. Roof Mount (right)

so guarantee a clear view for camera, LiDAR and/or RADAR systems

- heating system: can be integrated hidden into the outer lens like it was already done in some SAE head light projects
- wiring: up-to-date head lights are widely equipped with a high-speed data bus system like CAN or ethernet which may be re-used, and modern ECUs are available with system health monitoring, thermal control and other features known and used for LED light source functions



BLIND SPOT AREAS

Figure 2: Schematic illustration - Blind spots sensor integration in lamps

- levelling: head lights are pre-levelled and offer an active on-the-fly levelling that may be used for sensor adjustment or zero-km-positioning. Even dynamic scenarios with levelling when driving seems reasonable and

can be used for high beam like range boosting for sensors too.

- styling: head lights and rear lamps have the potential for aesthetical integration of sensors

By all the benefits we should not forget that head lights were enriched with a lot of new functionality generation to generation (Figure 3). When we look like an example to the head light of the Mercedes Class S 2006, it hosted low and high beam (LB, HB), Cornering Light (CL) and an infrared night view module (IR) covering 30% of the front area by function meanwhile 70% remained for styling. For the Mercedes Class S 2020 model the situation turned vice versa: low and high beam get assistance by a base light (Base) and a high beam booster (HB+) Pixel light (PXL), and DLP-Matrix functions are included. That brings a share of 70% functional to 30% styling area and with that the challenge of finding the mounting locations for sensors. The solution for finding the mounting space should and could not be to reduce the light functions. On the one hand side stylists will not accept a technical and only focused on function integration. But more important is that cameras are expected to get the lead in numbers of sensors required for ADAS as well as in turnover and most of the camera works within the visible spectrum and therefore, they rely on illuminated roads during the night [14]. Analysing the occupied space in a recent high end head light (Figure 3) we see that there is no space available and when we are looking at the trend in head light and rear lamp styling, we see that the visible outer lens area becomes smaller every year. So, one solution of these disaccord may be to take the space and areas freed by higher efficiency of the light sources and turn it into sensor space to enable a pleasant and high functional integration. In combination with other sensors, it will be soon

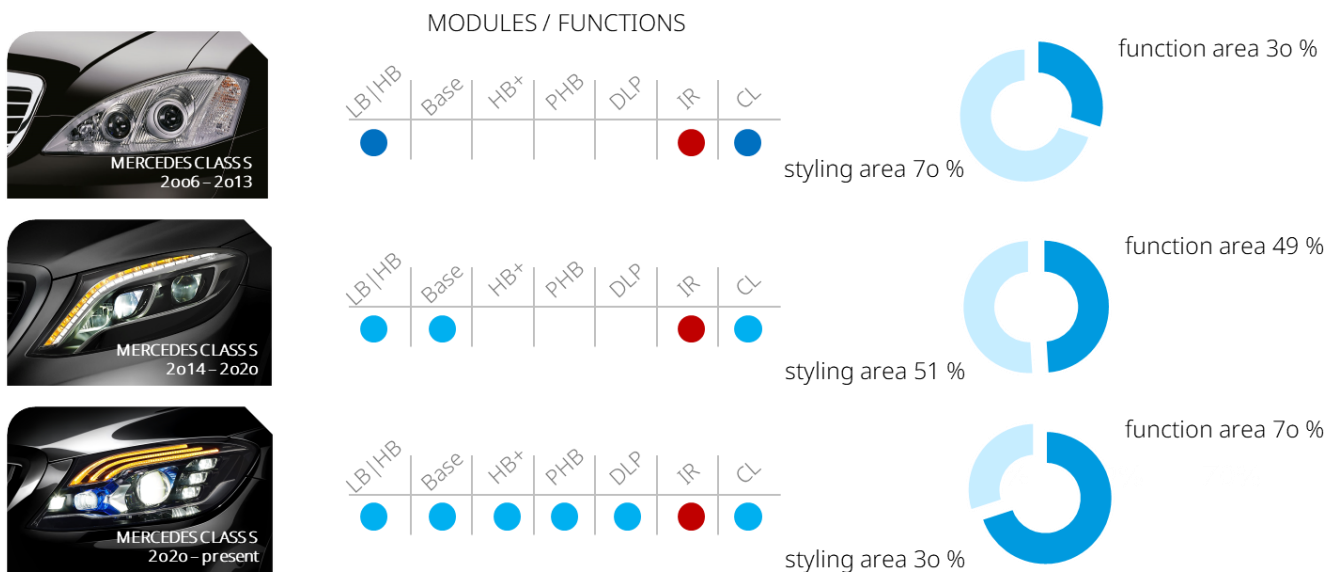


Figure 3: Change in Styling Area with Vehicle Generation

possible to take advantages for the sensor functions from vehicle's exterior lighting as well as vice versa [7].

2.2 Sensors, Sensor Potentials and Smart Corner Integration Constraints

2.2.1 Optical / visual Camera Systems

Cameras are also well known in automotive applications. The first applications are more related to comfort than to safety and found in the field of driving assistance. Step-by-step cameras are established for the use ADAS functions, and they had been the key enablers for functions like distance control, lane departure warning and more level 1 functions. The progress in the field of camera was so immense and fast that there is still a discussion if camera systems can support the whole autonomous driving functionality and will be sufficient for all functions as a stand-alone sensor system [8,9].

2.2.2 Ultrasonic Sensor

The most common sensor for the use in vehicles is ultrasonic sensors which are well known since decades and used for near distances (e.g., park sensors). Range and resolution are very limited and the sensor are not available at all driving speeds. Anyhow if RADAR or near field LiDAR systems starting to substitute these ultrasonic sensors step by step and a future without ultrasonic sensors which are nowadays mainly mounted in the bumpers seems possible. Due to these disadvantages the use of ultrasonic sensors for ADAS and Autonomous Driving is very limited.

2.2.3 RADAR

RADAR is also known since 1970 in the automotive world and in 1993 over one million RADAR systems had been sold only by BOSCH. With the development of the 3D RADAR systems and the so called 4D RADAR which enable additional object recognition

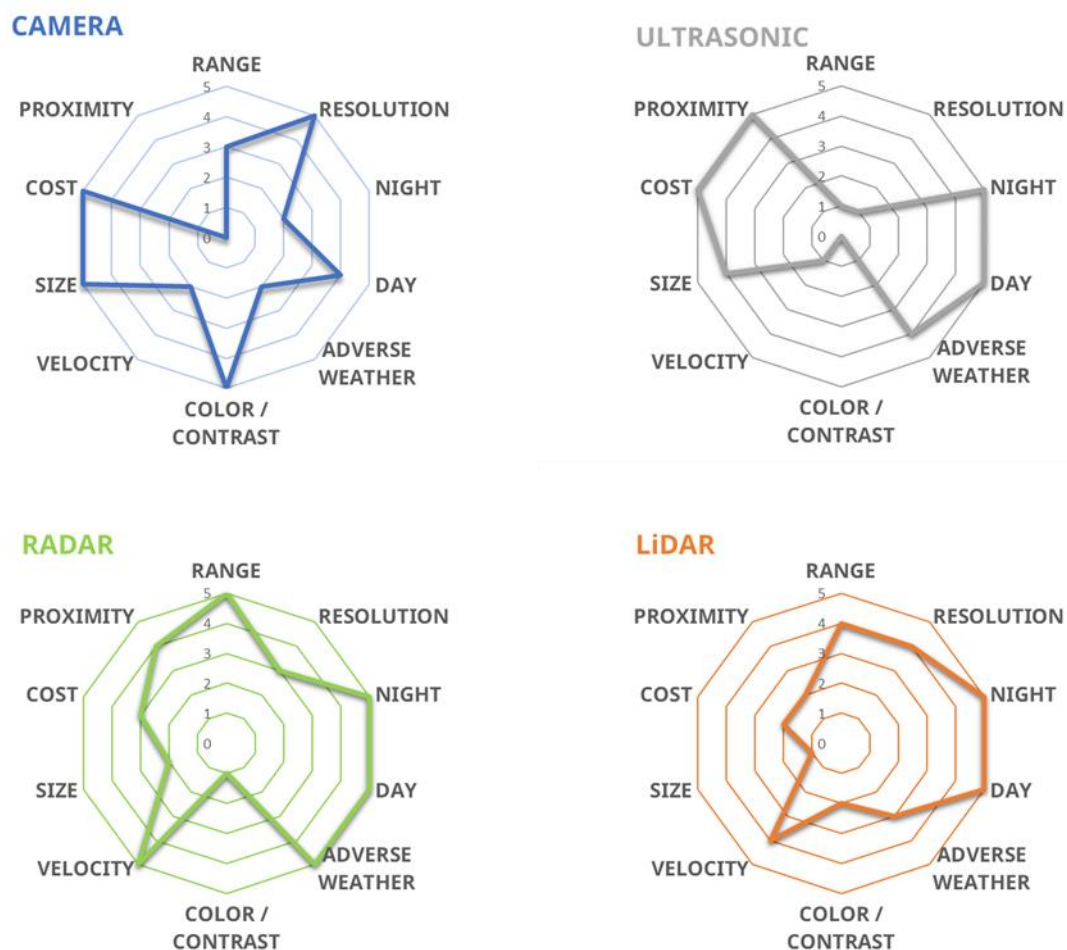


Figure 4: Sensor: Strength and Weakness

functionality there is still a progress in RADAR innovation. Acting in the range of microwaves RADAR is not visible for human eyes and do not interfere with lighting but object colour is not accessible and object size is not available in the resolution known from LiDAR and camera sensors.

another example, for a LiDAR the band path filter often used to block disturbing light can be placed in front of a LiDAR system with respect to the propagating waves. In the Smart Corner Concept an integration is made in an exterior part which was in the focus of the stylists for years and so a lot of constraints must be considered, and challenges must

SENSOR	HEAD LIGHT / REAR LAMP INTEGRATION	INTERACTION WITH LIGHT	LIGHT EMPHASIZING OPPORTUNITY
ULTRASONIC	DIFFERENT COVER NEEDED	NO INTERACTION	ONLY SURROUNDING
CAMERA	+	INTERFERE WITH VISIBLE LIGHT SOURCES / SHIELDING OR (ELECTRONIC) SHUTTER MANDATORY	WITH SHUTTER OR WHEN SYSTEM IS OFF
RADAR	+++	NO INTERACTION WITH VISIBLE LIGHT	IN ANY CASE
LIDAR	++	WAVELENGTH NEAR TO VISIBLE LIGHT / INTERFERENCE WITH SENSOR POSSIBLE	DETAIL INVESTIGATION ON OVERALL SYSETM

Table 2: Smart Corner Integration Constraints / Summary

2.2.4 LiDAR

LiDAR seems for a long term the most promising ADAS and Autonomous Driving sensor. Even if the potential is still high, the market penetration is low and behind former expectations [4]. Using infra-red light sources emitted rays will not be visible for humans and will not interfere with lighting.

2.3.5 Sensor Summary / Integration Strength and Challenges

When we focus on the Smart Corner Integration feasibility, ultrasonic sensors will not work fine behind a standard head light or rear lamp outer lens because they need a specific cover. Other sensor system which are using electro-magnetic waves are close to the lighting technology so that an integration behind the lens seems possible.

With the integration of sensors in head lights or rear lamps we face one essential change: as long the sensor is a dedicated stand-alone part, the housing can be designed to optimize the sensor function. This means for example for the RADAR that in a stand-alone part you will be able to design a radome as close to a sphere or a plane to minimize the interaction of the microwaves with the material. In

be solved.

In ADAS level 4 and higher also automated cleaning systems and heating for de-icing and defogging have to be considered.

In the following chapters we will focus on integration and illumination of RADAR sensors because the market penetration of RADAR is already high, the interaction and interferences with light functions is low and the overall system complexity is reasonable. Furthermore, the versatility of RADAR systems is high. All these make RADAR sensors to the most feasible sensor type for light emphasizing.

3. Illuminated Smart Corner RADAR Integration

3.1 RADAR Sensor Integration Essentials

New issues rise when integrating RADAR sensors in head lights and rear lamps. Among them the most important are [10,11]:

- all materials in the ray path must be as high as possible RADAR transparent to avoid absorption ($\tan \delta$) – so e.g., metal flares or graphite filled materials are not feasible

- air gaps or any other high delta jumps in permittivity should be avoided
- with respect to the RADAR wavelength inside the material thickness should be $\lambda/2$ to avoid reflection and interference.

Beside these RADAR transparency essentials, the targets for an illuminated radome are:

- the radome outer surface must resist all environmental impacts
- cleaning system (not integrated) must be available; the surface must resist cleaning solvents (at least for ADAS level 4 and above)
- heating system for de-icing / defogging should be available (at least for ADAS level 4 and above)
- the radome should be illuminated at least with a single colour light source
- coloured styling elements should be visible in in day and night styling

In order to add all these functionalities to the radome we follow a stacking layer approach: each functional layer like cover, heating, lighting, and styling is placed in a dedicated layer (Figure 5).

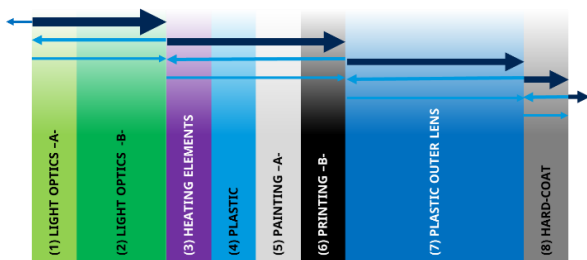


Figure 6: Illuminated Radome: Functional Layers and Main Ray Concept Illustration

In the first approach the stacking layers follow the function only. Once the layers and their function are defined it is necessary to proof the overall concept in terms of RADAR compatibility. Within the development progress first all suggested materials are checked for their RADAR properties to determinate any incompatible material. Base of these material check is a growing material database with permittivity and tan loss (RADAR frequencies 24 GHz and 76 – 80 GHz) results for nearly 100 common automotive head light and rear lamp materials. Bottom-up on this development a first optimize structure is proposed with adapted thickness based on the RADAR according to the RADAR wavelength inside the layer. After that the interference and reflectivity of each layer was checked followed by an over-all system main ray calculation. At the end of the workflow a total loss analysis was made. Once all

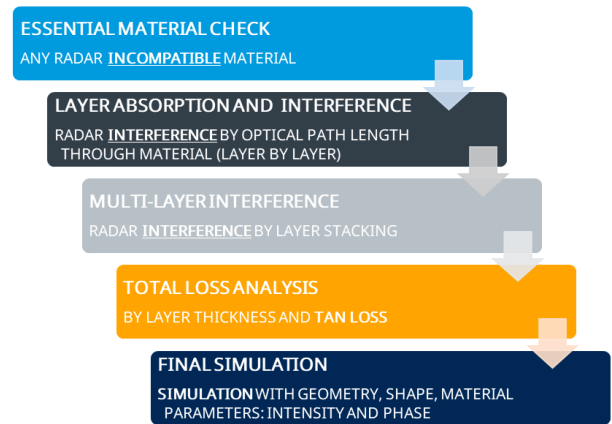


Figure 5: RADAR Transparency Check (schematic workflow)

optimizations from workflow step 1 to 4 are considered in the development, a final finite element simulation of the total head light, rear lamp, or grill geometry is used to proof the system and simulate parameters like overall transmission, interference, reflectivity, and phase shift of the Smart Corner integrated RADAR system (Figure 6: RADAR Transparency Check (schematic workflow)Figure 6).

3.2 RADAR Transmission Simulation

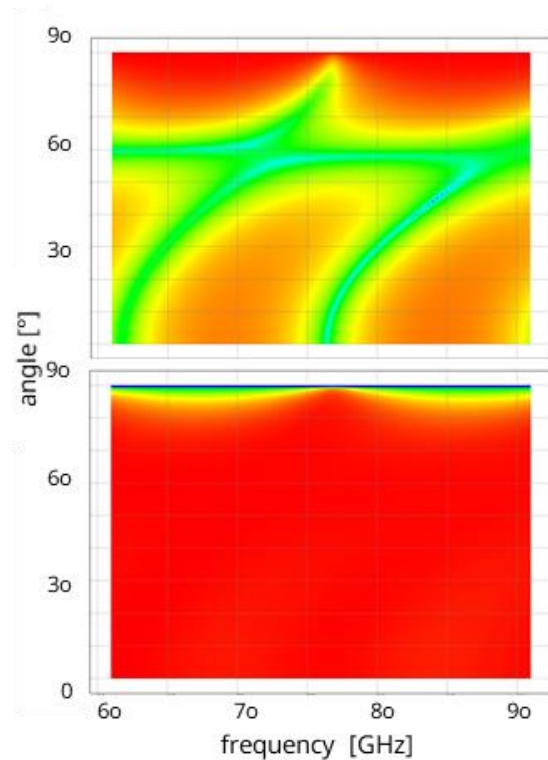


Figure 7: RADAR Transmission Simulation of a Stacking Layer Assembly: Transmission 77 GHz (left) and Reflection 77 GHz (right)

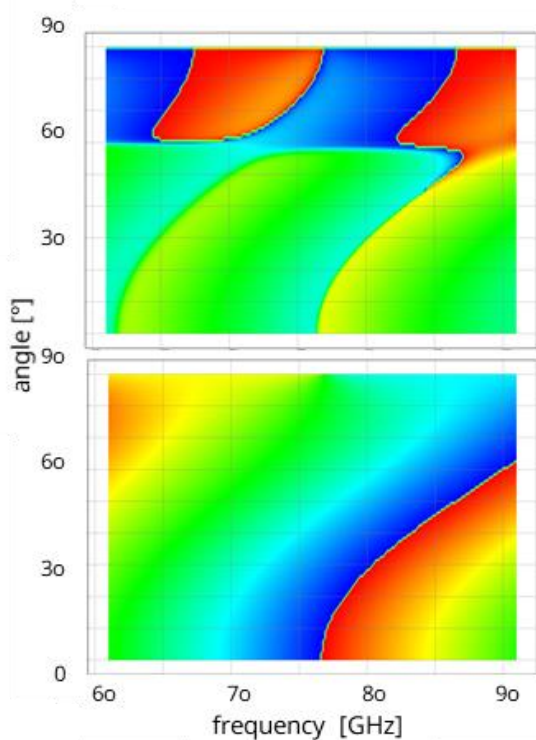


Figure 8: RADAR Transmission Simulation of a Stacking Layer Assembly: RADAR Phase Shift

The RADAR transmission simulation is the final step in the development before entering a prototype phase. With the tools of finite elements method first the stacking layer of the functional RADAR sensor assembly is simulated in terms of transmission, reflectivity, and phase shift (Figure 7, Figure 8).

This is essential to proof the layers and interfaces with all functional groups including lighting, heating, styling and protection parts. Also, thin layers for a metallic look like indium or silicone layers and lacquers (e.g., hard coats) must be include in these simulations. In case the results let expect an overall one-way attenuation of -1dB or lower the total system simulation finalize the RADAR transparency check.

The simulation of the RADAR transparency is the one of the first essential step to see if the layers and interfaces with all included functional groups like lighting, heating, and styling fulfil the specification and the expected RADAR attenuation is -1dB or better..

3.3 Radome Heating and Cleaning

Thinking of ADAS level 4 and above sensor cleaning and heating will be mandatory. Embedded wires in the outer lens ensure that the transmission and receiving areas are free of ice and snow under driving conditions. Simulation, experiments, and prototype measurements complete the development process.

Beside the manufacturing technology one of the challenges is to find the right balance between de-icing time, maximum temperature, and power consumption. Even if the simulation must be redone for every development status 0.3 W / cm^2 is a reasonable value for performing the de-icing process in approximately 3 min which are common specification parameters

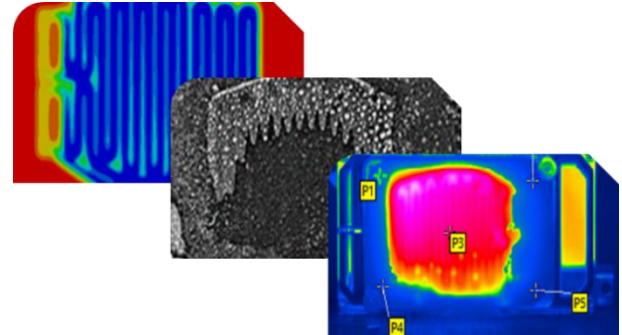


Figure 9: Heating Development Workflow: Simulation - Experiment - Measurement

3.4 Radome Illumination

With the light layers, it is possible give the radome an unique night styling. One or more functional lighting layers enlighten the radome mainly based on back illuminated light guide technology (Figure 10, Figure 11). The example shows a prototype development with to different stylings – one which with a homogenous area lighting, the other with a light outline styling.



Figure 10: Radome Illumination - Visualisation and Luminance Simulation for a Prototype



Figure 8: Radome Illumination - Visualisation Holographic 3D Effect

These stacking layer technology allows to illuminate the complete outer surface of the sensor especially the RADAR transmission surface. By stacking and shaping the lighting layers holographic 3D effects are reachable to emphasize the integrated sensors even more.

These stacking layer technology allows to illuminate the complete outer surface of the sensor especially the RADAR transmission surface. By stacking and shaping the lighting layers holographic 3D effects are reachable to emphasize the integrated sensors even more.

4. Summary

The Smart Corner Concept offers headlights, rear lamps, and vehicles' front end as a host for sensors needed for ADAS and Autonomous Driving. Camera, LiDAR and especially RADAR sensors may be integrated into an existing product with small impact on the styling. The integration offers new opportunities for the lighting technology but also come along with new challenges. Throughout past all component of a sensor follow its function since all parts of the sensors were hidden. Smart Corner integration allows to use or reuse environmental protection, cleaning and heating systems and wiring of the hosting part. Furthermore, the prominent position offers a different field of view which helps to complete a 360° - field – of - scenario.

The combination of sensor and automotive lighting functions open the field of sensor illumination and enlarge this field from a framing edge illumination to a 100% cover illumination with aesthetical styling integration. Stacking layer technology similar to light curtain light guide technology has the potential to generate illuminated holographic 3D lighting.

5. Conclusion

The process of turning driving into Autonomous Driving force to integrate more and more sensors into a

vehicle. In order to reach 360° field of view which will become essential for ADAS level 4 and above, more sensor mounting position must be considered. The Smart Corner Concept offers a lot of advantages by integrating sensors into new developments of head lights, rear lamps, and front ends. The combination with light emphasizes the sensors and allows a unique styling while driving by day or night.

6. Acknowledgement

Benjamin Allain, Fillion Vincent and Enguerrand, Quilliard

MARELLI AUTOMOTIVE LIGHTING
17 CHEMIN DES PRÉS
38240 MEYLAN, FRANCE

Sebastian Döhler, Johannes Brill, Uwe Schubert, and Christian Frank
MARELLI AUTOMOTIVE LIGHTING REUTLINGEN
(GERMANY) GMBH
TÜBINGER STR. 123
72762 REUTLINGEN
GERMANY

7. References

- [1] Bosch and Mercedes-Benz start San José pilot project for automated ride-hailing service. BOSCH (retrieved 2022-08-19).
- [2] We're building the World's Most Experienced Driver. Waymo, (retrieved 2022-08-19).
- [3] NHTSA. (retrieved 2022-08-19). *The Road to Full Automation*.
- [4] Yole Development. (2019). *Imaging for Automotive report*.
- [5] ST. (2019, 09 12). *Automotive ADAS Systems*. Retrieved from ST Developers Conference.
- [6] Davies, Dan (North American Lighting). (2020). *Improving Visibility by Integrating Sensors into Headlamps*. we.connect.US automotive.
- [7] i-MicroNEWS. (2020). *Automotive Lighting industry: positioning for ADAS*.
- [8] Elon Musk on Cameras vs. LiDAR for SELF Driving and Autonomous Cars. (2019, 04 27). <https://youtu.be/HM23sjhtk4Q>.
- [9] Morris, J. (2022, 06 11). Is Tesla Backtracking On Its Camera-Only Autopilot Strategy. www.forbes.com.
- [10] Emilsson, E. P. (2017). *RADAR Transparency and Paint Compatibility*. CHALMERS UNIVERSITY OF TECHNOLOGY.
- [11] Pfeiffer, F. (2009). *Analyse und Optimierung von Radomen*. Technischen Universität München.

- [12] Rohde & Schwarz. (2018, 10). *White Paper Automotive radar technology, market and test requirements.*
- [13] Woodside Capital Partners. (2016, 09). *Beyond The Headlights: ADAS and Autonomous Sensing.*
- [14] Yano Research Institute. (2020). No. 2574: *Global ADAS/Autonomous Driving System Sensor Market.*



LIGHTING EVERYWHERE

SMARTER, SAFER, GREENER and APPEALING
lighting systems to the whole mobility world.

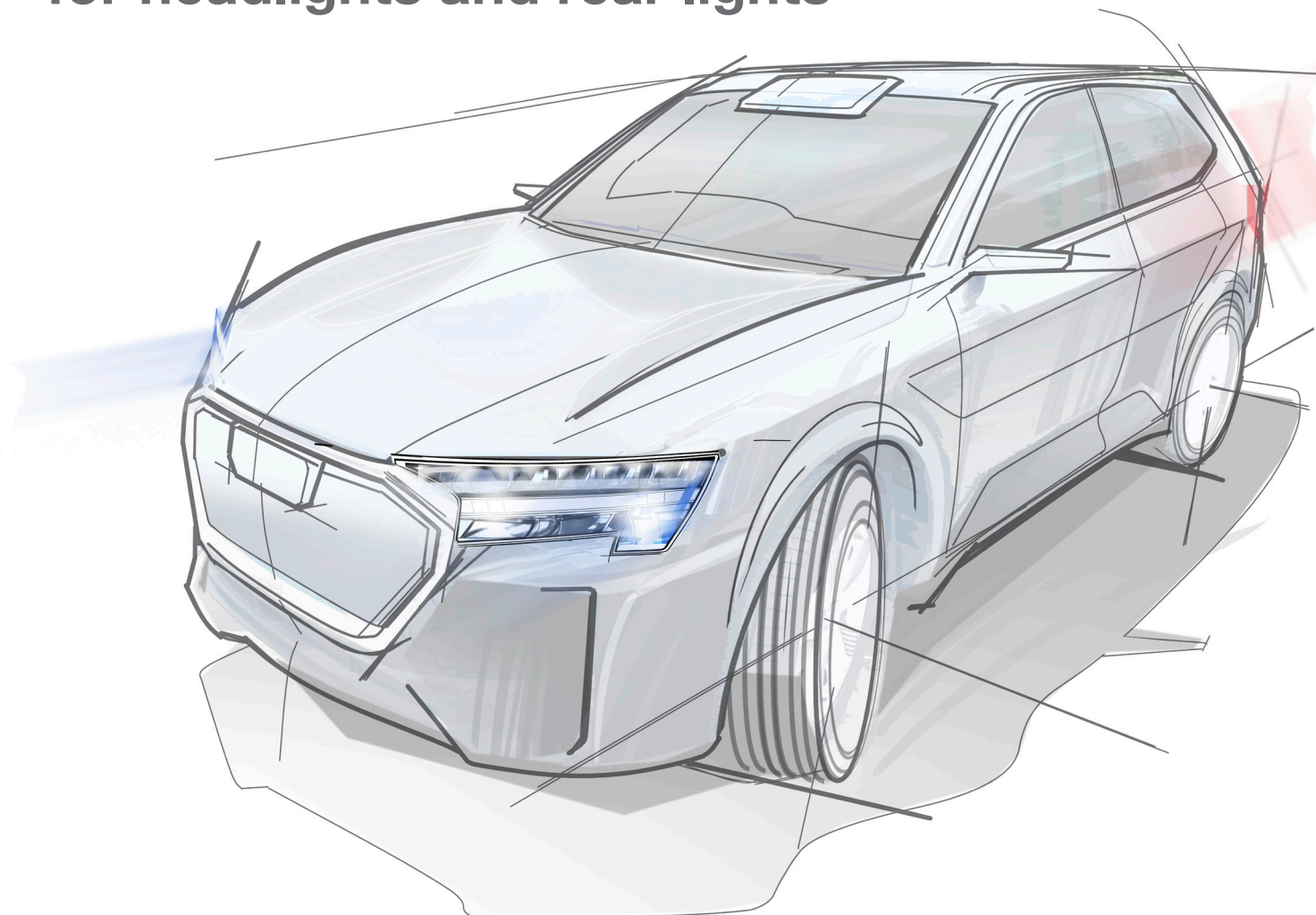
Visit our website www.valeo.com
to discover our latest innovations



SMART TECHNOLOGY FOR SMARTER MOBILITY

IMPROVED SENSOR PERFORMANCE

Engineered joining solutions for headlights and rear lights



Joining – Fastening – Adjusting

Adaptive and intelligent vehicle lighting will fundamentally change the driving experience in the future. Besides improving safety, the design plays a decisive role. The vehicle lighting increasingly merges with the exterior therefore creating ever higher requirements for the joining technology. All influences and parameters must be taken into consideration for the choice of the proper joining solution.

For decades, we have been a partner to the automotive industry offering special solutions to fasten lighting elements in vehicles.

Be inspired by our 360° joining technology for lighting applications.

Tel. +49 521 44 82-1387
fat@boellhoff.com
www.boellhoff.com

BÖLLHOFF

Detection of the road lighting using a conventional camera system

S. Vogel¹, G. Maar^{1,2}, M. Niedling^{1,3}, S. Völker³

1: HELLA GmbH & Co. KGaA, Rixbecker Str. 75, 59552 Lippstadt, Germany

2: Leibniz University Hannover, Welfengarten 1, 30167 Hannover, Germany

3: Technical University of Berlin, Straße des 17. Juni 135, 10623 Berlin, Germany

Abstract: Modern high-resolution headlamp systems can adjust to different driving situations. However, the existing road lighting situation is not yet taken into account in the headlamp's light distribution when illuminating the road. This is also due to a lack of information about the present road lighting in the car. Here a camera system for the detection of the current road lighting class while driving based on a luminance measurement with a conventional RGB camera system is presented.

After the spectral sensitivity of each color channel was measured, this data was used to fit the sensor characteristics to the luminous efficiency function of human visual perception. This could be done with a f1' mismatch index of 21%. The RGB camera system was then calibrated using a calibrated luminance measuring video photometer. The resulting pixel values were compared with different measured luminances to create lookup tables for different camera settings.

The new sensor was able to determine the average luminance ahead of the car with a mean relative deviation of 5.7% for several static measurements and of 19% for a dynamic measurement.

Next steps include further improvement of the dynamic measurement and the investigation of additional scenes with varying road lighting settings. This system would allow not only for the use in headlamp applications but also for big data road lighting analysis.

Keywords: Road lighting, luminance measurement, adaptive headlamp, energy efficiency, town light

1. Introduction

The main goal of automotive lighting is preventing traffic collisions and establishing a high safety environment for all road users. One key contribution to this is a high detectability of obstacles and hazards by the driver, which can be improved by changing the photometric conditions.[1,2]

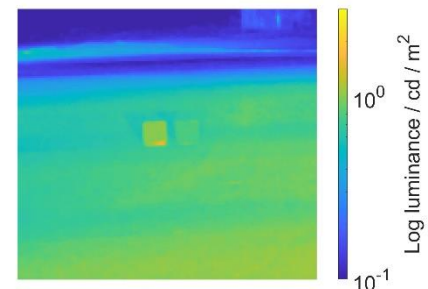
Modern automotive headlamp systems are capable of adapting to different environments. However, the present road lighting conditions are not yet considered.

Previous research has shown that an adaptation to the road lighting settings results in better visibility of objects.[3]

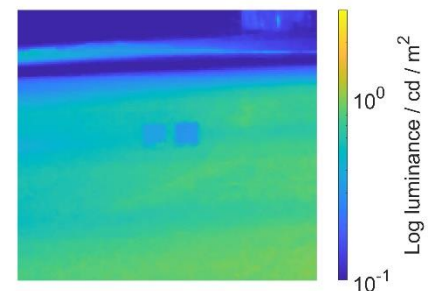
Reducing the illumination of the road by the headlamp creates more easily detectable negative contrasts [4,5], while the additional light of the headlamp actually decreases this contrast possibly rendering the target invisible.

Consequently, less light results not only in better energy efficiency, but also in greater road safety under certain conditions.

An example for this interaction of headlamp and road lighting is shown in Figure 1.



(a) Headlamp turned **on**.



(b) Headlamp turned **off**.

Figure 1: Example luminance measurement of (a) a positive contrast created by the headlamp and (b) the better visible negative contrast created by the road lighting of two targets with a reflectance of 30% (left) and 20% (right) in 60 m distance under M3 road lighting conditions.[3]

However, in order for the headlamp to adapt to the road lighting, it must be classified first.

Here an approach using a conventional camera system is presented. The system was used to measure the luminance created by the present road lighting on the road surface. This road surface luminance is one of the key photometric

characteristics used to classify road lighting according to DIN EN 13201.[6] For the most common road lighting classes it varies between 0.3 cd/m² and 2 cd/m².

2. Characterization of the camera system

The camera system used was a VCXU-23C of Baumer Optronic GmbH. The sensor was a 1/1.2" CMOS Sony IMX174 with 2.3 megapixel and a RGGB bayer filter. Exposure times could be varied between 28 µs and 60 s.

The system was characterized with special regard to its spectral sensitivity and the vignetting as described in the following.

2.1 Spectral sensitivity

In order to measure the photometric luminance of a surface the sensitivity of the measuring system must match the luminous efficiency function, which describes the spectral sensitivity of human visual perception of light shown in Figure 2.

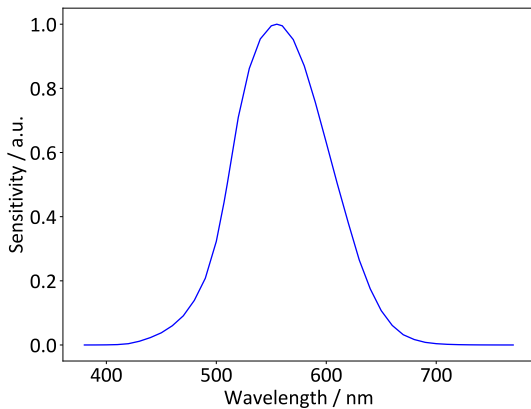


Figure 2: Photopic luminous efficiency function according to Williamson and Cummins. [7]

To characterize the mismatch between this sensitivity and the sensitivity of the camera system the $f1'$ mismatch index is used.[8] It is defined as:

$$f1' = \frac{\int |s_{rel}(\lambda)^* - V(\lambda)| d\lambda}{\int V(\lambda) d\lambda} \quad [1]$$

with

$$s_{rel}(\lambda)^* = s_{rel}(\lambda) \frac{\int S_A(\lambda) \cdot V(\lambda) d\lambda}{\int S_A(\lambda) \cdot s_{rel}(\lambda) d\lambda} \quad [2]$$

$S_A(\lambda)$ is the spectral distribution of CIE illuminant A, $s_{rel}(\lambda)$ is the relative spectral power distribution of the detector, in this case the camera system. Before trying to minimize this mismatch index $f1'$, the spectral sensitivity of each color channel of the camera needs to be characterized. This was done

using a OL490 tunable light source by Gooch & Housego PLC with a bandwidth of 5 nm. The light source emitted light of different wavelengths into an OL IS-3900 integrating sphere by Gooch & Housego PLC, which was then measured by a OL 770 spectroradiometer by Gooch & Housego PLC to determine the spectral radiant power of the light source. Subsequently, the camera system under test measured the emitted light. Its response was corrected by the spectral radiant power of the light source to determine the sensitivity of the camera system and its color channels. The results are shown in Figure 3.

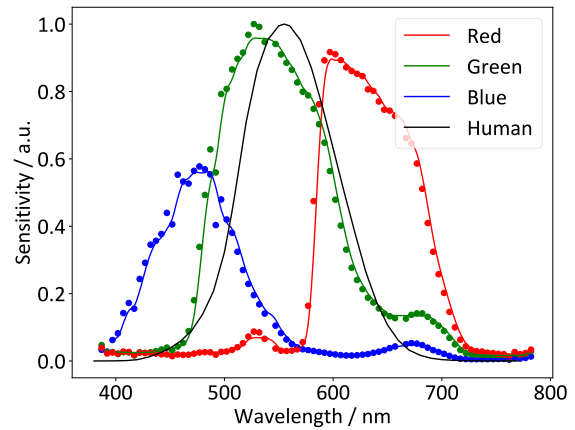


Figure 3: Measured spectral sensitivities of the color channels of the VCXU-23C camera system and the photopic luminous efficiency function of the human observer [7] as a comparison.

The sensitivities of the channels behave differently as expected with different peak sensitivities according to their “color”. However, the spectral sensitivity of human visual perception of light is not matching any of these channel sensitivities. Therefore, the measurement system required a specific adjustment as discussed in Section 3.1.

2.2 Vignetting

Vignetting describes the reduction of signal between the peripheral part of the image and its center. It is caused among others by lens limitations and the law of \cos^4 but can be corrected by postprocessing.

For that, the vignetting of the camera system had to be determined. This was done using an OL IS-3900 integrating sphere. In the sphere, a halogen lamp emitted light. This light was homogenized by several reflections inside the sphere. Before passing the detector feedthrough it was additionally diffused. The camera system was positioned directly behind the feedthrough. Intensity varied over the different pixels as expected. The measured signal of a single row including each color channel is shown in Figure 4.

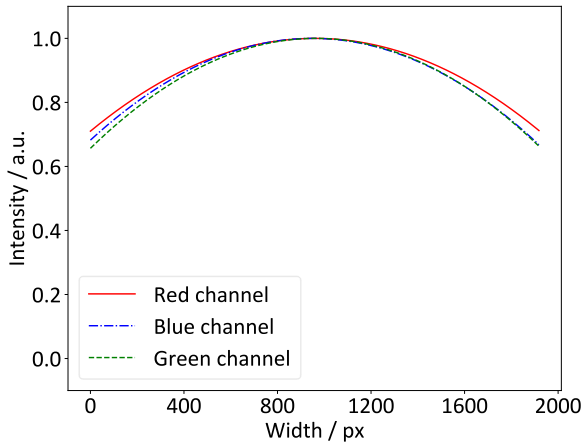


Figure 4: Vignetting of a single pixel row analyzed for each color channel, distinctive decrease to the edges is visible.

The decreasing intensity for pixels closer to the edge is clearly visible. There was also a slight variation for each channel. As a consequence, for each pixel a correction term was determined, which was then later applied to correct the measured signal.

3. Calibration of the camera system

The next step in the development of the system was its calibration to measure luminance values. This consisted of two steps: First, the adjustment of the spectral sensitivity to luminous efficiency function, such that pixel values of the system were proportional to the given luminance. Second, the allocation of pixel values to corresponding luminance values. This was done for different camera exposure times as well as specific gain settings.

3.1 Adjustment of the spectral sensitivity

In order to match the spectral sensitivity of the camera system with the spectral sensitivity of a human observer, the $f1'$ mismatch index introduced in Equation [1] had to be minimized.

For that a polynomial approach was chosen. It combined the different sensitivities of the channels to achieve the desired spectral sensitivity. This resulted in the formula:

$$s(\lambda) = 0.14 \cdot s_R(\lambda)^3 + 0.27 \cdot s_G(\lambda)^3 + 0.71 \cdot s_R(\lambda)^2 + 0.67 \cdot s_R(\lambda) \cdot s_G(\lambda) \quad [3]$$

with $s_R(\lambda)$ being the sensitivity of the red channel and $s_G(\lambda)$ being the sensitivity of the green channel. The resulting adjusted sensitivity function is shown in Figure 5.

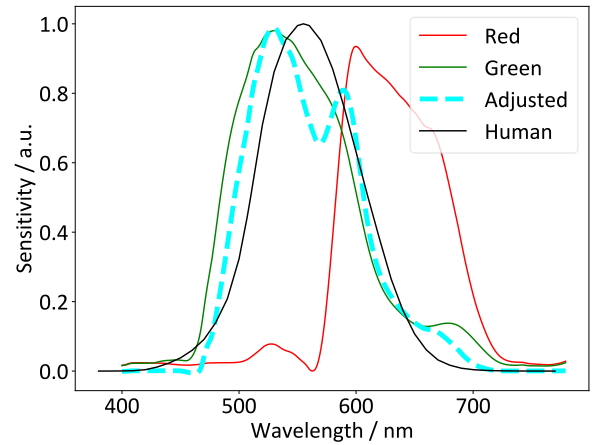


Figure 5: Adjusted sensitivity of the camera system to minimize the $f1'$ mismatch index based on a polynomial combination of red and green channel in comparison with the photopic luminous efficiency function.

In the adjustment only the red and the green channel were used. This was due to the fact, that the blue channel had the highest offset from the photopic luminous efficiency function. As a result, adding components of the blue channel did not result in any improvement of the $f1'$ mismatch. Neither did increasing the degree of the polynomial fit.

As a result, a $f1'$ mismatch index of 21% could be realized. This value was higher than the one of specifically developed luminance meters (typically below 5%) but should be sufficient for the intended application. The maximum difference between the sensitivity of the adjusted system and the photopic luminous efficiency was 26% at a wavelength of 569 nm. This had to be considered when measuring specific luminances in the field.

3.2 Determination of luminance levels for different pixel values

The next step was to investigate the relationship between the measured pixel values (determined using the adjusted sensitivity) and the actual luminance. For this purpose, a PA500A projector by NECDIS GmbH illuminated a screen. The resulting luminance was measured by a LMK 5 color video photometer with a relative expanded measurement uncertainty of 4.7%. The camera system under test was positioned right next to the video photometer to minimize the influence of different observation angles to the screen surface. Different luminances were then allocated to the pixel values determined using:

$$N = 0.14 \cdot N_R^3 + 0.27 \cdot N_G^3 + 0.71 \cdot N_R^2 + 0.67 \cdot N_R \cdot N_G \quad [4]$$

with N_R and N_G being sample values of the red and green channel.

The measurement was repeated for different exposure times and different gain settings. An example for 4 different exposure times between 30 ms and 70 ms for a gain of 12 dB is shown in Figure 6 and an additional example for 5 different gains between 6 dB and 18 dB and an exposure time of 30 ms is shown in Figure 7.

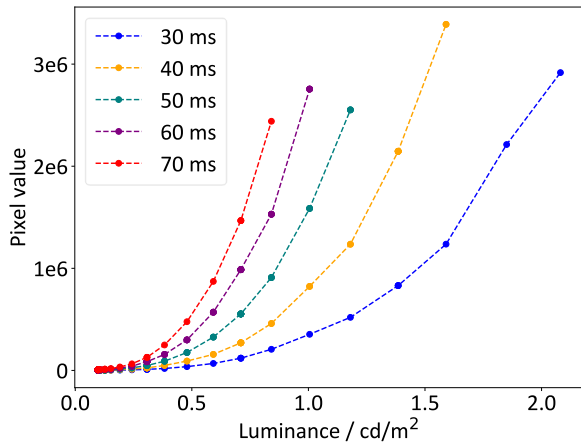


Figure 6: Relationship between pixel values and luminance for different exposure times between 30 ms and 70 ms and a gain of 12 dB, dashed lines for orientation.

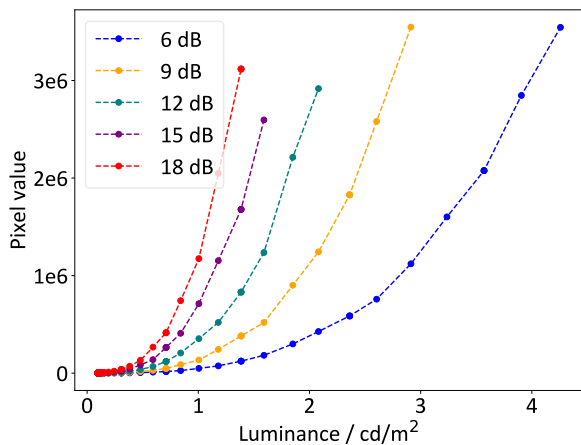


Figure 7: Relationship between pixel values and luminance for different gains between 6 dB and 18 dB and an exposure time of 30 ms, dashed lines for orientation.

The exposure time as well as the gain had an influence on the range of luminance values that can be identified with different pixel values. Higher exposure times made the system more sensitive for lower luminance values but on contrary overexposure was reached for lower luminances as well.

The gain has a comparable influence. Low gain values enable the resolution of higher luminances without the risk of overexposure. However, the slope became less steep for lower values. Thus, the distinguishability of close luminance values would have been limited.

The choice of exposure time and gain depends on the application. In the following measurements an exposure time of 30 ms and a gain of 12 dB was chosen in order to cover the full range of luminance values between 0 cd/m² and 2 cd/m², which were relevant for identifying the road lighting class.

4. Validation in the field

The validation in the field consisted of measurements in a static and in a dynamic situation. In the static situation the influence of light sources with different spectra as well as the capability to measure real road lighting scenes was examined. In the dynamic situation, a special focus was put on challenges in a real traffic scenario. For all following measurements, the camera system was positioned behind the windshield of a test car as shown in Figure 8.

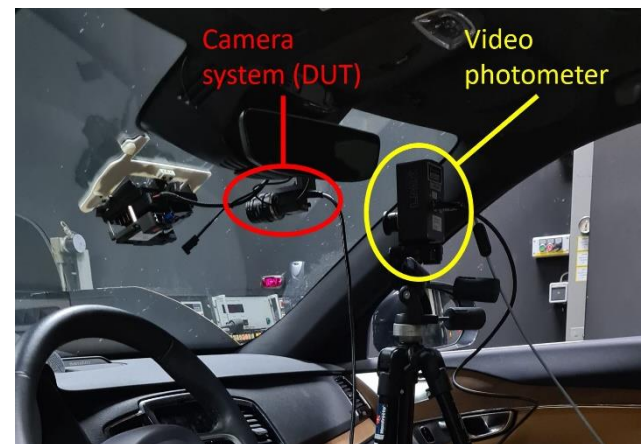


Figure 8: Camera system under test and video photometer LMK 5 Color positioned behind the windshield of a test car very close to each other.

4.1 Influence of different light sources

The influence of the spectra of different light sources was tested in the light channel facility of HELLA GmbH & Co. KGaA in Lippstadt. Several square targets were positioned ahead of the car in slightly different distances and positions. They were illuminated with four different headlamp systems: a halogen headlamp, a xenon headlamp and two different LED headlamps. The resulting luminances were measured with the camera under test - using the previously described relationship between pixel value and luminance - and the video photometer LMK 5 Color. The results were then compared, and a deviation could be estimated.

Additionally, the f1 error of the measurement and a Spectral Mismatch Correction Factor (SMCF, [9]) were calculated according to

$$f1 = \frac{\int S_Z(\lambda) \cdot s_{rel}(\lambda) d\lambda}{\int S_Z(\lambda) \cdot V(\lambda) d\lambda} - 1 \quad [5]$$

and

$$SMCF = \frac{\int S_A(\lambda) \cdot s_{rel}(\lambda) d\lambda}{\int S_A(\lambda) \cdot V(\lambda) d\lambda} \bigg/ \frac{\int S_Z(\lambda) \cdot s_{rel}(\lambda) d\lambda}{\int S_Z(\lambda) \cdot V(\lambda) d\lambda} \quad [6]$$

with $S_Z(\lambda)$ being the relative spectral power distribution of the used light source. The SMCF was used to correct the measured luminances by the camera under test. The luminances were determined for 8 different targets with different reflectances calculating the average relative error. The results are shown in Table 1.

Head-lamp	Error / %	f1 error	SMCF	Correct. err. / %
Halogen	4.4±1.6	-0.031	1.002	4.4±1.8
Xenon	5.8±3.0	-0.050	1.051	3.1±2.0
LED 1	12.0±1.6	-0.055	1.057	7.5±2.2
LED 2	12.1±2.8	-0.055	1.057	7.1±3.1

Table 1: Average relative errors of the luminance measurement with the camera system under test over 8 different targets, 4 different headlamps were tested, in each case the f1 error was determined as well as a SMCF, which was then used to calculate a corrected average relative error.

The results showed that different light sources with different spectra needed different corrections and resulted in varying relative errors. However, the maximum average error did not exceed 10 %. Even in the cases without a correction the average relative error did not exceed 15 %. The comparably large error when measuring the LED light sources can be explained by the non-perfect spectral match of the camera's sensitivity. The LED's spectral peak around 560 nm created by the phosphor layer is not well matched by the camera's spectral sensitivity.

4.2 Road lighting classification in a static scenario

The key challenge of the camera system was the identification of different road lighting settings. For this purpose, three different real scenarios around Lippstadt, Germany were investigated. In each scenario the luminance in a reference area was measured with the camera system under test and the video photometer LMK 5 Color. The reference area was chosen according to the DIN EN 13201-2. [6] It started 60 m ahead of the car and had a length equal to the distances between two road luminaires.

The width equaled the width of the road. The three different scenarios and the corresponding evaluation areas are shown in Figure 9.

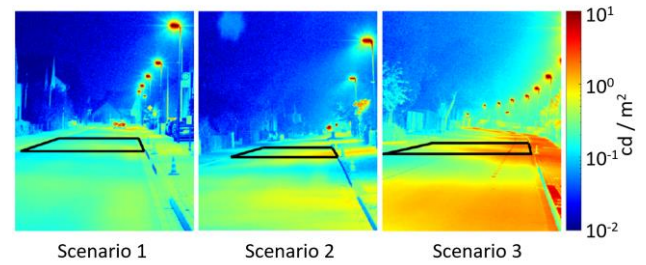


Figure 9: Luminance measurement of three different real road lighting scenarios around Lippstadt, Germany; evaluation area in the black square.

The measurement setup was the same as in Figure 8. The test car was not moving to prevent any motion blur of the camera systems and to have a fixed evaluation area. Three different cases were differentiated: the headlamp was turned off ("OFF"), only the prefield module of the headlamp was turned on ("PF") and a typical low beam light function was turned on ("LB"). The measured results are shown in Table 2.

Scenario	Light function	L _{LMK} / cd/m²	L _{DUT} / cd/m²	ΔL / cd/m²
1	OFF	0.25	0.22	0.03
	PF	0.25	0.23	0.02
	LB	0.29	0.26	0.03
2	OFF	0.33	0.34	0.01
	PF	0.36	0.34	0.02
	LB	0.41	0.42	0.01
3	OFF	1.13	1.16	0.03
	PF	1.14	1.19	0.05
	LB	1.18	1.21	0.03

Table 2: Measured average luminance in an evaluation area for three different scenarios and three different light functions by a LMK 5 Color video photometer (L_{LMK}) and by the camera system under test (L_{DUT}) including the absolute difference between both luminance values (ΔL).

The results showed only slight deviations between the measured luminance values by both systems. The maximum absolute error equaled 0.05 cd/m² or 12 %. Overall, the average relative error could be estimated to be (5.7 ± 3.4) %. Changing the light function did not have a measurable influence on the precision of the measurement. Additionally, the absolute error did not increase with higher

luminances on the road surface. An absolute error of 0.05 cd/m² was not exceeded.

4.3 Classification of a road lighting scenario while driving and its challenges

Previous measurements were done in a static setting, the next step of functionality was the testing of the system while driving.

The test car was driving along a straight road corresponding to scenario 3 from Table 2. 50 different measurements were done with an exposure time of 30 ms and a gain of 15 dB. For each measurement the evaluation area was defined in order to calculate an average road surface luminance. The average measurement error in this case was 19 %. This was primarily influenced by the manual choice of the evaluation area but can also be explained by motion blur due to the non-zero exposure time.

Additionally, different problems arise in a dynamic setting, which could be neglected during the static environment, and which were best possibly avoided during the previous measurement:

1. During acceleration and braking the tilt of the car is changing. As a result, the camera pixels corresponding to the evaluation area are not constant. Image processing algorithms are required to identify the new evaluation area in the picture and to determine its average luminance.
2. Different courses of the road also have an influence on the measurement process. With a turn in the road the evaluation area shifts to the left or to the right. In these cases, additional image processing is required as well.
3. Other traffic participants might be within the evaluation area and therefore alternate its luminance. This is even more severe when these traffic participants illuminate the road as well. Then, the road lighting class can be wrongly determined.

In order to successfully implement a camera system for road lighting classification, these challenges need to be addressed.

5. Conclusion and outlook

5.1 Conclusion

Adapting the headlamp's light distribution to the present road lighting is beneficial. However, information about the road lighting is required to do that.

It was shown that a conventional camera system is able to classify a road lighting setting according to DIN 13201-2 by measuring the average road surface

luminance in a specific evaluation area. The mean relative error in three different road lighting scenarios could be estimated to be 5.7 %. Different light sources of headlamps or road luminaires did not change that. Neither did the use of various headlamp functions.

This error would be sufficient for the classification because the luminance requirements of different road lighting class are separated by orders of 0.1 cd/m².

However, the functionality in a dynamic situation with other traffic participants, more complicated courses of the road and the vehicle's dynamics are challenging.

5.2 Outlook

While general functionality and proof of concept could be shown, additional features are needed.

Further image processing is required to individually determine the evaluation area, discard non-relevant objects in the area and subtract additional light of other traffic participants. Only then it is possible for the system to collect reliable information about the road lighting class.

Overall, much more testing in various scenarios is required to identify and understand further problems.

6. References

- [1] Commission Internationale de l'Éclairage: "Contrast and Visibility", CIE 95, 1992.
- [2] S. Völker: "Hell – und Kontrastempfindung – ein Beitrag zur Entwicklung von Zielfunktionen für die Auslegung von Kraftfahrzeug-Scheinwerfern" [Brightness and contrast perception: a contribution to the development of target functions for designing automotive headlamps], habilitation thesis, University of Paderborn, 2006.
- [3] S. Vogel, S. Fiedelak, M. Niedling, S. Völker: "Influence of automotive headlamp systems on the visibility of targets under different road lighting conditions", Lighting Research & Technology, 2022.
- [4] A. Bacelar: "The contribution of vehicle lights in urban and peripheral urban environments", Lighting Research and Technology, 36(1), 2004.
- [5] A. Ekrias, M. Eloholma, L. Halonen: "Effects of vehicle headlights on target contrast in road lighting environments" Journal of Light and Visual Environment, 32(3), 2008.
- [6] European Committee for Standardization: "DIN EN 13201-2 Road lighting - Part 2: Performance requirements", CEN, 2015.
- [7] S. Williamson, H. Cummins: "Light and Color in Nature and Art", John Wiley and Sons, 1983.

- [8] CIE International Commission on Illumination: "Characterization of the performance of illuminance meters and luminance meters", ISO/CIE 19476:2014, 2014.
- [9] U. Krüger, P. Blattner: "Spectral mismatch correction factor estimation for white LED spectra based on the photometer's f_1' value", CIE x038:2013, Proceedings of the CIE Centenary Conference "Towards a New Century of Light", Paris, 2013.

The Automotive Night & All-Weather Camera and Its Critical Role in the Automotive Sensor Suite

Ofer David¹, Daniel Kriger¹, Ran Ginat¹, Shalom Weinberger¹, Itai Winkler¹

Bright Way Vision, Haifa, Israel

Abstract:

Nighttime driving has been recorded as the most hazardous time of the day to drive [1]. In addition, current ADAS cameras and near-future cameras for autonomous driving cannot operate satisfactorily at night (darkness). Cameras based on GatedVision can perform very well in darkness while providing obstacle detection based on the unique features of GatedVision. Slicing can eliminate the background, and shadow detection can detect obstacles with zero contrast. We present some basic concepts of GatedVision and its associated detection capabilities. The basic automotive implementation of a GatedVision system is to have the GatedVision camera side by side with the visible (standard) camera. This will allow full visual operation in lighted conditions and darkness.

Keywords: GatedVision, Safety, automotive, CMOS image sensors (CIS)

1. Introduction

We present the current state of ADAS in darkness and adverse weather conditions (section 2). Current ADAS cameras are far from satisfactory when it is most needed [2]. In section 3, we describe what is needed from an imaging sensor for the automotive industry. Cameras should see better at night than in the day since nighttime is more dangerous. In section 4, we describe what GatedVision is followed by why it is needed in the automotive industry in section 5. GatedVision is a technology that shows promising results in evaluations by OEMs. It is mostly suitable for night driving and inclement weather. We use the definition of “visible sensor” for any imaging sensor operating in the visible spectrum; it could be RGB or RCC, for example.

2. The current state of automotive visual sensors

Current automotive image sensors rely on CMOS technology. CMOS image sensors (CIS) have made huge progress in recent years. As much as the technology advanced and the sensors got more sensitive, there is a lower limit of sensitivity where the input light cannot overcome the internal noise of the sensor. Figure 1 shows that at low signals, as the

SNR drops below 5, there is no usable image. SNR 5 is the imaging threshold.

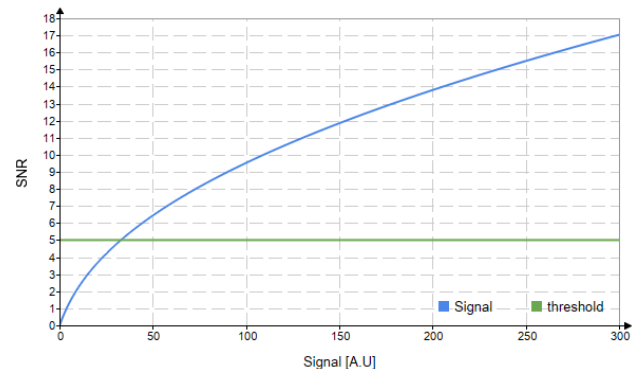


Figure 1- signal vs. SNR (theoretical)

In addition, the integration time of a CMOS image sensor is mostly controlled by the ambient light and thus is too long in dark scenes while driving, where short exposure is required to prevent the blurring of the image. Passive (regular) CIS do not sense the range information of objects in the scene. CIS cannot make any partition of obstacles and background, which might confuse detection algorithms. Looking at published data [3], we see that practically none of the OEMs equipped their cars with CIS that can perform automatic emergency braking in dark scenery. In addition, daytime performances are below the desired level and achieve accident mitigation only a third of the time. If one adds adverse weather conditions, things get worse. The current status, according to the IIHS, is: “Results showed that pedestrian AEB reduced the odds of a pedestrian crash by 32 percent (daytime)” and “Unfortunately, it also shows these systems are much less effective at night when three-quarters of fatal pedestrian crashes happen.”

A supporting fact for the need for pedestrian safety in darkness is the percentage of pedestrian (77%) casualties in these conditions (Figure 2). The industry is pushing LiDAR as a safety sensor, but LiDARs will fail in adverse weather, low reflectivity, and in some cases when targeting a specular reflective surface. If one looks at the cost of casualties at night, it is obvious that it is more expensive than equipping new cars with nighttime ADAS. OEMs should not bear the full cost of these systems and should provide close to 99% safety at all times.

¹These authors contributed equally to this work.

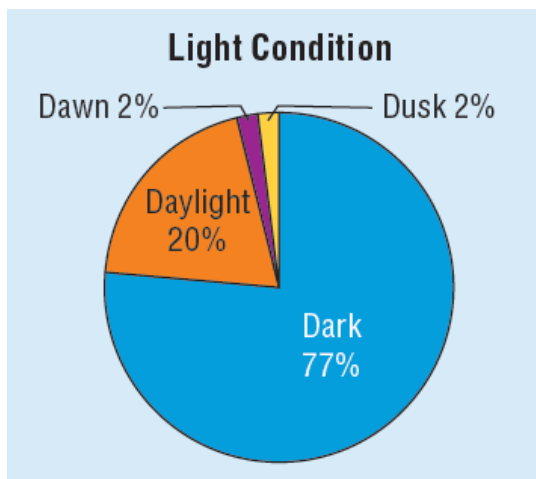


Figure 3 - Percentage of Pedestrian Fatalities in Relation to Light Conditions (NHTSA 2022)

3. What is needed

We now turn to evaluate what properties an ideal vision sensor for automotive applications should have.

3.1. Seeing day and night equally

There should be no difference in the level of safety between night and day. Nights are more dangerous due to several factors, such as limited visibility (facing the driving direction) of up to 50m and the range of the cars' headlamps in clear weather. Usually, nighttime driving allows for higher speeds as the roads are less congested. At night, we lack accurate distance estimation, are usually more tired, and our vision is degraded, especially with elderly drivers. While operating in the dark, the image sensor is not allowed for long integration times and must not be blinded by oncoming headlamps. So, an automotive image sensor should operate flawlessly in darkness with a short integration time and be resilient to blooming.

3.2. Weather

Adverse weather is one of the situations where drivers need their safety equipment to operate most efficiently. One cannot expect autonomous trucks or cars to stop when it starts raining. Although it will be acceptable to reduce the speed when raining, the vision system still needs to perform. When choosing the right imaging system, one must consider the wavelength to maintain optimal performance. When using active systems, especially at night, the backscatter caused by the air-carried aerosols will blind the camera, affecting the detection range [4].

3.3. Dynamic range

Dynamic range is important when using active illumination at night. Since brightness in the short to long range is squared law proportional and safe automotive operation requires achieving long-range and short-range imaging. A target at 10m will appear

100 times brighter than the same target at 100m. The image sensor should be able to capture both targets without saturation and with a reasonable SNR (>5). In the automotive sector, there are additional constraints, such as not being saturated and bloomed by oncoming headlamps, similar systems, and retroreflectors.

3.4. Relevant distance

If the visible sensor captures only the relevant range and ignores irrelevant backgrounds, it will allow less computation and lower false positives. It will also increase the contrast, as seen in Figure 4 where the pedestrian is more prominent in the GatedVision sensor than in the visible sensor. The contrast is higher in the GatedVision image than in the visual image. The selective range discrimination in GatedVision is referred to as a range slice. The location and width of the range slice vary in real-time and can correlate with the car's speed.



Figure 4 – Range discrimination as a detection enhancer (GatedVision - top)

3.5. Low cost

Any automotive sensor is price-sensitive. Up to L3 (SAE level), the price might be a limiting factor when it comes to mass market installation. At L3 and above, the cost of the sensor suite and the overall autonomous enabling system will have a higher budget. Trucks will allow for higher sensor costs if the driver is removed, especially in class 8 trucks on highway routes (hub to hub). In addition, L4 trucks will prefer nighttime driving, which flows more freely, making them more fuel-efficient and environmentally friendly.

There are additional requirements for safety, reliability (AECQ- 100) and cyber security which is true for all

CIS including the GatedVision which is beyond the scope of this paper.

4. GatedVision

GatedVision is an emerging imaging sensor technology for automotive applications. GatedVision relies on active laser illumination to allow for low-light imaging. The system flood illuminates the whole field of view (FOV) with a short light pulse and creates an image frame out of successive pulses of laser and short integration by the sensor. A GatedVision frame can be a portion of the whole range which is called a range slice (~1-100m wide) or a full range image (10m to 300m). The full range frame is constructed by multiple slices. Slicing enables to overcome backscatter, which is the dominant limitation in rain, fog, or snow.

4.1. Wavelength

There are several spectral regions to consider in active illumination sensing as is used in GatedVision. The visible spectrum can be eliminated since you cannot blind other road users. The spectrums to consider are NIR (0.78-1.2 μm Near Infra-Red), SWIR (1.2 -3 μm Short Wave IR), and thermal sensors (3-5 μm or 7-14 μm). Thermal imagers are sensitive to temperature differences in the scene. The 3-5 μm (MWIR) spectrum requires cooled detectors and costly systems, therefore it will not fit the automotive market. In the 7-14 μm (LWIR/FIR) band, there are moderate price systems that will detect hot targets (~300K). FIR and MWIR must be installed externally and suffer significant degradation in inclement weather. Thermal imaging is unsuitable for GatedVision since the scene radiation is very strong, and there is no need for active illumination. As for SWIR, it is still very expensive for reasonable performance. SWIR suffers strong attenuation by water molecules, so it is not useful for rain and fog. NIR is the best choice for automotive applications. Within the NIR spectrum, 0.8 μm is the preferred choice due to the following:

- High QE
- Low-cost Si detectors
- Windshield transparency
- Is blind to LiDARs
- Low aerosol attenuation (rain and fog)

4.2. Dynamic range

At night, GatedVision allows for each range slice to be optimized by itself. A range slice at 200m will have the same brightness as a range slice at 20m. Combining the slices linearly will provide a uniform illuminated scene with no need to adjust for a large intensity span. During the day, the dynamic range is the limiting factor for the available pulses (integration time) at a certain

slice width. Increasing the dynamic range will improve the SNR of a range slice. It is beyond the scope of this paper to analyze performance during daytime.

4.3. Backscatter

One of the major differences between active illumination systems and gated active systems (GatedVision), is the ability of GatedVision to suppress the backscatter created by the suspended water particles in rain or fog. The width of the slice and its distance from the system affect the backscatter intensity. In addition, the distance between the illuminator and the camera is another parameter that strongly affects backscatter.



Figure 5 - Backscatter in snow. GatedVision (top) vs. a visible HDR camera (bottom).

5. Why GatedVision for automotive applications

As presented in section 3, the requirements of the automotive image sensor are versatile and

demanding. In section 4, we described GatedVision technology. Gated Vision is showing great potential as an answer to these requirements. It will allow overcoming the limitations described in section 2. Automotive OEMs should broaden the scope of their ODD to allow for better safety by using adequate technology. In addition to answering all requirements listed in section 3, GatedVision technology provides additional capabilities, as we shall describe below.

5.1. Depth

Using several overlapping range slices created by GatedVision, one can calculate the range to any point in the scene [5]. The slice itself can provide a range at a lower resolution but is sufficient at the longer ranges.

5.2. Shadow

All vision systems rely on contrast; if there is no contrast, no AI or human can detect a target lying on the road. Any active system generates a shadow in the scene. The issue is to differentiate the dark spot as either a shadow or a non-reflective material. GatedVision is capable of spatially modulating the shadow in the captured image within a single frame time (<5msec). A dark spot or a non-reflective material will not be modulated.

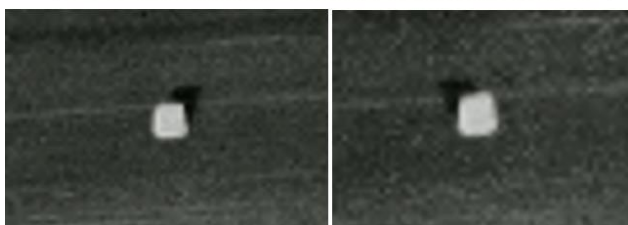


Figure 6 - Shadow left+right at top, left illuminator bottom left, right illuminator bottom right

5.3. Retro

GatedVision systems can distinguish between diffuse reflection and retroreflectors, which are not neutral and belong to road markings, traffic signs, or the rear end of a car. This is helpful in the rain for LIKE/LDW and for AEB cars with or without lights.

5.4. Non-trained obstacle detection

Slicing combined with shadow and passive NIR imaging can enable a new kind of detection.

4. Conclusion

While it has the smallest drive capacity, the highest number of casualties and fatal accidents occurred while driving at night and in adverse weather conditions [2]. ADAS and AVs must be able to see at night as clearly as in broad daylight. Gated imaging working in the NIR wavelength has the power and capability to fill the gap at night and in adverse weather to provide clear images with high contrast [6], with the ability to perform range discrimination as a detection enhancer. In addition, gated imaging suppresses adverse weather interferences, such as backscatter. Using the inherent capability of overlaying slices, a depth image can be extracted to provide an accurate enough depth map, as shown in recent studies [4]. The technology is now mature and ready to provide high performance at a low cost to be adopted by the automotive industry to fill the gap that the current ADAS and AV sensor suite has at night and in adverse weather conditions.

5. References

- [1] N. N. C. f. S. a. Analysis, "Traffic Safety Facts 2020 Data (DOT H Administration, 1200 New Jersey Avenue SE, Washington, DC 20
- [2] I. I. f. H. S. (IIHS), "Pedestrian crash avoidance systems cut crash Highway Safety, Highway Loss Data Institute, 501(c)(3) organiza
- [3] Joe Young, "Few vehicles excel in new nighttime test of pedestrian Highway Loss Data Institute, 501(c)(3) organizations, Arlington,
- [4] "Extended Photometric Model of Fog Effects on Road Vision," [C https://www.researchgate.net/publication/245560922_Extended_F
- [5] S. W. M. B. F. M. J.-A. M. L. W. R. F. H. Amanpreet Walia, "Gated Images," in *2022 Conference on Computer Vision and Patt June 2022, 2021*.
- [6] Mario Bijelic, Tobias Gruber and Werner Ritter, "Benchmarking Image Sensors Under Adverse Weather Conditions for," in *2018 IEEE Intelligent Vehicles Symposium (IV)*, Changshu, Suzhou, China, June 26-30, 2018, 2018.

6. Glossary

ADAS: Advanced Driver Assistance Systems

CMOS image sensors (CIS)

GatedVision – Active gated imaging

Range slice – An image having a start and end range

Investigation of the influence of camera parameters on data quality for highly automated vehicles

David Hoffmann¹, Anil Erkan¹, Korbinian Kunst¹, Markus Peier¹, Timo Singer, Tran Quoc Khanh¹

1: Technical University of Darmstadt, Laboratory of Adaptive Lighting Systems and Visual Processing, Hochschulstr. 4a, 64289 Darmstadt, Germany

Abstract: The development of highly automated vehicles, in which the driver no longer needs to observe the traffic area, is undergoing a significant push. Various sensor types such as LIDAR, RADAR and cameras are used to observe the surrounding traffic space. In this process, the analysis of the surrounding traffic space for the detection of objects, intentions of other road users or the recognition of the drivable area is carried out by various algorithms. The algorithms provide more reliable information when the data quality of all sensor types is known and used optimally. Although the various sensor types partially compensate for each other's deficiencies, each sensor type must be fully understood and interpreted to ensure usable data for the applied algorithms.

This paper provides a first insight into studies on the detectability of objects in nighttime road traffic under situations with an oncoming vehicle as glare source. In addition, this paper will highlight that cooperation between camera and headlamp development is essential for safe autonomous driving in nighttime traffic.

Keywords: Autonomous driving, Camera, Object Detection

1. Introduction

Future highly automated vehicles will rely on multiple sensors for environmental sensing to increase the certainty of detection through redundant sensors. The most common sensors are RADAR, LIDAR and cameras. These sensors partially compensate for weaknesses of the others, e.g. RADAR can see through fog compared to cameras and LIDAR and cameras have the advantage of high resolution and the recording of color values. The high resolution is helpful for better classification of objects or to recognize the faces of pedestrians to predict their intention. Capturing the color of objects becomes important, for example, to distinguish the yellow from the white lane markings in road constructions. Since each sensor must be read and understood optimally, this work focuses on the analysis of imaging camera sensors, as they will be an important component of future highly automated vehicles.

The main tasks of cameras in highly automated vehicles consist of detecting objects, recognizing the roadway and the individual lanes, and additionally recognizing the intentions of vulnerable road users such as pedestrians and cyclists. Intention recognition is an important tool that enables the vehicle to communicate with other road users via signaling devices and thus, for example, to solve dead lock situations or to avoid them completely.

Comparable to the human eye, most cameras operate in the visible light range from 380 nm to 780 nm. To support the human driver, headlights are installed in the vehicle, and these can also be used to support cameras. The optimization of light distributions and lighting functions has been an important topic in science and industry for several decades. With the development of automated driving functions, however, the focus must be shifted from human perception to the perception process of cameras and the underlying data processing algorithms. Compared to a human driver, who must pass a vision test when obtaining a driver's license, there is until now no comparable test for cameras. The IEEE P2020 working group [1] is currently working on this task. The EMVA 1288 standard [2] serves as the basis for describing the quality of imaging sensors.

The following experiments focus on nighttime scenarios. Here, the influence of glare from oncoming vehicles is investigated.

2. Experiments

2.1 Experimental design

Figure 1 and 2 show the measurement setup to investigate the influence of glare on the signal quality of cameras. This investigation was carried out in a light tunnel with an asphalt floor and no ambient light. A measurement grid consisting of 5 rows at a distance of 20 m, 40 m, 60 m, 80 m, and 100 m and 5 gray cards at a distance of 1.75 m per row was set up. One gray card was placed centrally in front of the vehicle, one on the right and three on the left. The gray cards have a reflectance of about 4%. There are no road markings in the light tunnel, so a road

width of 7 m and a resulting lane width of 3.5 m were assumed for this test. In the first step, data was recorded without an oncoming vehicle, and in the second step, a vehicle was positioned in the opposite lane at a distance of 60 m with the LED low beam switched on.

On the test vehicle, the LED headlights were modified so that they could be dimmed from 0 to 255 using 8 bit PWM coding. The dimming values used were 0, 42, 63, 84, 105, 126, 147, 168, 189, 210, 231 for the low beam and high beam in parallel.

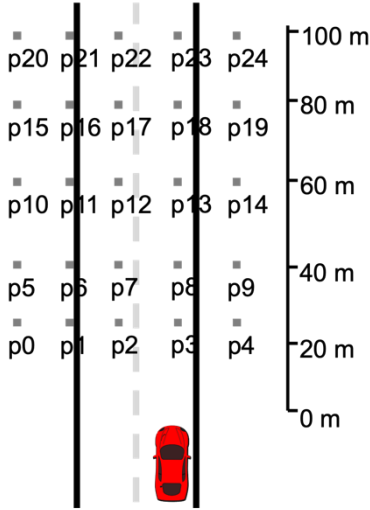


Figure 1: The figure shows the measurement setup for the detection investigation of cameras. The measurement cards with a reflectance of 4% and a size of 20 x 20 cm are arranged in 5 rows at a distance of 20 m, 40 m, 60 m, 80 m, and 100 m. Per row, 5 cards are placed at 1.75 m from each other. One card in the center in front of the vehicle, one card to the right of the vehicle and three cards to the left of the vehicle. (No markings were present on the test site; these were simulated with a road width of 7 m and a lane width of 3.5 m.)

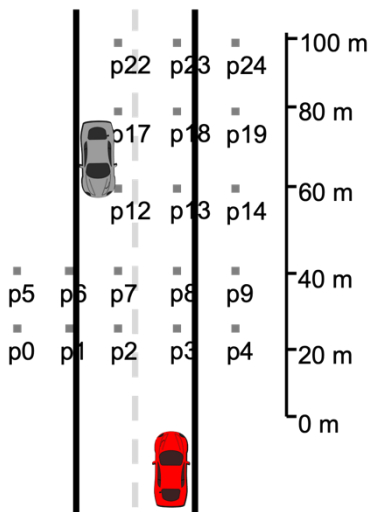


Figure 2: Comparable setup to Figure 1, but with a vehicle with its low beam switched on in the opposite lane 60 m away. Positions 10, 11, 15, 16, 20 and 21 were covered by the vehicle.

Two cameras with an identical 12 mm lens and aperture F4 were used. The first camera has a resolution of 1920 x 1200 pixels with a pixel size of 2.3 μm and the second camera has a resolution of 728 x 524 pixels with a pixel size of 6.9 μm . Raw images were captured with exposure times of 0.5 ms, 1 ms, 5 ms, 10 ms, 20 ms and 50 ms and analog gains of 0 dB, 10 dB, 20 dB, 30 dB, 40 dB and 48 dB. For each setting, 5 images were taken to average the results. In addition, dark images were recorded for each setting and luminance using a luminance camera. All cameras were mounted under the rearview mirror inside the vehicle.

2.2 Basics of data evaluation

In this work, the focus is on the signal to noise ratio (SNR) and the luminance where the signal exceeds the noise, i.e. has a non-log SNR greater than one. The SNR is calculated from the dark noise, temporal noise and fixed pattern noise. The dark noise is caused by the electronics surrounding the photodiode and is additionally temperature dependent. Temporal noise are fluctuations in the signal of each pixel in the array under constant illumination over time and fixed pattern noise are variations in mean pixel signal across the array under uniform illumination. It is also called structural noise and spatial non-uniformities. The SNR can be calculated as follows:

$$SNR(n) = \frac{\mu(n)}{\sigma_{total}(n)}$$

$$\sigma_{total}(n) = \sqrt{\sigma_{tot_temp}^2(n) + \sigma_{FPN}^2(n)}$$

$$\sigma_{FPN}(n) = \sqrt{\frac{1}{I_n \cdot J_n} \sum_{i=1}^{I_n} \left(\sum_{j=1}^{J_n} [\mu(i, j, n) - \mu(n)]^2 \right)}$$

$$\sigma_{temp}(i, j, n) = \sqrt{\frac{1}{K-1} \sum_{k=1}^K [S(i, i, k, n) - DN(i, j, n) - \mu(i, j, n)]^2}$$

$$\sigma_{tot_temp}(n) = \sqrt{\frac{1}{I_n \cdot J_n} \sum_{i=1}^{I_n} \left(\sum_{j=1}^{J_n} \sigma_{temp}^2(i, j, n) \right)}$$

where $\mu(n)$ is the cleaned signal (raw data minus dark noise), n is the index of the region of interest, K is the number of images, i and j are rows, and line index corresponding to the image S .

Figure 3 shows an example plot of a camera response as a function of luminance divided into raw signal, dark noise, fixed pattern noise, temporal noise and

resulting SNR for the first camera with a pixel size of $2.3\text{ }\mu\text{m}$ at 50 ms exposure time and an analog gain of 0.

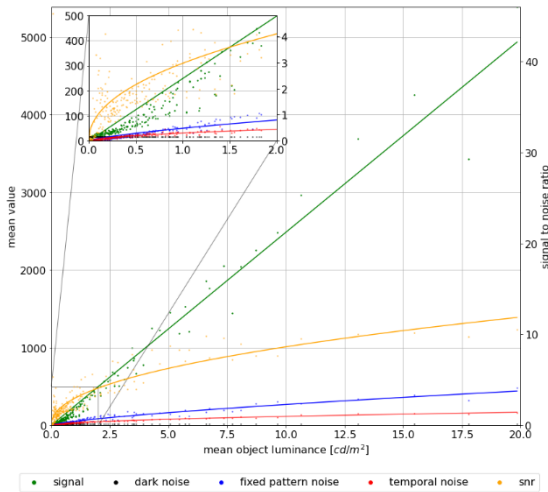


Figure 3: example plot of camera response as a function of luminance divided into raw signal (green, left y-axis), dark noise (black, left y-axis), fixed pattern noise (blue, left y-axis), temporal noise (red, left y-axis) and resulting snr (yellow, right y-axis)

Since noise can lead to isolated SNR values greater than 1 even at very low luminances, the luminance at which 90% of the SNR values are greater than 1 was used in the further evaluation.

3. Results

For a first evaluation, the results of all gray cards were combined. A detailed analysis of the individual positions will be carried out and is not the subject of this paper. Figure 4 shows the minimum luminance required to achieve a SNR of 1 for the first camera at the different exposure times and analog gains. In comparison, Figure 5 shows the minimum luminance required in the case of an oncoming vehicle with its low beam switched on.

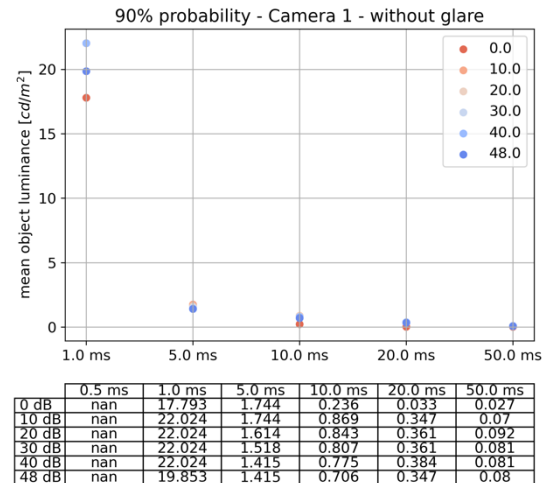


Figure 4: The figure and table show the minimum luminance required to achieve a SNR value of one for the different exposure times and analog gains for the first camera with a pixel size of $2,3\text{ }\mu\text{m}$.

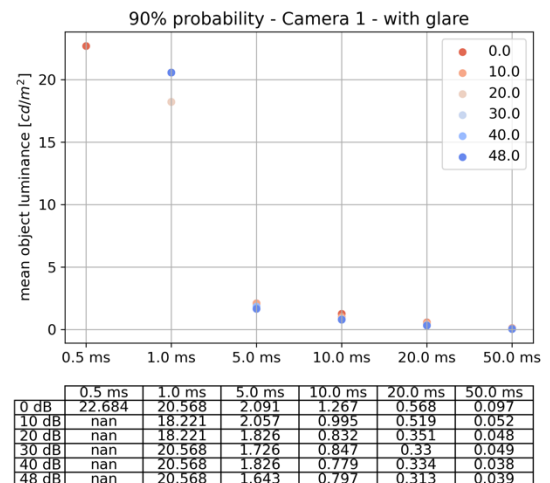


Figure 5: The figure and the table show the minimum luminance required to achieve a SNR value of one for the different exposure times and analog gains for the first camera with a pixel size of $2,3\text{ }\mu\text{m}$ in the presence of glare.

The results essentially show that in the presence of a glare source, the required luminance levels are increased. One reason for this behavior can be the stray light in the lens, which is caused by the glare source. Initial analysis shows that the presence of the glare source raises the fixed pattern noise. This suggests that the stray light causes an inhomogeneous increase of the signal. However, a detailed investigation is to be carried out.

For comparison, Figure 6 and 7 show the results of the second camera for the situation with and without glare. The behavior of the minimum luminance is comparable to camera 1. However, due to the

significantly larger pixels, it is noticeable that these require a lower luminance at the same exposure time and analog gain to achieve a SNR of one.

In order to put the values in relation to the set light distribution (PWM), figure 8 shows the resulting luminance levels and the difference between the two scenarios for the column in front of the vehicle and the column to the left of it, directly next to the glare vehicle. By looking at the data, it is now possible to either dim down the light distribution or reduce the exposure time. This is dependent on the speed driven and the resulting motion blur and the required detection distance. Furthermore, it can be seen that the glaring vehicle additionally illuminates the objects by back reflection and thus the object luminance is increased.

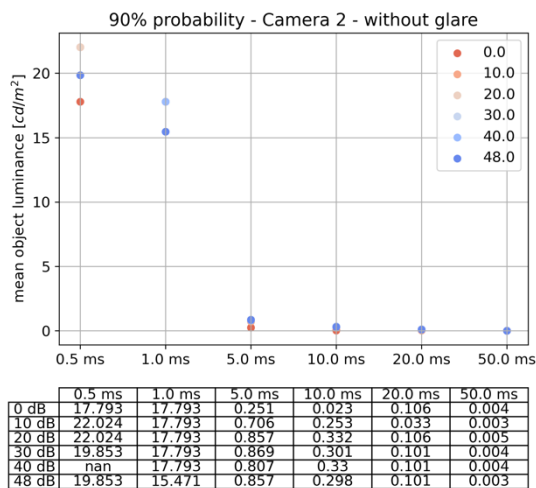


Figure 6: The figure and table show the minimum luminance required to achieve a SNR value of one for the different exposure times and analog gains for the first camera with a pixel size of 6,9 μm .

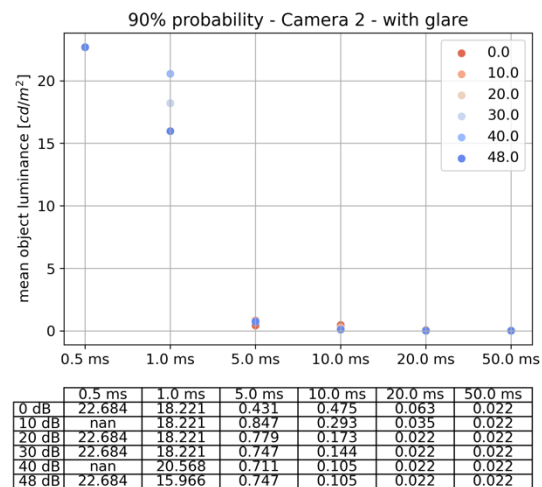


Figure 7: The figure and the table show the minimum luminance required to achieve a SNR value of one for the different exposure times and analog gains for the first camera with a pixel size of 6,9 μm in the presence of glare.

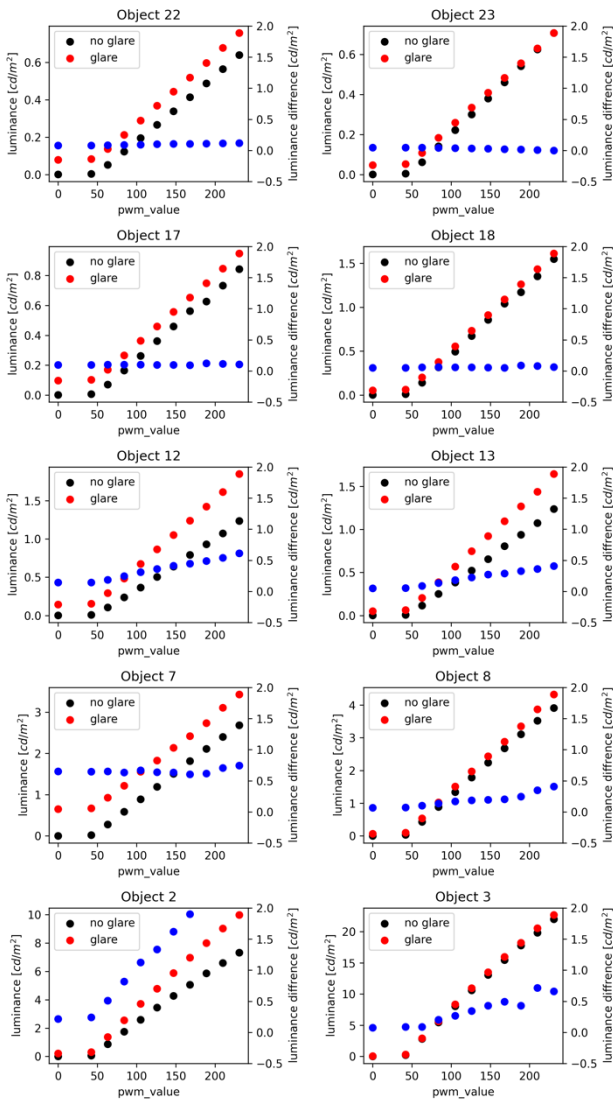


Figure 8: Luminance on objects 2, 3, 7, 8, 12, 13, 17, 18, 22 and 23 with and without glare source for the different PWM values. The figures on the right show the objects centrally in front of the vehicle and the figures on the left show the objects one row to the left directly next to the glare vehicle. In addition, the difference in luminance between the two scenarios is shown in blue (right y-axis).

4. Conclusion & Outlook

The first examination of the results shows that, comparable to humans, glare sources have a negative influence on the detectability of objects. Furthermore, the results showed that the minimum required luminance is reduced by a larger pixel size. This results in a tradeoff between resolution and pixel size. Large pixels are important for the detectability in night traffic and a high resolution is important to reliably detect objects in large distances and for example to estimate the intention of pedestrians by recognizing faces. However, in order to make a precise statement about the influence of glare, further

investigations must be carried out. On the one hand, the condition of the road has an influence on the amount of reflected light, which means, for example, that on a wet road only a small percentage of the light is reflected back onto the objects and thus more light is reflected into the camera. Furthermore, the influence of the position of the glare source as well as the quality of the camera lens is another influencing parameter that should be considered. For this investigation, a laboratory setup is recommended in order to achieve controlled measurement conditions and to measure different geometries in a reproducible process.

In the next step, it is necessary to consider the influence of street lighting and the contrasts required to reliably distinguish the object from the background. Studies by Aulhorn [3] and Damasky [4] show that negative contrast provides a better detection condition for humans than positive contrast. It is possible that a comparable behavior is also shown for the cameras.

In this work a SNR of 1 was chosen to see from which luminance the signal can be theoretically distinguished from the noise. In the case of highly automated vehicles, the data is further processed by neural networks in order to detect objects. Investigations are currently being carried out to determine which SNR is required by different networks for reliable detection.

5. References

- [1] Authored by Members of the IEEE P2020 Working Group: "IEEE P2020 Automotive Imaging White Paper", 2018.
- [2] European Machine Vision Association: "EMVA Standard 1288 – Standard for Characterization of image Sensors and Cameras", 16. June 2021.
- [3] Aulhorn E.: "Über die Beziehung zwischen Lichtsinn und Sehschärfe.", Albrecht von Graefes Archiv für Ophthalmologie Vereinigt mit Archiv für Augenheilkunde 1964; 167(1): 4–74.
- [4] Damasky J.: "Lichttechnische Entwicklung von Anforderungen an Kraftfahrzeugscheinwerfer.", Dissertation, Technische Hochschule Darmstadt, Darmstadt, 1995.

ROAD PROJECTION STAKES

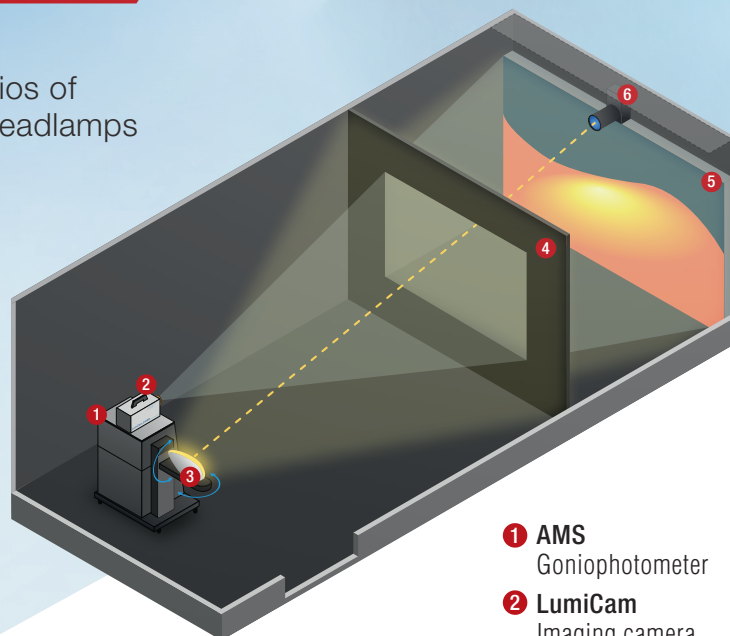
One System — All Light Distributions


12_{MP}

AMS Screen Imaging System

- ▲ **State-of-the-Art:**
All possible lighting scenarios of HD, ADB, Matrix or Pixel headlamps with one system
- ▲ **Time-saving:**
Ultra-fast camera-based screen photometry
- ▲ **Seamless:**
Simultaneous analysis with LightCon software

Visit us at
BOOTH #S307!



- | | |
|--------------------------|---------------------|
| 1 AMS Goniophotometer | 4 Baffles |
| 2 LumiCam Imaging camera | 5 Projection screen |
| 3 Vehicle lights | 6 DSP Photometer |



Digital Projections: Distraction Potential for Other Traffic Participants

Michael Hamm, Jonas Kobbert, Christian Hinterwälder

Audi AG Ingolstadt, Germany

Abstract:

The paper will focus on research on digital projections. The study presents research findings with test persons if and in which geometrical space road projections are visible to other road traffic participants. Such participants can be e.g. oncoming, passing drivers or pedestrians standing aside the road. Luminance Measurements under various Observation Angles are discussed. Published Eye mark studies on visual gaze and the 3-dimensional gaze direction of drivers are investigated and compared.

With the derived data, a grid was created to identify the areas where digital projections could be understood and where the digital projections are just illegible. As a dominant factor the grazing incidence by means of geometrical projection and luminance was identified. Since the projecting car is moving, for each of the traffic participant group, a realistic detection zone and time period was calculated in a dynamic traffic situation.

One of the big concerns regarding digital projections is potential distraction. The study will contribute to an evaluation of distraction and disturbance potential based on geometric data.

The results show that distraction for other road participants is unlikely for any position outside very limited areas. The dynamic "readability map" of digital road projections is given.

Keywords: Digital Projections, Driver Information, Distraction

1. Introduction

Some cars are already available with additional features of driver information. Digital projections have drastically increased the possibilities of communication in automotive applications.

Two fields of application can be identified:

Application #1: Beam support. Projections support low- and high beam by the ability to locally increase the illumination on the road (see Figure 1). With high resolution, also ADB (or Matrix Beam) function offers new potential e.g. of adapting and fine-tuning the glare

free zone according to traffic and regulatory needs. US ADB requirements might be probably best possible with digital ADB projector support.

In the specific application shown in Figure 1, the own lane is covered with increased illumination. Vehicle sensors give the width and geometry of the lane and with this information, the projection adds light to the standard low beam illumination, dynamically following the moving lane positions. This function is called "Guiding Light".

Application #2: Additional Information. Besides the local illumination adaptation, digital projectors can give additional information by individually on the road surface projected patterns, symbols or figures. Such patterns, symbols and figures are possible by the high-resolution ability of the digital projectors used. The new idea of digital projection is to present specific elements directly in the visibility area of the driver (see Figure 2 – 4). Unlike in a Head Up Display the information is independent of the angle and eye position. Due to the added light, positive or negative contrast is possible. E.g. the extra patterns inside the increased illumination (Figure 1) indicate the live car position in its lane. This negative contrast pattern is called "Orientation Light".

Since there was no regulation in advance, the discussion about how to assess digital projections is now very active. Lack of prototypes led to the fact that little research has been conducted to investigate the positive traffic safety benefits as well as the potential disadvantages. Meanwhile the situation has changed and test vehicles and serial applications are now available.

Independent of research, several regulatory working groups have started to look inside the digital communication possibilities [1]. During the first preparatory sessions for regulatory drafts, several concerns have been communicated, but with rare research base. Glare and possible distraction of third persons have been mentioned in several combinations. Such concerns were fueled by creative drawings and photoshop images. Marketing needs liked to transport in woodcut-like sketches the salient visions of the road projection idea. Since photoshop

cannot replace scientific investigations, this paper contributes to the research on real digital road projections.

Any live view of digital projections shows that because of the grazing incidence of a projection about 20 m in front of the car there is optical distortion. Depending on the intended position of the projection and readability, the correction of distortion must be considered by the engineers in the original picture.

Visibility and readability of projections play a crucial role in assessments about distraction for third parties like pedestrians, overtaking or oncoming traffic participants. This paper tries to assess where and how there is readability and where there is no readability and thus no distraction potential.

2. Digital Road Projection and Benefits: Traffic Safety Investigations

Investigations on digital projections and traffic safety effects have been conducted in recent years. This was motivated by giving proof that there are predominantly positive effects and such technology does not give harm or danger to other traffic participants.

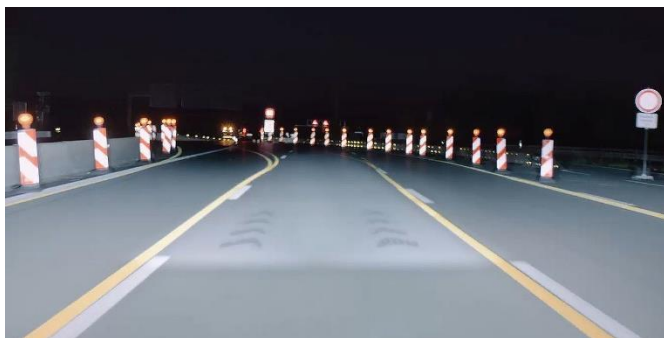


Figure 1: Video snapshot of real nightdrive by a serial solution with lane indicators ("Guiding Light") and width indicators ("Orientation Light")

2.1. Safety Investigations – Study Overview

Since the digital projections are new, studies have been published only in recent years. In SAE Paper 2018-01-0516, Audi [2] published the results of a study that investigated the effects of guiding lines in construction zones. The construction zone light as investigated in this paper projected two light stripes on the road anticipating the width of the vehicle on the coming scenery in the area of roadwork. As critical situations during nighttime driving an overtaking attempt in a double-lane construction zone was considered. Such overtaking could be considered critical in a roadwork area, where a truck drives on the right and massive delineators limit the road at the left

side. The overtaking situation needed to be evaluated whether the width of the lane during the dynamic driving situation is sufficiently safe for the driver to overtake.

The study showed that gas pedal position changes (-15 %) and decreased steering angle frequency (-20 %) lead to better results with the construction zone light used in the study. Overall questionnaire feedback of the drivers resulted only positive results. The drivers felt less forced to make abrupt braking manoeuvres and had much better estimation of the own lane width. The overall rating on the construction zone light achieved 95 % positive feedback.

Another study of Karlsruhe Institute of Technology [3] with 83 test persons investigated similar digital projections of a "Guiding Light" in road working zones. Positive effects were found on reduced steering wheel velocity (-16 %) and summed up steering wheel motion (-34 %). In a correlated questionnaire 97.26 % of the test persons agreed to the statement "I felt safer having the lines shown up in front of me". The study concluded that guiding lines have a high potential of helping the driver in stressful situations like in work zone or construction zone areas. Potential distraction of the driver and other traffic participants was not identified.

A study presented from Automotive Lighting [4] was able to give real numbers for a lane-keeping improvement of digital projections. Special interest was given to the ability to keep driving in the middle or center of the lane. The study was able to record the lateral distance between the position of the car axis and the center of its own lane with and without digital projections. By comparing the data in correlated conditions, the deviations were analysed. About 20% less deviations from the safe center corridor were shown.

2.2. Safety Investigations - Conclusion

Digital Projections improve safety in nighttime driving. The above referenced studies covered various parameters like gas throttle position, steering wheel constancy, steering wheel overall movements, lane keeping capability and questionnaires. In the answers more than 95 % were positive test person reactions. Especially the combination of digital projections and traffic safety feeling was the positive summary of the subjective questionnaire. Potential distraction was not mentioned in any questionnaire or situation.

3. Viewing Direction towards the Projections: Eye Mark Investigation

As mentioned above, Digital projections can also be intended to inform and guide the driver. In Figure 2..4 some of the actually discussed symbols [1] are shown. One information could be a warning symbol

for adverse road conditions like ice or snow, the other two photographs show general warning symbols. All are intended to warn the driver about critical issues along his driveway.

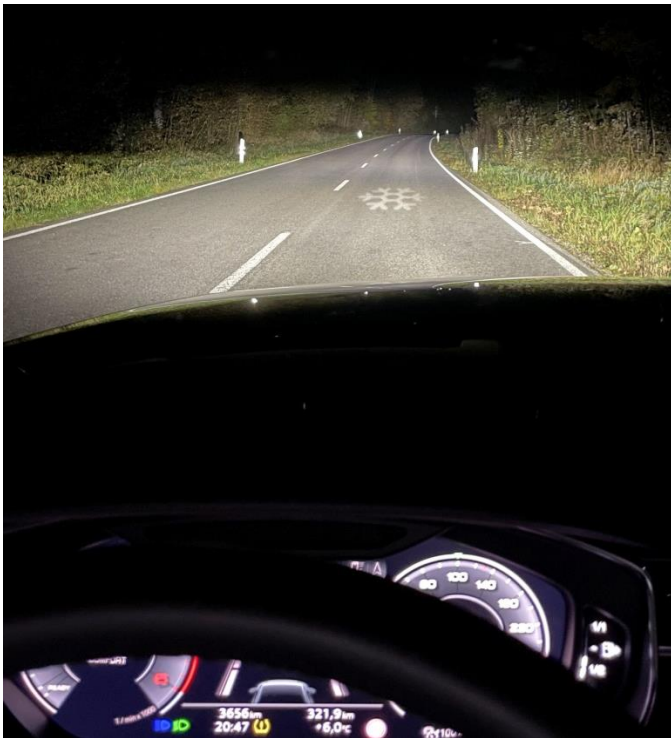


Figure 2: Snowflake projection indicating glossy or freezing road as example of a digital projection in front of the vehicle.



Figure 3: Possible Warning projection



Figure 4: Possible Danger/Collision Warning projection.

Concerns in the discussion arised that such projections might be visible to other traffic participants. And for curiosity this information might lead to eye movements and therefore potential risk of drivers not following their basic driving task of following their lane.

Under today's legal boundary conditions many events with active digital projections will happen at nighttime driving outside city limits. Thus other road users might potentially be involved while participating in nighttime driving, in being overtaken or overtake a vehicle with digital projections in its front area.

In order to address the potential of distraction (even when the previous studies showed no indication at all for such condition), some studies covered explicitly the hypothesis of distraction. The hypothesis of Distraction was investigated in 2 eye mark studies with live test setups of nighttime driving. Eye movement recording and analysis was considered as a significant parameter to identify distraction or even interest by digital projections.

3.1. Eye Mark Investigations – Study Overview

A study of Technische Universität Darmstadt [5] analysed the driver's gaze behavior in overtaking situations. In about 700 overhauls, 3 symbols were presented with a digital projection vehicle. Two situations were investigated, a digital projection car overtaking a test person's car or a test person's car overtaking a digital projection car. The results show that the viewing behavior of the test persons was not affected in all cases. The eye movement zones did not significantly differ, the main focus was always the drivers own lane to perform their driving task. Additionally, about 12 % of test subjects did mention they recognized a digital projection. The rest of 88 % did not see a projection at all, despite they were clearly present.

A study of Gottfried Wilhelm Leibniz Universität Hannover, Institute of Product Development [6] investigated the eye movements and potential of distraction by digital projections. 38 test persons did drive an identical 80 km motorway section without knowing that they would be overtaken several times by a projection vehicle. The distraction potential was examined with an eye-tracking system by recording the direction of the subjects' gaze. The digital projections were either presented in static or blinking mode. In a literature research, critical distraction was found to be longer than 1.6 seconds.

In the first part of the study where the test persons were not informed about the study target, only a few subjects looked at the projection with a duration of in average 492 ms, which was considered well below the reported critical threshold for the distraction of 1.6 seconds. In total, all glances towards the

projection corresponded to 0.7% (static) / 1.4 % (blinking) out of a total of 855 glances (Figure 5).

Since the actual and intended digital projections in the regulatory discussion are all static, the static research data delivers better transformation potential. Anyhow, the dynamic data reported did not indicate significant differences or distraction potential.

With or without information and with or without the projection the majority of the test driver's glances (about 65 %) concentrated their view on the own lane (Figure 5).

In the correlated interview only one of the 38 test persons stated that the projection on the road was recognizable.

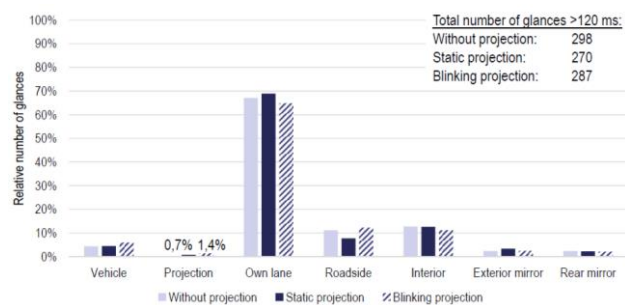


Figure 5: Eye Mark analysis of glances towards projections (static or blinking) during takeover maneuver. Source [6].

3.2. Eye Mark Investigations - Conclusion.

Digital Projections are quasi not registered from other drivers in situations of overtaking or been overtaken. Thus there is no eye movement in the direction of the symbols. Only 12 % in the first study and 1 test person out of 38 in the second study did register something. No study reported distraction in the interviews.

4. Experiments on Readability

The outcome of the two Eye Mark studies (see previous chapters) leads to the question why there were so few eye movements and no distraction was mentioned by any of the test persons in all the studies before.

4.1. Geometry

One direct explanation could be the geometry of the projected symbols. From first real street evaluations, it seemed obvious that there is a strong geometrical dependency for visibility or readability.

The angular constellation is that from driver's perspective all projections should be visible as if they were on an area perpendicular to the driver. If a projection is done from the headlamp mounting height of e.g. 0,8 m to a street surface in 20 m the grazing incidence leads to a distorted projection on the road, but it is made to make the driver in his specific geometry see a readable symbol or text.



Figure 6: Example of Readability Pattern "AE23P" used in the investigation from driver's perspective (20 .. 24m)

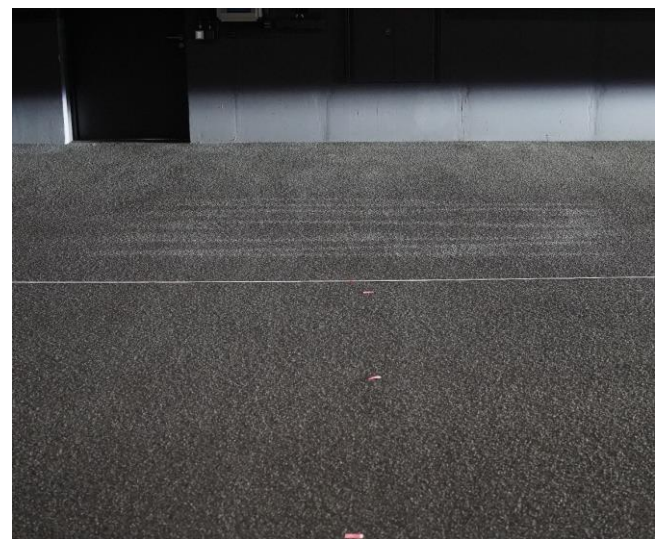


Figure 7: Readability Pattern "AE23P" from Figure 6 viewed at position direct at the projection (0 m) and 4 m lateral distance.

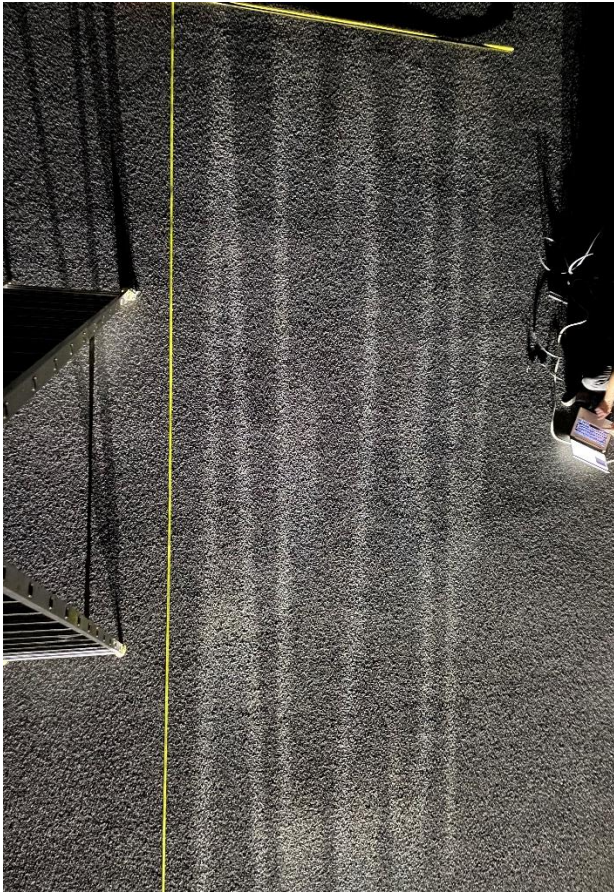


Figure 8: Readability Pattern “AE23P” from Figure 6 viewed at bird’s eye view direct (0 m) and 4 m height. Pattern Size on the road 4x2,4 m.

Looking to the 50 Letter-Number combinations used (see Figure 4 for example), the projection that looked quite readable for the driver is outside the car in reality much more stretched (For consistency, one of the 50 combinations “AE23P” was used throughout the images). Figure 4 and Figure 5 demonstrate the effect “AE23P” was visible from driver perspective in a shape of 5.6 x 1 (width x height) (see Figure 4). Standing perpendicular in front of the projection (like pedestrian would see), the geometry changes to 1 x 5.3 (see Figure 5). The enrolled projection on the street surface measured 4 m in length and 2,4 m in width. (see Figure 8) Most of the displayed combinations showed about 50 % fill factor.

Comparing the figures above shows that the same amount of photons delivers two different contrast and luminous intensity situations. The luminous flux is distributed over a large area in driving direction. Only the driver’s view delivers a virtual compression of the illuminated area in order to make the signals legible. In the compressed geometry, the letters are visible under 0,43°. Moving out of the driver’s position changes the visual field, increases the observation angle, reduces luminance and reduces the legibility.

4.2. Luminance

As the geometrical investigations show, the observed surface changes from each observation point additional to the legibility for a distorted Letter-Number combination.

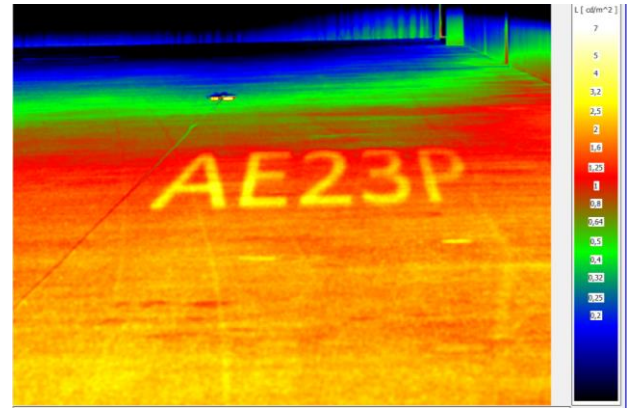


Figure 9: Luminance Analysis of Fig. 6
Average Luminance of the letters
was about 2 ± 1 cd/m²

The given contrast and luminance in the test depends on the performance of the low beam with illumination in about 20 m distance. The reflectivity of the road then leads to the perceived luminance and a positive contrast projection.

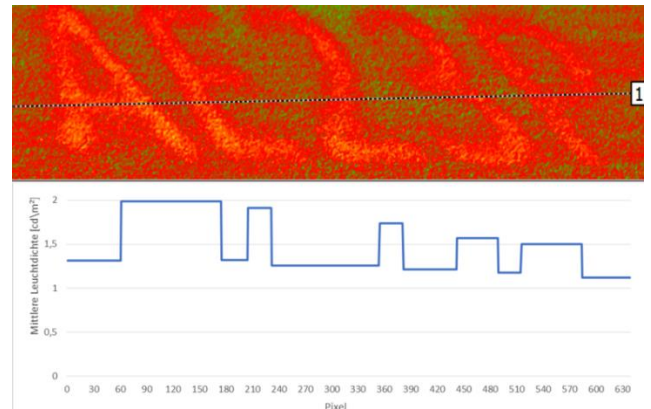


Figure 10: Contrast and luminance investigations with example “AE23P”.

The Luminance and the resulting contrast were not constant and additionally depending on the actually chosen observation position.

The maximum recorded luminance in the investigated window was $L=1,988$ cd/m², the minimum luminance in the field was $L=1.112$ cd/m².

$$C = \frac{L1-L2}{L1+L2} = \frac{1.988-1.112}{1.988+1.112} = 0.279 \quad \text{eq (1)}$$

Following the Michelson Contrast formula [8], (eq (1)) the contrast was determined to $C= 0.279$.

4.2.1 Luminance Analysis Letter "E"

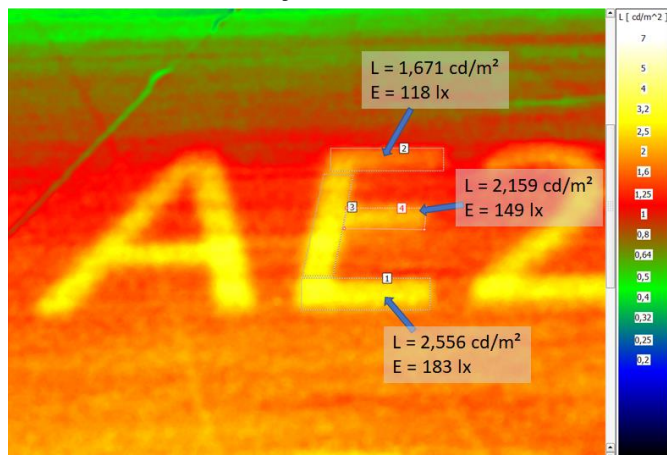


Figure 11: Luminance Analysis of Letter "E" out of driver's perspective. Average Luminance of complete letter was 2,31 cd/m²

A Look to the measured luminances in Figure 11 shows that due to illuminance decay of distance and also the lateral inhomogeneities the luminances are not constant. Overall the letters are measured with about 2 cd/m². A more detailed look to the letter "E" shows that the measured perpendicular illuminance varies from 183 lx at the bottom to 118 lx to the upper part of the letter. Thus also the luminance varies from 2,556...1,671 cd/m² in the different segments.

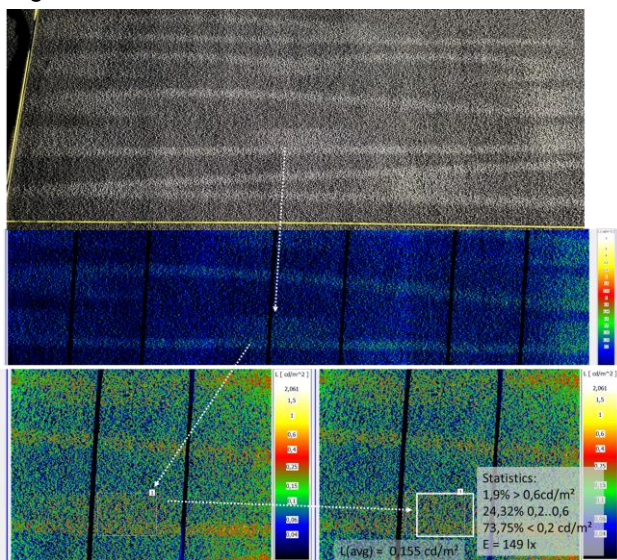


Figure 12: Photo and Luminance Analysis of the center of the Letter "E" out of bird's eye perspective. (see Figure 8, 9&11) Average Luminance of the "E" center was 0,155 cd/m²

A detailed analysis of the center of the letter "E" shows that the luminance from driver's perspective is 2,159 cd/m² (see Figure 11) but drops in bird's eye perspective to 0,155 cd/m² (see Figure 12).

This position-based luminance variation reaches a factor of 14.

Additionally the roughness of the street surface is heavily contributing to the inhomogeneous pixel-level luminance, supported by the grazing incidence. With headlamps mounted $a = 80$ cm and an object in $b = 2200$ cm there results a small illumination angle of $\alpha = 2,082^\circ$

The sub-segment of "E" in Figure 12 shows: Only 1,8 % of the surface carries 0,6 cd/m² and higher, but 73,75 % of the surface is quasi dark, below 0,2 cd/m².

4.3. Summary Geometry and Luminance

Both factors, geometry and luminance contribute heavily to the readability. On one hand the readability worsens because the original picture was distorted in such a way, that optimum readability is achieved from driver's perspective. The 5,6:1 shape (width x height) is quasi-inverted to 1:5,3. Luminance shows a dramatic decay with a factor of 14 from driver's to bird's eye perspective. Both elements make readability hard outside the optimum position.

5. Test Person Experiments

5.1. Test Setup

A total of 17 Test persons were involved. The average test person age was 38 years, spreading from 21 to 58 years. Gender distribution was 14 male, 3 female subjects. All test persons passed a visual performance check. Threshold was a visual acuity level with a visus $V > 0,8$.

Like in reality, Low Beam was switched on together with the digital projection. In total, the projections created a luminance of about 2 cd/m² from driver's perspective (see Figure 9-12).

5.2. Digital Mapping of the readability area.

In order to be able to allocate the geometrical readability, a mapping structure of 1x1 m squares was created around the scenery (see Figure 13). The grid was created in a light tunnel with the chance to create a map about 60 m in both directions and up to 8 m in lateral extension. A total area of 960 m² was covered. Under the assumption that the legibility of symbols is symmetrically possible from both sides, only the left side as shown in Figure 13 was used.

On each position in the grid a new letter-number combination was presented. The 50 letter-number combinations were used in order to extract the real data by avoiding any memory possibility. The test

persons were moved along the grid, task was to read each time the combination.

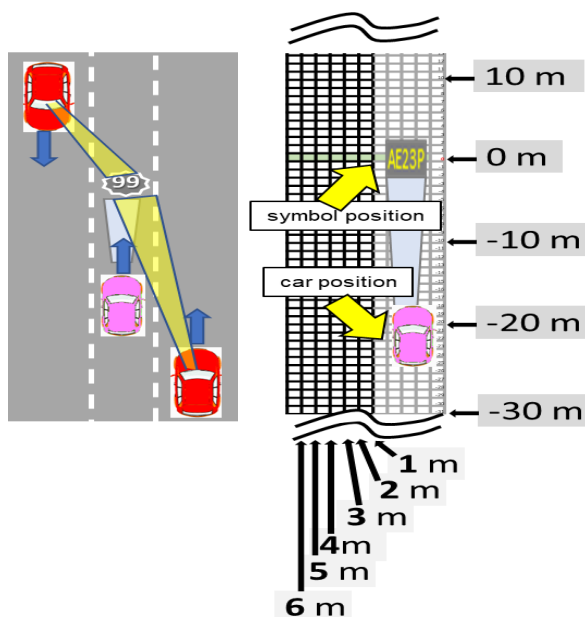


Figure 13: Potential visibility area and readability map used in the investigation. Overtaking and opposing could happen on both sides. The results were assumed to be mirrored for Left Hand Drive / Right Hand Drive.

The test persons were divided in two subgroups. One group was allowed to take whatever time they needed to identify the number-letter combination and tell it to the supervisor (Free Time group). The second group experienced a 5 second presentation slot on each position in the mapping grid. The 5 seconds were chosen due to the time recommendation for presenting 5 optotypes to special test persons [7] (5 Sec group).

A “heat map” was generated to visualize the variations on readability inside the mapping grid (Figure 14). The red areas indicate that none of the test persons were able to read the combination. The darkest green shows that all test persons were able to read the combination.

5.3. Overtaking Situation Total Readability

The overtaking situation investigated the perspective where a car from behind the test vehicle approaches. (See Figure 13) Like described above, the test persons were moved in the mapping grid in order to check their ability to read the combinations. They had no restriction in time to be able to read. Generally, the further the distance and the more lateral distance they had; the more time was needed to come to a result.

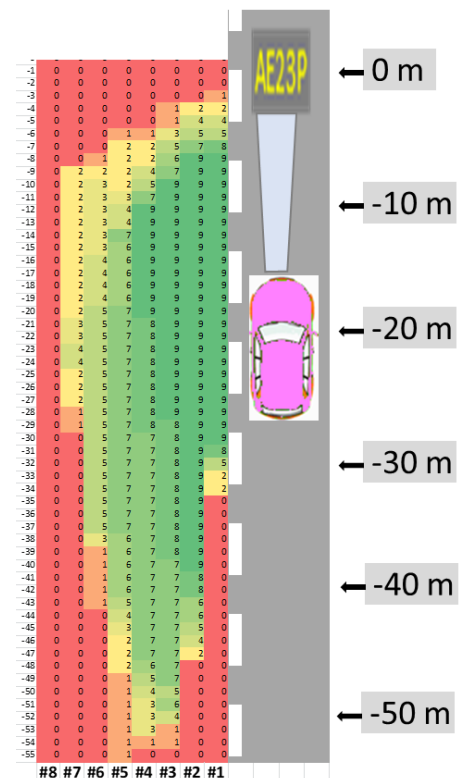


Figure 14: “Heat Map” Distribution of readability area with color variation from NONE can read (=red) to ALL (=green). Overtake Situation, Free Time.

Especially at the 5 m grid lane and further there were not all test persons able to identify the combination. Beyond 7 m distance not a single Test Person was able to read in any Position. Longest readability was found in grid lane #2 with full readability from -39 m to -8 m, giving 31 m full readability distance.

In total only 84 m² were found where all test persons could read the combination.

When looking to the average distances of readability, the heat map in Figure 14 indicates that the standard deviation in grid lane #1 must be significantly lower than in grid lane #5 and beyond.

5.4. Oncoming Situation Total Readability

The oncoming or situation investigated the perspective where a car from the opposite distance approaches the test vehicle (see Figure 13). The heat map is displayed in Figure 15. All test persons had Free Time to decide what the combination said.

Only in the inner lane #1 all test persons were able to read the letter combination in at least one position. In total only an area of 5 m² was determined where all test persons could read a combination. Starting from lane #2 the analysis showed that in the identical 1x1 m lane grid some persons were not starting to read, while others already stated they could not read any more.

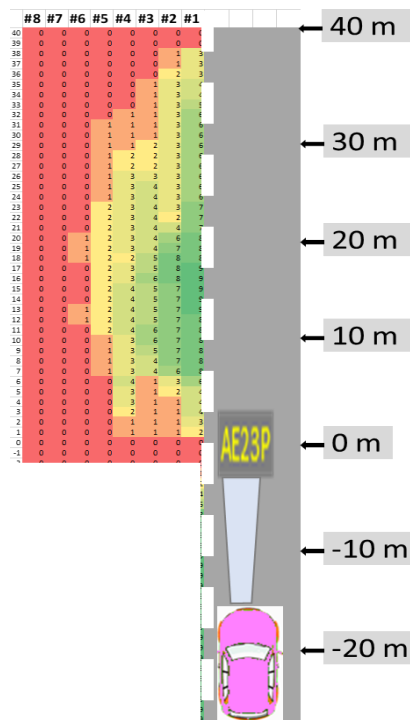


Figure 15: "Heat Map" Distribution of readability area with color variation from NONE can read (=red) to ALL (=green). Oncoming Situation, Free Time.

5.5. Statistical Average Area of Readability

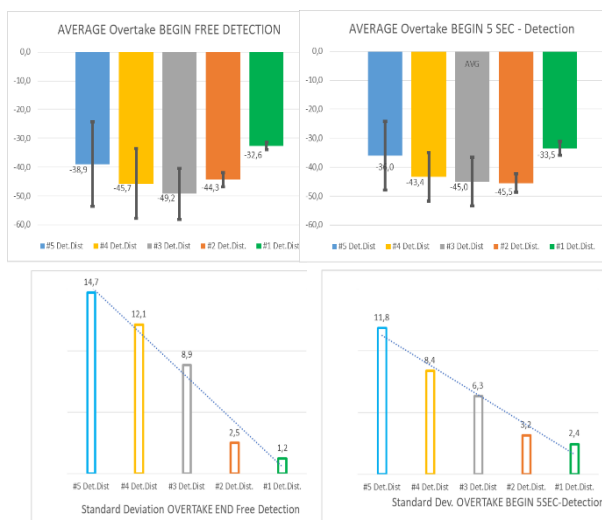


Figure 16: Statistics (Free Time and 5 Sec)
Average begin of the readability and Analysis of the standard deviation from line#1 to line#5.

From the recorded data of Test Person's beginning of detection, the average readability distance was created. (See Figure 17) Criterion was that minimum 50 % or more test persons were able to read the combinations at all.

As indicated by the heat map in Figure 14, the standard deviations show a strong increase with increasing lane distance to the projected

combinations. Figure 16 "Free Time" shows the statistics for the beginning of readability. Line #1 gives a being of 32.6 m with a standard deviation of 1.2 m. Line #5 gives an average readability start of 38.9 m and a standard deviation of 14.7 m.

That means, the standard deviation varies with a factor of about 12 between the lane #1 and lane #5. In short words: the longer the distance, the higher the uncertainty. Good readability is obviously no longer possible in bigger distance.

Both results of subgroups do not significantly differ. The average results of the "Free Time" group are within or close to the standard deviations of the "5 Sec" group.

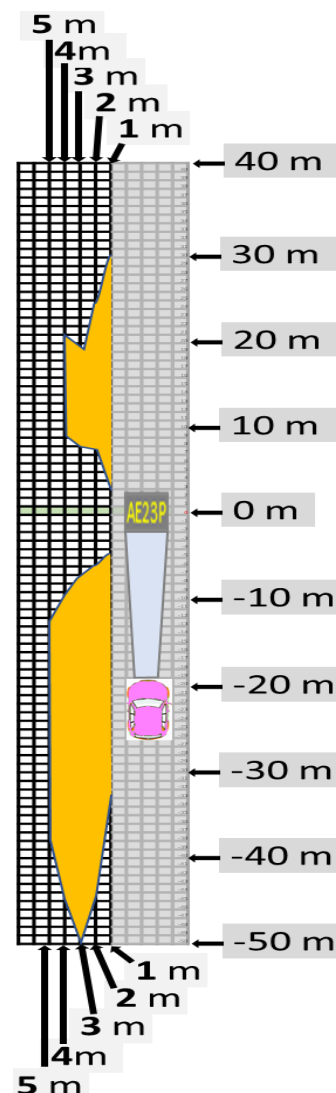


Figure 17: Average Readability Zone for the letter-number combinations.

For each grid lane and for both situations (oncoming, overtaking) the start and end of readability was recorded. From the above-described results, each start and end was averaged for all test persons. Thus, the statistical average area was built. In Figure 17 the complete Readability Zones for the symbol

projections are given. The “Oncoming” zone is compared to the “Overtaking” Zone significantly smaller. Figure 18 shows the Oncoming marking in the light tunnel with red pylons.



Figure 18: Average Readability Zone marked in the light tunnel with pylons. Oncoming Situation.

6. Transformation to Real Traffic

6.1. Overtaking Car

The Average Readability Length (see Figure 17) is translated into real traffic. Some speed assumptions had to be defined. In an overtaking situation, the car with digital projections was assumed with about 80 km/h, (i.e., about 50 mph) the overtaking car was assumed with about 100 km/h (i.e., about 62 mph). The resulting delta speed is 20 km/h (i.e., about 12,5 mph). 20 km/h equals 5.55 m/sec.

A normal lane width of 3.50 m is assumed and a normal overtaking lateral distance where the overtaking car is centered in its overtaking lane. As a result, the driver's eyes of the overtaking car are in about 3.5 m distance to the projection. For geometry reference, see Figure 17.

The average of both groups was built for an average begin and end of readability (or detectability).

Takeover Situation	FREETIME Begin	5 SEC Begin	FREETIME End	5 SEC End	Total Delta	Visible Timeslot
3m	-43,38	-45,67	-9,38	-9,67		
4m	-45,00	-49,22	-7,13	-7,33		
		Begin		End		
AVG Lateral Distance: 3.5m		-45,82		-8,38	37,44	
Assumption: Delta 20km/h = 5,55m/sec						6,7 sec

Table 1: Average Readability Length for Overtaking Vehicle (data in meters)

Table 1 shows: The average length of readability is about 37 m. An overtaking driver or respectively an overtaken driver would have 37 m to realize what is projected in front of the vehicle he is just overtaking.

Assuming 5.55 m/sec gives that he would have a window of about 6.7 sec to read or discover what the projections are giving.

Under the perspective that the eye tracking data showed that more than 98% of all glances the drivers

look to different areas, it is even more unlikely they will read or thus start to be distracted.

6.2. Oncoming Car

The average readability length for oncoming vehicles (Figure 17) are translated into real traffic.

In an oncoming situation, the car with digital projections was assumed with about 80 km/h, (i.e., about 50 mph) the oncoming car was also assumed with about 80 km/h (i.e., about 50 mph). The resulting delta speed is 160 km/h (i.e., about 100 mph). 160 km/h equals 44.44 m/sec.

A normal lane width of 3.50 m is assumed and for both cars each car is centered in its lane. (see the dimensions in Figure 17). As a result, the driver's eyes of the oncoming car are in about 2 m distance to the projection.

The average of both groups was built for an average begin and end of readability (or detectability).

Oncoming Situation	FREETIME Begin	5 SEC Begin	FREETIME End	5 SEC End	Total Delta	Visible Timeslot
2m	25,00	30,00	7,90	8,30		
		Begin		End		
AVG			27,50	8,10	19,40	
Assumption: Delta 160km/h = 44,44 m/sec						0,43 sec

Table 2: Average Readability Length for oncoming vehicle (data in meters)

Table 2 shows: The average length of readability is 19.4 m. An oncoming driver would have 19.4 m to realize what is projected in front of the vehicle he is just overtaking.

Assuming 44.44 m/sec he would have a window of about 0.43 sec to read or discover what the projections are giving. This is under normal conditions impossible to realize.

6.3. Pedestrians

Worst case scenario would be that pedestrians are close to the driving lane in about 1 m lateral distance. With an oncoming car of 80 km/h the relative speed would be 22.22 m/sec. Table 3 shows: A pedestrian would have about 26.4 m readability. With 22.22 m/sec he would have 1.2 seconds time to detect a moving projection and start to feel distracted. Pedestrians on the opposite side walkway (< 4m) would be completely unable to read or see.

Pedestrian Situation	FREETIME Begin	5 SEC Begin	FREETIME End	5 SEC End	Total Delta	Visible Timeslot
2m	30,40	34,50	4,20	7,90		
		Begin		End		
AVG			32,45	6,05	26,40	
Assumption: Delta 80km/h = 22,22 m/sec						1,2 sec

Table 3: Average Readability Length for Pedestrians close to the driving lane (data in meters)

All Transformation calculations assume as worst-case basis that there is comparable readability even when the observation geometry is dynamically changing. The observed objects change their shape

and luminance in each position. Thus the calculated reading areas in real life might be even smaller and should be subject to subsequent studies.

In [9] TU Darmstadt presented an investigation about visual latencies. Basic recognition latency was 300 msec for distortion-free perpendicular viewing for one letter. Considering results in this paper with dynamic and variable distortion, at or below a pedestrian detection time of 1,2 sec it can be assumed this is not sufficient to read a dynamically changing multi-letter figure or complex symbol.

7. Summary/Conclusions

There is a very small and limited area where digital projections are readable or detectable at all outside of the car. About 94 m² for overtaking situations were visible to all test persons. The anyhow limited area for visibility in overtaking shrinks in oncoming situation again by 95 % to 5 m². Only from driver's view the grazing incidence is virtually compressed and symbols are fully legible as an 0,5° object. The readability decay is very quick, 6 m aside of the projections the readability approaches zero. The Luminance varies due to the distorted projection by a factor of 14.

The time window for visibility for oncoming vehicles is with 0.43 sec negligible. No oncoming driver will realistically be able to read. Pedestrians at the side of the lane will not be able to follow the projections and read. Even when they are close to the driving lane, the resulting readability time of a moving pattern would be only 1.2 seconds.

Only when overtaking there might be sufficient time to read or detect the digital projections. But about 6.7 seconds visibility slot under the situation stress of overtaking (lane keeping, speed keeping, traffic scene observation etc.) seems to be not enough to create a window for reading, evaluating and feeling distracted or anything else.

Timeslot summary: Other traffic participants have an extremely limited time and geometrical window to even read what the driver sees. This corresponds well to the questionnaires and eye tracking research.

It can be derived that because of grazing incidence any road projection must be tailored to a very precise, most probable position for an out-of-car observer. Due to the dynamic change of the legible geometry and luminance the real time slot for understanding the meaning of the projection is even smaller than the worst-case assumption in this investigation.

The conclusion of the presented investigation: There is not enough time to be distracted by digital projections. They are made for the driver and permanently only visible for the driver and nobody else. The dynamic distortion change of the projection's shape is a fact of limitation to detect or read.

The remaining conclusion: There are only benefits found for digital projections and no negative effects for other traffic participants.

8. References

- [1] Driver Assistance Projections 2019. GTB Presentation to support informal document GRE-82-04
<https://unece.org/fileadmin/DAM/trans/doc/2019/wp29gre/GRE-82-40e.pdf>
- [2] Hamm, M., Huhn, W. Reschke, J.: Ideas for Next Lighting Generations in Digitalization and Autonomous Driving. SAE Paper 2018-01-0516.
- [3] Budanow, M. et.al.: Information System for Car Drivers Based on Projections on the Road. In: Proceedings IFAL 2018. Shanghai: Fudan University, 2018.
- [4] Rosenhahn, E.-O., Link, F.: Traffic Safety Benefits provided by High Resolution Headlamp Systems. In: ISAL, Vol 18. München: Utz, 2019. pp 239-248
- [5] Polin, D., Khanh, T. Investigation on Headlights with High-Resolution Projection Modules. In: ATZ Worldwide 70–73 (2018).
<https://doi.org/10.1007/s38311-018-0174-9>
- [6] Lachmayer R., Glück, T. et. al.: Distraction Potential of Road Projection Symbols. Leipzig Universität Hannover, 2020.
<https://unece.org/fileadmin/DAM/trans/doc/2020/wp29gre/GRE-83-34e.pdf>
- [7] Westermann, H.: Die Grenzen der Sehstärke, T.4. In: DOZ - Deutsche Optikerzeitschrift. V.02, 2002.pp.32-38
- [8] Colour Usage Research Lab. Nasa AMES Research Center: Luminance Contrast.
- [9] Klabes, J.; Babilon S. et.al.: The Sternberg Paradigm: Correcting Encoding Latencies in Visual and Auditory Test Designs. Vision 2021, 5, 21.
<https://doi.org/10.3390/vision5020021>

Contact Information

Dr. Michael Hamm, Audi AG, Germany.
email: michael.x.hamm@hotmail.com

Christian Hinterwälder, Audi AG D-85045 Ingolstadt, Germany. email: christian.hinterwaelder@audi.de

Dr. Jonas Kobbert, Audi AG, D-85045 Ingolstadt, Germany. email: jonas.kobbert@audi.de

The authors like to thank the Audi Bachelor and Master Students Julia Hoffmann, Markus Braun and Luca Fuso for their support in executing the research setup and generating the data.

Review of user's evaluation and the needs for road projections around a vehicle

M. Sc. Alexander Stuckert^{1,2}, M. Sc. Tabea Schlürscheid^{1,2}, Prof. Dr.-Ing. Tran Quoc Khanh²,

1: BMW Group, Germany

2: Technical University of Darmstadt, Germany

Abstract: Within the last years the development in projection technology, particularly the wide usage of DMD, LCD, or LCoS projectors, enables the broad application of pico-projectors in the automotive sector. Consequently, this implies a high demand to apply projections for various applications in future vehicles, such as communication between a highly automated vehicle and other road users. However, there are already projectors implemented nowadays in cars, yet mostly static projections next to the vehicle, typically showing brand or model illustrations, or simple design graphics.

This article evaluates the needs of participants from three independent studies regarding the projected content. In addition to the projection content, the characteristics of a high-quality projection are part of the surveyed customer opinion.

Keywords: near-field projection, user needs, projection content, quality aspects, additional lighting function

1. Introduction

The design of a vehicle determines not only the character and the look of a car, it is one of the main reasons for buying a new car according to the ADAC customer barometer [1]. Lighting technology gives the possibility to emphasize the vehicle design. Besides the widespread usage of daylight signatures in the vehicle's front or back, the use of a projection system gets more popular. Projection technology applications are projections for driver assistance [2, 3], such as navigation or indication of guiding lines, and for communication [4-6] with other road users, like pedestrians or cyclists. Other researchers include in their projects the importance of safety-related near-field projections with the corresponding prototype proposals for such projection engines [13,14]. Although so far, no research faculties have tried to investigate the user's needs for road projections around the car. Colley et. al [7] have investigated the requirements if the vehicle would be the projection surface and stated that the quality and sharpness of the projections play a significant role in the appearance.

Under these circumstances, it is necessary to evaluate the opinion of relevant content, which is displayed next to the vehicle. Another question is what aspects are meaningful for the users when

talking about high-quality projections. This article summarizes three independent surveys (n1=70, n2=50, n3=25) to evaluate the opinion on road projections. Therefore, the three studies vary among each other depending on two influence factors: First, studies No. 1 and No. 3 evaluate if the presented brightness of the near field projection influences the subjects' answers. This factor may influence the results because the participants get the questionnaire after participating in the study with a different brightness level in each study. Second, an analysis of the survey's timing in studies No. 1 and No. 3 compared with study No. 2 evaluates the conditioning of the subjects. If there is a recognizable bias of the answers when presenting the questionnaire before and after the participation in the subject study. This paper just focuses on the answers of the questionnaires of all three studies.

2. Materials and Methods

2.1 Overview and subjects

Overall, 145 subjects, who were workers in the company, participated in the three surveys. The independent surveys took place within a half year at the BMW campus. In all studies, the subjects viewed a ground projection in the near field of a vehicle. The setup used for the ground projection was the same in all studies.

Study No. 1 and Study No. 3 dealt with the required image quality of a high-quality ground projection. The subjects answered a questionnaire after the actual subject test where they saw the displayed ground projection. The study setup and investigated parameters were the same in studies No. 1 and No. 3, but under different environmental illumination. Study No. 2 investigated the required visibility of a high-quality ground projection in different illumination scenarios. The subjects of study No. 2 filled out a questionnaire before the study.

Table 1 displays the average age of the subjects in the respective studies.

Table 1: Depiction of the number and average age of the participants of the three studies.

Survey	No. 1	No. 2	No. 3
n	70	50	25
Average age (SD)	34,86 (10,75)	34,49 (10,47)	35,56 (12)

2.2 Questionnaire design

All three questionnaires were paper-pencil tests, as these suit best for on-site subject studies. They were individual tests, as each respondent completed one questionnaire.[8]

Possible formats of task types are free-response options, bound-response format, and atypical-response format. The ones used in the present questionnaires contained a bound-answer format. Bound-answer formats are subdivided into order-, choice-, and assessment tasks. Therefore, several alternatives for a possible answer are prefabricated. This facilitates an evaluation to record necessary and important factors of a ground projection.[8]

In all three studies, the first segment of the questionnaires consisted of personal questions about gender, age, and prior knowledge of lighting technology. All tasks except the question about prior knowledge of the subjects had a free-response format. The question about the lighting knowledge used a rating scale [9]. The second part of the questionnaires evaluated the characteristics content and important aspects of a vehicle's near field ground projection, such as content and aspects. Questionnaires No. 1 and No. 3 used a different approach compared to questionnaire No. 2.

To obtain an overview of the prior knowledge of lighting technology for the test subjects, the questionnaire raised the question, "Do you have previous knowledge of lighting technology?". The used answer format was a discretely graded bipolar Likert scale, which can be clearly distinguished by the participants [9,11]. The rating scale divided the knowledge level into six points from "1: Does not apply at all" to "6: Applies completely". For the evaluation, these knowledge levels corresponded to "expert" (answer options 1-2), "neutral" (answer options 3-4), and "layperson" (answer options 5-6).[8]

One question raised in all studies dealt with the importance of several aspects for a high-quality ground projection in a vehicle's near field. Questionnaire No. 1 and No. 3 used a bound response format with a multiple-choice task and seven possible answers. The response format of the questions was item-specific. The participant checked all the aspects they considered as important for a ground projection. In addition, own additional aspects could be specified. Possible aspects to select were: Brightness, Resolution, Contrast, Size, Colour, Colour fidelity, Sharpness. Some aspects, such as "Resolution" and "Sharpness" were mentioned several times by other expressions to get a better picture of the answers.[8]

Study No. 2 used a bound response format as well. The used assessment task worked with a discrete-graded, unipolar, asymmetrical 4-step Likert rating scale [9,11]. The task evaluated a total of eight

aspects. The task divided the response dimensions into intensities from 1 to 4 ("1: not important", "2: less important", "3: important", "4: very important"). To prevent the participant's tendency to tick the middle of the rating scale, the task used an asymmetrical scale [8,9,10,11]. Aspects to be evaluated in the question were: Colour, Size, Dynamic, Brightness, Resolution, Content, Visible during night, Visible during day. Since, all three questions included the four aspects "Resolution", "Brightness", "Colour" and "Size" these aspects will be compared with each other in the results.

Another aspect in the questionnaire dealt with the possible content for a ground projection in the near field next to the vehicle. However, the question in Study No. 1/No. 3 again consisted of a tied item-specific response format. A multiple-choice approach was used. There are a total of five answer options. All answer options that apply should be selected. Additionally, own answers can be given in a free field [8]. The possible content answers were: Welcome-Goodbye-Message, Weather information, Vehicle information, Design illustration, Route information.

In Study No. 2, the question on contents of a ground projection consisted of an ordering task with a bound-response format. The question consisted of an assignment task with five answer options [8,10]. The numbers 1-5 had to be assigned only once each to evaluate the individual contents ("1: best", "5: worst"). The subjects placed the contents "Design Illustration", "Vehicle Information", "Other Information", and "User Defined" in order. All three questions included the contents "Design illustration" and "Vehicle information". They will be compared with each other in the results.

The question method used in the questionnaires of Study No. 1 and Study No. 3 enabled a general overview of the preferred aspects and contents for a ground projection. The used rating scales in the questionnaire of study No. 2 assign a rating to the mentioned aspects and give a more precise and weighted insight into the opinions of the test person. Therefore, the comparison of individual aspects and contents is more important and simpler. In addition, the results can be statistically analyzed [8,10].

3. Results

In this section, detailed results of every study are illustrated regarding aspects for high quality and projection content.

3.1 Questionnaire No. 1 & No. 3

The questionnaire covers a subjective opinion of the participants regarding aspects for high-quality projections. The results are separated by the percentage below and above 50% of every study. Therefore, four characteristics gained more than 50% in study No. 1 and study No. 3: "Sharpness",

“Resolution”, “Brightness”, and “Contrast”, which are illustrated in detail in Figure 1. However, four characteristics were voted less relevant by the subjects: “Colour”, “Colour fidelity”, “Size” and “Others”, which are indicated in Figure 1 in detail with the corresponding percentages.

Altogether, Figure 1 summarizes the aspects in five groups. First, “Sharpness” and “Resolution” are indicators for image quality and are rated above 76% in both studies. Second, “Brightness” and “Contrast” are markers for the visibility of the projection and reached percentages from 74% to 80% in both studies. Third, the aspects “Colour” and “Colour fidelity” represent the colour aspects and gain a percentage from 28% to 44% depending on study No. 1 or No. 3. The fourth and fifth groups are “Size” and “Others” which are unique for themselves and indicate a specific condition. Given these points, all participants in studies No. 1 and No. 3 demonstrate that image quality and visibility are the most outstanding characteristics.

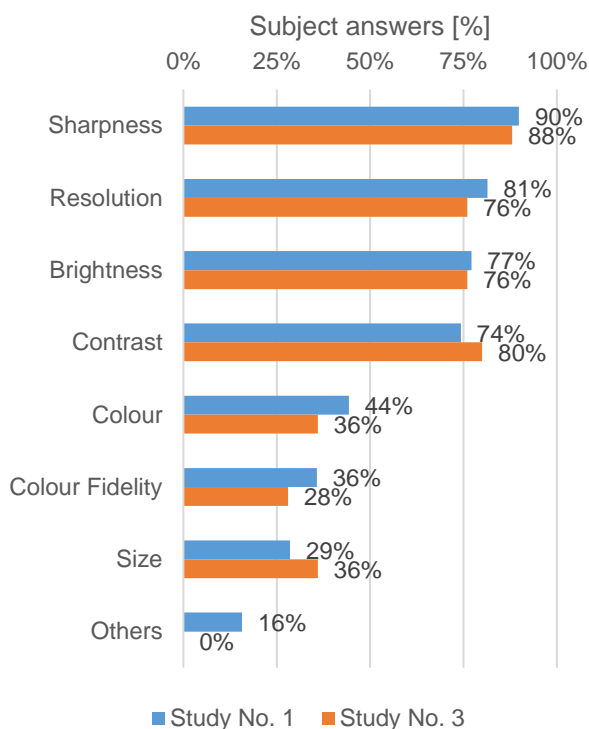


Figure 1: Illustration of the question “What other aspects are necessary for a high-quality projection?”, which includes aspects such as sharpness, resolution, brightness, contrast, colour, colour fidelity, size and others with the percentual. The aspects are sorted by frequency of study No. 1.

Figure 2 displays the response rate in percent according to the aspect of the preferred content for a ground projection. The results can be separated for both studies (No. 1 and No. 3) in two groups (over or

below 50% answer rate) for the preferred content of a near field projection. Therefore, three items in both studies are rated over 50% according to the answered questionnaires by the subjects: “Vehicle charging status”, “Design illustration” and “Welcome/ goodbye message”. Nevertheless, three other aspects reached less than 50% by every subject collective the questionnaire: “Other”, “Weather information”, and “Route information”, which leads to a lower priority compared to the other projection content aspects. After all, the most relevant content for the participants of study No. 1 or No. 3 is either informative regarding the charging status, a design statement, or a personalized message when entering or leaving the vehicle, which is covered with the aspects rated above 50% in Figure 2.

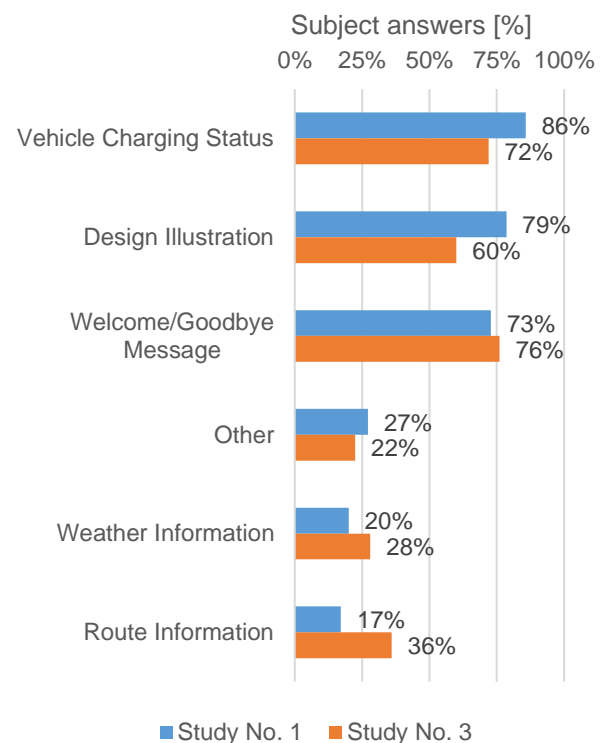


Figure 2: Illustration of the asked projection content items with the correspondent answers in. The aspects are sorted by frequency of study No. 1.

3.2 Questionnaire No. 2

The response distributions of the questions in study No. 2 related to the preferred contents and aspects of a high-quality projection in the vehicle's near field, which are illustrated in boxplots (see Figure 3,4,5,6). Therefore, two questions were answered with a Likert Scale including four or five points. The boxplots show the total of all answers for, first, the individual aspects and, second, the projection contents that were evaluated - outliers, upper and lower whiskers, the upper and lower quartile as well as the mean (marked

as a cross per boxplot) and the median (indicated with a red line per boxplot) are shown.

Figures 3 and 4 show the distribution of the answers to the question related to essential aspects of a ground projection in the vehicle's near field. The response scale of the question ranges from "1: not important", "2: less important", "3: important" to "4: very important". Based on Figure 1 all medians of the queried aspects are above the mean value of the rating scale of 2.5. Therefore, the medians of all aspects were in the agreeable range. The smallest median is 3, which is the case for the aspects "Colour", "Size", "Dynamic", "Content" and "Resolution". So, they are still considered as "3: important". The lowest mean value is found for the aspects "Colour", "Dynamic" and "Size". In all 3 cases, the mean value is below 3 and therefore in the lower range of the rating scale. These aspects are considered as less important since the mean value is below "3: important". Almost a quarter (23%) of the subjects rated the aspect "Colour" as "1: not important" (Figure 4). The highest ratings and thus the largest mean values are found in the aspect "Visible during the night", which has a mean value of 3.79 and a median of 4 (Figure 3). The spread of the answers, in this case, is low and predominantly the "4: very important" was given as an answer. In total 79% of the subjects rated the aspect "Visible during the night" with the highest answer "4: very important" (Figure 4). Likewise, high ratings of the Likert scale and thus median values result for the aspects "Brightness" (m=3.64) and "Resolution" (m=3.38). In this case, 66% of the participants rated the aspect "Brightness" with a "4: very important" and half of the collective (51%) for the aspect "Resolution" (Figure 4). None of the three aspects were rated with "1: not important" by the test persons. Overall, no clear tendency can be discerned for the aspects "Content" and "Visible during the day", as the spread of responses is large since the lower and upper quartile are far apart.

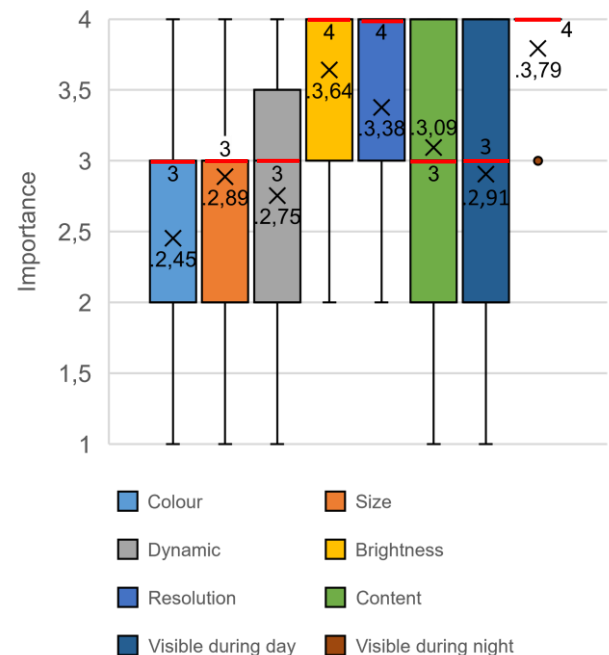


Figure 3: Illustration of the question: "How important do you consider the following aspects with regard to a road projection?", which displays the aspects "Colour", "Size", "Dynamic", "Brightness", "Resolution", "Content", "Visible during day", "Visible during night" with the correspondent answers shown in Boxplots over the rating scale from "1: not important", "2: less important", "3: important" to "4: very important" for study No. 2 with 50 participants. Values of the mean (marked with cross (X)) and median (marked with red line (-)) are included.

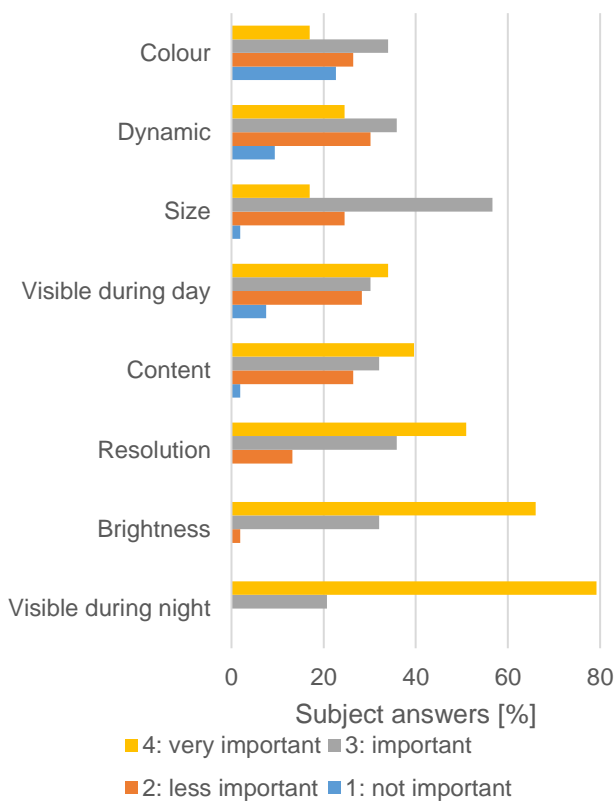


Figure 4: Illustration of the question: "How important do you consider the following aspects with regard to a road projection?", which displays the aspects "Colour", "Size", "Dynamic", "Brightness", "Resolution", "Content", "Visible during day", "Visible during night" (sorted by mean) with the correspondent answers shown in percentage of the subject answers (1 -4; 1: not important" to "4: very important") over the different aspects for study No. 2 with 50 participants.

Statistical tests are carried out to determine significant differences between the individual aspects. Since the dataset is normally distributed, a one-factor analysis of variance using ANOVA can be applied. There are significant differences, which are examined in more detail using a t-test ($\alpha < 0,05$). Table 2 lists the corresponding p-values for the comparison of the individual aspects regarding their importance. The aspect "Colour" is rated significantly lower than all other aspects and is therefore significantly less important. The aspect "Visible during night" is considered significantly more important in comparison. "Brightness" is rated significantly better for all aspects except for "Visible during night". There is no significant difference in the evaluation between "Size", "Dynamic" and "Brightness".

Table 2: Calculated p-values of the t-test with an error of $\alpha = 0,05$ for the importance of the aspects of a ground projection. Aspects listed by size of mean in descending order. If $\alpha < 0,05$ there is a significant difference between two aspects.

1.Visible during night	p-value	2.Brightness	p-value
X Brightness	0,02219	X Resolution	0,00247
X Resolution	0,00027	X Content	0,00023
X Content	1,55122 $\cdot 10^{-6}$	X Visible during day	1,03122* 10^{-6}
X Visible during day	2,54182 $\cdot 10^{-10}$	X Size	3,76807* 10^{-10}
X Size	2,46479 $\cdot 10^{-12}$	X Dynamic	3,37666* 10^{-9}
X Dynamic	1,38485 $\cdot 10^{-9}$	X Colour	1,91891* 10^{-11}
X Colour	4,10411 $\cdot 10^{-13}$		
3.Resolution	p-value	4.Content	p-value
X Content	0,03949	X Visible during day	0,14536
X Visible during day	0,00172	X Size	0,07339
X Size	0,00044	X Dynamic	0,02426
X Dynamic	4,08674 $\cdot 10^{-5}$	X Colour	0,00065
X Colour	3,37234 $\cdot 10^{-7}$		
5.Visible during day	p-value	6.Size	p-value
X Size	0,45639	X Dynamic	0,16097
X Dynamic	0,20471	X Colour	0,00261
X Colour	0,00799		
7.Dynamic	p-value		
X Colour	0,04779		

Finally, the aspects "Visible during the night", "Brightness" and "Resolution" are the most important aspects for a high-quality ground projection in the near field of a vehicle for the subjects. In contrast, "Colour", "Size" and "Dynamic" are considered less important.

Another question in the questionnaire of study No. 2 refers to the preferred represented content of a ground projection. The corresponding answer options are given from "1: worst" to "5: best". Each number could only be given once. Figures 5 and 6 show the distribution of the answers to the question related to the preferred content of a ground projection in the near field of a vehicle. With a median of 5 and a mean of 4.11, the content "Design Illustration" is rated best (Figure 5). In total 58% of the subjects rated the subject with "5: best" (Figure 6). The content "Vehicle Information" has a median of 4 and a mean of 3.49 and is therefore in the positive range of the rating scale (Figure 5). Additionally, the "Safety Feature" is rated greater than 3 with a median of 3 and a mean of 3.28 by the subjects, which corresponds to the middle of the rating scale, which is perceived positively

(Figure 5). The two contents "User-Defined" and "Other Information" are rated worst. Both medians of the response distributions are 2 and thus in the lower third of the given scale. The mean values of the two content examples show a value of < 2.5 . With a mean value of 2.11, the content statement "Other Information" is rated the worst. For "User Defined" 42% and for "Other Information" 38% of the subjects rated the contents with "1: worst" (Figure 6).

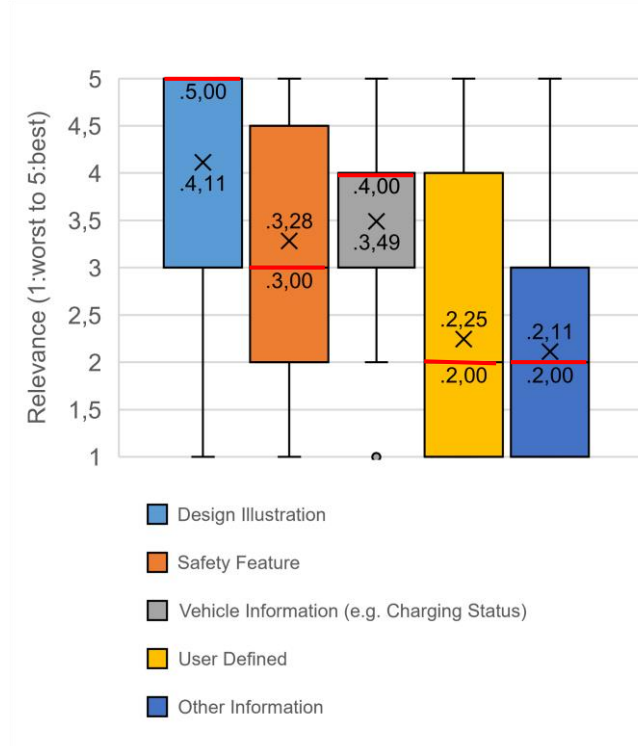


Figure 5: Illustration of the question: "What content of a road projection do you prefer?", which displays the items "Design illustration", "Safety feature", "Vehicle information", "User defined" and "Other information" with the correspondent answers shown in Boxplots over the rating scale from "1: worst" to "4: best" for study No. 2 with 50 participants. Values of the mean (marked with cross (X)) and median (marked with red line (-)) are included.

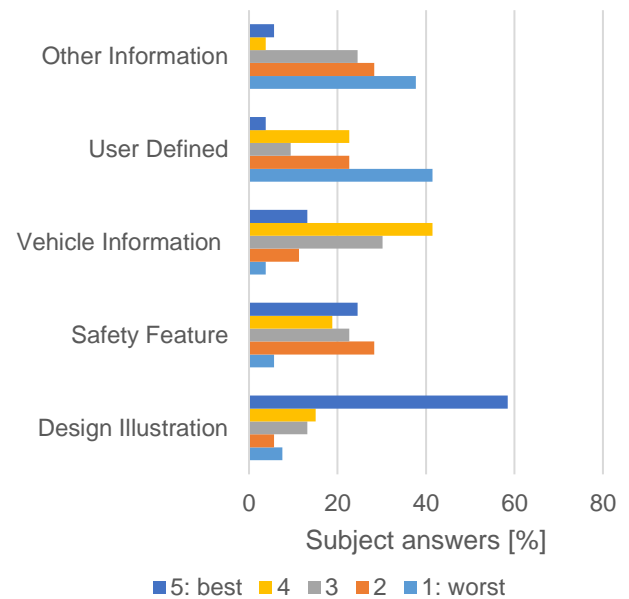


Figure 6: Illustration of the question: "What content of a road projection do you prefer?", which displays the items "Design illustration", "Safety feature", "Vehicle information", "User defined" and "Other information" (sorted by mean) with the correspondent answers in percentage of the subject answers for the items shown over the different ratings (1 -5; 1:worst" to "5:best") for study No. 2 with 50 participants.

When looking at the individual contents via statistical tests using the ANOVA and t-test, significant differences can be seen in some cases ($\alpha < 0,05$). Table 3 lists the corresponding p-values for the comparison of the individual contents about their preference. The content "Design Illustration" shows a significantly better rating compared to all other contents. There is no significant difference between the ratings of "User Defined" and "Other Information". However, all other aspects are rated significantly better than "Other Information".

Table 3: Calculated p-values of the t-test with an error of $\alpha=0,05$ for the preference of the contents of a ground projection. Contents listed by size of mean in descending order. If $\alpha<0,05$ there is a significant difference between two contents.

1. Design Illustration	p-Value	2.Safety Feature	p-Value
X Safety Feature	0,00566	X Vehicle Information	0,16878
X Vehicle Information	0,01048	X User Defined	0,00087
X User Defined	$7,3113 \cdot 10^{-12}$	X Other Information	$7,27595 \cdot 10^{-7}$
X Other Information	$5,21508 \cdot 10^{-10}$		
3.Vehicle Operation	p-Value	4.User Defined	p-Value
X User Defined	$1,84122 \cdot 10^{-5}$	X Other Information	0,31473
X Other Information	$7,42909 \cdot 10^{-9}$		

Overall, the subjects predominantly prefer "Design Illustration" and "Safety Features" as possible contents for ground projections in the near field of a vehicle.

4. Discussion

This paper aimed to evaluate the preferred content and which aspects describe a high-quality projection. Therefore, three studies, whereby study No. 1 and study No. 3 have a different questionnaire compared to study No. 2, have been completed. In total 145 participants took place in the study with various knowledge backgrounds to gain an overall opinion. Since the percentage of female subjects in all three studies was less than 35%, the analysis does not focus on the gender factor to the corresponding answers to the questionnaires. Additionally, previous studies show, that there is no significant influence by age [12]. The perception of a ground projection is assumed to be independent of gender and age to obtain a general opinion. After all, the results' comparison between study No. 1 and No. 2 states, that the participants are not influenced by different brightness levels of each study and indicate the same relevance of either the projection content or the aspects for high-quality projections. The relevance is shown by the responses of the two studies, as to whether subjects from study No. 1 or study No. 2 scored the same response options above 50% (see Figure 1 and Figure 2).

Additionally, the tendencies for the results of studies No. 1&3 and No. 2 are similar and therefore show no specific influence by the time of handing out the questionnaire. When comparing the questionnaires, the aspects "Brightness" and "Resolution" play an essential role in all studies and account for the largest share. Likewise, aspects such as "Size" and "Colour"

were less important by looking at the given answers in all studies. In study No. 1 and No. 3 the subjects had already seen and evaluated the projection with its size and colour. Compared to study No. 2 where the subjects saw the ground projection after answering the questionnaire. This leads to the conclusion that the timing of the query does not reveal a difference in this case. Therefore, the subjects are less concerned with size and colour, as these aspects are seen as less important. Rather, good recognition through brightness and resolution is advantageous.

A similar picture emerges for the preferred content representation. Design representations are dominant in all studies. As seen in Table 3, design elements and safety aspects show the highest rating, which is significantly substantiated. Especially for safety reasons, good recognizability of the representation is necessary. This is achieved by sufficient brightness, high contrast and resolution of the floor projection. Table 2 shows that these aspects are significantly rated best. This motivates and states aspects for safety projections which have to be observed in detail.

In study No. 2 there is a clear tendency towards the highest rating of 4 for "Visible during the night", this is less clear when viewed during the day. Consequently, this shows that the opinions of the test persons differ significantly in this respect. On the one hand, 24% of the respondents consider daytime visibility is crucial. On the other hand, 28% give the rating 2 and see daytime recognizability as less important. This finding must be addressed in more detail, especially concerning safety-relevant projections, as these must be seen in every light scenario. This projection content received a high impact from the participants in study No. 2.

5. Conclusion

The analyzed data indicates the importance of fundamental research to obtain main aspects for high-quality projections in the near field of the vehicle. Hence, the independent opinion of 145 participants shows the range of importance for the customer. This survey review indicates, that besides the design illustration or brand representation next to the car, the customers are interested in informative projections next to the vehicle, like the vehicle charging status or other vehicle information. Additionally, personalized messages are relevant for the subjects to illustrate individual welcome or goodbye messages to the car owner. Therefore, it is crucial, that the technology develops into the usage of digital projectors to enable this kind of projections which need a high degree of freedom to project changeable content. Another possible solution is to offer personalized projectors with conventional and not digital projection technology.

Furthermore, ground projection will play a major role as a safety feature in the future, although it did not

receive the highest ratings in study No. 2. This is an important aspect especially for automated vehicles. A clear, quick detection is of great importance for a safety feature. This is confirmed by the results of the importance aspects of a ground projection, which indicate the research focus for further investigations specifically for safety relevant near field projections. Therefore, this field of research is crucial in the future, which will deal with next-generation mobility such as a highly automated vehicle. The introduction of projections as new light functions must be examined in the specific use case. The popularity of near-field projections will increase when this function is used as a new communication medium for a highly automated vehicle to communicate the vehicle's intention with other road users. Furthermore, the acceptance of drivers and other road users will gain a certain level, where projections will enter the standard configuration status for most car manufacturers.

7. References

- [1] ADAC. (2021). Die TOP-10 Kaufgründe. https://www.adac.de/infotestrat/autodatenbank/kundenbarometer/kundenbarometer_top10.aspx (visited: 2022.11.11).
- [2] Krieft, F., Thoma, A., Willeke, B., Kubitz, B., & Kaup, M. (2019). Symbol Projections: Gain or Gadget? Proceedings of the 13th International Symposium on Automotive Lighting (ISAL) 2019, 321–330.
- [3] Reiss, B., & Cladé, S. (2019). Road Marking Solutions with Pixelized Light Source. Proceedings of the 13th International Symposium on Automotive Lighting (ISAL) 2019, 343–352.
- [4] Dietrich, A., Willrodt, J.-H., Wagner, K., & Bengler, K. (2018). Projection-based external human-machine interfaces – enabling interaction between automated vehicles and pedestrian. Proceedings of the Driving Simulation Conference Europe, 43–50.
- [5] Nguyen, T. T., Holländer, K., Hoggenmueller, M., Parker, C., & Tomitsch, M. (2019). Designing for Projection-based Communication between Autonomous Vehicles and Pedestrians. <https://doi.org/10.1145/3342197.3344543>.
- [6] Ackermann, C., Beggiato, M., Schubert, S., & Krems, J. F. (2019). An experimental study to investigate design and assessment criteria: What is important for communication between pedestrians and automated vehicles? Applied Ergonomics. <https://doi.org/10.1016/j.apergo.2018.11.002>.
- [7] Colley, A., Häkkinen, J., Forsman, M.-T., Pfleging, B., & Alt, F. (2018). Car Exterior Surface Displays: Exploration in a Real-World Context. 1–8. <https://doi.org/10.1145/3205873.3205880>.
- [8] Moosburger, H., & Kelava, A. (2012). Testtheorie und Fragebogenkonstruktion (H. Moosbrugger & A. Kelava (eds.)). Springer, Berlin, Heidelberg. <https://doi.org/10.1007/978-3-642-20072-4>.
- [9] Lozano, L. M., García-Cueto, E., & Muñiz, J. (2008). Effect of the number of response categories on the reliability and validity of rating scales. Methodology, 4(2), 73–79. <https://doi.org/10.1027/1614-2241.4.2.73>.
- [10] Buehner, M. (2008). Einführung in die Test- und Fragebogenkonstruktion. <https://doi.org/10.17877/DE290R-6148>.
- [11] Simms, L. J., Zelazny, K., Williams, T. F., & Bernstein, L. (2019). Does the Number of Response Options Matter? Psychometric Perspectives Using Personality Questionnaire Data. Psychological Assessment, 31(4), 557–566. <https://doi.org/10.1037/pas0000648>.
- [12] Stuckert, Alexander; Singer, Timo; Khanh, T. Q. (2022). Analysis and definition of resolution requirements for projections in the near field of a vehicle. ISAL 2021, 14, 521–530.
- [13] Schlöder, U. (2022). Dynamic Ground Projections around the Car: The Headlamp as Integrator. ISAL 2021, 14, 538-547.
- [14] Namyslo, S., Courcier, M., & Moisy, E. (2022). 360° Near Field Projection - Enhanced safety or just a nice gadget? ISAL 2021, 14, 511-520.

Digital Projections: The next level of freedom and customization in vehicle design

M. Rosenauer¹, T. Huber¹, C. Allgeier¹, P. Vogt²

1: Plastic Omnium, Im Gewerbepark C25, 93059 Regensburg

2: ams OSRAM, Leibnizstr. 4, 93055 Regensburg

Abstract: Road and ground projections have already established themselves as an additional pillar of vehicle lighting. Offering highly customizable content, digital projections now mark the next stage of this development and open new application possibilities for automotive manufacturers and end customers. Digital projection modules can be used to support important exterior safety features and to implement additional interaction lights. In this paper, we present the latest innovation in optomechanical engineering and a new system approach to vehicle architecture for digital projections.

Keywords: Projection, Electronics, Digitalization

1. Basis for digital projection

Previous ground projections are based on static and some dynamic approaches with compact optical lens and image systems in combination with high power LED sources. These currently available concepts for series applications are also a relevant basis for the requirements of the next generation of digital projection solutions in terms of brightness, integration, and durability.

2. Digital projection as an advanced lighting solution

Digital projection solutions offer OEMs a wide range of options for vehicle design and end customers numerous possibilities for individualization [1,2]. By allowing end customers to create their own personal "living room on wheels," digital projections, whether on the dashboard or the headliner, create a high-quality ambience and thus a fascinating driving experience.

This new experience is made possible by the combination of the exceptional performance of the modules with their very compact design, which offers a wide range of installation options. One application, for example, is the projection of a light surface in front of the driver and passenger doors for better visibility when entering the vehicle - a considerable relief for drivers and passengers, especially in the dark and with poor visibility. Alongside this, the technology can be used to display warning symbols next to the vehicle and even communicate signals to its

surroundings (see Figure 1). Beyond that, digital projections offer a new tool to stage vehicles with eye-catching welcome and goodbye scenarios [3].



Figure 1: Projection for communicating a vehicle's intention to its environment

3. Digital projection systems by Plastic Omnium

Plastic Omnium's projection solutions are based on a modular approach. The module consists of an efficient optical unit with high-power LEDs, digital mirrors (DMDs) and front-end electronics including the hardware and software to control the system (see Figure 2).

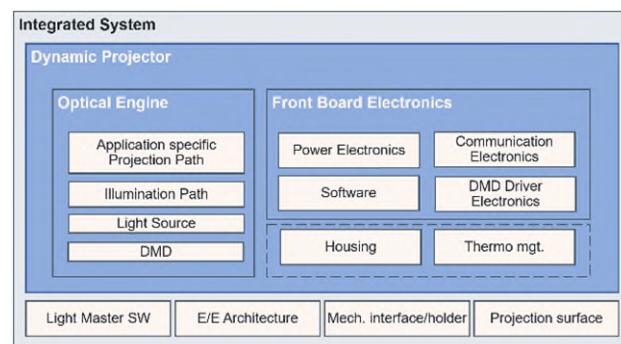


Figure 2: Main components of projection systems and vehicle interaction for a fully integrated system

DMDs are the state-of-the-art technology in the realization of digital projection solutions. This is due to their large number of pixels, which enables high digital resolution in combination with small digital mirrors, allowing compact yet efficient optical

systems. In addition, DMDs are available in different sizes and meet automotive industry standards at component level. Thanks to their compact design, the modules can be flexibly installed on and in the vehicle to display projections on a variety of surfaces both inside and outside the vehicle.

The modules can achieve a resolution of more than 400,000 chip-level microscopic mirrors and an optical lumen output of 25-200 lm (highly dependent on the application and module size) [4]. The power supply and signals are managed via the front board electronics with implemented LED drivers and signal control. The LED drivers can drive white or RGB LEDs to display animation or video content from internal memory (data refresh possible) or live via a streaming option based on modern communications such as 10Base-T1 Ethernet or LVDS, with the definition depending heavily on the application.

The optical engine consists of a complex lens system with a projection lens set with defined offset and throw ratio (TR). To achieve a completely passively cooled system, the module houses not only the optical module and the directly connected electronics, but also the thermal management system.

4. Ground projection application

Already well-known use cases for ground projection are the implementation in the rocker panel or side mirrors for welcome and goodbye scenarios (see Figure 3).



Figure 3: Ground projection with customized projections for welcome and goodbye scenarios

For both implementation options, the projection direction runs along the side of the vehicle with an installation height of the module of typically 20 to 30 cm from the floor for the rocker panel and 80 cm to 100 cm for the side mirror. The projection length is at least 1.80 m up to 3.00 m and depends on the distance and the projection field of the DMD implementation (see Figure 4). The length is ultimately limited by the brightness level, with a minimum brightness of < 150 lx for visibility at dusk and night.

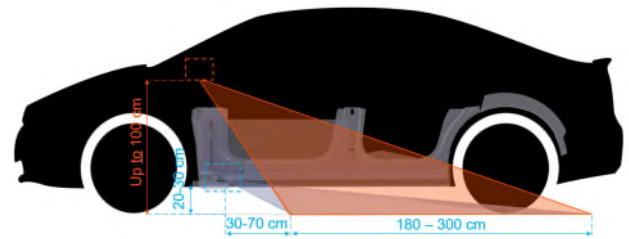


Figure 4: Integration of the projection module into the rocker panel or side mirror and usual projection dimensions

5. From exterior to interior projection application

In the car interior, digital projections unfold their full potential. An application example is a wave, abstract effect, pattern, or graphic starting in a central display and seamlessly continuing through projection onto the dashboard and doors. This is made possible by the combination of digital projection with additional technology in the interior lighting and a corresponding architecture that controls the complex orchestration of the various components. Another application example is the projection onto the headliner, which, with a possible size of 120 cm to 100 cm, offers completely new possibilities for passenger comfort and entertainment (see Figure 5).



Figure 5: Headliner projection application for widescreen display of animations over multiple materials and structures

Especially in the vehicle interior, installation space and integration are important factors. In addition to the compact space, the user experience requires limited daytime visibility of up to 150 cd/m², with a typical interior surface reflectivity of 5 to 18 %. This presents a challenge for the balance between minimum space requirements and maximum brightness and performance. To reconcile this, a significant part of the development work consists of managing the energy demand, the operating point, and the associated thermal load in such a way that both a power mode (e.g., a brief welcome scenario or a visualization when entering the vehicle) and continuous operation (functions during the entire

journey) are possible. To define the thermal and energy management, clear requirements for the use case with the key information are necessary (see Figure 6):

- Timing for each individual use case
- Definition of LED(s) for setting the maximum brightness (for power mode)
- Ambient temperature and derating profile
- After reduced LED current (= continuous operation) possible thermal reserve for power mode (e.g., good-bye scenario)
- Definition of the environment of the projection unit (additional heat sources near the projector, encapsulation, possible fresh air flow)

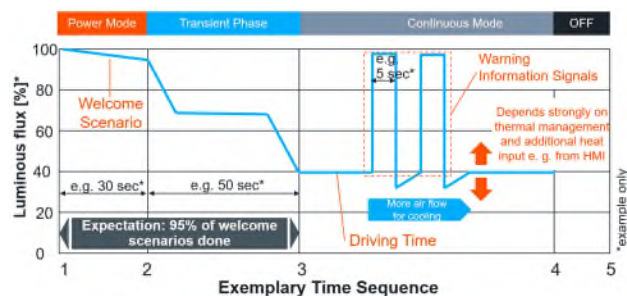


Figure 6: Definition of use cases to determine the potential brightness over time based on different scenarios like power mode or continuous mode

The overall goal is to always operate the LEDs below the maximum operating temperature, which is typically in the range of $T_j = 125 - 150^\circ\text{C}$ and dictates the overall system design and module size.

6. Projection module with video update option

To offer a fully customizable product, Plastic Omnium developed a single-box approach. The digital projection contains an optical engine with DLP technology and includes all electronics, integrated memory and communication parts with front-end electronic boards and heat sink in a single box (see Figure 7). This enables a module size of $80 \times 60 \times 50 \text{ mm}^3$.

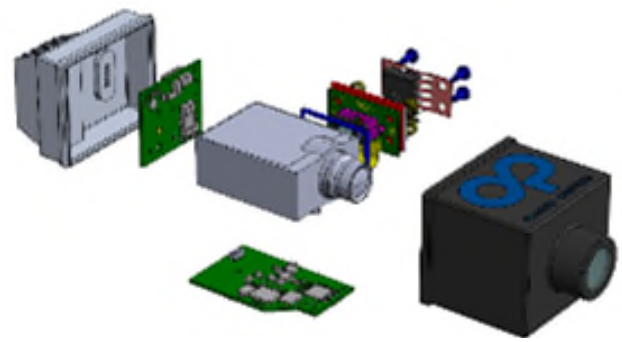


Figure 7: The digital projection module and its main components

The setup includes a DLP2021 chipset connected to a single white 0.5 mm^2 LED to achieve approx. 90 lm at $T_{\text{amb}} = 25^\circ\text{C}$ and an input power of approx. 8 watts. With an effective input resolution of 588×330 pixels, the technology exceeds the resolution of existing ground projection technologies.

An FPGA-based (field-programmable gate array) DMD controller enables a system architecture without a graphics processing unit (GPU).

The system stores ready-to-use image data and video sequences on a flash chip of up to 2 GBit in size, which are transmitted to the DMD via the DMD control logic. The microcontroller handles the communication with the vehicle as well as the configuration and parameterization of the system components. Via an Ethernet connection, video data from the vehicle ecosystem can also be live streamed to a high-performance microcontroller with GPU. The SRAM buffer supports the processing of the video data in the DMD controller as a buffer to ensure the necessary timing in the DMD chip [5].

7. Optical module architectures

When designing a projection solution for the ground, it is necessary to choose between different optical architectures. Typical designs can, among others, be divided into prism, field lens and freeform mirror approaches. These describes the coupling of the illumination light and the projection light path across the DMD chip in different ways (see Figure 8).

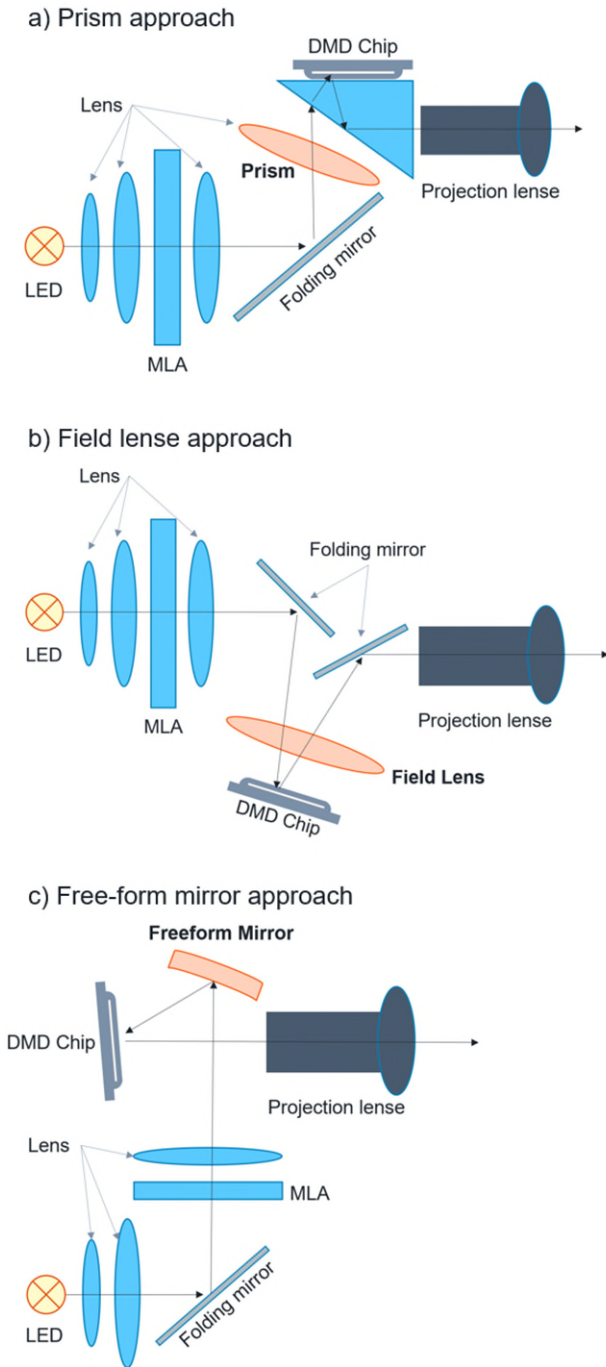


Figure 8: a) Prism approach, b) Field lens approach, c) Free-form mirror approach. For simplicity, only a single white LED is shown here as the light source

A particular disadvantage of the field lens approach over the other two architectures is a tendency to strong ghosting. The ghosting is nearly impossible to avoid and is caused, first, by a localized loss of contrast in the projection surface near the projector on the floor. Secondly, there is a lack of modularity as the field lens affects both the illumination and projection light paths. Unlike options a) and c), it is not possible to simply use a different projection lens if the

projection requirements change, e.g., across different car lines. Instead, the illumination path must be re-evaluated.

The advantage of the free-form mirror concept is the realization of the most compact optical modules possible, which have one less optical element than the prism concept. However, the disadvantages are poorer homogeneity of the DMD illumination, higher complexity of the design and fabrication of the mirror and, above all, lower optical efficiency compared to option a). This in turn is the main advantage of the prism concept, which achieves the highest luminous flux performance. In combination with a DLP2021-Q1 and a 0.5 mm² LED, the optical efficiency reaches up to 20%. The additional cost of higher luminous efficiency due to this extra optical element is negligible when choosing a simple wedge prism.

8. P-lens architectures (on-axis and off-axis)

The typical application of an outdoor ground projection has an offset of the target projection surface to the installation space of the projector. In a rocker-panel or side-mirror projection, the targeted projection surface is angularly offset from the installation space with grazing incidence of light and installation space severely limited (see Figure 9). For this reason, particularly compact designs that meet the critical requirements for installation space are preferred. The video or image content follows the spot definition of the main projection area but can be adapted to the desired main projection area.

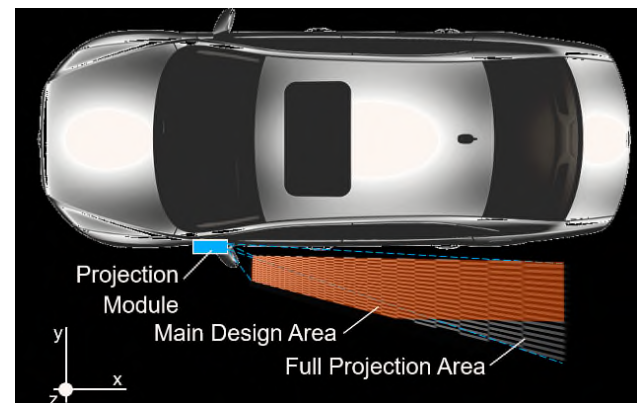


Figure 9: Offset of the projection surface and installation space for ground projection along the vehicle side

The lateral offset of the projection field can be realized by tilting the entire module (ON axis) or by choosing a P-Lens OFF axis design. The latter option offers the advantage of eliminating tilting of the projector module in the installation and aligning it along the x-axis to better address even the smallest installation spaces. In addition, the front impact edge of the

projection field can be more easily aligned parallel to the y-axis of the vehicle, if desired.

Compared to the ON-axis design, the OFF-axis projection lens has larger lens diameters and thus a slightly higher material cost. Normative requirements such as ECE-R48, on the other hand, can be met with both an ON- and OFF-axis design in the scenarios we investigated.

Another consideration when selecting an on/off axis design for P lens alignment is the orientation of the DMD mirror surface relative to the projection plane. By appropriately offsetting the projection lens from the DMD center, the tilt of the DMD mirror surface relative to the projection plane can be minimized. Figure 10 shows a simple pinhole camera model for imaging the DMD chip and illustrates the geometric relationships. The DMD chip is divided by the black and white pattern into four equal areas, shown here as a simplified representation of the DMD pixels.

The upper image in Figure 10 shows an "ON-axis" system where the optical axis coincides with the image center of the DMD chip. The lower image shows an "OFF-axis" arrangement where the DMD chip is offset relative to the optical axis. The geometric conditions in this example are designed in such a way that the different arrangement has a particularly strong effect: In the ON-axis design, the four areas of the DMD are distorted to varying degrees, resulting in a steeply sloping brightness gradient across the projection surface and larger maximum pixel spacing in the lower area. In contrast, the DMD surface sections in the OFF-axis design are less distorted, resulting in a less steeply sloping brightness curve and smaller maximum pixel spacings.

In a real application, the achievable effect is less distinct, calling for a compromise between the possible mounting position of the module, the optical imaging quality, and the brightness of the OFF-axis design versus the desired maximum pixel size and the brightness gradient in the projection area.

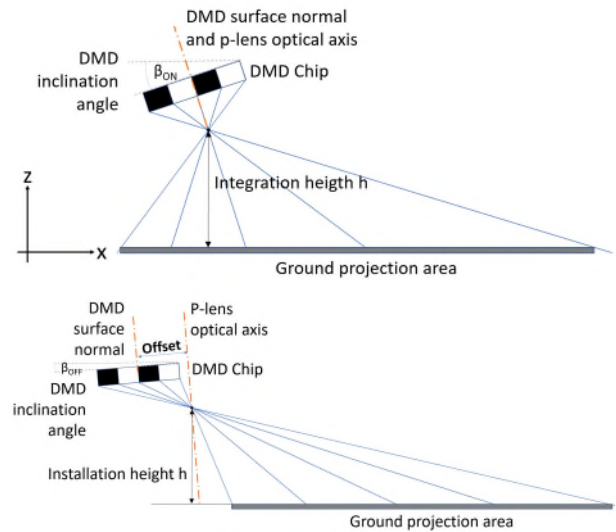


Figure 10: Simple pinhole camera model for imaging a DMD chip with an ON-axis (top) or OFF-axis (bottom) design

In summary, DMD-based projection systems allow the designer to choose from a variety of technical solutions to create a product that is perfectly tailored to the application at hand.

9. Electronics architecture

Based on an evaluation of various system architectures, in the following sections we will discuss the pros and cons for ground projection, including a comparison of the major E/E architectures and guidance on selecting the optimal electronic architecture for each application.

Based on the selected DMD chip, the DMD controller can be defined in combination with the microcontroller and the additional desired peripherals to design the main electronic architecture for the projection system. The microcontroller takes over both the task of communication with the vehicle and the parameterization of the system components (see Figure 11).

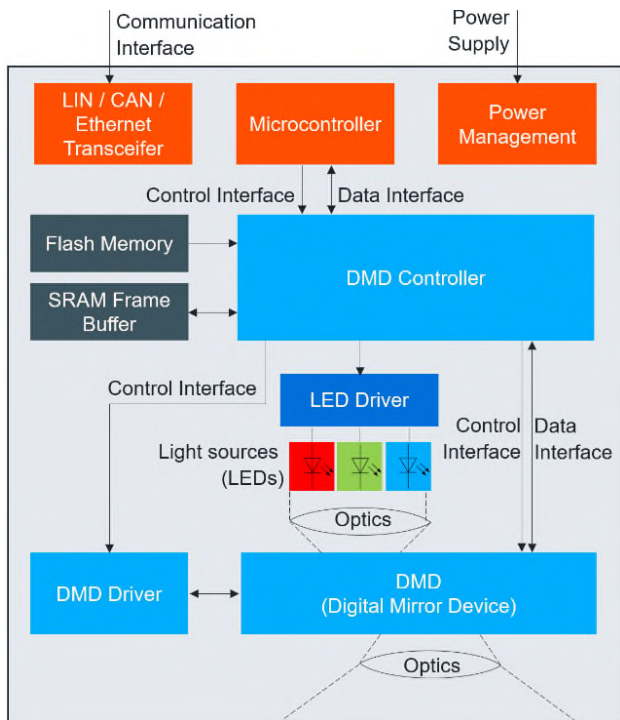


Figure 11: General electronic architecture of a DMD projection system

In general, the two projection data transmission methods "Live Streaming" and "Video Content Update" are available (for a direct comparison see Figure 12):

Live-streaming: Based on the automotive DLP3021-Q1 0.3" WVGA DMD chip in combination with the DLPC120 DMD controller, the video data from the vehicle ecosystem can be transmitted via live stream to a powerful microcontroller with GPU (Graphic Processing Unit). The SRAM buffer as intermediate memory supports the processing of the video data in the DMD controller to ensure the necessary timing in the DMD chip. With this setup, a main vehicle controller can send the video data (e.g., 25 fps) to the projection system via Ethernet or LVDS, for example, to display the requested data under real-time conditions. Complex calculations of video content such as live distortion or video interaction via chassis sensors can be performed on the vehicle domain controller before being sent to the projection module.

Video content update: A cost-effective solution based on an FPGA approach is to store the predefined data information in an integrated flash memory. In this way, the projection unit can display video content without an additional advanced control structure - all the necessary projection content and application data is on board. Current internal memory chips are available with 512 Mbit, 1 Gbit and 2 Gbit. Based on an advanced communication setup, updates of flash memory contents are also possible.

With 10Base-T1 Ethernet, an update time of less than 4 minutes can be achieved based on an FPGA approach.

In addition, a technical differentiation of data storage capacity and update rates for high-resolution actuators (e.g., DMD with 588 x 330 pixels at 50 Hz refresh rate) for existing and new vehicle bus architectures (LIN, CAN, LVDS, 10Base-T1 Ethernet) is performed, considering data compression for the projection streams.

Function-Focus	Live-streaming	Video content update
DMD Controller	DLPC 120	FPGA
Overall function	Live-streaming	Display stored video content, update possible
Controller setup	Controller + DLPC120	Controller + FPGA
External communication	LVDS or Ethernet-10Base-T1S for live-streaming	Ethernet-10Base-T1S or CAN-XL for update
Support of DMD	0.3", based on Package Type S247	0.3" and 0.2", based on Package Type S247
Max. flash memory	No memory	2GBit
Flash memory definition	No memory	NOR
Multiple flash memory possible	No memory	No
Control external signals (e.g. sensors)	Yes	Yes
Parallel video update/projection possible	No memory	No
Update timings (Ethernet-10Base-T1S)	-	~200s (2GBit)
File structure for update	-	Compiled image with application and video content
Live projection content adaption	-	Yes - dynamic picture sequence generation
Live video distortion	On-Board Control Unit	No
Evaluation status	Fully evaluated for RGB and White application with focus on 0.3" DMD	Fully evaluated for RGB and White application with focus on 0.2" DMD

Figure 12: Comparison of live streaming and video content update features

10. Regulation framework

In general, there are different regulations worldwide. In UN-ECE countries, projections into the vehicle environment are already permitted, but only in white and when the vehicle is parked or traveling at a speed of less than 10 km/h. Dynamic RGB projections while driving are not yet allowed.

However, the technical committees responsible for automotive lighting are constantly working to expand the use of projections to improve road safety at night. For example, a proposed regulation to allow digital projection of symbols on the roadway to assist drivers just cleared one of the biggest hurdles in the U.N. legislation. As early as next year, we will see more vehicles on the road using this new technology. In addition, there are intense discussions about the next generation of projection systems, so more applications may be possible in the future, such as advanced communications for autonomous vehicles.

11. Outlook and summary

With the development towards autonomous driving, light will become a decisive factor for communication between driver, vehicle and environment and thus contribute to the acceptance of autonomous vehicles. Thanks to their real-time adjustability and flexible installation options, digital projection systems could play a key role here. By enhancing existing lighting functions such as turn signals or brake lights and displaying relevant driving information on the road, they can contribute to significantly greater safety for all road users (see Figure 13). These benefits, along with the versatile opportunities the technology offers for more customized interior and exterior vehicle design, indicate that digital projections will be the next significant evolutionary step in automotive lighting.

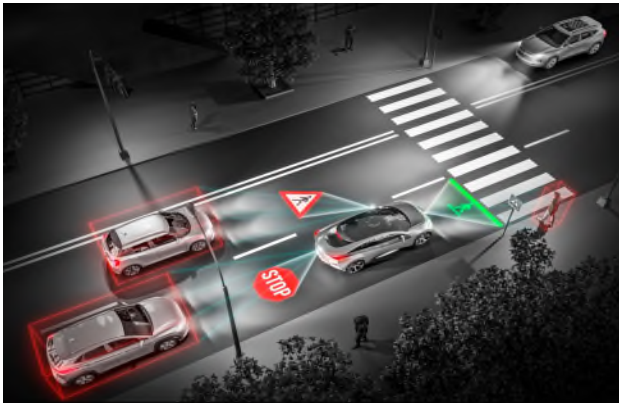


Figure 13: Possible future projection application to improve communication between driver, vehicle, and environment

12. References

- [1] V. Bhakta, B. Ballard: High resolution adaptive headlight using Texas Instruments DLP® Technology, ISAL Proceedings (483-494), 2015
- [2] M. Rosenauer et al.: Exterior Surround Lighting – From Static Logo Projection to 360° Dynamic Content Visualization, ISAL Proceedings (699-708), 2019
- [3] M. Rosenauer, J. Muster, G. Forster: Lichtlösungen zur Akzeptanzsteigerung autonomer Fahrzeuge, ATZ Elektronik, Springer Fachmedien Wiesbaden GmbH, Volume: 15, ISSN: 0005-6650, 2020-4
- [4] M. Rosenauer, C. Gärditz, O. Hering: Projektion ergänzt Scheinwerfer - Wie Licht Fahrzeugdesign und Funktionen verändern wird, Elektronik-Praxis Vogel, <https://www.elektronikpraxis.vogel.de/wie-licht-fahrzeugdesign-und-funktionen-veraendern-wird-a-1094401>; 09.02.2022, last access 23.09.22
- [5] Texas Instruments - DLP3021LEQ1EVM Evaluation Module; <https://www.ti.com/tool/DLP3021LEQ1EVM>; last access: 20.09.22

VALIDATION AND ADVERSE WEATHER CONDITIONS

Simulation of adverse weather as a basic requirement for the development and validation of bad weather robustness of ADS

W. Ritter¹, M. Bijelic¹, G. Hasna², K. Saad², P. Fomin², G. Prillwith²

1: Mercedes-Benz AG, D-71059 Sindelfingen, Germany

2: ANSYS Germany GmbH, 83624 Otterfing. Staudenfeldweg 20, Germany

Abstract: The development and verification of ADS (Automatic Driving Systems) suitable for bad weather stands and falls with the existence of a sufficiently large and suitable learning and test sample of bad weather sensor data.

Since such data cannot be obtained in sufficient quantity across all the important scenarios and all relevant weather variations by means of real-world recordings, the only alternative is to generate these data via a suitable adverse weather sensor data simulation.

The aim is for this simulated bad weather sensor data to correspond as closely as possible to the real-world sensor data from the point of view of a perceptual system. In the ideal scenario, the domain gap between the simulated and real worlds is zero, and the perceptual system will behave in the real world as it does in the simulated world.

This paper proposes an approach to achieve a stepwise alignment between the simulated and real adverse weather sensor data of environmental sensors for ADS, and it presents the first steps towards the realization of this approach in the form of implementations of the (adverse weather) simulators for camera, LiDAR and radar.

Keywords: Adverse weather sensor data simulation, Automatic Driving Systems.

1. Introduction

In the publicly funded project AI-SEE [1] we are developing an all-weather perception system allowing ADS (automated driving systems) to be operated safely in fog, rain, snow, and spray and enable automated driving in all weather conditions, to ultimately reach 365/24 service level for automated transport modes. The perceptual unit of this system is implemented by deep neural networks, which have to learn how to deal with these difficult conditions by example.

In the previous project DENSE [2] we already learned that the development and validation of the adverse weather operability of ADS implemented by deep neural networks is only possible with the help of simulated adverse weather sensor data. The adverse weather phenomena are too rare and too diverse, to be obtained from the real world via measurement

campaigns to the required extent, or only at economically and temporally unacceptable costs.

The goal must be that the performance of the deep neural network, trained on the basis of simulated data in the real world, deviates as little as possible from the performance in the virtual world. This is achieved when the deep neural network can no longer distinguish the virtual world from the real world, or in other words, when the simulated world is identical to the real world for the network. In AI-SEE, we aim to achieve this correspondence between the virtual and real worlds through a stepwise matching of the simulation data with (semi) real world data. Our bootstrap approach is explained in detail in this paper.

For modern perceptual systems for ADS greater than or equal to SAE Level III [3], the three main sensor types -camera, LiDAR and radar- are used in parallel due to the high safety requirements. We have defined the requirements for these sensors in AI-SEE five use cases, which allow statements/estimates about the sticking points of as wide an application area as possible.

Based on these use cases, the parameter space of the (adverse weather) simulation was defined for the sensors camera, LiDAR and radar.

The parameter space from sensor data simulation and the use cases serves as the base space for alignment between simulation and the real world. To make the alignment controllable, it must be performed in increasingly complex parameter spaces, starting with known, but still limited, variability of the bad weather and the scenarios reproduced in it from the previously defined use cases, via the less controllable or parameterizable adverse weather but still strongly limited scenario diversity on test sites, up to the greatest possible variability with regard to the occurring bad weather and the scene diversity on public roads in the real world.

2. Need of simulation data for training and verification of neural networks

Training the deep neural networks of the perception stack (unit) is done by so-called data loops. Typical data loop approaches cover the process from data capturing, algorithmic development, and identifying

weaknesses through to extensive tests. These weaknesses are addressed by additional data measurements in the area of weaknesses with which the process starts from the beginning.

This classic data loop has limited applicability because adverse weather events are rare in the real world, are therefore not usually included in the training data set and hence cannot be learned by the neural network. This difficulty can be explained by the fact that adverse weather conditions can be a combination of various rare individual effects, such as a mixture of sun and rain, which can vary independently in intensity. Hence, this data gap has to be closed using appropriate simulation techniques.

Our proposed approach therefore extends the data capturing with an intermediate step, replicating the captured data with simulation techniques. This allows us to expand the database with more adverse weather effects. In this way, the added simulations are always validated with the sensing setup providing crucial information on applicability of the found real-world approximations in simulation.

Misalignments and weaknesses can be identified in each validation step, triggering additional data capturing events. Finally, the validated data frames act as input to the training backend to enhance the training data sets for the perception function.

3. Our bootstrap approach to close the gap between simulation and real-world data

In order to obtain good simulation data, we propose a bootstrap approach depicted in Figure 1. Our working hypothesis is that the artificial data can be considered equivalent to the real data if the perception stack can no longer distinguish between them. However, general validity can only be derived if this applies to all forms of perception stacks. Since this cannot be done by us, we limit ourselves to our AI-SEE perception stack.

The aim is to minimize the differences between the data from the "different worlds" from the perspective of the perception stack. If the difference is no longer perceptible to the perception stack, it behaves in the real world as in the simulated world. Suitable measurement methods for this can be found in [4] [5].

The starting point to bridge the gap between real data and simulated data will be the weather chamber [6] [7]. In the weather chamber we can simulate a small part of the real world in terms of adverse weather. This simulation itself is an approximation of real rain or real fog by physical means, where, for example, size and distribution density of fog droplets in a closed

space can be kept constant over a longer period of time and thus simulated on average e.g., fog with a defined visibility. However, generally it will not reproduce natural, real-world fog exactly, with all the variations in droplet size, density and distribution that can occur even in small spaces, and which can also be disturbed by external influences such as temperature fluctuations, wind, etc. Nevertheless, it is a good simulation, because the artificial fog/rain is simulated with real material water and therefore comes very close to real fog in terms of the properties of wave propagation or scattering of light. Furthermore, this artificially generated adverse weather has the advantage that it can be reproduced, except for small variations, and thus can be used as a defined measure and in a repeatable way.

A first test for the quality of a simulation could be to record defined scenarios without adverse weather and with defined degrees of adverse weather in the weather chamber. These adverse weather scenarios could then be reproduced via augmentation, or a complete simulation, and the reproductions compared with the initial scenarios from the weather chamber. As proposed, the AI-SEE perception stack [5] can serve as a comparison tool. However, there will also be investigations to see if simpler measurement methods can be derived for this comparison (first step see for example [4] [5]).



Figure 1: Illustration of the extended data loop with adjustment stages

The next level to be added to real weather data are the recordings from measurement campaigns with defined scenarios on the test sites [9]. Here, procedures and, to a limited extent, weather influences such as spray generated over a driving surface with a constant water film or rain generated by an outdoor rain system can be defined and repeated. Adverse weather is less precisely defined here, as it is influenced by environmental factors such as temperature and wind, but at least the range of variation in the experiment is limited compared to recordings from normal road traffic. As in the weather chamber, “good-weather” recordings can be made here and transferred to “adverse weather” recordings via augmentation. A complete simulation of the manoeuvres performed is also possible, although it is very time-consuming. As proposed, the AI-SEE perception stack can serve as a comparison tool. However, there will also be investigations to determine whether simpler measurement methods can be derived for this comparison.

Once the hurdles of the weather chamber and proving ground have been cleared for the simulation, the last step is to match the simulation data with data from real-world images. Again, the AI-SEE perception stack will serve as a matching tool. As mentioned previously, the artificial data are equivalent to the real data for the perception stack if it can no longer distinguish between them.

4. Use Cases

The goal in AI-SEE is to cover as large an area of application as possible in the development of the system and thus also in the supporting tools. For this purpose, we have defined four representative use cases in AI-SEE with the goal that the most important performance data of such a system can be investigated and responded to. These are:

- **Use Case 1 - Adverse weather detection¹:** Test of the sensor-specific ability of the system to predictively perceive severe weather.
- **Use Case 2 - Road debris detection² in adverse weather:** Test the detection limits of the sensor system.

¹ Under adverse weather detection we understand recognize (classify) adverse weather in the sensing range of the sensor (in a matrix of sensor scans) possibly without exact localization.

- **Use Case 3 - Detection of road vehicles in adverse weather conditions:** Test of the detection capability of the system with and without degraded sensor data.
- **Use Case 4 - Pedestrian detection in adverse weather:** Test of the system’s detection ability when radar data is uncertain.

5. Simulation and Validation

The goal of the simulation in AI-SEE is to generate synthetic raw sensor data for the sensors most commonly used in ADS environment sensing systems, i.e., the camera, LiDAR, and radar. For validation, this synthetic sensor raw data will be compared with real sensor raw data achieved by measurements within the weather chamber or test tracks. This means that we will start to generate digital twins of the weather chamber and the test tracks, we will create similar scenarios and use measurements of real materials within the chamber and the test tracks as much as possible. The sensor-specific simulation techniques we implemented are described in the following subsections.

5.1 Camera

We have implemented two processing chains for the camera simulation. The first processing chain calculates the synthetic image very close to reality but is very time-consuming in the calculation taking approx. 10 minutes for one image. Since this already causes a computation time expenditure of nearly one year (exactly 347 days) with relatively small learning samples of approx. 50,000 images, its application for the generation of large learning samples is not purposeful. The reason for the extremely high computational time requirement is that Monte Carlo estimation methods are used for the simulation. Taking into account the interaction of each ray with rain, fog or snow particles is especially time consuming, whereas single scattering events on a surface can be treated in sufficient simulation time.

Therefore, this more accurate simulation is mainly used for quality comparison with simpler simulation techniques only or for the verification of trained deep neural networks.

For the generation of large learning samples, we implemented another processing chain, in which first

² Under object detection we understand recognize (classify) the object with bounding box in a matrix of sensor scans such as a pixel array.

the clear image of a scene is generated and on top of this clear image, the bad weather is augmented in a separate computational step. This processing chain requires about 20 ms for the generation of a bad weather image and is thus real-time capable.

Both processing chains are presented in the following.

5.1.1 Accurate but elaborate simulation

The camera model contains three main parts, the optical lens system, the electric receiver model and the digital processing. We are using a Monte Carlo simulation model, which means that all light sources within the scene, headlamps like road lights as well as the ambient sky and sun, will emit electromagnetic radiation.

As it would take too much time to emit all the rays by the sources and integrate only the small part of radiation getting to the receiver, inverse ray tracing technology is used. It is much more efficient to emit the rays by the detector, as we are hitting back a source it is possible to calculate back the radiance on the sensor.

It is key to also include the realistic behavior of the environment, so in addition to specular reflections one must take into account the surface roughness. This can be done by using a so called BSDF (Bidirectional Scattering Distribution Function) on all geometries present in the simulation.

Finally, to simulate the interaction of these light rays with rain and fog, it is necessary to model the volume scattering effects. This can be done by modelling the droplets themselves, which is the most detailed but also the slowest method to simulate the wave propagation of light. To speed up this simulation process (at the cost of accuracy, of course), it is possible to use a more phenomenological description of the fog, rain and snow by using the volumic absorption coefficient, the scattering coefficient and the phase function related to each particle.

The optical lens model can be simulated by a black box model containing the optical response like an MTF (Modulation Transfer Function) or PSF (Point Spread Function) equation. The electrical receiver model needs to contain the quantum efficiency transforming photons to electrons including the noise, which is generated. The DSP will finally convert the electrical raw signal into camera raw data related to the spectral filters of the camera and its dynamic

limitations (for example an RGB Sensor digitized with 12 bits).

A result of a camera simulation of a weather chamber scene, once as a clear image and then again as a fog image, is shown in Figure 2.



Synthetic camera image without fog



Synthetic camera image with fog

Figure 2: Synthetic clear image and fog image from a weather chamber scene.

5.1.2 Less accurate but real-time simulation

To achieve a camera simulation in real-time, we connect the driving simulator Carla [10] via AVL Model.CONNECT™ [11] to Ansys AVxeleration™ [12] software. The output of this simulation will only contain ideal clear view synthetic sensor raw data which needs to be augmented with weather related effects based on the research of [13] [14].

The volume scattering is not considered in the real-time process, but surface scattering and all light sources in the scene are taken into account. These images containing the projected radiance in the scene for each pixel can then be augmented for bad weather using, for example, the standard Koschmieder

formula [15]. With this formula the scattering of light sources within the image are not modelled well enough, so as a next step, a more realistic approach can be used to correct these effects. As soon as the comparison with the physics-based simulation is validated, we can use this approach to simulate a multitude of synthetic frames needed for training a neural network.

5.1 LiDAR

The LiDAR sensor is an active sensor. It consists of a radiation source (laser diode) with a wavelength of about 950 nm (NIR = Near Infra-Red) as standard. Since the wavelength in the NIR range is not eye-safe, the maximum light intensity of the laser diode must be limited, which leads to a limitation of the range or resolution of NIR LiDARs. Newer, more powerful LiDAR sensors operate in the SWIR range (Short Wave Infra-Red) with a wavelength of around 1500 nm. Since they operate in the eye-safe range, the light intensity of their laser diode can be up to a factor of 50 higher than conventional NIR LiDARs. This allows higher resolution or longer range of the SWIR LiDAR. In AI-SEE, we study and simulate both NIR and SWIR LiDARs, i.e., we model the LiDAR beams in the NIR band as well as in the SWIR band.

A LiDAR is described in the simulation by three models, one for the transmitting and receiving optics, one for the electrical model of the source and the receiving diode and finally one for the digital signal processing to evaluate the raw signals. In contrast to the camera sensor, LiDAR delivers a three-dimensional result as raw data, the so-called point cloud. The parameters here are the coordinates x , y and z of the point as well as the reflection signal of the point and the time between sending and receiving the signal (time of flight, ToF).

In the case of bad weather, the laser beam of the LiDAR is attenuated, multiple reflections occur within the interfering particles (e.g., fog droplets) and there are further interfering reflections from the possibly wet road surface. The modeling of these interfering influences is done in AI-SEE according to [16] [17] [18].

Depending on the manufacturer, different techniques are used to filter the reflected signal, which influence both ToF and the measured intensity. Furthermore, since multiple objects can be located within a beam, modern LiDARs often detect and output multiple signal maxima. To accurately model this sensor, it is therefore imperative to have an exact model of the

DSP of the sensor. An example of a LiDAR simulation of a fog scene is shown in Figure 3.

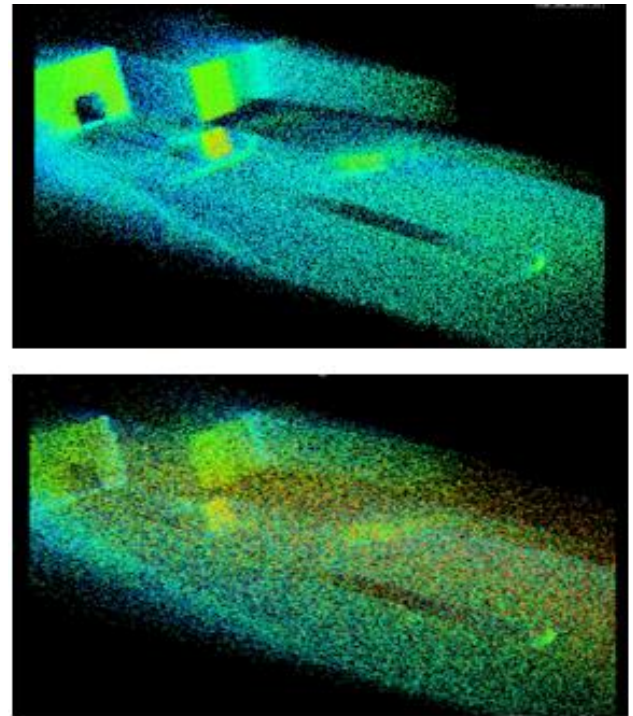


Figure 3: Synthetic LiDAR data with low (top) and high (bottom) fog density.

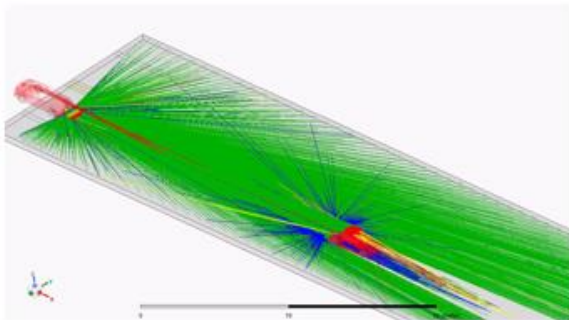
5.1 Radar

The last sensor we focus on is a new radar technology called MiMo radar (Multiple Input – Multiple Output). With this technology we have analog to LiDAR sensor an active sensor consisting of multiple emitter antennas as well as multiple receiver antennas. A Radar sensor emits specific signals called “chirps”. As these chirps are reflected by objects it is possible to obtain the speed of the objection by analyzing the frequency shift of the signal.

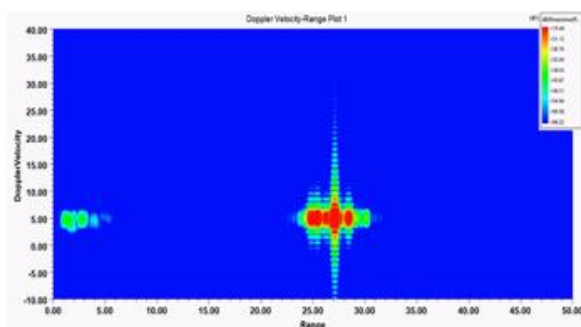
Within the simulation model we have once again three parts, the antenna model itself, which has an influence on the far field distribution diagram of the antenna, as well as the description of the angular sensitivity diagram of the receiving antenna. The raw signal is then transmitted to the analog digital converter (ADC) where we can find the complex radar raw data. The digital signal processing is the final and most important step within a radar sensor. With several mathematical operations based largely on FFT (Fast Fourier Transform) the complex radar signal is filtered and processed with different methods. At the end of the analysis, we get a so-called Doppler range plot, with the Doppler velocity on

one axis over the range on the other axis. Finally, with more sophisticated approaches, it is possible to export a radar point cloud as a raw signal containing as parameters the x, y, and z positions, as well as the signal strength (RCS, Radar Cross Section) and the Doppler velocity.

The images in Figure 4: Typical outputs of a radar simulation show typical outputs of a radar simulation:



Radar ray tracing



Doppler range diagram

Figure 4: Typical outputs of a radar simulation

Since the radar wavelength is, in principle, hardly influenced by normal fog and rain, it may not be necessary to include these effects in the simulation. Only water films in the near field of the radome as well as snow aggregates and ice structures influence the radar signal. The approach in this project is to simulate in detail the effects of such water, snow, and ice films on the far-field pattern of the antennas and then to include these results in the phenomenological simulation.

5.1 Validation and verification of the simulation

The training of perception systems with synthetic, simulated data has already started. We can see a

significant improvement of the detection rate (up to 20 percent) within adverse weather compared to a standard approach using only empirical test data [19] [18]. So, the concept of the improvement of AV driving by using synthetic sensor data for training shows a good tendency.

We have already started implementing the first data loop step according to Figure 1: Illustration of the extended data loop with adjustment stages. In this work step, the simulated data will be compared with data from measurements in the weather chamber. For each AI-SEE use case, scenarios will be simulated in the weather chamber and recorded at defined fog and rain densities. For these weather chamber scenarios, the same scene with the corresponding fog and rain densities will be then simulated and compared with the weather chamber scenarios. The simulation algorithms are optimized until a good match is achieved and the perception algorithms can no longer distinguish between measured and simulated data.

6. Conclusion

This paper proposed an approach to achieve a stepwise alignment between the simulated and real adverse weather sensor data of environmental sensors for ADS. Implementations of the (adverse weather) simulators for camera, LiDAR and radar were presented for realizing this approach.

Detectors trained with the simulation data showed significant improvement over purely conventional, clear weather detectors when applied to real bad weather scenes.

As a next step, work has begun on the verification of simulation performance based on the comparison of simulation data with real data from weather chamber scenarios.

7. Acknowledgement

The research leading to these results is part of the AI-SEE project, which is a co-labelled PENTA and EURIPIDES2 project endorsed by EUREKA. Co-funding is provided by the following national funding authorities: Austrian Research Promotion Agency (FFG), Business Finland, Federal Ministry of Education and Research (BMBF) and National Research Council of Canada Industrial Research Assistance Program (NRC-IRAP).

8. References

- [1] „AI-SEE - Enhancing vehicle vision in low visibility conditions 24 hours and 365 days of the year,“ [Online]. Available: <http://www.ai-see.eu>.
- [2] „DENSE - 24/7 AUTOMOTIVE SENSING SYSTEM,“ [Online]. Available: <https://www.dense247.eu/>.
- [3] „SAE Levels of Driving Automation™ Refined for Clarity and International Audience,“ [Online]. Available: <https://www.sae.org/blog/sae-j3016-update>.
- [4] M. Bijelic, T. Gruber und W. Ritter, „A Benchmark for Lidar Sensors in Fog: Is Detection Breaking Down?,“ in *IEEE Intelligent Vehicles Symposium (IV)*, 2018.
- [5] M. Bijelic, T. Gruber und W. Ritter, „Benchmarking Image Sensors Under Adverse Weather Conditions for Autonomous Driving.,“ in *IEEE Intelligent Vehicles Symposium (IV)*, 2018.
- [6] M. Colomb, J. Dufour, M. Hirech, P. Lacôte, P. Morange und J. Boreux, „Innovative Artificial Fog Production Device, a Technical Facility for Research Activities,“ 2004.
- [7] S. Hasirioğlu, „A Novel Method for Simulation-based Testing and Validation of Automotive Surround Sensors under Adverse Weather Conditions,“ in *Doctoral Thesis*, Linz, 2020.
- [8] „AI-SEE Enhancing vehicle vision in low visibility conditions 24 hours and 365 days of the year,“ 2021. [Online]. Available: <https://www.ai-see.eu/>. [Zugriff am 2 10 2022].
- [9] B. Mario, T. Gruber, F. Mannan, F. Kraus, W. Ritter und K. Dietmayer, „Seeing Through Fog Without Seeing Fog: Deep Multimodal Sensor Fusion in Unseen Adverse Weather,“ in *CVPR*, 2020.
- [10] „CARLA - Open-source simulator for autonomous driving research,“ [Online]. Available: <https://carla.org/>. [Zugriff am 2022 2 10].
- [11] „Model.Connect,“ [Online]. Available: <https://www.avl.com/documents/10138/2699442/Model.CONNECT%E2%84%A2+Overview>. [Zugriff am 2 10 2022].
- [12] „Technische Simulationssoftware von Ansys,“ [Online]. Available: <https://www.ansys.com/de-de>. [Zugriff am 02 10 2022].
- [13] S. Geiger, A. Liemert, D. Reitzle, M. Bijelic, A. Ramazzina, W. Ritter, H. Felix und A. Kienle, „Single scattering models for radiative transfer of isotropic and cone-shaped light sources in fog,“ *to be published in Optics Express*, 2022.
- [14] A. Liemert, S. Geiger und A. Kienle, „Solutions for single-scattered radiance in the semi-infinite medium based on radiative transport theory,“ *Journal of the Optical Society of America*, 19 Feb. 2021.
- [15] H. Koschmieder, „Theorie der Horizontalen Sichtweite.,“ *Beiträge zur Physik der freien Atmosphäre*, 1924.
- [16] M. Hahner, C. Sakaridis, M. Bijelic, F. Heide, F. Yu, D. Dai und L. van Gool, „LiDAR Snowfall Simulation for Robust 3D Object Detection,“ in *IEEE/CVF Conference on Computer Vision and Pattern Recognition (CVPR)*, 2022.
- [17] M. Hahner, C. Sakaridis, D. Dai und L. Van Gool, „Fog simulation on real LiDAR point clouds for 3D object detection in adverse weather,“ in *IEEE International Conference on Computer Vision (ICCV)*, 2021.
- [18] C. Linnhoff, D. Scheuble, M. Bijelic, L. Elster, P. Rosenberger, W. Ritter, D. Dai und H. Winner, „Simulating Road Spray Effects in Automotive Lidar Sensor Models,“ in *Eingereicht bei der IEEE Sensors Journal*.
- [19] F. Julca-Aguilar, J. Taylor, M. Bijelic, F. Mannan, E. Tseng und F. Heide, „Gated3D: Monocular 3D object detection from temporal illumination cues.,“ in *IEEE International Conference on Computer Vision (ICCV)*, 2021.

Comparing Vehicle Safety Systems in Adverse Condition Splash and Spray between Road and Test Site

Dr. Jan-Erik Källhammer¹, Dr. Werner Ritter², Dr. Paul Otxoterena af Drake³, Roine Stenberg¹,
Peter Eriksson⁴, Erik Ronelöv⁴

1: Veoneer Sweden AB, Wallentinsvägen 22, SE44737, Vårgårda, Sweden

2: Mercedes-Benz AG, Werk/Plant 05919 - HPC G023-BB D-71059 Sindelfingen, Germany

3: RISE, Safety and Transport, Box 857, SE-50115 Borås, Sweden

4: AstaZero AB, Lindholmspiren 3 SE 41756 Göteborg Sweden Company

Abstract: Perception systems in current serial vehicles were designed for fair weather conditions, resulting in degraded performance in adverse visibility conditions such as fog, snow, rain, or spray from vehicles ahead. Addressing this shortcoming brings challenges in the development and validation of such systems. Consistent adverse conditions are quite rare, imposing a challenge to collect sufficient relevant data to validate the system. A key difficulty in adverse conditions testing is therefore the lack of repeatability. Tests done at different instances in time and location are difficult to compare and measures of variability essential to consider when assessing differences.

Keywords: Adverse weather, Perception systems, Repeatability test methods

1. Introduction

The American Automobile Association found that adverse weather can severely impair Advanced driver assistance systems (ADAS). In tests, vehicles hit a static other vehicle in 33% of the cases when traveling at 56 km/h and lane keeping failed in 69% of the cases in tests at 72 km/h [1]. Although it is not clear that the test method used by AAA is fully realistic, it should be beyond dispute that the perception systems in future car releases need to improve in low visibility and adverse weather conditions.

During the 2010-2014 period 20.7% of crashes occurred in adverse weather in the USA. Assuming these numbers are still valid, this means that current perception systems on average have degraded performance in one out of five crashes. Of the crashes in adverse weather, 14.2% occurred on wet roads, 3.0% occurred on snow-covered roads, 2.6% on roads with ice, and 0.9% in other conditions. Fog was on average only reported in 0.4% of the crashes [2]. Although crashes in fog are relatively few, they appear to be more severe and an important factor in fatal multi-vehicle pileups [3-4].

Addressing the shortcomings in current ADAS perception systems brings challenges in the development and validation of such systems. These challenges get emphasized with the move towards

Automated Driving Systems (ADS) with driving automation of SAE level 3+ [5]. An essential step in a widespread industrialization of such systems is reaching repeatable methods for test and validation under controlled circumstances.

However, not only ADAS and ADS systems should be concerned with adverse weather conditions. The performance of modern lighting systems such as Adaptive Driving Beam (ADB) should benefit by adopting its behavior to adverse weather conditions. Drivers are accustomed to restricting the use of the high beam when driving in fog. An adaptive driving beam that adapts to fog and other adverse weather conditions should be a reasonable continuation of ADB but will need repeatable validation techniques. Additional synergies are expected as ADB headlights and matrix headlights use cameras to control the direction and extent of the headlight beam. Laser lights and emerging systems that use pulsed laser illuminators in the non-visual range are additional areas which should benefit from more standardized test methods for adverse weather.

Ambient conditions vary due to varying intensities of rain and snow, varying types and density of fog, and spray from the vehicle ahead depends on the amount of water on the road, vehicle speed, tires, and factors changing the turbulence behind the vehicle such as the shape of the vehicle, presence of mudflaps and other features affecting the airflow. This result in that tests done at different instances in time and location are difficult to compare and measures of variability between test occasions are essential to consider when assessing differences between systems and their possible configurations. Parallel data collection of all relevant sensors is currently essential for comparison.

Today, tests and validations in adverse weather are largely confined to naturalistic field tests. A key difficulty is the lack of repeatability, giving uncertainties associated with the results as ambient conditions lack consistency. We treat the field data as 'ground truth' which we aim to replicate in controlled test conditions. Artificially generated conditions generated in a controlled manner enables better

repeatability and freedom to effectively plan and conduct such tests.

Repeatable tests under controlled circumstances will therefore not only reduce variabilities in the tests but also greatly reduce the costs and time duration of testing. Examples of such controlled environments could be a weather chamber, wind tunnel or other type of indoor environment, but these facilities are few and rarely adapted for all adverse weather conditions occurring in the field. Furthermore, comparing the results between such test facilities are difficult due to lack of establish test procedures and measures.

Another difficulty is that the occurrence of adverse weather conditions is not evenly distributed over the year. The validation period may therefore have to be extended, affecting development duration and launch dates.

Although radar has much better all-weather capability than optical based systems, radar systems are not sufficient as stand-alone systems. Optical systems provide higher resolution required for classification. We are therefore focusing on optical perception systems for ADAS. Emulation of spray was the first focus as it appears to be a major factor influencing perception system performance and driving on wet roads is the most common adverse weather condition according to [2].

Our project aims to map the conditions for testing perception systems under the influence of adverse weather conditions. The primary objective for the work is to evaluate different kind of sensor and camera technologies at an early stage and under real-world conditions. This kind of early evaluations can help us to make decisions about future product capabilities. It is also possible to invite customers for technology test drives strengthening existing or creating new relationships.

2. Visibility

Visibility is defined as the distance at which an object can be identified with an unaided eye. A visibility of 100 m means that only 5% of the unaffected contrast remain. Reduced visibility is mainly caused by darkness and adverse weather. The visibility reduction in darkness is caused by low light levels while the visibility reduction in adverse weather is mainly caused by obscurants (particles) in the atmosphere.

Visibility can be classified into four classes as shown in Table 1 [6]. For our evaluation, we concern ourselves mainly with lower visibility, in ranges 2-4.

Table 1: Visibility range classes

Visibility range	Visibility distance [m]
1	200-400
2	100-200
3	50-100
4	< 50

The obscurants can be in the form of rain, snow, water droplets in fog or spray from other vehicles, haze, or pollutants in smog. In certain areas of the world dust and sandstorms can significantly influence visibility, but elsewhere the most common particle is water. Ambient light and reflected light from an object are absorbed and scattered by these obscurants. The optical scattering causes an offset in the image also called airlight [7]. The absorption and scattering lead to a loss of contrast. The reduced visibility conditions reduce both human visibility as well as sensors performance. Dirt accumulation on sensors are additional factors to consider, especially in Nordic type winter with lots of salt and dirt particles on the road.

In [8] was shown that attenuation for visual wavelengths is in the order of 200 dB/km in fog vs 10 dB/km in heavy rain (25mm/h). Thus, besides fog, it is usually not rain directly that is the main issue in reducing visibility, but the spray generated from other vehicles and the water accumulation covering the sensor window. It is thus important to have a mounting location behind a clear area such as behind the area of the windshield swept by the wipers.

Mist and fog are caused by suspended microscopic water droplets or wet hygroscopic particles. Thus, both conditions have the same cause, but with different size and densities of the droplets. Fog occurs during high relative humidity, usually above 95% [9].

The meteorological definition of mist is having a visibility that exceeds 1 km while fog has a visibility less than 1 km. When comparing the meteorological definition of mist and fog with the classes of Table 1, we see that mist will not be an issue for driving visibility. Another implications of the definition of fog to less than 1 km visibility means that established reference in civil aviation etc. may not be fully applicable to driving. Military applications usually involve long distance surveillance issues and beyond distances of concern for driving, why experiences from these areas should be dealt with caution.

Attenuation is a function of particle size distribution, density, and refractive index of the particles. Particle size distribution is the most important factor to determine the optical features of light passing through the atmosphere. Depending on fog type, the mode of droplet size can vary in the range 1-10 μm [9]. Rain and spray on the other hand can have water droplets in the order of millimeter. This means that the size of

the particles in the atmosphere is larger to much larger than the visual wavelength and the short-wave infrared region, affecting what physical phenomena that govern the scattering and reflections.

3. Method

SAE J2245 is a recommended practice for splash and spray evaluation [10]. It provides a guideline for assessing spray by either measuring light extinction or by contrast measurements. It describes two methods of analysis. Quantifications are done either by means of laser methods for light extinction or video digitizing for contrast measurements. The recommended practice notes that splash and spray are turbulent phenomena with complex interactions of involved variables. The document highlights some important caveats. Two notable ones are that caution should be exercised when comparing results of tests done at different test sites and that results should be reported as differences between 95% confidence intervals and not as differences between averages.

SAE J2245 was issued in 1994 and “stabilized” in 2011. The, ADAS and ADS systems were at best at its infancy at the time of drafting the practice. It is thus reasonable to assume that specific issues related to ADAS, and ADS were not considered specifically. A major limitation of J2245 is that there is no implied relationship between laser methods for light extinction or video digitizing for contrast measurements. Separately, we are comparing these measures. The first analysis was presented by [11].

In this early stage of developing test methods for spray evaluation, we use SAE J2245 as a guide to assess levels of spray in various situations. We collect data in various naturalistic conditions in the field and compare with generated spray at the test site as well as by spray generating devices. Strict adherence to J2245 is not possible in traffic such as repeated runs and runs in different directions to compensate for wind directions. With moving vehicle wind influence should be low compared to vehicle speed. As we are assessing how we can replicate natural variability at the test track and using spray simulator devices we don't apply the Figure of Merit measure at this stage.

In the comparison between field test and simulated spray we selected to focus on contrast measurements in video data. Given that optical systems are most affected by particles in the atmosphere we considered it a more direct measure on the influence on the camera images. Contrast was measured across checkerboards as prescribed in J2245. We also compare it with histograms applied to the intensities over the checkerboard. The shape of the histogram changes with increased spray. The test site conditions are adjusted with the aim of giving

reasonable consistent and comparable results with the collected field conditions.

A common deficiency in many evaluations of sensors is that not all relevant sensors are available, and comparisons are made at different points in time when conditions are not consistent over time. A way to address this shortcoming is to equip a test vehicle with all considered cameras and record simultaneously to allow uniform conditions for all involved cameras. We therefore built a test vehicle with a distributed sensor data collection system that can be expanded with more PC's if bandwidth or CPU/GPU limitations is reached. An internal software plugin architecture makes the system easy to adapt to new sensors, new interfaces, and new processing technologies. The graphical user interface is designed for simplicity allowing it to be easily used by the driver without undue distraction. During post-drive sensor data evaluation, the full resolution and framerate of the sensors is available for further analysis. The data collection software has been deployed in a Mercedes S-class, currently equipped with seven different cameras/sensors.

For vehicle tests a 'Grid module' with a checkerboard consisting of contrasting pattern of 12 by 12 black and yellow squares each sized at 10x10 cm. Figure 1 shows the grid module mounted on the back of a car.



Figure 1 Checkerboard contrast target mounted on a Volvo V70

Videos were recorded in normal traffic and on the test track. Normal traffic tests were documented at speeds 50/70/85/110 km/h for cars and 90 km/h for trucks. Track tests were carried out on AstaZero's road course. The tests were recorded from the following vehicle. Track test speeds documented were 50/70/90 km/h for both cars and trucks.

4. Results

Figure 2 shows examples of videos recorded in normal traffic on RV40 motorway near Borås,

Sweden. The events occurred shortly after each other with only a few seconds separation. The left side show low amount of spray, while heavy spray was generated in the situation in right image. Posted speed limit was 110 km/h. Figure 3 shows example images recorded on the AstaZero test track. The images produced an average contrast 20% in 50 km/h (left), while under similar conditions on the test track the contrast had decreased to only 8% at 90 km/h (right).

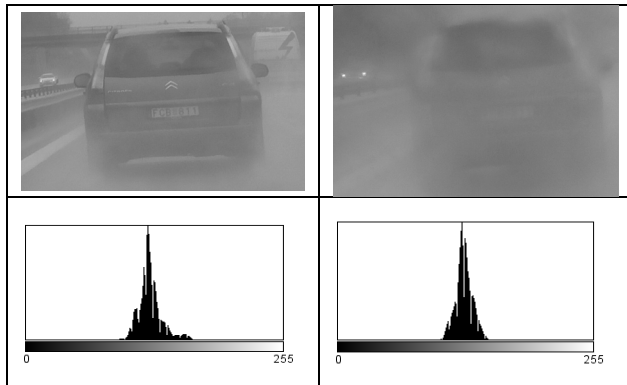


Figure 2 Image and Histogram of car travelling on motorway.

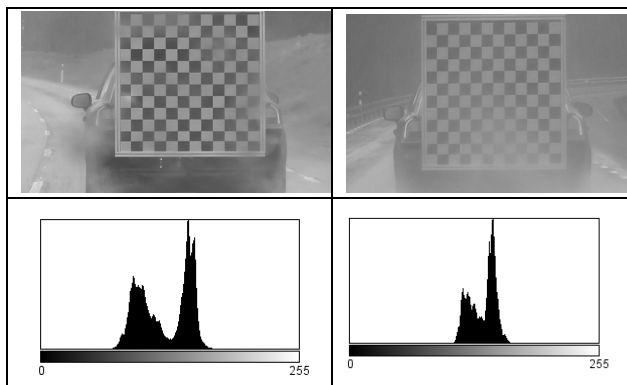


Figure 3 Checkerboard behind car at AstaZero test road and its histogram at 50 km/h (left) and 90 km/h (right).

When analyzing the films from tests at AstaZero's test track, it was discovered that the corresponding test on public roads rendered more water spray. The road where Figure 2 was recorded is rather worn with slight depressions where water can accumulate. This difference was especially apparent at the AstaZero high-speed area, which has a surface with an alternative asphalt surface with a very high horizontal precision. The amount of water that could be accumulated on the surface was less than what was accumulated in the worn areas of the regular roads where most of the trucks drive.

The lesson we drew from this is that test tracks with its controlled surfaces may not be fully representative

and that surface conditions of the roads where naturalistic field tests are done must be documented with regards to depth of water accumulation on the road surface.

Two different types of static spray simulators have been evaluated. An example of the uniform spray that can be achieved is shown in Figure 4.

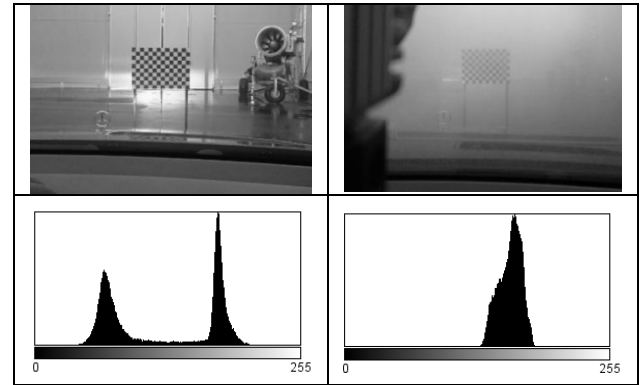


Figure 4 One version of spray simulator. Left: Baseline without spray. Right: with simulated spray

The recorded images of the checkerboard shown in Figure 4 had an average contrast of 41% as baseline without spray exposure. The contrast dropped to only 4% with the artificial spray. We can observe that the histogram contracts with more spray. The two peaks without spray have merged into one with the heavy spray from the spray simulator.

We did not measure the Figure of Merit described in SAE J2245, as it is very difficult to have the fixed exposure as described in SAE J2245 with the varying ambient conditions. We instead focused on the contrast of the checkerboard in in each image and the influence on the histogram shape the spray caused. Our working hypothesis is that histogram shape will be at least one important criteria in comparing the effect of spray and other adverse conditions.

5. Conclusion/Summary

The speed of the vehicle ahead and the amount of water on the road both have major effects on the spray generated. We started with spray measurements on regular roads and two attempts for simulation of artificial spray.

Further work is needed in other adverse weather areas as well as better means of controlling e.g., droplet diameter ranges as droplet size affect contrast degradation differently with different sensor wavelengths.

In following steps, we intend to apply lessons learnt on spray investigation applied to fog and snow conditions.

6. Acknowledgement

The work is part of the SEVVOS project with support from Sweden's Innovation Agency. The project is also associated with the project AI-SEE, which is funded by the following National Funding Authorities: Austrian Research Promotion Agency (FFG), Business Finland, Federal Ministry of Education and Research (BMBF) and National Research Council of Canada Industrial Research Assistance Program (NRC-IRAP). AI-SEE is a co-labelled PENTA and EURIPIDES² project endorsed by EUREKA.

7. References

- [1] AAA: *"Effect of Environmental Factors on ADAS sensor Performance"*. Washington, D.C.: AAA Foundation for Traffic Safety, 2021.
- [2] Tefft, B.C.: *"Motor Vehicle Crashes, Injuries, and Deaths in Relation to Weather Conditions, United States, 2010-2014"*. Technical Report. Washington, D.C.: AAA Foundation for Traffic Safety, 2016.
- [3] Whiffen, B.: *"Fog: Impact on aviation and goals for meteorological prediction"*. Proc. Second Conf. on Fog and Fog Collection, St. John's, NF, Canada, Environment Canada, and International Development Research Center, 525–528, 2001.
- [4] Hamilton, B., Tefft, B.C., Arnold, L.S. & Grabowski, J.G.: *"Hidden Highways: Fog and Traffic Crashes on America's Roads"*. Technical Report. Washington, D.C.: AAA Foundation for Traffic Safety, 2014.
- [5] SAE International: *"J3016_202104 Taxonomy and Definitions for Terms Related to Driving Automation Systems for On-Road Motor Vehicles"*. Warrendale, PA., 2021.
- [6] AFNOR: *"NFP 99 320:1998 Road Meteorology – Gathering of Meteorological and Road Data – Terminology"*. Association Francaise de Normalisation. Saint-Denis, France, 2013.
- [7] Oakley, J. P., and B. Satherley: *"Improving image quality in poor visibility conditions using a physical model for contrast degradation"*. IEEE Trans Image Processing, Vol. 7, No. 2, 167-179, 1998.
- [8] Hautière, N. and Tarel, J-P.: *"Simultaneous Contrast Restoration and Obstacles Detection: First Results"*. Proceedings of the 2007 IEEE Intelligent Vehicles Symposium. Istanbul, Turkey, 2007.
- [9] Muhammad, S.S., Flecker, B., Leitgeb, E., Gebhart, M.: *"Characterization of fog attenuation in terrestrial free space optical links"*. Opt. Eng. 46(6) 066001. <https://doi.org/10.1117/1.2749502>, 2007.
- [10] SAE International: *"J2245 Recommended Practice for Splash and Spray Evaluation"*. Warrendale, PA., 2011.
- [11] Otxoterena Af Drake, P., Willstrand, O., Andersson, A., Henrik Biswanger, H.: *"Physical characteristics of splash and spray clouds produced by heavy vehicles (trucks and lorries) driven on wet asphalt"*. Journal of Wind Engineering & Industrial Aerodynamics, 217, 104734, 2021.

8. Glossary

ADAS: Advanced driver assistance systems

ADB: Adaptive Driving Beam

ADS: Automated Driving Systems

Use and development of the PAVIN fog and rain platform in the framework of the H2020 AWARD project

P. Duthon^{1*}, F. Bernardin¹, S. Liandrat¹, A. Ben-Daoued¹

1: Cerema, Equipe Recherche STI, 8-10 rue Bernard Palissy, 63017 Clermont-Ferrand, France

*adweather@cerema.fr

Abstract: Cerema is a member of the European All Weather Autonomous Real logistics operations and Demonstrations (AWARD) project which aims to bring major innovations to the transport industry, fleet operators and the entire logistics sector. The project contributes to the accelerated deployment of innovative, connected, and automated freight transport solutions in Europe and worldwide.

The Cerema ITS research team plays an important role in this project. Among other things, it is involved in setting up the protocols and carrying out tests in degraded weather conditions. For this, the PAVIN Fog and Rain platform, located in Clermont-Ferrand, is used for the development of the sensor suite and associated algorithms. It is also an opportunity for the research team to develop this physical simulation platform, particularly concerning the production of maritime fogs, by extending the size range of the reproduced fog droplets.

The results of the tests carried out and the innovations obtained are presented in this communication.

Keywords: Adverse weather conditions, automated freight transportation, logistic, maritime fogs, controlled artificial fog and rain

1. Introduction

Mobility issues are being transformed and the massive development of Autonomous Vehicles (AVs) or more generally Automated Driver Assistance Systems (ADAS, e.g. pedestrian and obstacle detectors) seems to become more and more a reality as regulations evolve and allow their deployment. However, while the world is watching demonstrations of autonomous vehicles evolving in ever more advanced scenarios, the question of driving in adverse weather conditions remains an issue to be addressed.

For freight applications, the H2020 All Weather Autonomous Real logistics operations and Demonstrations (AWARD) project¹ aims to bring major innovations to the transport industry, fleet operators and the entire logistics sector. The project will contribute to the accelerated deployment of innovative, connected and automated freight transport solutions in Europe and worldwide. The Cerema Intelligent Transportation Systems (ITS)

research team has an important role in this project. It participates in more than half of the project's work packages (WP). Within the framework of WP3, the research team participated in the implementation of the protocols and in the realization of the tests in adverse weather conditions. The PAVIN platform was used during the development of the sensor suite and the associated evaluation of processing algorithms.

The following section describes the main features of the PAVIN Fog and Rain platform, but also how it is generally used today. Section 3 proposes a focus on a use case of the platform, realized in the framework of the AWARD project. Section 4 shows what are the next developments in the actual platform, before the construction of a new platform. Finally, Section 5 concludes.

2. The PAVIN Fog and Rain platform

2.1. Main features

The Cerema PAVIN (INtelligent Vehicle Platform of Auvergne region) Fog and Rain platform is one of the few testing facilities over the world which is capable to artificially generate controlled fog and rain in such a volume (Figure 1).

This platform is operated by the ITS research team of Cerema, a French public agency attached to the Ministry of Ecological Transition, which ensures its

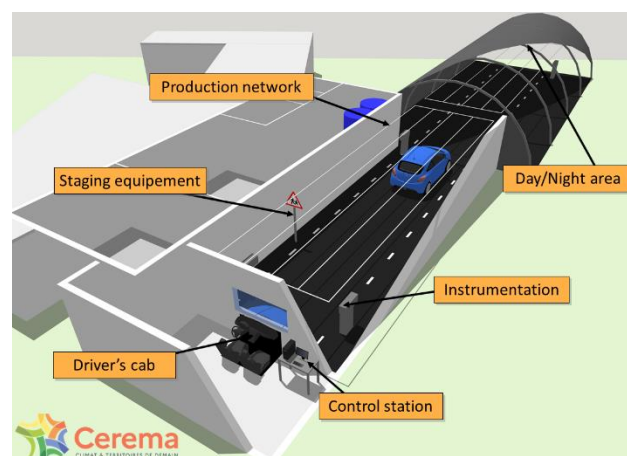


Figure 1: The PAVIN platform scheme

¹ <https://award-h2020.eu/>

independence, confidentiality and neutrality. The platform is 30 m long, 5.5 m wide and 2.20 m high. This volume allows for the reproduction of realistic road scenarios, including vehicles, pedestrians and road equipment, in day or night conditions. It is also possible to set up reference tests with targets calibrated in reflectance and thermal black bodies. The platform is mainly dedicated to the automotive (ADAS, AVs, lighting) and road (marking, traffic signs, monitoring) domains but also to other advanced domains such as rail, aeronautics, maritime, construction or military.

Into the chamber, fog and rain of varying intensities may be produced on demand. Fog density may be replicated in the Meteorological Optical Range (MOR) range of 10m to 1000m. The Droplet Size Distribution (DSD) is representative of continental or maritime fogs. Rain conditions may be produced with rainfall rate ranging from 10 to 180mm/h.

The MOR [1] is defined as the maximum distance (in meters) at which a calibrated object is visibly distinct from its background. The lower the MOR, the denser the fog. Fog with a MOR of 10m is considered extremely dense and is occasionally encountered on roads.

Rain intensity [1] is characterized by the rainfall rate in mm/h, corresponding to the height of water in mm that falls on a surface area of 1m² over a 60-minutes period. The greater the rainfall rate, the heavier the rain. A rainfall rate of 120mm/h represents violent storm peaks in Europe.

2.2. Main activities

While the platform was first used to analyse the impact of fog on human vision, it is now mainly used to evaluate computer vision systems that are installed in vehicles, whether for ADAS or AV, but also to make roadside surveillance cameras smarter. Research on computer vision has become predominant since 2010, with the rise of ITS and the AV development. Concerning the use of the PAVIN platform, it can be classified into three main areas:

- measurement of weather conditions by camera (artificial intelligence)
- numerical simulation of meteorological phenomena
- measurement of the impact of adverse weather conditions on vehicle perception systems

Concerning the measurement of weather conditions by camera, camera-based weather measurement initially derived from work on the impact of rain on cameras. Indeed, it was shown that rain has a quantifiable impact which is proportional to the rainfall intensity on common image features of the literature [2]. The impact on the image features was then used to detect the actual weather conditions, including fog and rain conditions. Then, the use of image features was left aside, and Deep

Convolutional Neural Networks (DCNN) were successfully used in the WeatherEye solution (up to 90% of good detection) [3] [4]. For the artificial intelligence optimisation, a first learning step can be done from images recorded in the PAVIN platform, before being transferred and fine-tuned on images that are acquired on a real site.

Concerning the numerical simulation of adverse weather conditions, the first numerical simulation tools developed with the PAVIN platform were about fog. The work started in 2000 and continued until 2010. Authors first used visible light cameras only in night conditions. These researches were resumed by the Cerema team in charge of the platform in 2020 and are currently in progress. First, some experiments were conducted to check the impact of the wavelength and the fog droplet size distribution on the transmission of electromagnetic radiation [5]. According to the literature, they show that the light transmission is not the same for all wavelengths. The objective is now to use these first results to develop and validate a new fog numerical simulator based on radiative transfer equation and Monte-Carlo method (Figure 2) [6].

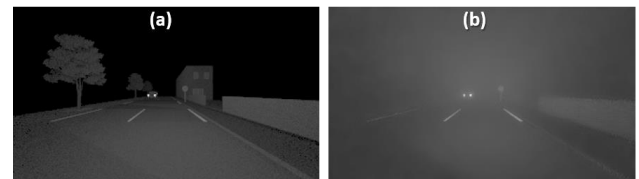


Figure 2: Simulated road scene in the visible: (a) without fog, (b) with 3D fog with MOR = 21 m [6].

Concerning the measurement of the impact of adverse weather conditions on vehicle perception systems, the first public work was conducted in the context of the AWARE project, from 2014 to 2017 [7]. The objective of this project was to analyse which wavelength bands are least penalized by fog. Several cameras in the visible light (VIS), Short-Wave Infrared (SWIR), Mid-Wave Infrared (MWIR) and Long-Wave Infrared (LWIR) ranges were thus compared in the platform [8] [9]. This topic was then continued in the DENSE project, from 2016 to 2019 [10] [11]. The DENSE project aimed to develop a series of all-weather sensors, allowing the automation of a particular vehicle. The conditions targeted included fog, rain and snow. The sensors set was composed of stereoscopic cameras in VIS, (Near-Infrared) NIR and SWIR domains, LiDARs (Light Detection And Ranging), radars and time-of-flight cameras. The research studies characterized the boundary weather conditions for each of the sensors [12] [13] [14] [15] [16] [17] (Figure 3) and used data fusion to extend the admissible conditions. This work was then continued in the AWARD project, which is the subject of a focus in the next Section.

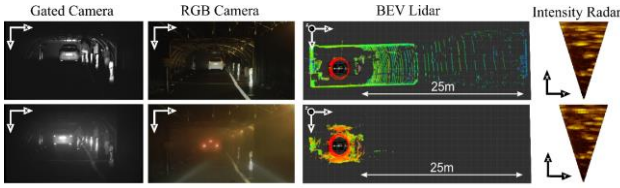


Figure 3: Multimodal sensor response of camera, LiDAR, gated camera, and radar in fog. Clear conditions in the first row, fog (MOR=23m) in the second row [18].

3. AWARD project results: a case study

3.1. Scope

Within the AWARD project, some partners, like Easymile [19], Navtech, Foresight Automotive [20] or Adasky have carried out tests within the PAVIN platform. In this paper, we will give a focus on works done with Foresight Automotive's QuadSight® vision system.

This proprietary technology (Figure 4) is based on the utilization of 3D video analysis and advanced image processing algorithms to achieving accurate obstacle detection in adverse environmental conditions. This technology can be customized to address the numerous challenges facing ADAS and AVs.

The QuadSight vision system consists of 2 pairs of stereoscopic vision channels: a visible light stereo channel in conjunction with a thermal stereo channel, providing depth perception to obtain a clear 3D view of the environment. Stereoscopic vision technology uses two synchronized cameras to generate a depth map, allowing for the detection of an object, either classified or non-classified, and its accurate size, location, and distance. Monocular vision object detection technologies are usually based upon inferencing and rely on Deep Neural Networks (DNN) object recognition. Using DNN for object recognition will always encounter corner cases where there is an unknown object to the trained network. Foresight's stereoscopic technology provides a hybrid 3D detection solution for both classified and non-classified objects.



Figure 4: QuadSight vision system by Foresight²

² <https://www.foresightauto.com/solutions/quadsight/>

According to the latest published literature, most of the 3D object detection studies address only favourable climatic conditions. This is the case of most of the datasets in the field [21] [22] [23] [24]. Some recent datasets deal with adverse weather conditions, but only address visible light cameras and contain only few images [25] [26]. Other datasets that include many images exist for traffic surveillance applications [4] [3], fog removal [27] [28] [29] [30] [31] [32] or weather classification [25] [26]. These do not concern 3D object detection for automotive purposes and they do not contain thermal images. Concerning automotive sensors for autonomous driving, some recently published studies propose algorithms to deal with fog conditions by incorporating data fusion from LiDAR and stereoscopic visible light cameras [33] [18] [34]. Other studies analyse the impact of fog, rain and snow on LiDARs [35] [36] [17]. These studies do not use thermal cameras for detection, such as the QuadSight vision system. Some other studies use data fusion with the use of thermal cameras [37] [38] but they don't address adverse weather conditions.

The QuadSight vision system was tested under a range of artificially reproduced weather conditions. The novelty of the work done with Foresight Automotive is to present results of 3D object detection: (a) on a commercialized system, (b) using visible light and thermal wavelengths, (c) in controlled fog and rain conditions. This work allows for a demonstration of the characterization of the Operational Design Domain (ODD) under harsh weather, and a scientific analysis on a commercialized system.

3.2. Protocol

A specific scenario was designed to characterize the quality of object detection of the QuadSight vision system in poor weather conditions. The system software allows 3D detection of various objects, in this case, vehicles and pedestrians. As seen in Figure 5, a human pedestrian producing a true-to-life thermal signature, and an electric Renault Kangoo vehicle was used as test subjects. Various target-sensor distances, weather and illumination conditions combinations are tested. These include day/night, fog of varying densities (MOR = 10m, 20m and 50m), and rain of varying intensities (rainfall rate = 11mm/h, 70mm/h and 120mm/h).

In daylight conditions, only the ambient light is present. In nightlight conditions, the headlights of the vehicle on which the QuadSight vision system is placed are turned on. In total, we have 84 experiments (2 targets [car + pedestrian] x 2 illumination conditions [day + night] x 7 weather conditions [1 clear + 3 rains + 3 fogs] x 3 target-sensor distances [10, 17 and 25m]).

For the analysis, the measures of precision and recall were used. First, the position of the pedestrian

and the vehicle over the entire dataset was manually annotated. The 3D object detection algorithm was then applied to the images. To determine whether a detection is valid, the Intersection of Union (IOU) metric was utilized. These are common state of the art metrics.

3.3. Results

The results of precision and recall scores are recorded in Table 1. The results confirmed the expected system performance for both visible light and thermal channels based on past experimental data (Figure 5). The visible light cameras are highly dependent on the environmental lighting conditions and subsequently, show reduced performance at low lighting (night) levels. This is not the case for thermal cameras; however, as they are dependent entirely on object heat and emissivity. On this basis, the results of different lighting conditions do not show any change in performance.

The rain at all levels had minimal effect on the performance of both visible light and thermal channels. The results show improved detection of pedestrian target compared to the electric car target at fog levels 10 and 20m. This can be explained by the difference in heat emissivity of pedestrian and car. As opposed to combustion engine vehicles which

expel a large amount of heat, an electric vehicle is more similar in temperature to the surrounding environment. The improved detections of both pedestrian and car by the thermal channel compared to the visible light channel at fog 10 and 20m is explained by the reliance on object emissivity as opposed to lighting conditions (Figure 6). All fog scenes tests were performed immediately following the rain scenarios, while all objects were still wet, reducing contrast between the object and the surrounding environment. Sometimes the results drop slightly, but this can be explained by local variations in the test conditions, such as the exposure time setting or the position of the pedestrian.

Despite technical complications during the testing period, Foresight's technology achieved quality results for both stereo vision light and thermal imaging. Combining the advantages of stereo systems using visible light and thermal cameras will help to increase road safety for all road users and will pave the way for better ADAS and autonomous vehicles. The thermal cameras enhance ADAS systems, allowing improved performance under many weather and lighting conditions. The concurrent use of these camera-based sensors provides a complete image of the surrounding environment, under challenging conditions, where other sensors' performance may be compromised.

Table 1: QuadSight system detection results (Precision / Recall)

		Pedestrian - IOU 0.5						Car - IOU 0.7					
		VIS			IR			VIS			IR		
Target dist. →		10m	17m	25m	10m	17m	25m	10m	17m	25m	10m	17m	25m
Day	Clear	100/100	100/100	100/100	100/100	100/100	100/100	100/100	100/100	100/100	100/100	100/100	100/100
	Fog 10m	100/100	NaN	NaN	100/100	100/100	100/100	100/100	NaN	NaN	97/100	NaN	NaN
	Fog 20m	96/100	99/100	99/100	100/100	100/100	100/100	100/100	100/100	NaN	100/100	100/100	100/100
	Fog 50m	100/100	100/100	100/100	100/100	100/100	100/100	100/100	100/100	100/100	100/100	100/100	100/100
	Rain 11mm/h	100/100	100/100	100/100	100/100	95/100	96/100	100/100	100/100	100/100	100/100	100/100	100/100
	Rain 72mm/h	100/100	98/100	99/69	100/100	100/100	100/100	100/99	100/100	100/100	99/100	98/100	100/100
	Rain 120mm/h	100/100	100/100	100/100	100/100	100/100	100/100	100/100	100/100	100/100	100/100	100/100	100/100
Night	Clear	100/100	100/100	100/100	100/100	100/100	100/100	100/100	100/100	100/100	100/100	100/100	100/100
	Fog 10m	NaN	NaN	NaN	98/100	100/100	NaN	NaN	NaN	NaN	97/100	NaN	NaN
	Fog 20m	100/92	NaN	NaN	98/100	98/100	98/100	100/100	NaN	NaN	98/100	96/100	78/93
	Fog 50m	100/100	100/99	100/56	100/100	98/100	100/100	100/100	100/100	97/100	100/100	100/100	100/100
	Rain 11mm/h	100/100	100/100	99/100	100/100	100/100	95/100	100/100	100/100	100/100	100/100	100/100	100/100
	Rain 72mm/h	100/100	100/100	100/97	100/100	100/100	81/57	100/100	98/100	98/99	100/100	96/100	100/100
	Rain 120mm/h	100/100	100/100	94/74	100/100	100/100	93/100	100/100	100/100	100/100	100/100	100/100	100/100

*NaN values - There was no visible detection of the objects at the listed ground truth distances.

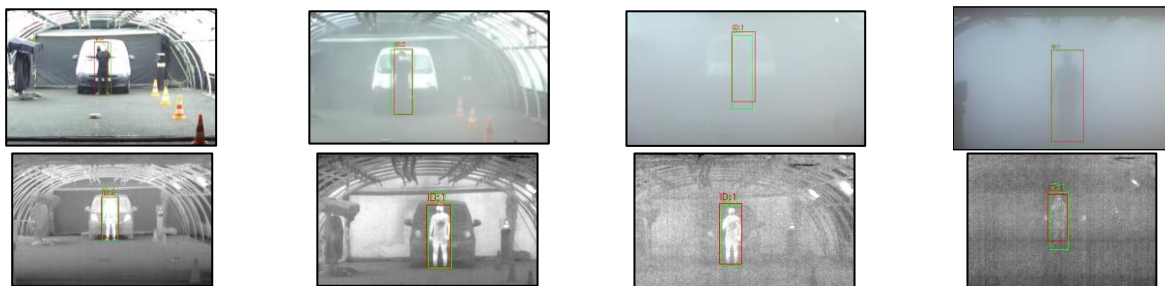


Figure 5: Example of detection results, in fog conditions at the maximum distance of detection. From left to right : Clear, Fog 50m, Fog 20m, Fog 10m. Up: visible light camera, down: thermal camera.

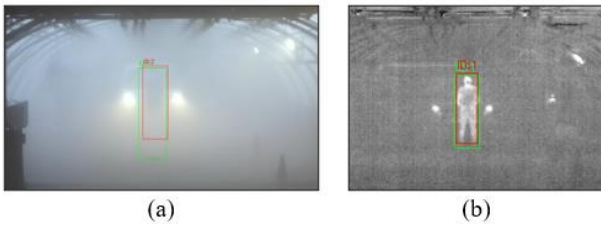


Figure 6: Example of the pedestrian who is totally invisible on the visible light camera (a), while he is perfectly visible on the thermal camera (b).

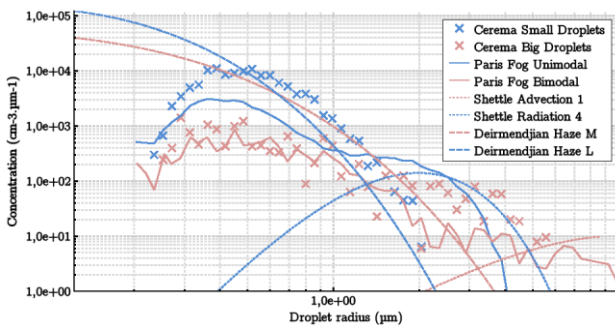


Figure 7: Particle size distribution of the PAVIN platform fogs compared to different models found in the literature [39]

4. The future PAVIN platform

4.1. The near future: research works to better address maritime fogs

Into the current platform, the two types of fog reproduced are similar to natural fogs. Indeed, as shown in the Figure 7, they have the same DSD as natural fog recorded in an outdoor measurement campaign [39]. However, it can be noticed that the fog models in the literature sometimes present droplets of even larger diameter (ex: Shettle Advection 1). For this reason, Cerema has proposed to study new ways of artificially producing fog in the framework of the AWARD project. Thus, measurements are underway and the exploitation of the results will allow to better address the large droplet fog.

4.2. A brand-new platform in 2024

From its construction in 1984, Cerema's PAVIN fog & rain platform has always evolved in order to stay correlated with actual stakes, renewing, improving and evolving its technical capacities and offer [40]. However, the building has achieved its maximum transformation and evolution possibilities and a complete redesign of the whole installation is inevitable. Then, Cerema initiated a new platform project in 2018 and its construction is planned for 2023 thanks to co-financing from the Auvergne-Rhône-Alpes region (France). One of the main

objectives was to increase the dimensions of the building. The new building is 50 meters length, 7 meters width and 6 meters height (Figure 8). These new dimensions will enable to consider new realistic scenarios and also to include other types of vehicles such as trucks, shuttles or even not urban vehicle (agricultural, etc.). Moreover, the positioning of the whole building in the continuity of its access road will enable to consider dynamic tests with vehicle entering or exiting of the tunnel, at realistic speed.

Beyond the strong evolution of the dimensions of the tunnel, this new platform is also improving thermal and lighting properties of the climatic chamber. The main purpose is to provide particularly optimized stable conditions over time, especially among a testing campaign for example. It consists then in a strong optimization of thermal isolation and sun exposition of the whole building, which will make possible to produce an even much better-quality fog. For lighting purposes, both natural and artificial sources will be used with adapted goals. The main idea is to obtain a good homogeneity on ground irradiance and a minimal average value. The natural light will allow to make daytime tests with the real spectrum of the sun. This will be useful for the dimensioning of the sensors of the future which use more and more varied ranges of wavelengths (SWIR, MWIR).

The rain production quality will also be strongly improved thanks to the height of the test chamber; indeed, the nozzles will be at about 5.50 m and then the rain will be very realistic from 3.5 m height (better falling velocity). In addition, the platform will be built with the possibility to recover all the rain generated and then be able to reuse it, thus working with very low water consumption, and much longer rain production time.

This new platform will offer the Cerema a great evolution at a larger scale to address adverse weather stakes with AVs, and for other applications. The building of this new adverse weather platform will be correlated with the development of fog modelling with the objective to get a numerical twin of the facility. Then, the Cerema will propose both physical and numerical simulations of fog and rain visibility conditions. One of the final purposes will be to propose a full standardized testing platform for ITS within adverse weather conditions.



Figure 8: New Cerema's PAVIN fog & rain platform

5. Conclusion

After presenting the actual PAVIN Fog and Rain platform main features, we showed the main applications of this platform. These ones may be classified into three main areas: measurement of weather conditions by camera (artificial intelligence) ; numerical simulation of meteorological phenomena ; and measurement of the impact of adverse weather conditions on vehicle perception systems.

Regarding the last area, we have shown an example of use case realized within the AWARD project: we presented a method to characterize an ODD under controlled weather conditions. The QuadSight vision system was tested in the Cerema's PAVIN platform under harsh weather conditions: fog and rain at day and night lighting conditions. Foresight's technology achieved quality results for both stereo vision light and thermal imaging.

Finally, we presented the future developments of the platform. First of all, and still within the framework of the AWARD project, we will propose new production methods in order to obtain fogs containing larger droplets. Then in 2024, a brand-new platform will be created, in order to better respond to the future challenges of ADAS and AVs development.

6. Acknowledgement



This project has received funding from the European Union's Horizon 2020 research and innovation program under grant agreement No 101006817.

The content of this reflects only the author's view. Neither the European Commission nor CINEA is responsible for any use that may be made of the information it contains.

The research team currently in charge of the PAVIN platform (F. Bernardin, S. Liandrat, J-L. Bicaud, D. Bicaud, A. Ben-Daoued, M. Ferreira Fernandes and P. Duthon) will be delighted to welcome you and discuss with you to carry out your own tests, or set up new collaborative projects. Do not hesitate to contact us via the email address adweather@cerema.fr.

7. References

- [1] W. M. Organization, Guide to Meteorological Instruments and Methods of Observation (2014 edition updated in 2017; WMO-No. 8), World Meteorological Organization, 2014, p. 1163.
- [2] P. Duthon, F. Bernardin, F. Chausse and M. Colomb, "Benchmark for the robustness of image features in rainy conditions," *Journal of Machine Vision and Application*, 2017.
- [3] K. Dahmane, P. Duthon, F. Bernardin and M. Colomb, "Weather Classification with traffic surveillance cameras," 2018.
- [4] K. Dahmane, P. Duthon, F. Bernardin, M. Colomb, F. Chausse and C. Blanc, "WeatherEye-Proposal of an Algorithm Able to Classify Weather Conditions from Traffic Camera Images," *Atmosphere*, vol. 12, 2021.
- [5] P. Duthon, M. Colomb and F. Bernardin, "Light Transmission in Fog: The Influence of Wavelength on the Extinction Coefficient," *Applied Sciences*, vol. 9, no. 14, p. 2843, 2019.
- [6] A. Ben Daoued, F. Bernardin and P. Duthon, "Comparison of 3D and 1D methods for automotive optical sensor simulation in foggy conditions," in *14th ITS European Congress*, Toulouse, 2022.
- [7] AWARE, <https://nextmove.fr/projets/aware/>, 2014.
- [8] N. PINCHON, O. CASSIGNOL, F. BERNARDIN, A. Nicolas, P. Leduc, J. P. TAREL, R. Bremond, E. BERCIER and J. BRUNET, "All-weather vision for automotive safety: which spectral band?," in *AMAA 2018, Advanced Microsystems for Automotive Applications*, Berlin, 2018.
- [9] N. PINCHON, M. IBN-KHEDHER, O. CASSIGNOL, A. Nicolas, F. BERNARDIN, P. Leduc, J. P. Tarel, R. Bremond, E. BERCIER and G. JULIEN, "All-weather vision for automotive safety: which spectral band?," in *SIA Vision 2016 - International Conference Night Drive Tests and Exhibition*, Paris, 2016.
- [10] DENSE Project, <https://www.dense247.eu/>, 2016.
- [11] M. Colomb, P. Duthon and F. Bernardin, "A Controlled Environment for Testing Sensors under Adverse Weather Conditions : The Cerema R&D Fog and Rain Platform," 2016.
- [12] M. Bijelic, T. Gruber and W. Ritter, "A Benchmark for Lidar Sensors in Fog: Is Detection Breaking Down?," *IEEE Intelligent Vehicles Symposium, Proceedings*, Vols. 2018-June, no. Iv, pp. 760-767, 2018.
- [13] M. Bijelic, T. Gruber and W. Ritter, "Benchmarking Image Sensors under Adverse Weather Conditions for Autonomous Driving," *IEEE Intelligent Vehicles Symposium, Proceedings*, Vols. 2018-June, no. Iv, pp. 1773-1779, 2018.
- [14] T. Gruber, M. Kokhova, W. Ritter, N. Haala and K. Dietmayer, "Learning Super-

- resolved Depth from Active Gated Imaging," *IEEE Conference on Intelligent Transportation Systems, Proceedings, ITSC*, Vols. 2018-Novem, pp. 3051-3058, 2018.
- [15] M. Jokela, M. Kutila and P. Pyykönen, "Testing and validation of automotive point-cloud sensors in adverse weather conditions," *Applied Sciences (Switzerland)*, vol. 9, no. 11, 2019.
- [16] M. Kutila, P. Pyykönen, W. Ritter, O. Sawade and B. Schäufele, "Automotive LIDAR sensor development scenarios for harsh weather conditions," in *2016 IEEE 19th International Conference on Intelligent Transportation Systems (ITSC)*, 2016.
- [17] M. Kutila, P. Pyykönen, H. Holzhüter, M. Colomb and P. Duthon, "Automotive LiDAR performance verification in fog and rain," 2018.
- [18] M. Bijelic, F. Mannan, T. Gruber, W. Ritter, K. Dietmayer and F. Heide, "Seeing Through Fog Without Seeing Fog: Deep Sensor Fusion in the Absence of Labeled Training Data," *CoRR*, vol. abs/1902.0, 2019.
- [19] K. Montalban, C. Reymann, D. Atchuthan, P.-E. Dupouy, N. Riviere and S. Lacroix, "A Quantitative Analysis of Point Clouds from Automotive Lidars Exposed to Artificial Rain and Fog," *Atmosphere*, vol. 12, 2021.
- [20] P. Duthon, N. Edelstein, E. Zelentzer and F. Bernardin, "Quadsight® Vision System in Adverse Weather Maximizing the benefits of visible and thermal cameras," in *2022 12th International Conference on Pattern Recognition Systems (ICPRS)*, 2022.
- [21] P. Sun, H. Kretschmar, X. Dotiwalla, A. Chouard, V. Patnaik, P. Tsui, J. Guo, Y. Zhou, Y. Chai, B. Caine, V. Vasudevan, W. Han, J. Ngiam, H. Zhao, A. Timofeev, S. Ettinger, M. Krivokon, A. Gao, A. Joshi, S. Zhao, S. Cheng, Y. Zhang, J. Shlens, Z. Chen and D. Anguelov, *Scalability in Perception for Autonomous Driving: Waymo Open Dataset*, 2020.
- [22] H. Caesar, V. Bankiti, A. H. Lang, S. Vora, V. E. Liong, Q. Xu, A. Krishnan, Y. Pan, G. Baldan and O. Beijbom, *nuScenes: A multimodal dataset for autonomous driving*, 2020.
- [23] A. Geiger, P. Lenz and R. Urtasun, "Are we ready for autonomous driving? the kitti vision benchmark suite," in *2012 IEEE conference on computer vision and pattern recognition*, 2012.
- [24] F. Yu, W. Xian, Y. Chen, F. Liu, M. Liao, V. Madhavan and T. Darrell, "Bdd100k: A diverse driving video database with scalable annotation tooling," *arXiv preprint arXiv:1805.04687*, vol. 2, p. 6, 2018.
- [25] K. Dahmane, P. Duthon, F. Bernardin, M. Colomb, N. E. B. Amara and F. Chausse, "The Cerema pedestrian database : A specific database in adverse weather conditions to evaluate computer vision pedestrian detectors," 2016.
- [26] C. Sakaridis, D. Dai and L. V. Gool, "Semantic Foggy Scene Understanding with Synthetic Data," *International Journal of Computer Vision*, vol. 126, pp. 973-992, March 2018.
- [27] C. Ancuti, C. O. Ancuti and R. Timofte, "Ntire 2018 challenge on image dehazing: Methods and results," in *Proceedings of the IEEE Conference on Computer Vision and Pattern Recognition Workshops*, 2018.
- [28] Y. Zhang, Y. Tian, Y. Kong, B. Zhong and Y. Fu, "Residual dense network for image super-resolution," in *Proceedings of the IEEE conference on computer vision and pattern recognition*, 2018.
- [29] S. Ki, H. Sim, J.-S. Choi, S. Kim and M. Kim, "Fully end-to-end learning based conditional boundary equilibrium gan with receptive field sizes enlarged for single ultra-high resolution image dehazing," in *Proceedings of the IEEE Conference on Computer Vision and Pattern Recognition Workshops*, 2018.
- [30] Y. Lei, T. Emaru, A. A. Ravankar, Y. Kobayashi and S. Wang, "Semantic Image Segmentation on Snow Driving Scenarios," in *2020 IEEE International Conference on Mechatronics and Automation (ICMA)*, 2020.
- [31] H. Sim, S. Ki, J.-S. Choi, S. Seo, S. Kim and M. Kim, "High-resolution image dehazing with respect to training losses and receptive field sizes," in *Proceedings of the IEEE Conference on Computer Vision and Pattern Recognition Workshops*, 2018.
- [32] O. Kupyn, V. Budzan, M. Mykhailych, D. Mishkin and J. Matas, "Deblurgan: Blind motion deblurring using conditional adversarial networks," in *Proceedings of the IEEE conference on computer vision and pattern recognition*, 2018.
- [33] N. A. M. Mai, P. Duthon, L. Khoudour, A. Crouzil and S. A. Velastin, "3D Object Detection with SLS-Fusion Network in Foggy Weather Conditions," *Sensors*, vol. 21, 2021.

- [34] A. Pfeuffer and K. Dietmayer, "Robust semantic segmentation in adverse weather conditions by means of sensor data fusion," in *2019 22th International Conference on Information Fusion (FUSION)*, 2019.
- [35] Y. Li, P. Duthon, M. Colomb and J. Ibanez-Guzman, "What happens for a ToF LiDAR in fog?," *Transactions on Intelligent Transportation Systems*, 2020.
- [36] R. Heinzler, F. Piewak, P. Schindler and W. Stork, "Cnn-based lidar point cloud de-noising in adverse weather," *IEEE Robotics and Automation Letters*, vol. 5, p. 2514–2521, 2020.
- [37] M.-g. Cho, "A Study on the Obstacle Recognition for Autonomous Driving RC Car Using LiDAR and Thermal Infrared Camera," in *2019 Eleventh International Conference on Ubiquitous and Future Networks (ICUFN)*, 2019.
- [38] V. John and S. Mita, "Deep Feature-Level Sensor Fusion Using Skip Connections for Real-Time Object Detection in Autonomous Driving," *Electronics*, vol. 10, 2021.
- [39] P. Duthon, M. Colomb and F. Bernardin, "Fog classification by their droplet size distributions. Application to the characterization of Cerema's PAVIN BP platform (under review)," *Atmosphere*, 2020.
- [40] M. Colomb, K. Hirech, P. André, J. J. Boreux, P. Lacôte and J. Dufour, "An innovative artificial fog production device improved in the European project "FOG"," *Atmospheric Research*, vol. 87, no. 3-4, pp. 242-251, March 2008.

ADB TECHNOLOGIES AND COMMUNICATIONS

The transition for ADB in the US market and lighting strategy

V. Molto¹, N. Costa², D. Novack³, M. Collot¹

1: STELLANTIS, Route de Gisy - 78943 Vélizy-Villacoublay - France

2: CRF – Corso L. Settembrini 40, 101135 Turin - Italy

3: STELLANTIS – 800 Chrysler Drive, Auburn Hills, Michigan 48326 - United States

Abstract: In this presentation, we are going to present the Stellantis strategy to deploy the ADB on a large range of vehicles by using the same SW and keeping offering freedom on headlamp design to style teams.

With the recent ongoing evolutions in the US regulations to allow ADB, Stellantis see the opportunity to enlarge this strategy to US, deploy it on a higher number of vehicles models and brands, and reduce diversity between European and US market, but faces the difficulties linked to the US constraints and specificities.

Keywords: AFS, ADB, US, standardisation, ECU.

1. Introduction

It's not necessary to present anymore ADB system, as it has been deployed for 10 years in Europe on many brands and vehicles. The benefits of this function are shared by a lot of customers.

A very big number of devices belong today to the family of ADB lighting modules. The variety of shapes, performances, number of rows, number of segments, external lens dimensions and other characteristics are countless.

One component is very important for the final performance on vehicle and is often neglected because not visible from outside: the ECU which includes all the intelligence of such function.

For Stellantis group, the device has to be standardized in order to increase volumes, reduce cost R&D hours, and time of performance and functional validations.

2. First generation

The C- Hatch program has been launched from 2017 to 2021.

It includes 5 vehicles of 4 different brands: 308, 408, DS4, C5X, Astra.

As we can see in the images below (Figure 1 & Figure 2), each vehicle has its own signature, its own optical modules, its own animations, its own AFS and ADB modes but share the same ECU, with the same HW and the same SW.



Figure 1 : DS4 Front face upper version



Figure 2: 308/408 front face – upper version

The management of the different light sources in order to be compliant with design intention, marketing request, regulation and performance targets is done by a specific calibration for each version.

For this program, Stellantis has developed with its partners two versions of standard ECU:

- one for mainstream level headlamps with limited functionalities,
 - one for high level headlamps with advanced functionalities (Figure 3) as AFS functions, matrix 1 row, specific animations, ...
- The headlamps equipped with such system are compliant with European and Chinese regulation.

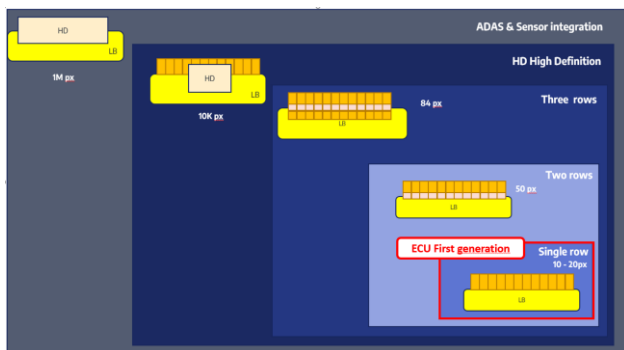


Figure 3: Perimeter covered by the ECU first generation

The benefits of this strategy are:

- the cost reduction due to the ECU massification,
- A unique software and the possibility to choose some features from a wide list,
- the simplification of the validation phases for the vehicles coming after the launcher,

But there are some difficulties too, as:

- the behaviour of each feature, the electrical interfaces between the different components, shall be specified by Stellantis several months before the beginning of the vehicle program. At this stage the design content of each vehicle is not known.
- several suppliers are involved in the development of the complete system and it's sometimes difficult to manage it.
- Stellantis becomes responsible of the performance tuning and functional check on the vehicle.

3. Second generation

Despite these difficulties, it's been decided to continue this strategy on the next programs.

The C-Suv and D-Cross program are under development since 2019 and composed of 9 vehicles for 6 brands.

The design and technical content can't be revealed at this stage.



Figure 4: C-SUV and D-Cross not revealed yet

As for the first generation, two versions of standard ECU are under development:

- one for mainstream level headlamps with limited functionalities,
- one for high level headlamps with much more available features than in the first generation (Figure 5): digital dynamic bending light, specific management of the cornering and static bending light, High Beam Boost, GFHB with motorway restriction and traffic sign anti-glare, ...

Moreover, it's possible to drive systems with one single row, two rows, three rows and it is also compatible with High-Definition Module. A large flexibility is possible for the global design of the vehicle as the signaling functions can be implemented in different locations: headlamp, bumper, grill.

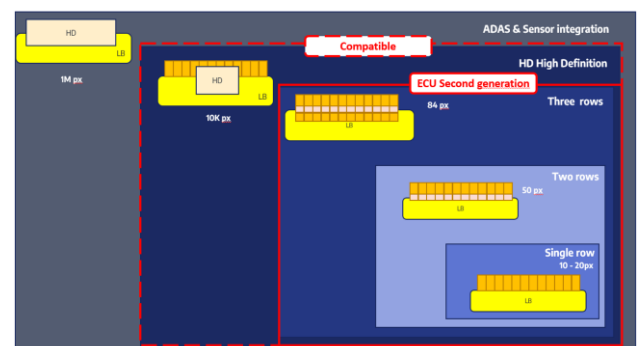


Figure 5: Perimeter covered by the ECU second generation

4. Next steps

The authorization of ADB function in the US is for Stellantis an opportunity to enlarge the number of vehicles with ADB and to reduce diversity linked to marketing countries.

However, there are unique requirements in the U.S. Adaptive Driving Beam Final Rule which Stellantis, and the industry, are currently evaluating. These unique requirements include:

- The Adaptive Driving Beam must comply with the lower (low) beam photometry in the shadow area, and upper (high) beam photometry outside the shadow area, with only a 1.0 degree transition zone.
- Includes both ADB lamp level laboratory photometric testing, and vehicle level driving tests where the ADB equipped vehicle is evaluated against test fixtures with standardized lamps. There is ambiguity in the laboratory test requirements. Stellantis is unclear at this time what the laboratory photometric test report needs to contain (e.g., how many different locations of the shadow need to be included in the test report?).
- The allowable ADB glare limit in the vehicle level driving tests appear to present challenges for some existing lower beam photometry requirements, particularly in the right curve driving test.
- The ADB Final Rule maintains the FMVSS 108 upper beam (high Beam) maximum intensity limit of 75,000 candela per headlamp in the area of the ADB unreduced intensity. This is considerably less than the 215 000 candela maximum limit per driving beam headlamp specified in UN Regulation 149.
- Horizontal aim only permitted if the ADB headlamp is equipped with a Vehicle Headlamp Aiming Device (VHAD).

One of main differences between ECE ADB and US ABD is the “tunnel” or “Shadow”:

- In ECE the regulation required to have the “tunnel” around the vehicles (oncoming or preceding) as dark as possible (Figure 6).
- In the US, the regulation requires lower beam requirements to be met in the “tunnel” or “shadow” area (Figure 7) and upper beam

requirements to be met outside the “shadow” area.

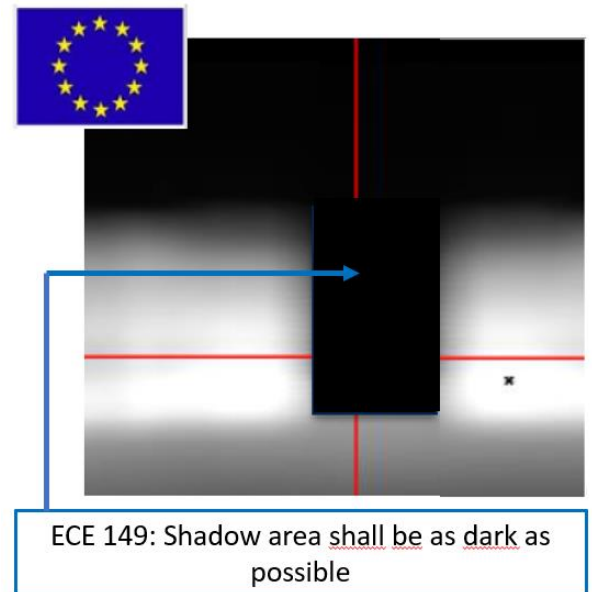


Figure 6 [1]

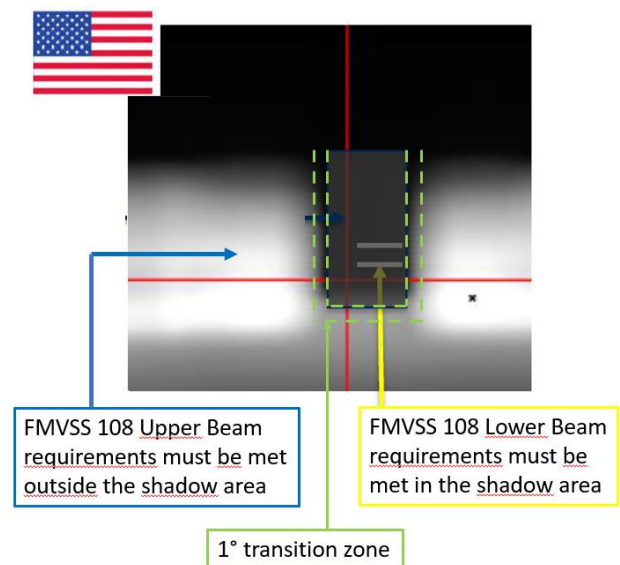


Figure 7 [1]

We know that the existing Stellantis ADB algorithm used in Europe will not be able to meet the US ADB Final Rule requirements and there is still a lot of work to do to answer to every open point.

Our target would be to develop optical modules and ECU with hardware and software capable of meeting,

or being easily modified to meet, ADB headlamp requirements for both the UNECE and US markets.

5. Conclusion

Stellantis lighting strategy is well defined and closely linked with the AFS and ADB functionalities and the development of standard ECUs.

The recent regulatory changes of ADB in the US are a good opportunity to integrate the US into this lighting strategy but it seems difficult to apply it in short term. Stellantis rely on the support of its suppliers and partners to find solutions and enable us to achieve this target.

6. Acknowledgement

The authors acknowledge the contribution of their colleagues and our partners companies to this work.

7. References

[1] Images from a Marelli's technical presentation

8. Glossary

ADB: Adaptive Driving Beam

ECU: Electrical Command Unit

HW: Hardware

SW: Software

AFS: Advanced Front light System

FMVSS 108: Federal Motor Vehicle Safety Standard 108

VHAD: Vehicle Headlamp Aiming System

Communication with exterior lighting through high definition front & rear signalling functions

Antoine de Lamberterie¹, Eric Moisy², Gregory Planche¹, Jose Afonso¹, Rezak Mezari¹, Onoriu Puscasu¹

1: Valeo, 34 rue Saint André, 93012 Bobigny, France
2: Valeo, Feringasträße 11,13a, 85774 Unterföhring, Germany

Abstract: Current trends toward the digitalization of exterior lighting and the development of L4 - L5 autonomous vehicles emphasize the need and added value for pixelated signalling and lighting systems that are able to communicate. The possibility of displaying symbols and text on the car outer surface answers new usages. It brings signalling to a higher level of interaction and gives a new dimension for stylists to explore.

Display for automotive exterior lighting is a new field of application of display technologies coming from consumer electronics and it brings new technical challenges to ensure that key parameters such as contrast, brightness and reliability are fitting with the exterior lighting environment. Beside contrast and reliability, style and regulation should be taken into account to achieve a regulatory, consistent and harmonious association with existing signalling and lighting functions. Do displays have to be merged with existing signalling functions? How can it be possible and what changes does it imply in terms of styling and performances?

In this paper, we will present how display integration brings different challenges for rear and front lighting systems, how best in class and innovative technologies can be provided to solve these challenges.

Keywords: Display, MiniLED, MicroLED, Automated Vehicles, Communication and pedestrian interaction, Signalling, external Human Machine Interfaces

1. Introduction

Digitalization of exterior signalling is shaping the vehicle design more than ever. Desire of personalization and differentiation will continue growing in the future to enhance brand signature.

This trend is being pushed by the development of the electric vehicle market, which enables higher space for digitalization in exterior vehicle lighting. Digitalization of signalling is also being accelerated by the development of autonomous vehicles: their use requires communication functions, amongst others, safety functions between road users, which can be pedestrians, two wheelers, vehicles and so on.

The implementation of exterior displays is key to answer to Digitalization. Moreover, smart integration and selection of the best display technology will effectively bring signalling to a higher level, improving style, communication features and safety.

In this paper, we will start from the usages of displays in the automotive exterior signalling. Then we will specify exterior displays: size and contrast, according to the usage identified. At last, before focusing on display technologies, the three next parts will be respectively focused on three key aspects of display integration: Style, Optics and Electronics.

2. Usage of Exterior display

Exterior display shall add a new value with new usages to go further in the personalization of the style, the signature of the vehicle and to provide various information to the driver or the other road users. They will also be part of humanizing the vehicles with warmer, friendly, engaging and immersive communication.

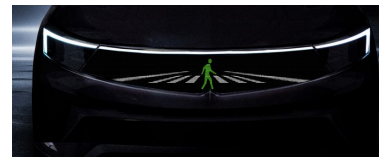


Figure 1: Stellantis OpenLab in Germany (Technical University of Darmstadt) display replaced the traditional grill for Internal Combustion Engine

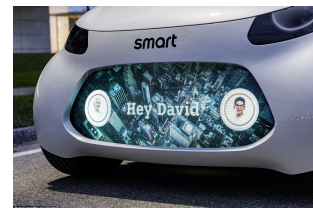


Figure 2: EV Smart Concept with immersive welcome scenario

2.1 Specific cases dedicated to autonomous vehicles

Exterior displays will also contribute to communication and safety in automated driving scenarios. They will enable a better acceptance of the autonomous vehicles for the other road users. The EU Hi-Drive collaborative project, where Valeo is a key partner, addresses a number of challenges

to reach high automation readiness (SAE Level 3 & 4). The project ambition is to considerably extend the operation design domain (ODD) and reduce the frequency of the takeover request by selecting and implementing technological levers. This requires that the AV manages its ODD safely but also communicates, interacts, and negotiates with the different road users (pedestrians, cyclists and other car drivers) to improve flow and reduce conflict. With these aims, Valeo focuses on (1) the definition, and specification of several use cases, (2) the study of road users interactions, (3) establishing what types of communication will be used between an AV and pedestrians and (4) investigating how this information can be used to design external HMI (eHMI) for AVs.

Therefore, activities started with an agreement on and definition of relevant Hi-Drive use cases that an AV could be confronted with. The Hi-Drive use cases have been selected using a step-wise process of discussions within the consortium, starting with literature, the analysis of accident statistics and some open brain-storming discussions. The use cases were aggregated and rated against several criteria (such as relevance for safety, need for interaction behaviour etc.) to agree on the most relevant ones. Two relevant use cases were identified in which the introduction of a display would add a real value to improve traffic flow and safety, without interfering with other road-users' behaviours.

2.2 Use cases

In this part, the two relevant selected use cases are described. The location of the displays will be based on them. These use cases are to be evaluated and showcased in the Hi-Drive demonstrator vehicles at the end of the project. They are the following:

Pedestrian crossing

The Autonomous Vehicle approaches a zone where a pedestrian intends to cross the road. The pedestrian is not sure if she/he was detected by the AV. The AV communicates that it will wait for pedestrians to cross the road (C2P).

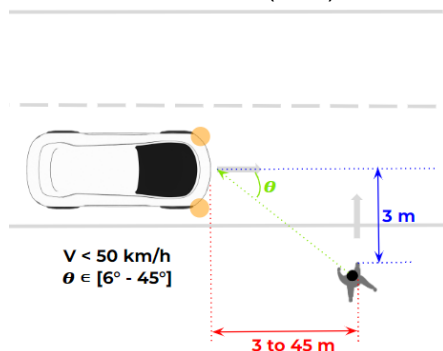


Figure 3: Pedestrian crossing : use case description

Vehicle departing from parking lot

The AV gets out of a perpendicular parking while its vision is limited (blind spot). This might cause dangerous situations for cyclists, pedestrians and other vehicles. The AV indicates the manoeuvring intention of the Valet Parking mode and creates a Safety zone around the vehicle to warn the Vulnerable Road Users about that dangerous situation.

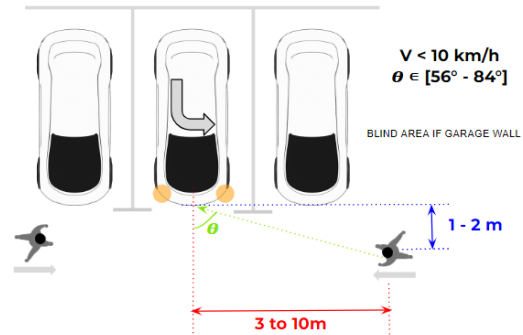


Figure 4: Vehicle departing from parking lot (front) - Use case description

3. Display Specifications

The description of the above use cases helps to understand the added value of exterior display. Moreover, the distance of observation, dynamic conditions (speed) and environmental conditions are key inputs to build display specifications and provide both the required range of display size and the required display contrast ensuring good visibility.

3.1 Display Size Specification

The ISAL paper [1] presented by VALEO in April 2022 shows clear specifications of display size relying on two needs: visibility of the display and good identification and understanding of the pattern which is displayed. As shown in Fig 5, the typical display size required for a viewer placed at 20m must be higher than 70mm and must reach 140mm when considering a more complex displayed pattern.

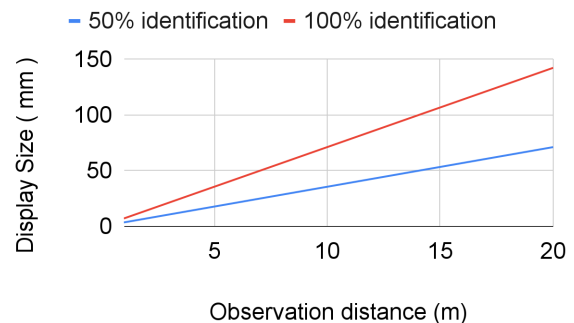


Figure 5: Display size needed for symbol identification

3.2 Display Contrast specification

In addition to size, the visibility of displayed patterns mainly relies on contrast between ON display area

and OFF display areas. Our definition of contrast is based on the Weber Contrast formula:

$$C_W = \frac{(L_{ON} - L_{OFF})}{L_{OFF}} \quad [1]$$

where L_{ON} and L_{OFF} are respectively brightness in ON and OFF areas, as seen also in Fig. 6 showing a display with a pedestrian crossing pattern.



Figure 6: Contrast definition

First approach is to consider a specification of contrast through the theory of eye sensitivity to contrast. From 1962 [2] to 1993 [3], several measurements have been conducted to evaluate eye sensitivity to contrast before the building of a model by Barten [4] in 1999. Fig. 7 shows measurements done in 1978 [5] with a brightness of 100cd/m² and the Barten model is observed in a continuous curve.

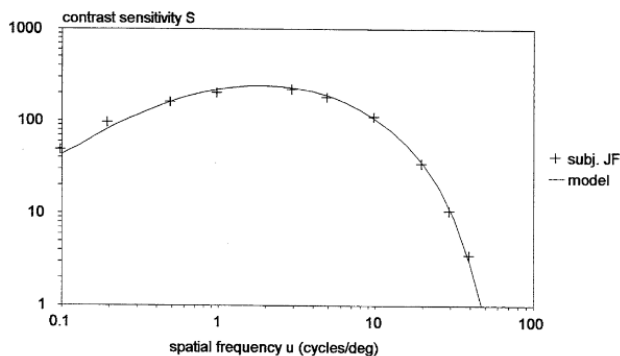


Figure 7: Barten Model and measurement from Howell & Hess (1978) [4]

An important information given by this measurement and this model is the fact that eye sensitivity continuously drops for a value of 50 to 60 cycles/deg. This justifies that higher contrast must be delivered when viewer distance increases while display size remains unchanged. However, practical use of Barten's model in the context of Automotive Signalling remains difficult. Driver's acuity is not always at the highest level, the pattern is not always placed in central vision and the driving situation is obviously not static. This explains that the real required contrast is by far higher than the contrast given by the model. In addition, comfortable visibility much higher than physiological thresholds has also a

positive impact on perceived quality. If the theoretical model remains a good reference, we have chosen to conduct a field test to evaluate the required contrast. More than 20 participants, having various visual acuity and placed at various distances were asked to give their feeling about various patterns' visibility and perceived quality. Four sessions were organized, giving the possibility to consider various locations but also various exterior/ambient light environments. The key outcome of all sessions confirmed that Weber contrast must be higher than 2, and sometimes more when considering higher distances.

3.3 Coming back to usages

Considering the two usages presented in the previous section, we can conclude on the specifications detailed on Fig. 8, knowing that activation of display in pedestrian crossing case starts when the car is located at 20m from pedestrian.

Usage	Display Size [Must]	Display Size [Nice to have]	Weber Contrast [Must]	Weber Contrast [Nice to have]
Pedestrian crossing	100 mm	200 mm	3	4
Vehicle departing from parking lot	50mm	100mm	2	3

Figure 8: Display specification according to usage

4. Integrations and Styling

4.1 New features

In the automotive industry sector, LEDs and OLEDs have opened up new horizons in the field of style and functionalities. Enhanced design freedom was made possible, through the graphic treatment of light in 2 or 3 dimensions and it has also brought a degree of animation, thanks to the electronic control of each element giving an evolution of the functionalities: running turn indicators, proximity warning, customization of lit areas or leaving home scenarios are significant examples of these new functionalities.



Figure 9: Customization - Audi Q4 - 2021 - Audi Mediacenter

Without this technological step, the design trends we know today would probably not have existed. In addition to changing the general design and details of our vehicles, this step can be also considered as the first level of a more evolved type of communication, with an increasing accuracy and relevancy of the messages delivered to other road users.

Today, the emergence of display technologies opens a new era that will allow ever-advanced communication. Display integration may create new impacts on style, depending on the selected technology. It is also a great opportunity thanks to the awesome possibilities offered by the display itself through the images displayed.

4.2 Specific style impacts

First design key: Curvature

The stylist's dream of having a full free form display matching with bodywork, as demonstrated with the Audi Swarm study shown in 2013 (figure 10) is still far from being mature for production today.



Figure 10: Audi Swarm - 2013 - Audi Mediacenter

If curved display technologies progressively emerge in the consumer market, shapes remain ruled and not fully free form. In addition, specific reliability constraints limit curvature threshold to flat or slightly curved shapes. This impacts the style of surfaces and volumes, as experienced with the first generation of OLEDs and overcome by using floating 3D elements or by faceting displays bricks when the designer seeks to follow a main volume.

Second design key: Sizing

The beginning of the decade has seen a strong styling trend to refine signatures of front and rear fascia with increasingly reduced heights. This height reduction seems part of a trend to emphasize the minimalist and pure graphic signatures while demonstrating how new technologies such as LEDs and Laser are able to take up challenges of maintaining legal specifications with ultra homogeneous thin aperture.

Optimised added value of exterior display requires to consider all use cases including communication use

cases where a large surface is required to ensure good understanding of message as stated above.

Therefore, display sizing for long distance and resulting display height will be one of the important data to be taken into account by the designers, to integrate it suitably into their design, while display width should have less impact considering current trends.

Third design key: Location

Location of the display on the car is also a key element. Location at the centre of fascias, two symmetrical displays disposed on each side on fascias, but also display located on the car side are three options that need to be considered according to the use case, i.e. according to the relative position of the viewer with respect to the car. Fig. 11 provides a simple illustration of how the location of the display on the front side is linked to viewer position and how this position modifies the display perception due to car body shape.

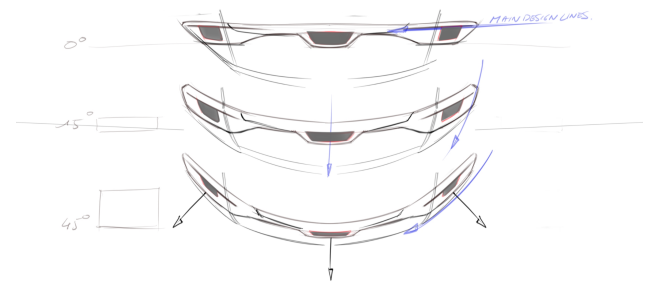


Figure 11: Front location - Valeo Design

Mastering the design

The compatibility of these 3 design keys with a mastered style harmoniously matching the car body and headlamp design rely on the flexibility offered by display technologies: especially on free form contour - as illustrated in Fig. 12.

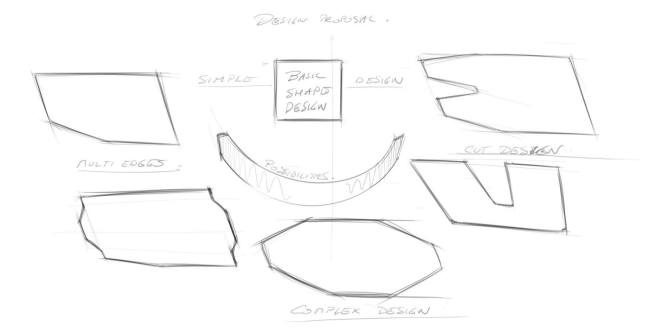


Figure 12: Front location - Valeo Design

Current display flexibility, and also future flexibility offered by technology improvements are key, but in any case, successful harmonious style requires that display integration occurs as early as possible within the car development process, as illustrated in Fig. 13.

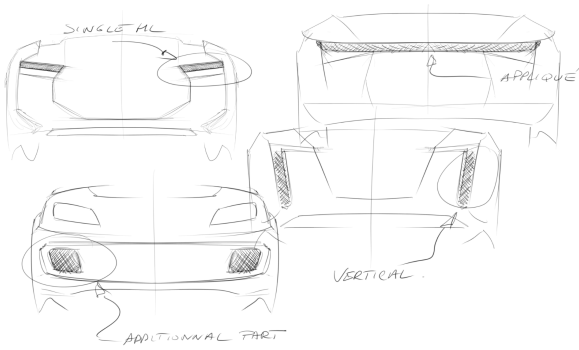


Figure 13: Front location - Valeo Design

4.2 Display content

If regulatory constraints are limiting display content, especially the colour, animation and activation rules, there is still some room to create awesome possibilities of contents to offer customized signalling functions. The use of grayscale to create a 3D effect is a good example of what can be done, as illustrated in Fig. 14.

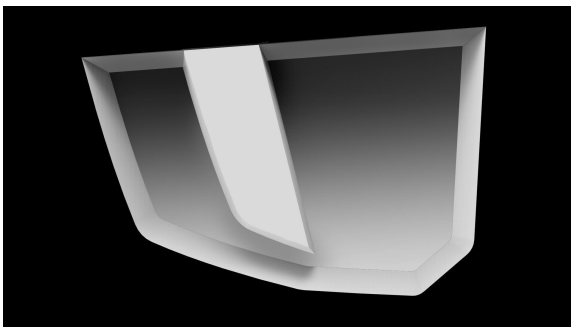


Figure 14: Sample of 3D effect - Valeo Design

Animations are possible in the context of leaving home scenarios without impairing road safety. All these contents require the development of a new domain inside the exterior light design departments, opening an evolution of designers know-how and designers tools that are closely linked with the 2D or 3D animation world. This evolution will increase driving experiences and interactivity for end users.

4.3 New Possibilities

Several design proposals have been presented on concept cars in the last decade, revealing the need to communicate, highlighting the "hype" of hyper connectivity and keeping up with the pace of the society/generation.

Most of these proposals conceal a consumer display under a smoky cover. This approach shows the use cases and functionalities but it is not sufficient to provide a harmonious and automotive robust design. Despite today's limitations of display technologies, a first step will initiate the revolution that will arrive in the more distant future with much deeper impacts on future vehicles. The Fun VII prospective concept (Fig. 15) made by Toyota in 2011 already showed

some of these new possibilities and design impacts. Now, it is to the design studios to exploit all the new features and characteristics to propose their visions of the communication based on the displays.

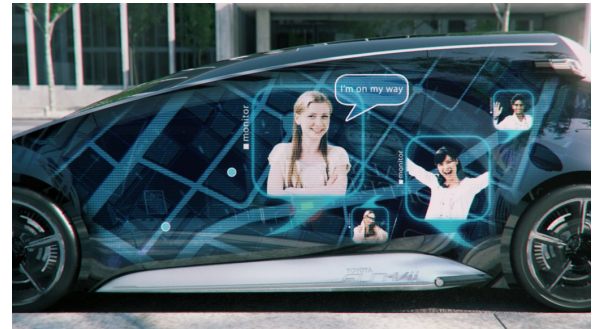


Figure 15: Toyota Fun VII - 2011 - Toyota Press Site

5. Integration and Visibility

As explained above, Visibility relies on contrast between L_{ON} and L_{OFF} areas. Majority of the L_{OFF} contribution is linked to the reflection from the exterior light surrounding the car's environment: sky by day, street lights or headlamps of oncoming drivers by night. This contribution is by far much higher in comparison to potential crosstalk effects that may be observed in some display technologies. Fig. 14 clearly shows some of these effects also called "Phantom effects"



Figure 16: Phantom effect on Rear Lamp

Considering brightness coming from exterior light (L_{ext}), we can easily specify required display brightness to ensure the good visibility:

$$L_{ON} = L_{ext} + L_{display} \quad [2]$$

$$L_{OFF} = L_{ext}$$

$$\text{thus : } L_{display} = C_w \cdot L_{ext} \quad [3]$$

Beside required contrast, brightness specification depends on exterior light configuration but also on the way light is distributed by the headlamp, the rearlamp or central module. Reduction of these effects maintains good visibility while having a huge impact on cost and power consumption. We present here 2 key design factors having significant effect on the brightness specification.

5.1 Outer lens

Vitreous reflection on the outer lens is a strong contributor to the background brightness and some relevant design choices are preferred. Anti reflection coating, but also matching between outer lens and display colour are relevant ways to reduce the

brightness reflected by the outer lens. Fig. 17 shows the brightness specification by day considering a large sky area with high turbidity (providing a brightness of 15 kcd/m²).

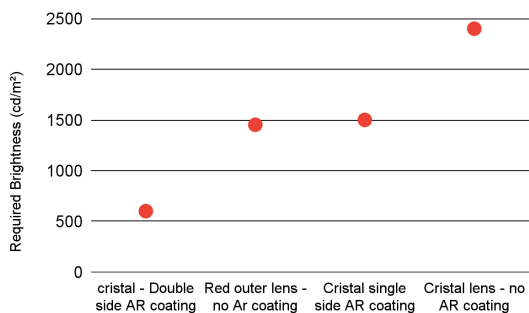


Figure 17: Brightness request according to lens design

If the added value of AR coating is obvious, the use of a red outer lens provides a huge benefit. For rear red display, this option is efficient and remains quite cost effective. Inclination of the outer lens is also a key design factor having an impact on specified brightness. Lower inclination reduces by far the statistical chance that the viewer sees an image of the sky reflected by the outer lens since the sky areas toward low angular height are hidden by all objects surrounding the roads and streets (trees, walls or buildings). This is clearly illustrated by Fig. 18 showing cars in the same environment. In the upper image, the outer lens has an inclination of 5° whereas the one from the lower image has an inclination of 30°.



Figure 18: Impact of the outer lens inclination on contrast and required Brightness

5.2 Veiling Luminance and Disability glare

Brightness specification must also consider glare effects coming from various sources. Other functions located in the rear lamp (Stop, Turn) or in the headlamp (DRL, Turn, Low Beam) are obviously to be considered, but some style objects such as bezels or even the car body itself may create disability with reduction of the contrast. A concrete example is observed in Fig. 19 showing required brightness according to distance between various glare sources and the display. Veiling luminance is

evaluated using CIE 2002 standard formula which is known as being valid for small angle values. Viewer is placed at 10m and is 60 years old.

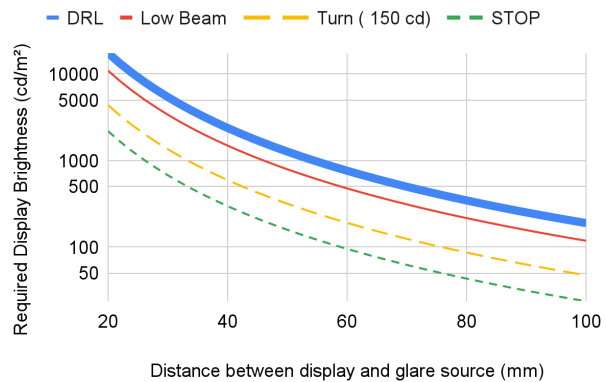


Figure 19: Brightness specification with various glare source

As clearly observed in the graph, the contribution of veiling luminance cannot be neglected, but more than that, it shows how smart integration that limits veiling luminance can avoid specifying high brightness and thus, reduces power consumption.

6. Integration and Electronics Systems

Each car maker, or group, has their own platform for their different models. This leads to a huge diversity of system architectures. Moreover, the fast evolution of the different platforms with different protocols and communication buses (including CAN, FPDLINK, RGB24, Ethernet) requires a strong knowledge of the vehicle architecture and customer, in order to give the best performance. To face those high variety and fast evolution, two architectures are able to drive the display and control high definition images: the Driver Module can be seen as a “Player” or as a “Streamer”, as illustrated in Fig. 20.

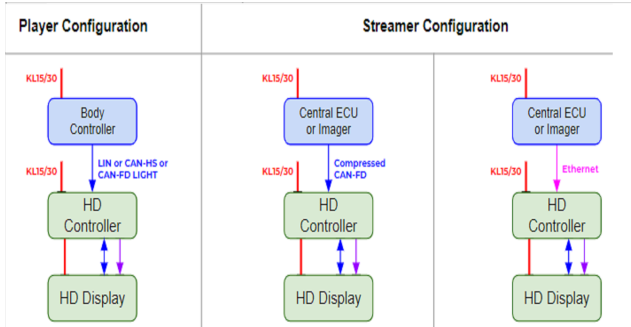


Figure 20: HD Module Vehicle architecture options

Player mode

As a “Player”, the display module corresponding to the display itself and its controller stores various images or animations (“images bank”). When the vehicle sends a request to the module according to the driving use case and scenarios, the module

answers to the request by displaying the expected scenario. Player mode allows fast transfert of the request without impacting vehicle system architecture: the use of classical CAN bus remains possible, even a LIN.

The main drawback is the bus bandwidth limitation in case we want to update the bank in the vehicle, leading to a long update time.

Streamer mode

In “Streamer” mode, “bank Images” are stored in the vehicle ECU. Therefore, the ECU transfers the image to the display module which directly displays it. This version has a strong need for data bandwidth requiring different solutions such as Ethernet bus or a traditional CAN SIC (of 5 Mbits) if data is compressed. However, Ethernet protocol is more and more used and will likely become the standard communication bus in the next vehicle platform generations.

This “bank” of images/videos/animations can be loaded and updated by the car maker through OTA (“Over-the-Air”) or by the vehicle owner through his smartphone. The owner is able to select from the library (defined by the car maker) the different options for each use case such as a personalized signature of the vehicle. In the same way, a company owning a vehicle fleet would be able to apply standard personalization on all cars. Both are challenging solutions for which Valeo has developed relevant solutions and tools.

Thanks to years of expertise and strong investments in this field, each element is being designed & defined taking into account performance, cost and CO₂ neutrality.

7. Display Technologies

In the consumer display world, high competition but also a high variety of needs and applications lead to a high variety of technologies. Development of displays for exterior automotive application requires a rigorous selection of the technologies in two steps. First step is to identify the key criteria that are used to select the technology, while the second step is the evaluation of the technologies and their roadmap.

7.1 Identification of key criteria

For any system dedicated to automotive business, several constraints criteria must be considered corresponding to the following key criteria.

Light Efficiency

This criteria is inevitable in the current context of CO₂ reduction, and is emphasized in the context where visibility by day may require relatively high brightness.

Cost

Cost is obviously an important factor but it should be considered cautiously as regards added value of the product, and as regards car segmentation.

In addition to these criteria, we also must consider specific criteria relative to the display application and to the display integration.

Brightness

As observed in the previous page, Visibility relies on contrast and brightness. Even if some smart integration helps to decrease specification, Required brightness by day remains higher in comparison to display used in the consumer Business.

Style Flexibility

As seen above, mastered design relies on display style flexibility: free form edge and curvature are therefore to be taken in account.

Scalability

Scalability is the ability to tune the LED pitch, colour and display size. This is very important when willing to easily adapt the technology to customer needs and requirements.

7.2 Technologies

We can make a distinction between self-emissive technologies and technologies requiring light modulation added to a backlighting unit.

Self Emissive Technologies

LEDs & OLEDs are currently the two light source technologies used to build self emissive displays. Two typical kinds of LEDs are used: MiniLEDs above about 100µm are associated with passive matrix drivers whereas MicroLEDs below 100µm are usually used with active matrix drivers to maintain good brightness. Last but not least, OLED is associated with a thin film active driver to build AMOLED. Fig. 21 presents a radar mapping of these 3 technologies relatively to the 5 key criteria presented above, and considering performances reached today.

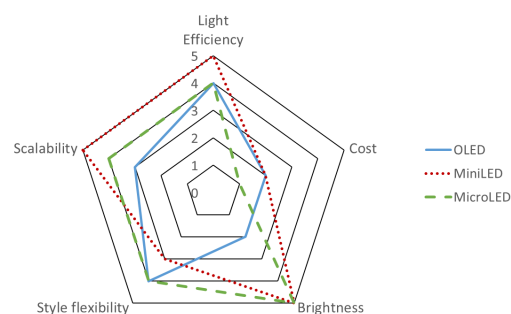


Figure 21: Ranking of self emissive technologies

Technologies with Light Modulation

LCD is the most common technology to modulate the light thanks to polarised light. Recent improvements have been made possible with Mini LED by using local dimming of back lighting illumination, thus reducing power consumption and crosstalk effects at iso brightness. Fig. 22 shows a radar mapping of the two existing LCD technologies: standard technology without local dimming, and standard technology with local dimming.

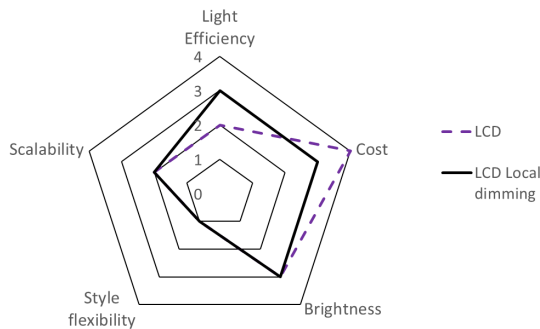


Figure 22: Ranking of LCD technologies

As clearly observed on these graphs, some technologies such as MiniLED and MicroLED are very promising since they can provide both good brightness and good efficiency. Moreover, these solutions are quite flexible. If the cost is high today, we can expect a decrease in the future thanks to the volume effect. Moreover, scalability through pitch and size gives the possibility to tune the compromise between cost and pitch and address a large panel of car segments.

8. Conclusion

Exterior display is the next step of digitalization and beyond continuing to shape the style of the vehicle, it will bring new usage for communication pushed by the automation of the vehicle. The regulation must continue to evolve to open these new possibilities.

As we can see in this paper, once the right display technology is selected, the key activities are its integration into the vehicle. Based on a full system approach from the analysis of the use cases down to reliability tests, Valeo develops all the technical solutions for display integration whilst mastering the impact on the style of the vehicle, the compliance with the electronic architecture and ensuring its visibility on the vehicle whatever the exterior light surrounding the car's environment.

All aspects of these developments are also driven by the VALEO commitment to reach carbon neutrality by 2050.

In the context of the EU Hi-Drive collaborative project, the display implementation and the relevant use cases will be tested in real conditions. These tests will contribute to understanding the needs of other road users interacting with autonomous vehicles in order to increase the acceptance.

9. Acknowledgement

This work is part of the Hi-Drive project. This project has received funding from the European Union's Horizon 2020 research and innovation programme under grant agreement No. 101006664. The authors would like to thank all partners within Hi-Drive for their cooperation and valuable contribution.

10. References

- [1] J. Petit, E. Moisy, A. de Lamberterie: "Style and signalling: display sizing for an optimised perception", II. Sine-Wave and square-Wave Contrast Sensitivity SAL 2021 proceedings.
- [2] J.J. DePalma, E.M. Lowry: Sine_wave response of the visual system. II. Sine-Wave and square-Wave Contrast Sensitivity, Journal of Optical Society of America - 52(3) 328-335 (1962)
- [3] J. Rovamo, O. Luntin, R. Näsänen: Modelling the dependence of contrast sensitivity on grating area and spatial frequency.
- [4] P. G.J. Barten: Contrast sensitivity of the human eye and its effects on image quality, HV Press, (1999)
- [5] E.R. Howell, R.F. Hess: The functional area for summation to threshold for sinusoidal gratings, Vision Research, 18, 369-374 (1978)

11. Glossary

eHMI : external Human-Machine Interface
 EU : European Union
 AR : Anti Reflection
 AV : Automated Vehicles
 ODD : Operational Design Domain
 C2P : Car to Pedestrian
 LCD : Liquid Crystal Display
 LED : Light-Emitting Diode
 AMOLED : Active Matrix Light-Emitting Diode
 OLED : Organic Light-Emitting Diodes
 OTA : Over The Air
 CAN : Controller Area Network
 CIE : Commission Internationale de l'Eclairage
 SAE : Society of Automotive Engineers
 DRL : Day Running Light
 HD : High Definition

Low Profile Headlamp System with efficient Light Guide Technology and improved safety standard (HSPR)

Dr Rainer Neumann¹, Tejaswi Challa², Petr Ferbas³,

1: Varroc Lighting Systems, GmbH, Germany

2: Varroc Engineering Ltd (Lighting Division), India

3: Varroc Lighting Systems, s.r.o., Czech Republic

Abstract: Automotive lighting systems have witnessed tremendous technological advancement in the recent years. Advancements in LED and manufacturing technologies have inspired the lighting designers to develop compact yet high performance systems for a variety of functions including the front lighting. In this work, we demonstrate low profile headlamp systems having just ~15mm height at the exit surface. The module(s), developed using novel light guide technology, satisfy photometry requirements imposed by ECE R149 regulation. The on-road performance of the module(s) is evaluated using the recent proposed HSPR standard to verify the safety benefit for all road users in night-time traffic. The satisfactory results indicate the scope to achieve competent light performance despite the smaller height of the headlamp.

Keywords: LED lamps, Slim headlamp, headlamp safety, HSPR.

1. Introduction

Automotive exterior lamps have benefited substantially with the advent of Light Emitting Diode (LED) light sources, especially in terms of lamp compactness and scalable light output. Several technologies have evolved over the recent years to fulfil the high optical requirements despite reduced light emitting areas and other challenges. Varroc has been actively working to address such challenges enabling headlamp technology transformation from bulky optical systems of ~100mm in height to few tens of millimetres in the recent days [1,2]. One of the milestones in the transition has been a 35mm height module designed for Jaguar E-pace produced in 2018. A 15mm height Adaptive Driving Beam (ADB) has been presented in 2019 using silicon optics and very recently developed a 15mm height light guide-based solution for fog, static bending, and base beam. A micro-LED low beam has also been prototyped. All the systems have been developed in adherence to United Nations Economic Commission for Europe (ECE) regulations. Figure-1 shows the evolution of headlamp systems developed at Varroc.

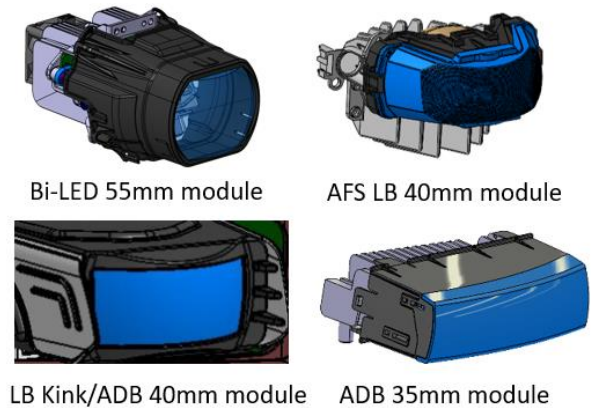


Figure 1. Varroc Headlamp modules

With the increasing demands of the market and customers, it has been deemed necessary to develop a complete compact headlamp module that fulfils both legal and safety requirements. Major concern associated with the compact headlamps is their on-road performance, especially the glare. An interesting study on these lines has been conducted by L-Lab to investigate the effect of glare in compact headlamps having 15-30mm height. Their study indicated that, for compact headlamp, the glare evaluation on DeBoer scale is like that of standard lamps having 60-80mm height [3]! The DeBoer scale approach, however, is widely used only for glare and a better tool for overall headlamp safety performance evaluation is necessary.

Headlamp Safety Performance Rating (HSPR) is the latest tool, recommended by GTB, to evaluate overall headlamp considering both the glare and on-road performances [4,5]. HSPR is the pioneer in headlamp safety evaluation in a way that it not only evaluates just low beam and high beam but for the first time ever, an ADB beam too! The evaluation methodology is based on TC 4-45 publication by CIE (*Performance Assessment Method for Vehicle Headlamps*) and applicable for any headlamp satisfying ECE regulations. The individual headlamp functions are rated on a 5-point scale, which are further subjected to varied weightages to evaluate the overall headlamp score. Accordingly, the overall headlamp rating (including all the auxiliary beams on the vehicle) is

classified into Standard, Good, Advanced, Excellent, Premium and Premium+.

This article describes a compact 15mm height headlamp prototype developed at Varroc Lighting Systems and evaluates its performance in terms of HSPR criteria. Investigations done on a relatively less compact, yet safe micro LED ADB headlamp are also mentioned in brief.

2. Low Profile Headlamp

2.1 Low Profile Headlamp Technology:

The low-profile headlamp prototype is developed using the light guide technology. Light guide is conventionally a single transparent part that redirects light from a remotely positioned light source (usually, an LED) to achieve uniform light distribution at the exit surface. Depending on the geometry of the light guide channel light pipe, light blade, light plate etc have come into light. The ability to customize the shape & profile of the exit surface has enabled light guides to be used in a variety of automotive lamps, most prominently the signalling functions. The recent advancements in LEDs to deliver higher output flux and evolution of new optical concepts has extended light guide applications to headlamp functions including the complex front lighting systems such as low beam, adaptive driving beam (ADB) etc.

The design of light guide headlamp is based on the concept of a single transparent light channel comprising of a series of elements. A variety of ideas have been investigated for this purpose and best suitable proposal to achieve the desired light distribution has been taken up. The concept is based on the principles of refraction, total internal reflection and has the potential to achieve efficiency as high as 45% with just 15mm height using PC material! The prototype headlamp in discussion comprises of two such compact modules: one for low beam and another for ADB high beam.

The low-profile low-beam module is a single part comprising of two units contributing to kink and base beams. Base beam is designed using a 3-segment light guide system, each having double chip LEDs @ 550lm each. Kink beam is designed using a compact light-guide-based-projector emitting 330lm output. The complete low beam prototype module has been observed to have an efficiency of 35% with PMMA. The system, with just ~15mm opening at exit surface (shown in Figure 2), has been designed to fulfil ECE 149 regulation and fulfils AFS modes country, motorway, and city.

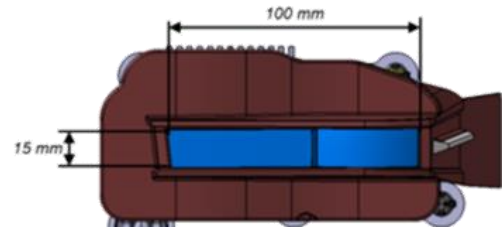


Figure 2: Light guide based slim low beam module

An ADB high beam has been developed using similar light guide technology. The 4-segment ADB prototype uses 4 No. of 2-chip LEDs @ 550 lm each and has been observed to have an Emax of 60000cd with optical efficiency of 38 %. The photometry performance and light distribution of the modules are shown in sections 2.2 and 2.3 respectively.

2.2 Low Profile Headlamp Performance:

Key photometry parameters (on 25m screen) of low beam are summarized in Table 1 and the corresponding light distribution is shown in Figure 3

Table 1: Light Guide Low beam performance

Parameter	Compact Low Beam Module (15mm)	Standard Low beam Module (35mm)
Max intensity	27627 cd	36609 cd
Intensity @ 75R	25486 cd	14621 cd
Intensity @ Zone 3	338 cd	472 cd
Intensity @ B50L	183 cd	216 cd
Intensity @ Zone IV	14363 cd	6776 cd
1 lx spread (horizontal @ 5D)	42° outboard 25° inboard	48° outboard 27° inboard
1 lx spread (vertical)	9.5 ° down	11 ° down
Flux (H: +/- 50, V: +/-15)	823 lm	996 lm

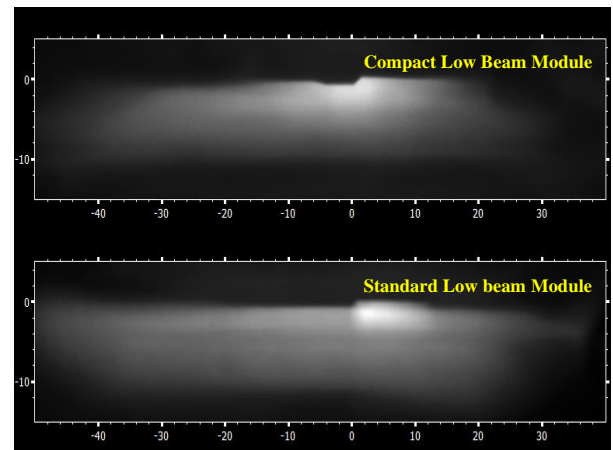


Figure 3: Low Beam light distribution on 25m screen

2.3 On-Road Performance and HSPR Evaluation:

The on-road performance of the low beam is evaluated considering installation conditions (on vehicle) as 800mm height and 1400mm width. The bird's eye view projection is shown in Figure 4 and night drive simulation is shown in Figure 5. The ADB functionality is shown in Figure 6.

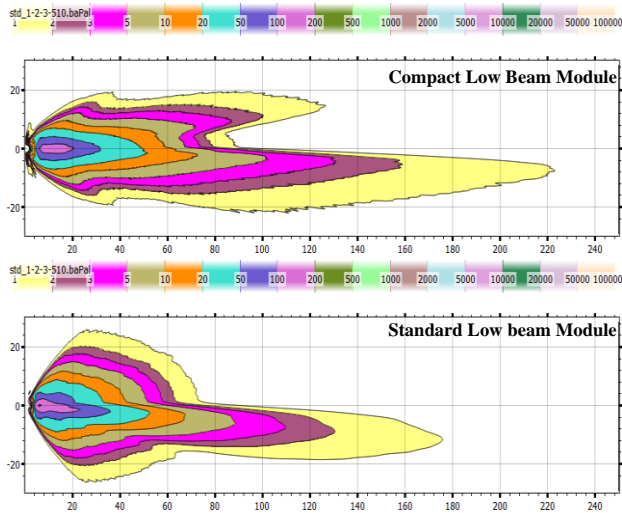


Figure 4: Birds' Eye view of the Low beam

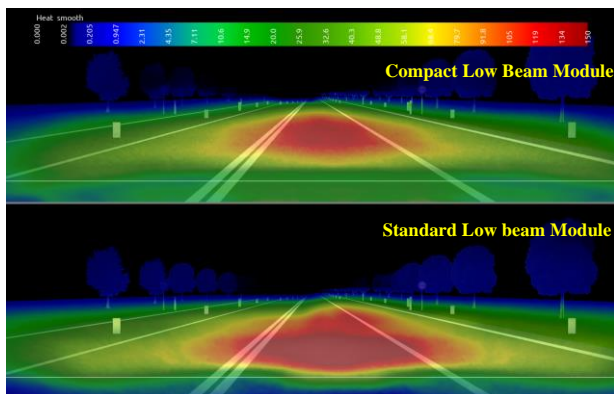


Figure 5: Drivers' view of the Low beam

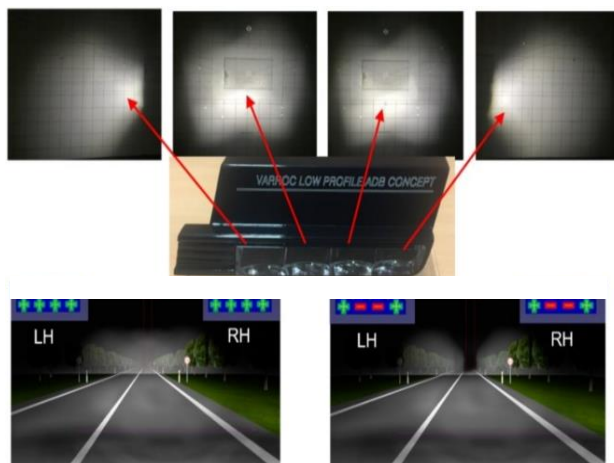


Figure 6: ADB functionality of compact headlamp

The performance of the low-profile headlamp is evaluated using the HSPR criteria and the results indicate safety at par with standard headlamp. The evaluation is done using an internal tool, developed in accordance with TC4-45 guideline. The performance results of the headlamp system are shown in Table.2. The overall headlamp performance of the compact headlamp is evaluated using the low beam in combination with the combined mode ADB high beam. '**Advanced**' HSPR rating of the system is comparable to that of standard headlamp modules, indicating the suitability of the concept for compact yet safe headlamps.

Table 2: HSPR performance of compact headlamp

Performance Parameter	Compact Headlamp	Standard Headlamp
Low Beam Score	4	3.6
High Beam Score	2.3	3.5
Overall headlamp Score (<i>manual</i>)	Advanced	Advanced
Overall headlamp Score (<i>automatic</i>)	Excellent	Excellent

2.4 Design Challenges & Future scope:

Slim headlamps have no doubt been a major market interest in recent times. However, the technology suffers from many challenges/limitations as of now. Few key challenges to realize the concept into serial production are mentioned below:

2.4.1. Tolerance: Owing to the compactness of the system, resulting in minimized active optical surfaces, the slim headlamps tend to be very sensitive to LED position and surface deviations. Hence, it is necessary to have precise manufacturing technology and assembly methods.

2.4.2. Efficiency: Another key challenge with compact lamps is the reduced efficiency due to minimized optical areas. This demands for innovative and optimized optical concepts to avoid increase in the light input (resulting in higher power consumption) or very long dimensions of the optical system.

Motivated by the encouraging results from the low-profile headlamp, investigations are being done to realize a complete-light-guide-based headlamp satisfying AFS modes with acceptable HSPR rating. Studies are also in progress to evaluate and improve the performance of light guide headlamps having smaller than 15mm height. In addition, other novel technologies, like the micro LEDs, are also in consideration to design smaller yet safer headlamps.

2.5 Micro-LED headlamp:

Micro LED headlamp is an advanced multifunctional system having both the light distribution and symbol projections within the same module. The micro-LED headlamp system comprises of 3 projector modules: a micro LED Kink Beam with symbol projection developed using a 20k pixel μ LED, a base beam projection module and an ADB matrix. Layout of the μ LED headlamp prototype is shown in Figure 7. The safety performance of the system is evaluated in terms of HSPR under two cases: first, considering the combined ADB high beam and second, considering the different ADB modes. In combined mode, the high beam light distribution remains same throughout and acts a typical high beam. In the second case the six modes of ADB High beam, as specified by ECE 149, are considered for the evaluation. The lamp has been rated '**Advanced**' in first case and '**Premium**' in second case. This improvement in rating confirms the safety performance of the compact ADB systems as compared to conventional manual headlamp.

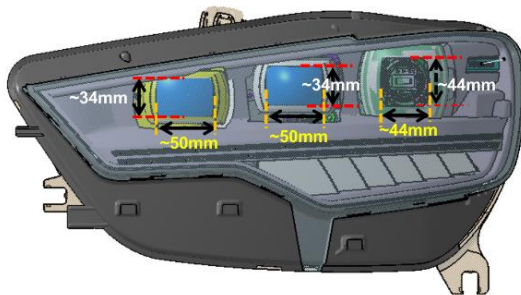


Figure 7: μ LED headlamp prototype
[layout (from right to left): μ LED Kink, Base, and matrix]

3. Conclusion

We have presented the performance of low-profile headlamp system using light guide technology. The HSPR rating of the prototype design has been evaluated for low beam and combined ADB mode of the high beam. The satisfactory rating of the headlamp, comparable to that of standard headlamp module, indicates better performance and safety standards possible despite the compact height of the optical systems. The results motivate us to explore further on compact headlamp technologies. In addition, investigations on micro LED has also been mentioned, indicating the scope to have improved safety of ADB headlamps using the novel μ LED technology.

4. Acknowledgement

We would like to thank our colleague Mr. Jan Martoch for his contribution to the design of light guide low beam. We would also thank our colleagues from Mr. David Hynar's group for providing the information on standard headlamp modules and micro LED system.

7. References

- [1] P.Nemec: "OptiLED Matrix – Compact Efficient Reflector", 13th International Symposium on Automotive Lighting [ISAL] (Germany, Darmstadt), 2017
- [2] J. Martoch, P. Ferbas, S. Büttgen, H. Groner: "*Opti-ADB – Study on Low Number of Segments*", 13th International Symposium on Automotive Lighting [ISAL] (Germany, Darmstadt), 2019
- [3] Mathias Niedling: "*Field Study: Glare of Headlamps with small Light Emitting Areas*", L-Lab, Germany, 2022
- [4] GTB, "*Headlight Safety Performance Rating (HSPR) - Recommended Practice*", (CE-5815, <https://www.gtb-lighting.org/publications/>)
- [5] Rainer Neumann: "*Headlamp Safety Performance Rating (HSPR), Rating System including ADB approved as a GTB standard in 2022*", DVN (Rochester Michigan), 2022

ADVANCED LIGHT SOURCES

Highest luminance color LEDs

for a next level of visual safety experience around the car

B. Springer¹, A. Timinger¹, R. Fuchs¹, D. Vanderhaeghen¹, W.J.M. Schrama²

1: Lumileds, Aachen, Germany

2: Lumileds, Eindhoven, The Netherlands

Abstract: With the emergence of very bright and compact LED (light emitting diode) projection optics, OEMs are exploring new lighting territories surrounding (360°) the car. Going beyond today's welcome entry light, these new-of-a-kind signaling road projection will bring a next level of visual safety experience to drivers and other road users. Paving the way for these new kinds of applications, also regulatory preparation work is already ongoing.

In this paper we assess from a technical application perspective, the OEM requested brightness requirements for a variety of lighting functionalities such as park-assistance marker lines, back-up light patterns, front- and rear-turn signals, and warning signals, and translate them into appropriate specifications for enabling LED light sources. Hereby we consider not only night-time operation but also the viability for potential daytime operation. Optical system efficiency is being simulated/characterized for these highest luminance color (white, red, amber, cyan) LEDs in various compact-size projection systems.

The learnings from this application study gives input for further assessment of new light-source developments for highest luminance color LEDs. This will ultimately enable compact size, energy-efficient and cost-effective road projection solutions, creating new opportunities to enhance road safety.

Keywords: Signaling, road projection, high luminance, optical systems

1. Introduction

The automotive industry together with government and regulatory bodies are continuously scouting for ways to improve road safety. Lighting plays a significant role to enhance road safety in twilight and night conditions. New high-luminance LED offerings in the market open possibilities to project light symbols and features at night as well as in dusk and dawn conditions that enhance comfort and safety around the vehicle. In 2019 there were 2035 cyclist fatalities in the European Union and cyclist were the only type of road users for which the fatality rates did not decline. Increased visibility of the operation intentions of cars on the road may decrease the

number of fatalities through of car-cyclist interactions [1]

In Japan there were 22,243 bicycle accidents with fatalities and injuries in the situations where the other vehicle's direction indicators were lit at night. A discussion is taking place now together with the regulatory bodies on the implementation of these road projection systems and their contribution to road safety and it is expected that these new regulations will come into effect in the next couple of years [2,3].

In this paper we present the results of optical prototyping efforts to investigate the required LED properties for high brightness, sharp contrast systems expected to be applied in new vehicles in 3-5 years from now.

A variety of different optical concepts was identified and made into prototypes targeting different realistic applications like turn indicator, welcoming light and back-up support.

2. Road projection requirements

Required luminosity of road projection applications is strongly depending on the ambient illuminance. It is clear there will not be a practical road projection solution available in the near future that enables use in full sunlight conditions. However, already under clouded weather conditions or at least starting from sunset, surround projections should be clearly visible. From literature [4] we can find 100 lx for symbols to enable good twilight visibility. From [5] we can even find required illuminance values in the range of 700 lx. As such the prototypes we show have been developed with ambient illuminance levels of 150 lx to 1000 lx in mind.

Also, the required illumination area varies between different applications. We can find reported symbol sizes in the ranging from 2 m² [4] for turn signals up to 20 m² for road projection to the front [6].

For the extension of the turn signal on the ground the required field of view can be relatively small, like seen

before. Also, the projection distance needs to be close to the car, typically 1 to 3 m. From this we can derive the required intensity levels of 225 cd to 6300 cd. If we want to create a symbol with 2 m² area the required flux on the road will be 300 lm to 1400 lm – not including any optical loss from the illumination optic. If the symbol size should be increased the required flux will increase accordingly.

For entry-light applications maybe a visibility under lower ambient light conditions is acceptable. On the other hand, typically the symbol size is increased. Most critical seems to be a warning application that needs to be extended over a wider area, like a back-up function. Here, high intensity requirements are combined with a large area.

To realize such high intensities also the luminance of the source needs to be high enough, to avoid large optical systems. With 60 Mcd/m² from the source we will need already a 12 mm diameter optic to realize 6300 cd – without any transmission loss. With realistical system transmission losses of >50% we can expect something like 3000 cd from such a system. In the following we will discuss an optical system that can fulfil such requirements and verify whether these assumptions are reasonable.

The demonstrated applications are not intended as proposed applications but for study purposes only, although keeping in mind possible future use.

A specific note should be made on the regulatory status. Currently, there is a very limited number of symbol projections allowed and these are related to front of the car projection [7]. The main application of road projection currently on the market is related to puddle or welcoming lights next to the car. Given the various proposals currently under discussion or in preparation it is expected to see more applications being legalized in the next few years [8].

3. Optical system requirements

3.1 Turn-indicator function

To support the turn indicator function, a projection of amber colored arrows on the road surface has been proposed and demonstrated by various OEMs and set makers [9,10]. There is evidence that the response time to the direction indicator lamp is decreased when road projection is added. The most likely locations for optical systems for turn-signal indicator lamps are on the corners of the car already being used for headlamps and turn indicators.

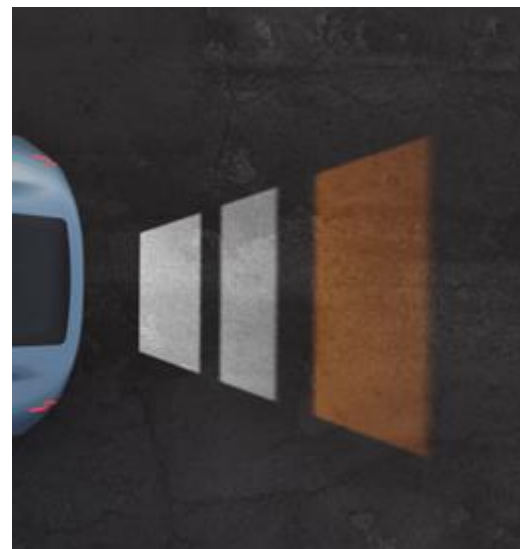
It is therefore essential to minimize the dimensions of the optical system, electronics and thermal solutions.

Blinking of the projection will need to be synchronous to the indicator lamp. The color of the projected arrows will need to be amber and is proposed to closely match the color of the indicator lamps.



3.2 Back-up illumination and dynamic warning

For back-up we show a potential application where white lines are projected in the area where the car will back into. An additional amber line can be projected on the ground when another road user is detected that may potentially cross the path of the vehicle backing up. An integrated solution for the different lines will reduce the number of exit windows in the back of the vehicle.



3.3 Welcoming projection

Welcoming projection is already commonly used in cars by projecting light or images on the ground from the side-view mirror. With limited physical space available in the side-view mirror it is important to have a high efficiency (low thermal load) and compact system.



4. Application examples

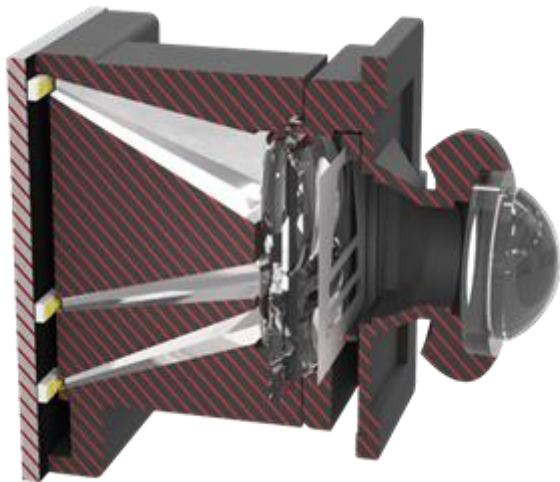
In the following we describe different possible optical systems for the discussed applications.

4.1 Static front-turn signal pattern projection

The intention of this optical system is to demonstrate highest optical efficiency - maintaining a small optic. With an overall depth of 25 mm (without heatsink) and 12 mm diameter of the lens it is quite compact. Here we used a pre-optic collimating the light to the Gobo (Graphical optical blackout) into the acceptance cone of the lens. The combination of high source luminance from a LUXEON FX2-L Plus PCA LED yielding 250 lm of amber light and the corresponding optical system enable an overall system efficiency of >31% including the losses at the Gobo for the shown symbol. With 3000 cd from a 12 mm diameter lens, we achieved the expected performance of 78 lm on the road.

4.2 Dynamic back-up light with warning function

To enable dynamic projections within one module we need to combine several LEDs under one projection lens. Again, we use per-collimating optics to selectively illuminate the Gobo. Since a wide area needs to be covered by the projection it is beneficial to illuminate under different angles. This increases the overall depth a little and requires some additional space in vertical direction (25 mm). However, with an overall depth of 44 mm (w/o heatsink) and still 12 mm lens diameter it is still extremely compact, especially as compared to the alternative of using multiple projection units. Here the overall efficiency is even a little higher, partly caused by the better adaption of the collimation optic to the symbol shape. Since here many LEDs are combined, luminance cannot be maintained as good as in the system above. So, the achieved intensity is, with only 1500 cd lower but still enables good visibility under twilight condition. For an even improved conspicuity we combined LUXEON FX2-L Plus PCA and LUXEON FX2 L Plus CW to enable multi color projection, with overall 460 lm on the road.



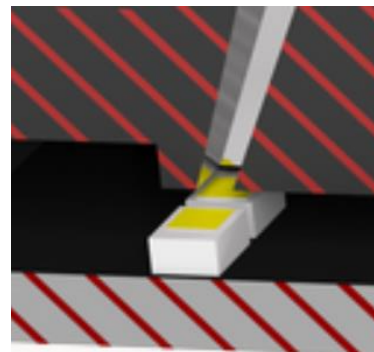
4.3 Dynamic, segmented and homogeneous carpet light:

For improved homogeneity and even more compact design we combined a 3x3 LED array of LUXEON Altilon Intense Gen2 1x1 with a micro-lens array (MLA) provided by SUSS [www.suss-microoptics.com]. We used here a Köhler-type MLA with dedicated designed masks. Within the MLA nine different sections are defined, where three different types of masks - create three different images. To enhance brightness of the symbol further away from the car, the light of several LEDs is combined. Köhler illumination with single lens for each LED is used match the numerical aperture of the MLA. With about 5% overall efficiency the flux out of the system is comparably low, but the system offers highest flexibility in a really compact design. Most of the light is lost at the masks – since we generate three disjunct symbols the average transmission of the mask is less than 25%. Additionally, the preoptic is only collecting 50% of the light. Due to the combination of nine high-power LEDs, we can still realize 40 lm on the road and a maximum intensity of 1000 cd with this approach.



5. Light-source requirements

As discussed above we need high-luminance sources to enable small optics with high intensity output. On the other hand, we see that many of the applications will require a large quantity of light – often not possible - with only one LED. So, the combination of several LEDs is often necessary. Here it is critical to not dilute the luminance of the source. E.g., in the optic for the dynamic back-up light, always two LEDs were combined under one pre-collimator. It is therefore important to use packages where a close placement is possible.



Alternatively, the combination can be realized at the projection plane like in the example of the carpet light. In this case an accurate lateral placement of the LEDs is required to avoid crosstalk between in the micro-lens channels.

Finally, we need to consider the thermal management. We have demonstrated three compact optical systems. However, if several high-power LEDs are combined the thermal system can -become the most space-consuming element. In case of the carpet light the light source itself could be operated up to an input power of more than 40 W. Even an active cooling system would be significantly larger than the

module. Additionally, we need to consider absorption losses in the optical path. Even at medium drive current of 300 mA per LED, about 2.8 W optical power will be emitted to the optical system. Here the high-luminance LED is operated at comparably low drive current but yields with >35% wall plug efficiency a good compromise between luminance and efficiency.

6. Conclusion

With the increasing interest in surround projection in automotive, we also see an increase in the need for small and compact optical systems. We demonstrated various optical concepts by selecting a few show-case examples that are illustrative for possible future applications.

As regulation discussions have only just started on surround projection, actual requirements will determine the specifications of the light sources and optics to be used. The different systems shown give an indication of what is possible at various levels of complexity

- The simple GOBO projection demonstrates that with only one high-power LED a compact system can be developed that can be used for simple static (or flashing) projection applications while being small enough to be embedded in the car corner
- The back-up demonstrator shows an example how three LEDs can deliver a wide projected image with sufficient brightness while emitting from a single cavity in the rear of the car
- An even more compact and flexible design can be achieved by an MLA system as is demonstrated in the welcoming application.

From all applications shown and studies done it is clear that for all optical solutions small compact LED light sources with high luminance and high efficiency are essential to achieve high contrast, high brightness road projections.

7. Acknowledgement

The authors acknowledge the contribution of all colleagues at Lumileds worldwide.

8. References

- [1] European Commission (2021) Facts and Figures Cyclists. European Road Safety Observatory. Brussels, European Commission, Directorate General for Transport.
<https://road->

[safety.transport.ec.europa.eu/system/files/2022-03/FF_cyclists_20220209.pdf](https://road-safety.transport.ec.europa.eu/system/files/2022-03/FF_cyclists_20220209.pdf)

- [2] Michael Hamm, Christian Hinterwaelder: „Road Projection of Turn Signals“, Driving Vision News, April 21, 2020
<https://www.drivingvisionnews.com/news/2020/04/21/road-projection-of-turn-signals/>
- [3] Informal document GRE-85-38: „Signalling Road Projection“, 85th GRE Oct 26-29 2021
https://unece.org/sites/default/files/2021-10/GRE-85-38e_5.pdf
- [4] Christoph Bremer, Cornelius Neumann, Burkard Lewerich: „Realisierungsmöglichkeiten für hochaufgelöste Umfeldprojektionen im Automobil“, VDI-Bericht Nr. 2323, 2018
- [5] Y. Shibata, M. Kito, H. Ishida: „Requirement Performance of Road Projection Lamp in Conjunction with Turn Signal Lamp“, Page. 362, ISAL Proceeding 2019
- [6] Gerolf Kloppenburg: „Scannende Laser-Projektionseinheit für die Fahrzeugfrontbeleuchtung“, Dissertation Fakultät für Maschinenbau der Gottfried Wilhelm Leibniz Universität Hannover, 2017
- [7] Informal document GRE-85-20,
<https://unece.org/sites/default/files/2021-10/GRE-85-20e.pdf>
- [8] Ulrike Schlöder, „Dynamic Ground Projections around the Car: The Headlamp as Integrator“, page 538-547, ISAL Proceeding 2021
- [9] Mitsubishi Electric: „Mitsubishi Electric System Uses Road-surface Projections and Car-body Displays to Indicate Vehicle Movements Clearly“, Mitsubishi press release, October 10, 2017
<https://www.mitsubishielectric.com/news/2017/1010-a.html>
- [10] Rainer Neumann: „Future Light Performance Requirements - Visibility, Comfort, Information“, Vision 2018

8. Glossary

LED: Light Emitting Diode
GOBO: Graphical Optical Block Out
MLA: Multi Lens Array

Exploring the challenges in micro-LED pixelated light source, μ PLS, for high-resolution headlamps

M. Schakel¹, H. Kuroda², X. Denis¹

1: Nichia Europe GmbH, Westerbachstrasse 28, Kronberg, Germany

2: Nichia Corporation JAPAN, 491 Oka, Kaminaka-Cho, Anan-Shi, Tokushima, Japan



Abstract: Emerging research and development of high-resolution pixelated headlamps is enabling glare-free high-beam and foreground projection overlay to increase the safety of road-users at night. There are many challenges for LED to enable full field-of-view illumination: pixel resolution, luminance, efficiency, and the flexibility of light control for all driving conditions.

The four years research and development have led to a light source with 16,384 pixels, fully integrated with an ASIC. The ASIC integration is designed with support for a large variety of current and future car electronic architectures in mind and the optical performance is top of its class.

Keywords: High-resolution head lamps, ADB system, micro-LED pixelated light source, μ PLS

1. Introduction

The market requests for pixelated light sources have increased in the last few years. Since the introduction of the first matrix Adaptive Driving Beam (ADB) LED solutions several years ago it was only a matter of time for the first OEM companies to start thinking about the possibilities of a high-resolution light source. Conventional LED technology enabled the first step into dynamic headlamp technology, and now micro-LED pixelated light sources are taking dynamic headlamp technology into the future.

2. Legal Requirements

If the purpose of a high-resolution light source is to be used in ADB systems, the legal requirements should be firstly considered. The requirements that are most important include the Field of View (FOV), angular resolution and brightness on the road.

The FOV should be sufficient to cover the full ADB area, which means it should be at least $\pm 10^\circ$ horizontal and 5° vertical. With the FOV defined, the aspect ratio then is quickly calculated and found to be 1:4.

To define the minimum angular resolution, the distance at which an object is to be shaded out needs to be considered. At 100m, an object with a 2m width has an angular width of just under 0.6° . Ideally the

shaded area should consist of more than a single pixel, or the result would be needing to shade at least two pixels if the object is not centred on a single pixel, leaving an area that is shaded twice the size of what is required. In stationary situations, this might even be acceptable, but in actual driving conditions this could mean constantly changing size of the shaded area even if the distance to the object causing the shading remained constant. A higher resolution, i.e., smaller pixels, drastically reduces this effect, as the percentage of overshaded area drops significantly with smaller pixels. With 256 pixel-columns and the 20° horizontal FOV mentioned before, this gives an angular resolution of just under 0.08° and reducing the extra shaded area from 100% down to 14%.

The resolution also has to be considered for other use cases, symbol projection and road-marking, and for these applications an angular resolution of 0.08° would be considered sufficient. If road-marking and symbol projection are to be used as the primary application, a different optics system could be chosen, delivering a higher angular resolution at the cost of the overall FOV. For lane-light or road carpeting, a horizontal range of 20° might not be required and this means an even higher angular resolution on the road.

The next requirement to look at is then the brightness on the road. From purely a light-source point of view calculating the final brightness on the road is not easy, as of course the optical system efficiency plays a major role. For ADB solutions generally a luminous flux value around 2000 lumen is desired and a source luminance of 70 cd/mm^2 . With these values the source is also bright enough to clearly display road-markings and symbols on the road.

3. micro-LED Technology

The light source required for a micro-LED headlamp solution, might resemble a micro-LED source for display applications, mainly due to the pixelated nature of both sources. There is however a significant difference between the two applications. Display applications have a much lower requirement for luminance. Besides the luminance requirements, display applications also tend to be RGB, where for headlamp applications only white light, so far at least,

is considered. A headlamp micro-LED light will very likely consist of a blue LED chip, combined with a phosphor converter material.

To achieve the resolution required to meet the legal requirements, pixels pitch and hence LED pixel size needs to be in the micrometre range (this will be discussed in more detail in the next paragraph).

There are currently two primary technologies to achieve a pixelated light source with micrometre pixel size able to deliver enough luminance, monolithic technology and individual pixel technology. Both technologies have their advantages and disadvantages.

One of Nichia's core-strengths is the capability to develop its own LED chip. This strength is best leveraged when developing an individual pixel micro-LED pixelated light source, which is why the initial research into pixelated light sources has been in this direction. Besides leveraging Nichia's core strength, several advantages of the individual pixel technology were identified as deciding factors in the decision to further pursue this technology.

The advantages that were identified are:

- A reliable method of replacing and repairing defect pixels during assembly, leading to a potential higher yield.
- A good reliability under thermal stress.
- Increased light extraction from the active material, i.e., the LED chip.

4. Pixel considerations

With the legal requirements setting the first boundary conditions on the light source, the biggest decision point becomes the actual pixel pitch. Pixel pitch is defined as the centre-to-centre distance. It is important to make the distinction between pixel pitch and actual pixel size as they might end up not being equal.

To avoid having a too large optical system, the size of the light emitting surface (LES) needs to be kept as small as possible. Make it too small however, and the light output will suffer significantly. There is a fine balance between these two conditions that needs to be considered. When looking into the market, a horizontal dimension between 10 mm and 15 mm seems to be accepted for an ADB optics system. Taking the 15 mm as the absolute maximum width and the previously mentioned 256 pixel-columns, this gives a maximum value for the pixel pitch of just over 58 μm . Decreasing the pitch will obviously increase the angular resolution, it will also lead to a decrease in LED brightness. LED brightness is strongly (and negatively) linked to the chip-size and at micrometre scale this effect is quite significant. Quantum efficiencies (QE) drop considerably the smaller the active area becomes.

In addition to the QE dropping, there is the effect of relative active area to consider. LED chips, and micro-LED chips are no exception, cannot be placed in a matrix, while physically touching adjacent chips. First of all, due to the actual ability to physically place the chips that close to each other as this would require incredibly precise equipment. But more importantly this should be avoided any way from a reliability point of view. The active material that the chips are manufactured will expand or contract under different thermal conditions. Which means, that if the chips were to be physically touching neighbouring chips during placement, under different thermal conditions, i.e., higher temperatures, when the chips would expand, they would collide with each other. Since the chips have no room to move, some would most likely crack under these stresses, or even become detached from the surface they are mounted on.

To avoid these catastrophic failures, a certain distance between the chips needs to be considered. As this gap between the chips is non-emitting, this distance influences the effective brightness of the micro-LED matrix. Manufacturing limitations mean there is a minimum distance for the LED distance that the LED's can be placed at. For chips with a size around 50 micrometre, this placement accuracy is around 5 micrometres and is mostly independent on the exact chip size. For a chip size of 45 micrometre or 60 micrometre, there is no difference in this placement accuracy. It is not entirely fixed and can be somewhat optimized, but only marginally. It is this fixed gap size why a smaller chip has a lower effective luminance, there is a larger ratio of non-emitting area. Figure 1 shows two schematic representations of a 4x4 LED chip matrix. The difference between the matrix on the left and the right is the chip size. The gap between the chips is kept the same.

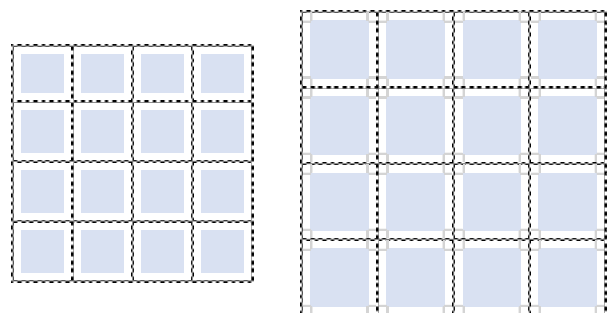


Figure 1: Two representations of a 4x4 pixel matrix with different chip sizes. The shaded parts indicating the LED chips.

Nichia has identified 50 micrometre as the optimal pixel pitch, and during the development has experimented with over 20 prototypes, varying the epi-structure, reflective materials and even the integration processes itself. During the research and development phase in the last two years, this has

resulted in an output of the device currently at 70 cd/mm² at a nominal input current, leaving still enough room to overdrive the pixels to achieve even more luminance.

Taking every consideration into account, the final pixel count of the μ PLS device then comes to 16,384, divided in 256 columns and 64 rows. And with a pixel pitch of 50 micrometre, the size of the LES amounts to 12.8 mm x 3.2 mm.

5. Heterogenous Integration

With thousands of micrometre sized pixels on such a small area, the obvious question is how to connect and drive each individual pixel. With an Application Specific Integrated Circuit (ASIC), this is possible. This number of pixels to control and a size that is quite large in the semiconductor domain, where ASIC's come from, it is still a challenge. Not just from a design point of view, but also when considering the production, manufacturing, and testing of the ASIC.

The next challenge was to bring the micro-LEDs and the ASIC together, placing the LEDs with micrometre accuracy on the ASIC surface. This process, Mass-Transfer technology, needed to be developed and perfected and was developed in-house. This technology enabled the accurate placement of all pixels in a single shot.

A schematic cross-section of the full stack can be seen in figure 2.

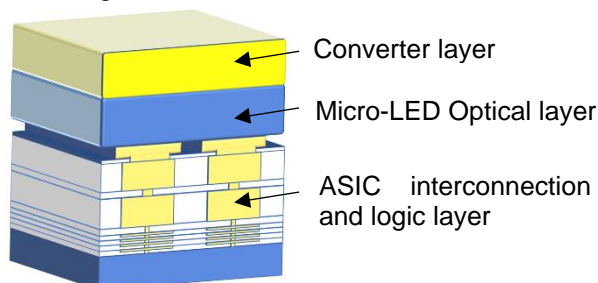


Figure 2: A schematic cross-section of the μ PLS product (not to scale).

6. Packaging

The package design was implemented to meet the unique requirements of headlight applications. Having the final product being a surface mount device (SMD) was very important and set as a requirement from the start of the development. In Figure 3, the package structure shows a substrate part, on which the ASIC (the green part in the figure) is mounted. The micro-LEDs are consequently mounted on this area.

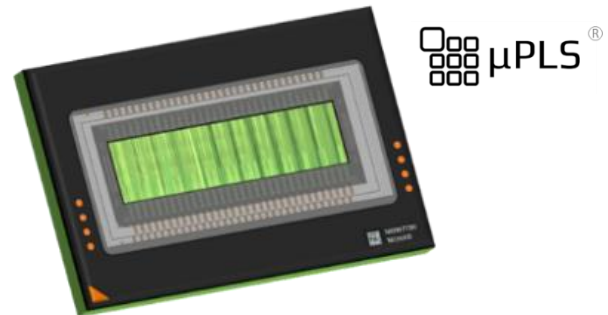


Figure 3: Package design of the μ PLS product.

The multiple signal and power supply wires coming from the ASIC needing to be guided to the substrate material.

6.1 Heat Dissipation

Thermal modelling was used extensively during the design process. Unlike conventional LEDs, this product has not just a single LED junction where heat is generated, but several thousands. And to complicate the modelling even more, additional heat is also generated in the ASIC part. The package was optimized by reviewing the package materials, the package structure and each step was verified by actual product testing, not just thermal modelling.

Another challenge with such a product is the dynamic behaviour. This light source is not intended to always display the same light pattern, and this means that the thermal behaviour of the device is also very dynamic. There are large thermal stresses inside the device, and once again, by building prototypes and actual testing, the structure and package was optimised to be able to withstand these forces.

6.2 Optical

In advanced optical control, stray light due to package reflection must be minimized. Optical simulation and physical property analysis were conducted to minimize stray light effects by arranging components with different transmittance and reflectance. By building several parts with different reflective components and materials, the trade-off between light output and minimising unwanted reflection was optimised.

6.3 Converter

With chips in the micrometre range, and most phosphor conversion materials having particles in the same order of magnitude, the design of the phosphor converter needed to be considered carefully. A thick converter layer would furthermore result in lower contrast due to light leaking easier to nearby pixels. A converter film with a thickness in the micrometre range was identified as the ideal compromise between contrast, homogeneity, and light output.

Reflective walls between the chips would in turn increase the contrast and increase the light output by reflecting the internal light outward. In figure 4, the inside structure is shown. The

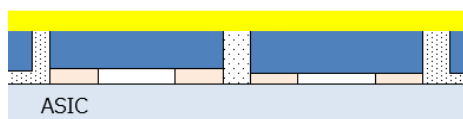


Figure 4: Converter film (at the top) placed on the LED chips, with the LED chips separated by a thin white separation.

6.4 Reliability

As an automotive product, the final μ PLS product needs to have a high robustness and high reliability. At the time of the development of this product (and the time of this publication) there is no in-vehicle reliability test standard for an integrated device such as the μ PLS. Therefore, it was decided in collaboration with our partners to qualify and test the ASIC part of the device according to AECQ100 and the full product according to AECQ102 where possible and applicable.

With this product being the first on the market, it does mean that there were still many open questions about the testing details as it was not possible to fully follow AECQ102, or the standard simply wasn't clearly specified for a pixelated device. One such example is the fact that it is not possible to run every pixel of this device at maximum current at the same time. Both the ASIC and the package were not designed to handle this amount of power as this is not expected to have any practical applications and would have led to over dimensioning of the product. And this is yet again, where the collaboration with our partners helped in determining the application boundary conditions and relevant parameters for the AECQ102 testing.

6. Features

To enable the usage of the light source in car architectures, there was the additional requirement that digital communication was somehow added into the device. The ASIC is the solution to this challenge. Included in the ASIC are three video interfaces, each supporting different car architectures. The integration of these interfaces (parallel RGB, V-UART, and SPI) offers the car manufacture complete freedom on where the data is built and created that is to be shown by the light source. This can be done completely locally in the headlamp and the SPI interface can be integrated with little effort, or with fully central intelligence in the car, the data can be streamed directly through the RGB interface from the main processing unit in the car, or a hybrid solution can be chosen.

The video stream is internally converted in the ASIC and drives the individual 10-bit Pulse Width Modulation (PWM) engines under each pixel.

In addition to the video interface, there is a control interface. Through this interface, the device can be controlled, and diagnosis functions can be read out. A watchdog function is implemented in this interface as well.

The diagnosis functions in this device include several Analogue to Digital Converters (ADC) to enable reading out different voltages. Each pixel's voltage can be read out, as well as the supply and internal voltages. A pixel failure diagnosis, sensing both dark and bright pixel failures is also available and there are 16 temperature measurement points under the LES that can be read out individually, but can also be used together with temperature warning flags. The μ PLS does not take actions based on these warnings, and all the warning and diagnosis functions are fully user customisable, leaving the control in the hands of the car manufactures.

Figure 5 shows the structure of the ASIC with the different interfaces and functions as described. To enable storage of some essential settings, and to load a Fail-Safe picture in case of communication failure, a final interface is implemented, an I2C interconnect to an EEPROM that can be connected to the μ PLS product. Through this interface the EEPROM can be addressed, without the need of a separate additional I2C connection to the EEPROM.

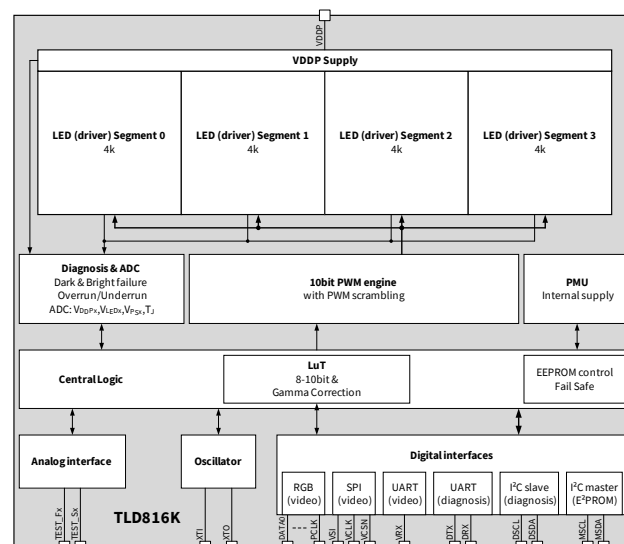


Figure 5: Structure of the ASIC of the μ PLS

7. Other challenges

7.1 Thermal resistance

As the expected power usage of this device will be around several tens of Watts (depending on the exact light pattern between 10 W and 40 W), the thermal resistance (R_{th}) is a critical parameter of the device. Especially since this power is generated in such a

small area. The LEDs are the main power generators in this product, but unlike conventional LEDs the chips cannot be placed directly on a PCB, since they are integrated in the device. This means the thermal resistance is expected to be higher than for conventional LEDs. In the end, the package thermal resistance was found to be less than 1 K/W (around 0.7 K/W) with an all pixel on light pattern.

The thermal resistance for a pixelated device is however only an approximation of the reality. Effectively there are 16,384 different thermal resistances as each pixel has its own thermal resistance path. The thermal resistance can be used for initial validations, but better tools should be used to validate the thermal design.

Nichia has developed an algorithm that can estimate the maximum Junction Temperature of the device for different light patterns. The basis for this algorithm is a large amount of testing on actual products. With this software Nichia can support customers by reducing some of the testing in early introduction and evaluation stage of the device.

7.2 Measurement tools

The development of the μ PLS product has also prompted the need for development of specific measurement tools. To measure and calculate the luminance of each pixel an area luminance measurement does not suffice. There is a discrepancy between each pixel of the CCD luminance camera used in the measurement, and the micro-LED pixel. To obtain accurate pixel luminance, the coefficient of the CCD pixel area and the micro-LED pixel area is calculated and used to correct the luminance reading of the camera. Using this method has improved the accuracy of the luminance measurement especially since it eliminates variations due to misalignment and edge-pixel areas.

7. Outlook

With the μ PLS being the first product of its kind on the market, it is no surprise that even during the development of this product already areas for improvement have been identified. To keep the development timeline as set out at the start of the project, some of these improvements had to be deferred to its successor product. Furthermore, Nichia is always looking to improve the chips and converter materials, thereby increasing the light output and efficacy of the product in successor products.

Nichia expects improved versions of the initial μ PLS to follow not long after with improved specs.

Besides the current generation of pixelated light sources there is a strong desire in the market for even

higher pixel count devices, which will challenge the technical minds of Nichia even further.

8. Acknowledgement

The authors acknowledge the contribution of their colleagues and partner companies to this work.

9. Glossary

μ PLS: brand name for micro-LED pixelated light source
LED: Light Emitting Diode
ADB: Adaptive Driving Beam
FOV: Field of View
RGB: Red Green Blue
LES: Light Emitting Surface
QE: Quantum Efficiency
PWM: Pulse Width Modulation
UART: Universal Asynchronous Receiver Transmitter
SPI: Serial Peripheral Interface
ASIC: Application-Specific Integrated Circuit
AEC: Automotive Electronics Council
ADC: Analog to Digital Converter
 R_{th} : Thermal Resistance
I2C: Inter Integrated Circuit
EEPROM: electrically erasable programmable read-only memory

Advancing OLED Lighting Technology for Automotive Applications

Soeren Hartmann¹, Michael Boroson², Kathy Vaeth², Joerg Knipping¹

1: OLEDWorks, Philipsstrasse 8, 52068 Aachen, Germany

2: OLEDWorks, 1645 Lyell Avenue, Suite 140, Rochester, NY 14559, USA

Abstract: Organic light emitting diode (OLED) is a premium quality, energy efficient, solid-state lighting technology. It has several noteworthy advantages for automotive lighting solutions compared to LED or microLED. OLED produces homogeneous surface light. It does not need any additional reflectors, light guiding films or any additional optics to achieve smooth uniform emission, making it very thin with minimal package requirements. Combined with the ability to create individually controllable, high contrast lighting sections within the panel, or segments, opens up new approaches for lighting designers that enable car manufacturers to set their vehicle apart.

We have successfully commercialized OLEDs for rear lamp applications. These introductions to the market have proven automotive compatibility, giving our customers the opportunity to capitalize on the key differentiators of this technology: light quality, function, contrast, and personalization. In this paper, we will look at OLED products available today, as well as the future generation of OLED panels under development with higher segmentation, the ability to perform Car-to-X communication and a wider range of legal functions. Additionally, we will review the transitioning from rigid OLED on glass towards a bendable device that will allow lighting to follow the outer car contours with a bend radius as low as 180mm.

Keywords: OLED lighting, automotive lighting, OLED technology, personalization

1. Introduction

OLED lighting panels offer a unique approach for exterior vehicle lighting. Illumination is diffuse, highly uniform, and low in glare. This makes the technology ideal for applications where the light is viewed directly from a wide angle by drivers and passengers, such as the tail, stop, and turn functions. These properties are inherent to OLED technology and have the additional benefit of not requiring lenses or diffusers to achieve high quality light. This allows for assemblies on the order of a millimeter in thickness or less. The compact profile also provides easy integration in tight spaces, and bendable OLED panels offer a form

factor for seamless incorporation of light over curved surfaces. The crisp segmentation characteristic of OLED lighting technology provides opportunities for unique branding and personalization, as well as car communication of icons or other symbols. This will pave the way for new form factors for lighting design, as well as the potential for closer integration of the various car systems. This will also enable more effective Car-2-X communication and superior safety systems.

2. OLED Panel Segmentation

A unique characteristic of OLED lighting technology is the ability to have individually addressable and dimmable segments within the panel (Fig 1).



Figure 1: OLED Panels with 60 Individually Addressable and Dimmable Segments

These segments have extremely homogeneous emission (> 90% uniformity) combined with high contrast. Current OLEDs on the road today have up to ten (10) segments per panel. This allows for unique styling by vehicle as well as personalization of the tail signature pattern, as seen in the Audi A8, A8L, and A8 Hirsch (Figure 2). In addition, the static tail position signature lighting with sharp, high contrast dimmable segments enable unique 'hello' and 'goodbye' sequences not possible with any other lighting technology. In these panels, the segment sizes tend to be >100 mm², which are well-suited for this application.

Panels with 50 to 100 segments have already been qualified and will soon be introduced in new car



Figure 2: Audi A8 OLED Taillights with Personalized Tail Position Signatures

models. These designs will have segment areas as small as 25 mm², which will enable more dynamic animations for styling, more static tail position signature options and the ability to communicate Car2X in ways well beyond the traditional brightness change. Using the sharp, high contrast segments of the OLED panels along with car-based sensors and/or web-based information these OLED lighting enhanced cars will be able to automatically communicate safety information to the car's surroundings by displaying a variety of symbols such as snow, ice, bicyclists, pedestrians, and hazard triangles (Figure 3).



Figure 3: Demonstration OLED Rear Combination Light Displaying Snow Hazard Information

Greater and more flexible Car2X communication will require even smaller segment areas and larger panels. To enable this OLEDWorks is developing technologies to decrease segment areas on OLED

lighting panels first to ~5-10 mm² over the next few years and eventually to less than 1 mm². Correspondingly, the number of segments will shift from 50-100 per panel to a few hundred per panel and eventually to 1000s per panel (Figure 4). These developments will be enabled in part by new materials and OLED architectures, as well as developments in driving electronics for the panels.



Figure 4: OLED Panels with Over 200 Segments per Panel and 3-15 mm² Segments

3. High Brightness Red Emission

OLED automotive lighting panels must be significantly brighter than the OLED displays used in mobile phones and TVs. A typical OLED display is only operated at a maximum brightness of ~500 cd/m², and only needs a lifetime of a few years. For the tail position function an OLED automotive lighting panel must operate at 2000 cd/m² to produce the legally required amount of light for the function and must last for 15 years. Other RCL functions such as stop and turn require 5-10x higher brightness than the tail position function and must also last for 15 years.

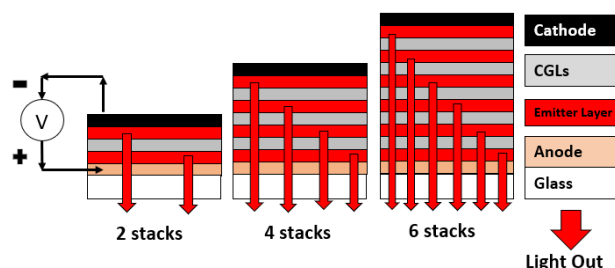


Figure 5: OLED Stacked Architecture

To achieve such high brightness and lifetime OLED automotive lighting panels use stacked architecture technology where multiple OLED emitting layers are stacked one on another with intermediate charge generation layers to increase the brightness and lifetime of the OLED automotive lighting panel (Figure 5). OLEDWorks is the world leader in multi-stack OLED lighting technology. Our OLED lighting panels are the world's brightest, longest lifetime and most

reliable commercial OLED lighting panels. For the tail position application two automotive red OLED stacks are needed. These structures are optimized for uniform brightness, minimal color shift with viewing angle, and color coordinates that meet deep red SAE and ECE requirements. The panels are designed to last the lifetime of the car, and extensive validation testing has been performed and passed to ensure their reliability and longevity (Figure 6).

Test	Duration	Result
-40C (2,000 cd/m ² operational and storage)	>2,000 hr	Pass
60C (2,000 cd/m ² operational)	20,000 hr	Pass
85C (2,000 cd/m ² operational)	>5,000 hr	Pass
85C (storage)	>5,000 hr	Pass
105C (storage)	>1,000 hr	Pass
85C/85%RH (storage)	>9,000 hr	Pass
85C/85%RH (2,000 cd/m ² operational)	>2,000 hr	Pass
-40C/85C Thermal Shock (storage)	>1,000 cycles	Pass
-40C/85C Thermal Cycling (2,000 cd/m ² operational)	>2,000 hr	Pass
ESD HBM/MM		Pass
Mechanical Shock and Vibration		Pass
H2S, Mixed Gas and Solar Environments		Pass
Combination Testing (2,000 cd/m ² operational and storage)	Up to 4,000 hr	Pass

Figure 6: Sample of Validation Testing

Other legal red automotive exterior functions such as stop, and rear turn (the latter in North America) will require higher brightness to achieve the required output. Based on the typical legally required light values and, in North America, lit area, it is expected that red OLED surface brightness of 10,000 to 20,000 cd/m² will be required for the stop and rear turn functions. Requirements for daytime communication through light in the rear of the vehicle will be similar. This will be achieved through increased number of stacks and further optimization of OLED materials. As with the tail function, these panels will also be designed to last the lifetime of the car. An example of a red six-stack OLED panel designed for stop function is shown in Figure 7.

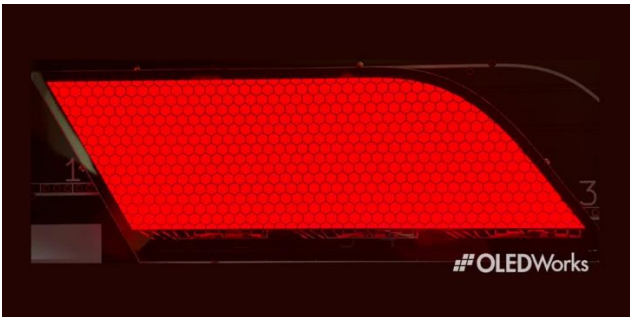


Figure 7: Six Stack Red OLED Panel

4. Other Colors

In some regions, amber light is required for the rear automotive turn signal. By adjusting the materials in the OLED stack and overall stack design, the emission color from the panel can be designed to meet the required color point and light output. For amber turn, it is estimated that a brightness of 20,000 cd/m² is required to meet legal requirements. Segmentation of the panel allows for smooth, glare-free horizontal animation in the panels that enhance the turn function. An example of an amber turn panel is shown in Figure 8.

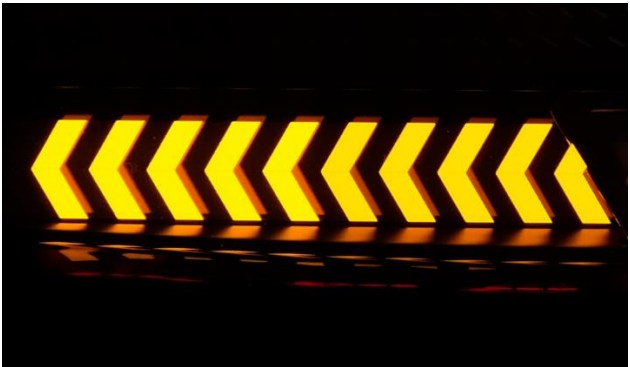


Figure 8: Amber Turn Signal OLED Panel

In addition to red and amber, automotive lighting currently uses white for various functions and plans to use cyan for future autonomous vehicles. These colors are also possible by adjusting the materials in the OLED stack and overall stack design. One application for white emission that is particularly well suited for OLED is badging in the front grill, hood, and side regions of the vehicle, particularly for electric vehicles which have more opportunities for unique lighting in the front of the vehicle. This application is optimal for OLED lighting technology, as the thin form factor, uniform emission, segmentation, and animation can create unique styling and branding, and also serve as an indication of vehicle charging levels. An example of a white OLED badge panel is shown in Figure 9.



Figure 9: Example Badge OLED Panel

5. Bendable OLED Panels

The next step in design freedom is to go from a rigid 2D OLED device into the flexible third dimension. In automotive applications for example, it would allow light to follow the outer contours of the car with the OLED taillight.

To achieve this, OLEDWorks is developing the technology to coat the automotive qualified OLEDs onto thin glass substrates which allow a bending radius as low as 180mm while having the same electro-optical performance and lifetime data as the rigid product. Additionally, segmentation and color variability are possible on the same scale as for the known rigid products.

In figure 10, a bendable panel is put into curved state to demonstrate the flexibility. In the final application, the curvature is defined by a holder onto which the panel is attached.

A side effect of the panel thickness reduction is reduced raw material consumption and a significant weight reduction.

Of course, automotive is not the only application where bendable OLED panels can be used, they can be used whenever light needs to follow a curved surface which bends along one axis.



Figure 10: Example of a Bendable OLED Panel

6. Conclusion

OLED lighting technology allows designers to explore unique appearances that have the ability to set the vehicle apart. The compact profile allows easy integration in tight spaces, and bendable OLED panels offer a form factor for seamless incorporation of light over curved surfaces. The crisp segmentation characteristic of OLED lighting technology opens up opportunities for unique branding and personalization, as well as clear

communication of icons or other symbols. This will pave the way for new form factors for lighting design, as well as the potential for closer integration of the various car systems, which will enable more effective Car2X communication and superior safety systems.

Glossary

OLED (Organic Light Emitting Diode): thin carbon-based organic layers sandwiched between two electrodes. When DC current is applied, holes and electrons are injected from the anode and cathode into the organic layers creating electroluminescence.

Segmentation: the splitting up of the OLED light emitter into separate and distinct areas or segments that can be individually lit and controlled.

Stacks: OLED technology wherein different layers of organic compounds are used to produce more light over a given area and/or using a mix of different organic compounds, produce a broad spectrum of light.

Substrate: Base material or device on which an OLED light is built. Glass is a common substrate, and different substrates can yield different looks, colors and designs.

LIGHTING AND SUSTAINABILITY

Exterior lighting function and better understanding about their usage

A. Paul-Henri Matha, B. Andrey Andreev, C. Ignacio Cadenas

Volvo Cars Company

Abstract:

Power consumption has become the main focus for most of the car makers during the last 5 years. with electrification of the lineup of the car makers, battery capacity and range have totally changed the design of the cars. Power consumption, even for exterior lighting has become a challenge for lighting engineers, even if every was thinking that the job was done with the transition from bulbs to Leds technology. we would like to focus with this presentation about the usage of the lighting function. do we have the same needs in urban city, in north of Europe, in California, when we have a manual gearbox or a BEV car what is the real usage of ADB, stop function, turn indicator? Volvo cars has equipped the company cars of its employees with a software system to know the activation of all functions, including lighting. We will present some of the results from Sweden, UK, Belgium, USA and China. we will be able to compare with the factor usages defined by European commission for WLTP cycle and/or eco-innovation

Keywords: Power consumption, customer usage factor

Introduction:

To face climate change, governments are taking decision to reduce CO2 footprint and automotive industry has to adapt itself very quickly. In Europe, for example, in 10 years, CO2 emissions must be reduced by 2 and Internal combustion engine (ICE) vehicles will be ban in 2035. (See figure 1)

2020-2030 CO2 STANDARDS FOR CARS AND LCVS IN EUROPE

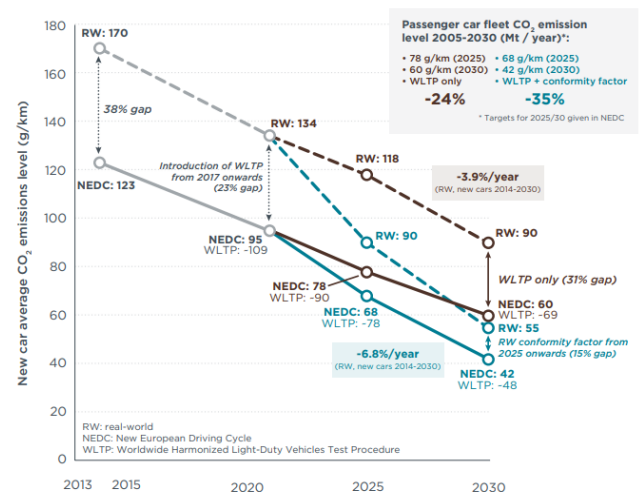


Figure 1: European Co2 emission roadmap for cars

To be able to reduce CO2 emissions, automotive industry must work on different topics:

1/ material production

2/refining

3/ use

4/ end of life treatment

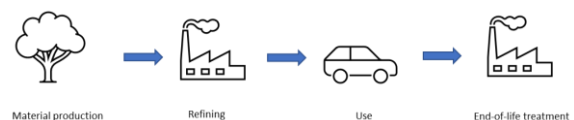


Figure 2: Life cycle for a vehicle

All automotive industry is tackling this challenge with especially cars electrification within the target to sell 100% Battery electrical cars (BEV) in 2035.

At Volvo Cars company, our willingness is to be climate neutral in 2040, as explain in our annual and

sustainable report : [Annual and Sustainability Report 2021.pdf \(volvocars.com\)](#) [1]

A first step is to reduce tailpipe emission by 50% in 2025 thanks to electrification of our vehicle line-up (with BEV and PHEV vehicles) and power consumption reduction.

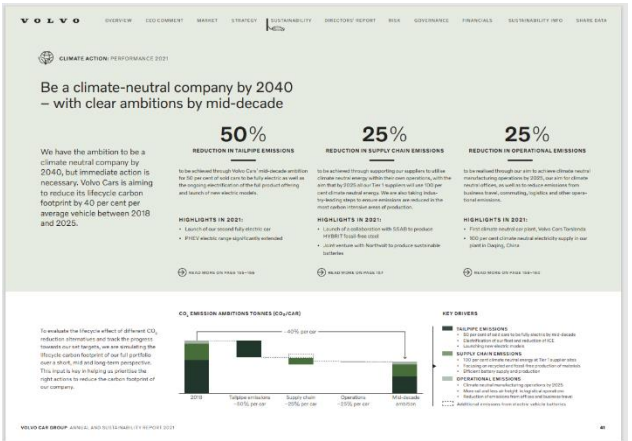


Figure 3: Volvo Cars strategy to be climate-neutral company in 2040

Last year, in 2021, for example, Volvo cars succeeded in reducing 9,5% of CO2 emission

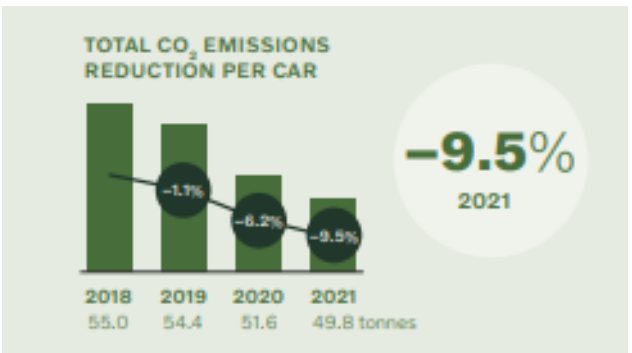


Figure 4: Volvo Cars CO2 emission reduction in 2021

How is automotive lighting business part of the global CO2 reduction?

Whatever the technology we use to produce light, we need electricity, and we are talking in Watt (W) power consumption.

In 1980's it was quite simple to know what the power consumption for each lighting function was. Low beam was produced by a H1 or H7 bulb for example, and a stop function by a P21 bulb. And all bulbs were

grouped in a standard (UNECE R37 legal requirement) : [E/ECE/324/Rev \(unece.org\)](#) [2]

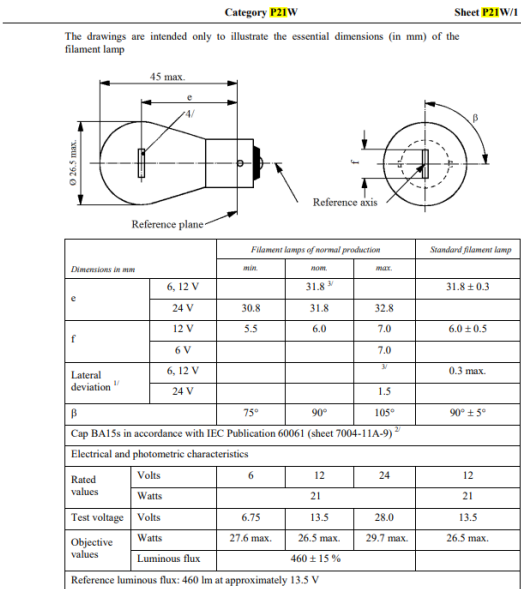


Figure 4: Example of R37 P21 bulb with power consumption indication

To define automotive lighting power consumption, European commission has done a synthesis in the document 32019D1119 about exterior lighting eco-innovation for:

1/ power consumption per lamp with standard Bulb (table 3)

2/ usage factor per lamp (table 6)

Table 3

Power consumptions for different baseline vehicle lights

Vehicle light	Total electric power (P _e) [W]
Low beam headlamp	137
High beam headlamp	150
Front position	12
License plate	12
Front fog lamp	124
Rear fog lamp	26
Front turn signal lamp	13
Rear turn signal lamp	13
Reversing lamp	52
Cornering lamp	44
Static Bending lamp	44

Figure 5 : power consumption per lamp according to table 3 of document 32019D1119, [EUR-Lex - 32019D1119 - EN - EUR-Lex \(europa.eu\)](#) [3]

Table 6
Usage factor for different vehicle lights

Vehicle light	Usage factor (UF) [-]
Low beam headlamp	0,33
High beam headlamp	0,03
Front position	0,36
License plate	0,36
Front fog lamp	0,01
Rear fog lamp	0,01
Front turn signal lamp	0,15
Rear turn signal lamp	0,15
Reversing lamp	0,01
Cornering lamp	0,076
Static Bending lamp	0,15

Figure 6 : usage factor per lamp according to table 6 of document 32019D1119, [EUR-Lex - 32019D1119 - EN - EUR-Lex \(europa.eu\)](#) [3]

Thanks to this information, we are able to define an average power consumption for our exterior lighting functions:

- During homologation according to WLTP cycle (Worldwide Harmonized Light Vehicle Test Procedure) [EUR-Lex - 32017R1151 - EN - EUR-Lex \(europa.eu\)](#) [4]. Only Day time running lamp is activated + ~25% of stop lamps
- during normal usage

For a vehicle with only bulb, we get:

- Exterior lighting power consumption in WLTP homologation: 69 Watts
- Exterior lighting power consumption in standard usage: 115 Watts

Function	CO ₂	Low beam (when light)	Passing beam (when light)	Driving beam (when light)	Front Position light	Front Turn indicator	Rear Turn indicator	side turn indicator	license plate light	reverse	stop	HBES	Rear fog	Rear PL	average consumption	WLTP consumption
Bulb	20	84%	17%	17%	17%	17%	17%	17%	17%	17%	17%	17%	17%	17%	115	69
LED	20	10%	1%	1%	1%	1%	1%	1%	1%	1%	1%	1%	1%	1%	62	51

Figure 7: calculation of WLTP and average usage power consumption for a vehicle equipped with Bulb technology

With LED technology it is more complicated to calculate because a lamp can be design with a multitude of different technology. If I calculate the values for our current Volvo XC40 vehicle, we get:

- Exterior lighting power consumption in WLTP homologation: 51 Watts
- Exterior lighting power consumption in standard usage: 62 Watts

This mean that in average usage you can save around 50 Watts power consumption compared to a car equipped with bulb technology



Function	CO ₂	Low beam (when light)	Passing beam (when light)	Driving beam (when light)	Front Position light	Front Turn indicator	Rear Turn indicator	side turn indicator	license plate light	reverse	stop	HBES	Rear fog	Rear PL	average consumption	WLTP consumption
Bulb	20	84%	17%	17%	17%	17%	17%	17%	17%	17%	17%	17%	17%	17%	115	69
LED	20	10%	1%	1%	1%	1%	1%	1%	1%	1%	1%	1%	1%	1%	62	51

Figure 8: calculation of WLTP and average usage power consumption for XC40 Volvo cars.

If we translate the power consumption in CO2 emission, or battery additional cost to keep same range autonomy with usual rule of thumb:

1 watt equivalent to 0,002g CO₂ → - 1g Co2/km

1 extra watt equivalent to 1€ extra battery cost to keep same range → -50€ battery cost

As a conclusion, we should say that thanks to LED introduction, power consumption has been reduced drastically for exterior lighting during the last decade.

However, sometimes it is not the case. It may happen that LED lamp consumes more than a bulb lamp. It may be common in the future due to styling trend.

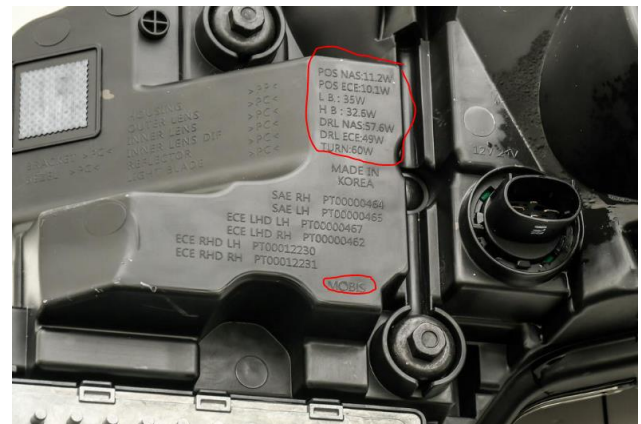


Figure 9: example of high-power consumption for a DRL

Limitation in usage factor knowledge

In the European document about usage factors, we can do some remarks:

1/ Stop function is not included. However, it is mentioned in the technical guidelines from 2018 about Eco-innovation that average usage is 11%, when in NEDC cycle it was 15% and in WLTP cycle 25%



Technical Guidelines

for the preparation of applications for the approval of innovative technologies pursuant to Regulation (EC) No 443/2009 and Regulation (EU) No 510/2011

July 2018 Revision (V2)

Note 26. The temporal share of deceleration phases during the NEDC amounts to 15.1% in relation to roughly 11% of braking during 'real-world' conditions. Potential improvements of brake lights technologies are therefore fully covered by the type approval measurements and cannot qualify for an eco-innovation.

Figure 10: Technical guideline book for Eco-innovation, European commission, [Technical Guidelines February 2013.pdf \(europa.eu\)](#) [5]

2/ High beam usage: 3% of the time seems to be very conservative, especially with the democratization of automatic high beam activation and Adaptive driving beam. We can find a lot of literature about additional usage of high beam. For example, publication from TU Darmstadt in ATZ magazine, 06/2020, Objective Assessment of the Safety Contribution of Today's Automotive Headlamps

The work has also shown that adaptive switching significantly increases the usage of the high beam. While with manually switched high beam, the duty cycle is approximately 10 %, an automatically switched high beam increases the usage to approximately 30 % – with the ADB

even an average high beam usage of approximately 70 % is possible

Figure 11: Extract of ATZ article about Objective Assessment of the Safety Contribution of Today's Automotive Headlamps [6]

3/ turn indicator usage (15%) of the time seems to be a bit too much

4/ rear position lamp usage is mentioned only by night, whereas a lot of car makers (like Volvo cars) is switching ON the rear position lamp by day also for safety reason. This activation will also become mandatory from September 2024 with the new 08 series of UNECE R48

On top of that, on Volvo exterior lighting switches (stalk), The customer can select different functions by day and night, and we were interested in knowing which functions are currently used:

- position "0" on the stalk (DRL by day without rear position lamp)
- Position "Position lamp by day"
- Position "low beam by day"
- Position "auto": DRL + rear position lamp by day
- Position "automatic high beam"
- foglamp activation
- turn indicator activation

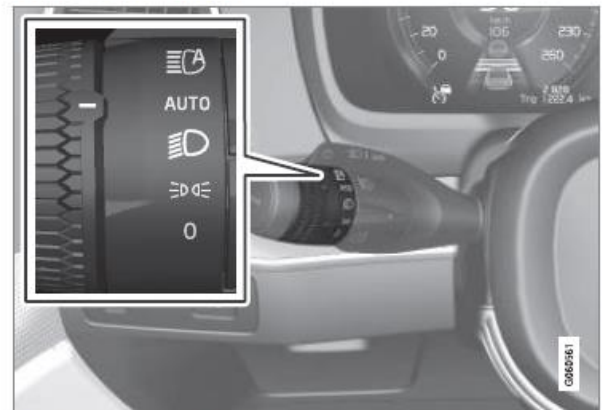


Figure 12: Volvo XC40 stalk

This study is very important for 2 main reasons:

- to know better the habits of our customer
- to know and improve the global average power consumption of the vehicle

Our goal was also to see if we have different usages by countries / region between USA, China and Europe, which are the main markets for Volvo cars

Top 10 retail sales by market (k units)	2021	2020
China	171.7	166.6
US	122.2	110.1
UK	48.3	46.5
Sweden	47.8	53.7
Germany	43.8	46.9
Italy	19.8	17.7
France	18.9	16.5
Japan	16.6	15.5
Netherlands	15.9	16.2
Korea	15.1	12.9

Figure 13: Volvo cars main markets

Investigations

To be able to run investigations, we developed 2 methods:

First idea was to use Volvo Cars community. We have different groups, with Apps to be able to connect them, with millions of users. The idea was to run a survey

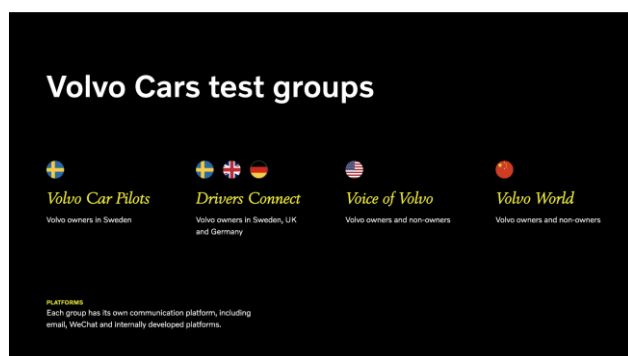


Figure 14: example of Volvo cars community

Second idea was to use the company cars that are all linked to a WICE database. On this database, we can find a lot of information about car usage and especially lighting usage. More than 1000 signals can be found on a database with updated information every day.

For this study, we analysed around 4000 cars in Sweden, 100 vehicles in Belgium, 100 vehicles in USA and 100 vehicles in China

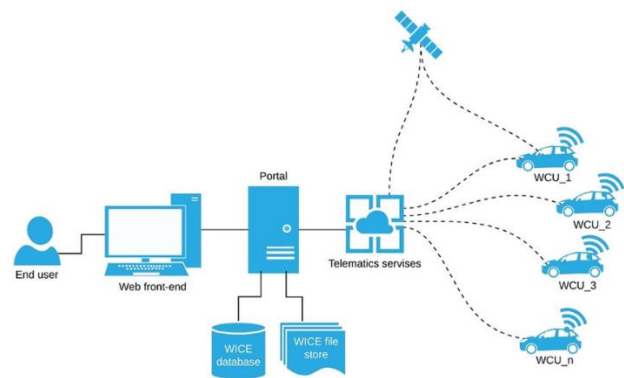


Figure 15: WICE principle

First results and next steps

You can find below some interesting analysis about car usage:

1/ Daytime running lamp: average value is 70% compared to 66% in European commission document

2/ Turn indicator usage is much less: 6% compared to 15% usage in in European commission document. On top of that, we have seen that average duration usage in 7 seconds

3/ Stop lamp usage: we have analyze cars that have only automatic gear box, then we estimate a quite important percentage of usage, much more than the 11% value from European commission document.

In Europe, for ICE vehicle, Result is around 15% average value for time usage, with a standard deviation of 3%, which is quite a lot. That means that not all the drivers have the same usage.

In USA, for ICE vehicle, average usage is around 20%, much more than Europe

For BEV cars, we can see that the usage increase to a value between 30% and 35%, much more that the WLTP cycle.

This can be explained by the One pedal drive system equipped on Volvo BEV cars

[Volvo XC40 Recharge One Pedal Drive Animation - Volvo Cars Global Media Newsroom](#) [7]

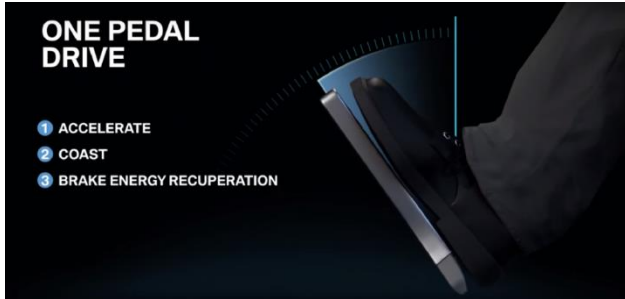


Figure 16: Volvo one pedal drive system

Average duration for stop light is around 15 seconds, with a maximum duration of 10 minutes

4/ Combined function

We can analyze also the usage of 2 functions in the same time, this is quite interesting to calculate the maximum thermal constraint in a lamp.

For example, turn signal and brake light are switch ON together only during 3% of the time of their usage

5/ stalk usage by the driver

Because Volvo is proposing different positions on the stalk by day and by night, it was interesting to see how often the stalk in "AUTO" position is. This position will be the unique one, while driving, from September 2024 with the new serie of UNECE R48 (08 serie)

- Around 2% of the users are switching ON the low beam by day
- Around 5% of the users are switch ON the low beam by night (where they have low beam if they are in AUTO position)
- In Europe, only 0,5% of the drivers are using the stalk in "0" position by day (to have no rear position lamp ON by day)
- Compared to Europe, in USA, 2% of the drivers are using the stalk in "0" position, more especially in parking conditions, which is a common usage in USA
- For remaining time, "AUTO" position is used. Around 95% of the time in USA and 98% in Europe
- "Position light" position is not used. This is especially a function used as "parking lamp function" for some specific countries like Germany. But we have not collected any data about this usage.

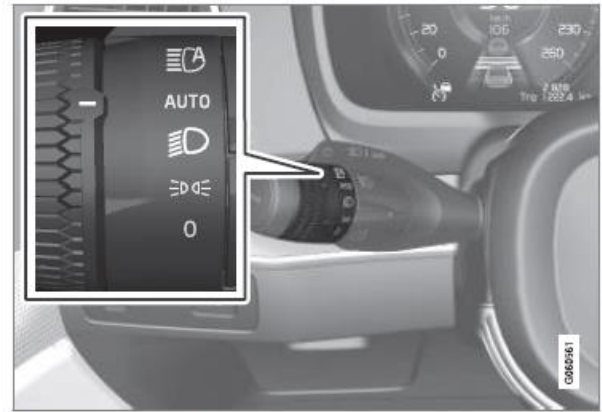


Figure 12: Volvo XC40 stalk

Conclusion

This study is showing the first Volvo analysis thanks to the car data usage with WICE system.

These results can help car makers to know better the average power consumptions values of exterior lighting (and other functions).

It may help also clarify some aspect of the mission profile like maximum and minimum temperature, level of durability needed for each component like fan, stepper motors, leds. What is needed is "just" a signal in the WICE database.

The potential is huge. Data collection is one of the key point for the new era of automotive industry, and not only for autonomous driving.

Acknowledgement

The authors acknowledge the contribution of their colleagues to this work: Matteo Lemmonier, Nils Olofsson and Jonas Frunk

References

- [1] Volvo annual report. [Annual and Sustainability Report 2021.pdf \(volvocars.com\)](#)
- [2] UNECE R37. [E/ECE/324/Rev \(unece.org\)](#)
- [3] document 32019D1119, [EUR-Lex - 32019D1119 - EN - EUR-Lex \(europa.eu\)](#)
- [4] Worldwide Harmonized Light Vehicle Test Procedure) [EUR-Lex - 32017R1151 - EN - EUR-Lex \(europa.eu\)](#)
- [5] Technical guideline book for Eco-innovation, European commission, [Technical Guidelines February 2013.pdf \(europa.eu\)](#) [5]

- [6] ATZ MAGAZINE 06/2020, Objective Assessment of the Safety Contribution of Today's Automotive Headlamps, Dr.-Ing. Jonas Kobbert, Prof. Dr.-Ing. Tran Quoc Khanh
- [7] [Volvo XC40 Recharge One Pedal Drive Animation - Volvo Cars Global Media Newsroom](#)

Analysis of Energy Consumption of modern Headlamp Systems and Options for Energy Consumption Reduction

Dr. Ernst-Olaf Rosenhahn

Marelli Automotive Lighting & Sensing Reutlingen GmbH, Tübinger Straße 123, 72762 Reutlingen

Abstract: In the field of improving the sustainability of exterior lighting products around the car the average power consumption of the main beam lighting functions is often the most important contributor.

In the presentation cost and energy optimized basic headlamp systems will be compared to ADB headlamps up to high end systems in terms of energy consumption for different driving situations taken on real test drives.

The important aspects like safety by lighting performance, headlamp styling and energy efficiency have to be balanced in the next generation of headlamps and exterior lighting components.

Field test measurements of the above mentioned systems and a detailed analysis will be presented, options for optimizations are discussed. The proposal is to adapt low beam illumination during driving in urban areas and to define an appropriate definition of an adaptive DRL to compensate the energy consumption offset for improved performance and safety.

Keywords: headlamp energy consumption, ADB power consumption, automotive power consumption reduction, adaptive town lighting, adaptive DRL

1. Introduction

Modern frontlighting systems often offer adaptive driving beam functionality (ADB) to increase range and safety also in situation with oncoming or preceding traffic. In comparison to headlamp systems, which provide low beam and high beam only the average power consumption of such systems is increased. This depends on the much more often activated segments in the high beam area, but also on the performance and the efficiency of the used modules.

In addition for future frontlighting systems also an increase in power consumption is expected by the illumination of the front panel including the emblem in the center of the front panel. In terms of sustainability it is the task to balance electrical power consumption and lighting functionality. After the analysis of the current situation especially concerning different ADB systems the way for smart and intelligent power consumption savings will be described.

2. Energy Consumption of Headlamp Main Functions

In a first step of analysis different headlamp system types have been investigated in detail concerning their energy consumption for low beam, high beam and adaptive driving beam (ADB). As a basic performance system a base version headlamp with an LED reflector system for low and high beam was analysed. As a standard matrix system an ADB system with 12 segments (1 row) was taken and for the high end system a prototype headlamp equipped with a micro-LED module (high resolution) combined with a bifunction low beam / high beam projection system as a background module was chosen.

For a fair comparison headlamp control data are collected from a 15 minutes ride along a test course in real traffic during nighttime. These data are used to control the different systems on simulation base and the resulting electrical power consumption was calculated and summarized in time intervals of 1s.

The power consumption of each lighting function for each headlamp system is shown in table 1.

Headlamp system	base version reflexion system	ADB headlamp system (12 segm.)
low beam mode	18,0 W	17,8 W
auto high beam mode	+4,7 W	-
auto high beam + ADB mode	-	+16 W

Table 1: Electrical power consumption for lighting functions per headlamp

In figure 1 the power consumption of the system with reflexion type low / high beam is shown for a 15 minutes ride along a country road. In the first half of this section there was a preceding car in front and the high beam can't be activated (low beam $P = 18 \text{ W}$ / headlamp). In the second half of the section there was no car in front, but there were several cars coming from ahead and switching the high beam to low beam is needed several times. In average the power consumption for this system (low beam + high beam) on this section (automatically switched) is at $P = 22,7 \text{ W}$, that means $\Delta P = 4,7 \text{ W}$ above the low beam consumption level. During this section in average

about 2,5 HB-LB-transitions / min are carried out by the system.

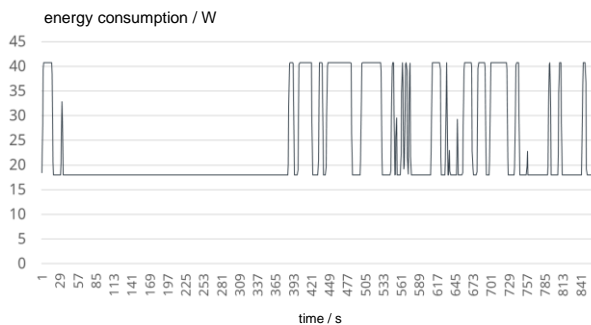


Figure 1: Electrical energy consumption for low / high beam controlled by automatic switching

In figure 2 the same section is shown with the function of power consumption of a low beam in combination with a standard ADB module (1 row of 12 segments per headlamp). In this case also in the first half of the same track with preceding traffic parts of the high beam can be activated in ADB functionality and an increased range in comparison to the low beam can be provided. Matrix segments right and left of the car in front are switched on and therefore the power consumption is increased in average by about $\Delta P = 9 \text{ W}$ above the low beam power consumption level. A second effect of the larger power consumption for the ADB headlamp is seen with $P = 45 \text{ W}$ power consumption for low beam plus full high beam. The main reason is the slightly reduced efficiency of the high beam optical system for ADB functionality in comparison to the standard high beam of the reflexion system.

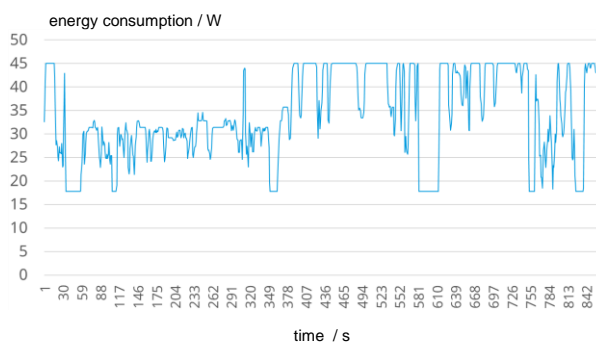


Figure 2: Electrical energy consumption for low beam in combination with ADB (12 segments)

The shown ADB system is a typical system with a large spread in the market of ADB systems. Normally ADB systems are designed in terms of the number of LEDs, number of rows and resolution according to the car segments and commercial budget. Therefore there is a brought variety of ADB-systems existing on the market and it has to be checked in detail about their individual power consumption.

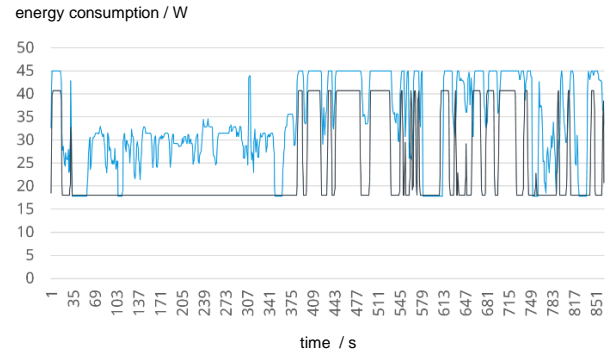


Figure 3: Energy consumption comparison between auto high beam switch and ADB high beam control

Looking to the above shown system we checked the advantage of performance in range and safety for such a system. In figure 4 the light distribution is demonstrated with the isolux-diagram on the road from the bird's eye view.

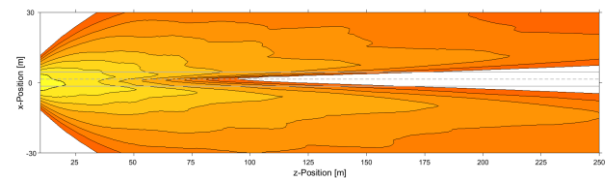


Figure 4: Isolux-diagram on the road of the ADB lighting function with 12 seg. in a one row high beam

For quantification of the advantage provided by an ADB system the HSPR rating (Headlamp Safety Performance Rating) score gives an idea. In table 2 the HSPR score comparison of an ADB headlamp system for manual switching, automatic high beam switching and full automatic ADB mode is summarized.

	HSPR effective performance in m	HSPR rating score
Manually	97,1 m	24,4 advanced
Automatic	108,9 m	31,7 excellent
ADB	124,5 m	41,5 premium

Table 2: HSPR ratings and effective performance of the ADB system switched manually, automatic and in ADB mode

The comparison proves that the increased power consumption of an ADB systems in comparison to automatic high beam switching is creating a significant amount of improved safety during nighttime. Average range down the road is

$\Delta d = 15,6$ m larger than without the ADB lighting function.

This increase of energy consumption is even higher by using an ADB system with more pixels and higher resolution. For example an HD headlamp system with a module using 25.000 pixels in addition to the background module with 12 segments is consuming on this test track in the ADB mode in average $\Delta P = 19$ W more electrical power than a standard system with 12 segments, but it can boost such a system to "Premium+" in the HSPR rating with a significant increase in safety and comfort for the driver.

3. Analysis of the Road Luminance

On the basis of several spot checks during daytime and nighttime the luminance of the road surface was measured as a function of the illumination level at the road surface. The results are illustrated in figure 5 from lower luminance levels for the illumination by the car's headlamp system only ($L_{\text{road}} < 1,5$ cd/m²), for road lighting in urban areas up to daytime situations with a cloudy sky or bright sunshine (L_{road} about 3.000 cd/m²). It's a wide range of about 4 decades of road luminance levels.

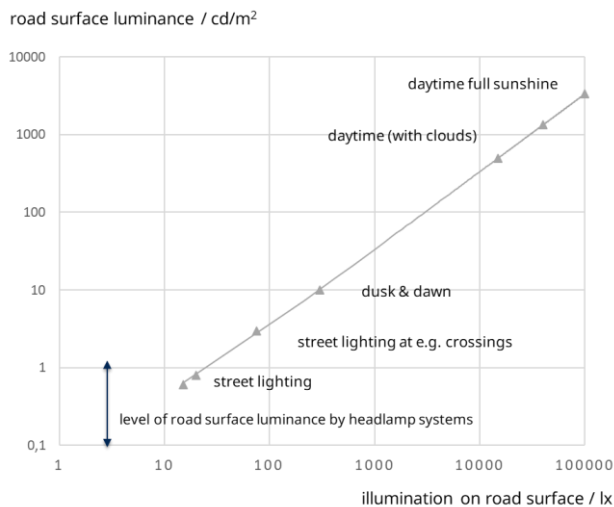


Figure 5: Road luminance as a function of the illuminance level at the road surface

Based on this analysis of road luminance levels especially for driving situations in urban areas are investigated concerning the potential of energy consumption savings.

Erkan [2] found out in his investigations at Technical University Darmstadt in 2019 that in urban areas all

drivers are o.k. with an average road luminance level of about $L = 0,8$ cd/m² (see figure 6).

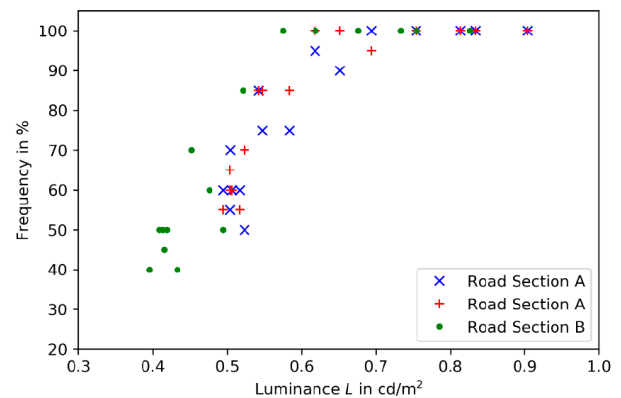


Figure 6: Subjective ratings about the road luminance levels requested by drivers during night in urban areas (Erkan [2])

The average luminance level of $L = 0,8$ cd/m² was rated by 100 % of all subjects as sufficient. Static road illumination is providing in a lot of situations such luminance level without any illumination by headlamps. In some crossing situations with a high level of illuminance up to $L_{\text{road}} = 3$ cd/m² can be measured.

In such driving situations with sufficient street illumination the low beam intensity can be reduced to save energy consumption. In case vehicle speed is low this reduction can be additionally balanced for the range, foreground and side spread area individually without loss of comfort or safety. In most of the optical low beam systems range and side spread are fired by different LEDs and therefore these two parts can be controlled mostly independent.

Weber [3] is proposing up to 75 % reduction in such good illuminated urban area situations. Also other driving situations like "nose to tail" or "vehicle speed 0" are driving situations which do not need maximum range and therefore can be reduced for energy consumption reduction. The proposal is to adapt the low beam luminous flux (class V and class C) to the illumination level of the road and other urban driving situations. The overall driving time in urban areas could be quite long, because of the low average speed and as consequence can lead to a significant energy consumption reduction. In some cases the homogeneity of road illumination is on a low level (because e.g. of the large distance between the street lamps), this has to be taken into account for the dimming factor. Safety should not be jeopardised.

In addition to driving in urban areas all driving situations with an illumination level of more than

$E = 300 \text{ lx}$ on the road should be checked, because with $E = 300 \text{ lx}$ on the ground the luminance level is at about $L = 10 \text{ cd/m}^2$ (see figure 5), which is 10x higher than the luminance, which is typically produced by the low beam. So with $E = 300 \text{ lx}$ on the road the light powered by the low beam to the road with about $P = 40 \text{ W / car}$ doesn't produce a visible effect for the driver on the road. In such cases the DRL lighting function is completely sufficient, because the car has to be seen by the other road users. Therefore in such cases of low illumination level (dusk & dawn, cloudy sky) to the front DRL is sufficient and also the rear lamps should be switched on for better signalling. In addition also the dashboard illumination is helpful for the driver and automatic switching on independent from the low beam activation could be comfortable. The usage of the DRL instead of the low beam in such driving situations is reducing the power consumption in such driving situations by about $\Delta P = 20 \text{ W}$ per car.

4. Daytime Running Lamp Lighting Function

The DRL lighting function is switched on for about 2/3 of all driving time, therefore the contribution of the total power consumption in frontlighting can be significant.

4.1 DRL power consumption

The analysis of frontlighting signal lamps (DRL & position lamp) showed up in the beginning of DRL lighting functions with LEDs e.g. a bumper module fired with one single LED and a power consumption of about $P = 2,5 \text{ W / lamp}$ and $P = 5 \text{ W / car}$. This was a functional application without any priority on styling and was used as a standard part integrated in the front bumper in Mercedes-Benz projects (Figure 7).

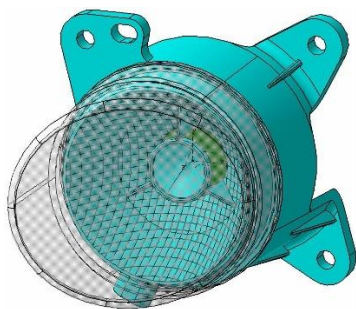


Figure 7: Daytime Running Lamp with a power consumption of about 2 W / lamp

With increased styling requirements for creation of the signature of the vehicle front the power consumption of DRL lighting functions increased over time. Especially with lightguide solutions for the optical concept power consumptions of up to $P = 20 \text{ W / lamp}$

($P = 40 \text{ W / car}$) or even more are existing in the meanwhile.

For further discussions a typical consumption of $P = 10 \text{ W / lamp}$ ($P = 20 \text{ W / car}$) is taken into consideration in the following discussion.

4.2. Energy Consumption Reduction by adaptive DRL

With an electric power consumption of 10 W for a typical DRL system / lamp the total amount of energy over lifetime is the same as for the low beam with about $P = 20 \text{ W}$ consumption per lamp, because of double activation time for DRL in comparison to low beam.

So it makes sense to understand, what can be done for decreased energy consumption within the DRL lighting function. Today in ECE a range between $I = 400 \dots 1200 \text{ cd}$ max intensity for DRL is defined.

And the switching level between low beam and high beam by sensor control is by ECE regulated to switch on low beam at a horizontal illumination level on the road of $E = 1.000 \text{ lx}$ at the latest and switch off at $E = 7.000 \text{ lx}$ latest.

The usage of this switching limits is resulting currently in the following statistic taken at German roads during dusk & dawn periods, which shows the low beam activation as a function of the horizontal road illumination level. This data also includes the low beam usage with manual switching. Under the assumption that cars without DRL (indication of the vehicle age) are not equipped with automatic switching this data in figure 8 are a mixture of manual and automatic switching according to the above mentioned limits. In Germany on the road about 25% of all cars are today not equipped with DRL, because of their age.

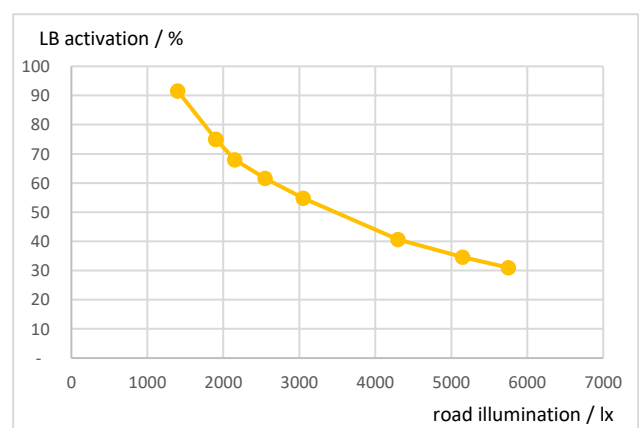


Figure 8: Percentage of low beam activation as a function of horizontal illumination level on the road

The statistic shows that at $E = 3.500 \text{ lx}$ road illumination 50% of all low beams are switched on.

The dusk & dawn periods every day contribute to power consumption disproportional, because these

phases show the highest traffic density (excluding summertime). According to figure 5 the luminance on the road is at $E = 1000 \text{ lx}$ road illumination about $L_{\text{road}} = 30 \text{ cd/m}^2$. At this luminance level and above the low beam flux on the road is not visible, it makes no sense to spend in this situation about $P = 20 \text{ W}$ / lamp low beam power for road illumination. Taking this into account the switching level with today's modern car sensors should be rechecked.

In this situations DRL, RL and dashboard illumination are the propriate illumination of the vehicle to guarantee a safe recognition by other traffic participants.

In addition, another aspect can support energy consumption reduction in such driving situations: The luminous power of the DRL could be adapted to the adaptation level of the drivers. With an average luminance of $L = 30 \text{ cd/m}^2$ / $E_{\text{road}} = 1000 \text{ lx}$ the human eye is not full adapted to the photopic adaptation level, therefore the sensitivity for signal lamps is increased as during higher luminance levels. The proposal is to drive with DRL, but to adapt the intensity level of the DRL to the adaption luminance respective the road illumination as an indicator.

Reduction of 50% of DRL intensity could lead to a power consumption reduction of about $\Delta P = 10 \text{ W}$ per car during these situations. At least for LED fired DRLs, because the LED spectrum with the higher amount of blue radiation give a significant higher brightness at these adaptation levels than halogen bulbs.

A proposal out of the above-described findings could be that electric power consumption reduction can be achieved by introducing 3 levels of automatic switching:

- DRL at $E_{\text{road}} > 7.000 \text{ lx}$,
- Adaptive DRL + rearlamp + dashboard:
 $500 \text{ lx} < E_{\text{road}} < 7.000 \text{ lx}$,
- LB + position at $E_{\text{road}} < 500 \text{ lx}$.

These proposed switching levels incl. hysteresis should be adapted and confirmed by additional input data.

4. Conclusion

The adaptive driving beam during nighttime traffic and new trends in signal lighting (illuminated front panels and logos) are important out of different reasons. Increased road safety and styling differentiation create additional value, but energy is needed to drive these features. Beside the continuous improvements in efficiency of the LEDs and optical systems other options have to be installed to follow the path of sustainability. Power consumption reduction should never lead to decreased safety level, but an additional contributor for reduced energy consumption in frontlighting could be a smart and intelligent light

control algorithms based on existing car sensor signals:

Following ideas should be consolidated upon their potential according energy consumption reduction:

1. Switching levels between DRL and low beam
2. Adaptive DRL intensity based on surrounding lighting conditions in combination with rearlamp and dashboard illumination.
3. Adaptive low beam lighting characteristics based on light levels provided by road illumination and other parameters like vehicle speed.

For a better quantification of the different measures on the total electrical power consumption reduction of frontlighting more data e.g. concerning the total duration of specific driving situations are needed for a consolidated strategy, but promising effects could be shown in the above discussed investigations. For quantification the values discussed above are related to typical optical systems. The energy consumption of each lighting function depends on the individual styling and the applied optical systems. Therefore stylists, optical engineers and a smart electronic control should contribute to energy consumption reduction in future frontlighting systems.

5. Acknowledgement

Thanks to my colleagues Bernd Dreier and Martin Reichelt, who strongly supported on the data collection and analysis.

6. References

- [1] Wagner, M. Erkan, A., Khanh, T.Q.: Reducing Head Lighting Level on Urban Roads for different Street Lighting Situations, ISAL Symposium, Darmstadt, 2019.
- [2] M. Erkan, Kosmas, K., Khanh, T.Q.: Energy Saving Potential of Headlights by determing the current utilisation rate of headlight functions, ISAL symposium, Darmstadt, 2019.
- [3] Weber, S., Köhler, S., Duhme, D.: Development of energy-efficient car lighting systems with focus on battery electric vehicles. Joint research project EFA 2014.

Efficiency enhancement opportunities for automotive lighting systems by traffic situation analysis

Anil Erkan¹, Lily Antoinette Engelbrecht-Schnür¹, David Hoffmann¹, Markus Peier¹,
Korbinian Kunst¹, Timo Singer¹, Tran Quoc Khanh¹

1: Technical University of Darmstadt, Laboratory of Adaptive Lighting Systems and Visual Processing,
Hochschulstr. 4a, 64289 Darmstadt, Germany

Abstract: In all socially relevant areas, the demand for more energy efficient solutions is increasing steadily. Thus, also driven by the switch to electric vehicles, the demand for energy efficient concepts for the realization of each component is also increasing in the automotive industry. This naturally includes the vehicle's lighting systems. The aim is to develop lighting concepts that are more energy efficient than current systems. In this context, it should be noted that the lighting systems are of great importance in terms of safety and perception in road traffic at night. For this reason, the question arises when and how the efficiency of automotive lighting systems can be increased without compromising safety and perception.

The aim of this work is to identify night time traffic situations that have potential to increase efficiency to a large extent by analysing traffic statistics. These can include traffic jams, rush hour traffic, or night time traffic in illuminated areas. Then, these situations will be sorted based on their potential and the adaptation possibilities of the corresponding lighting functions to increase efficiency will be analysed. For example, switching from low beam to daytime running lights in congestion situations could be such an adaptation option.

Keywords: Sustainability, automotive lighting, efficiency enhancement, traffic statistics

1. Introduction

Talking about the sustainability of lighting components on the vehicle, the entire product life cycle from development to product disposal has to be considered [1-4]. In terms of the sustainability of automotive lighting components in the various phases, there are already some considerations and approaches for improvement.

For Schmidt et al. the motto for sustainability improvement is "Reduce Reuse Recycle" [3]. There are two approaches to the topic of Reduce. On the one hand, the energy demand of the luminaires during the operating time should be reduced. On the other hand, material reduction in the sense of material savings and simultaneous weight reduction represents an important aspect. In addition, the

production of components and semi-finished products and the transport of individual components between facilities are possible reduction parameters that can be optimized, since in some cases components are installed in the vehicles that have already covered greater distances at the time of vehicle sale than the vehicle will later cover in the entire operating cycle. [3] Compared to the Reduce aspect, the Reuse idea is more difficult to implement, since here many parts cannot be installed in the next vehicle directly after the operating time of another vehicle has expired due to the high integrity (e.g. soldered LED on a circuit board) or high quality standards. Here, however, there are already components, such as the heat sink, which could be reused when using a universal concept. Work is also already being done on LEDs that are separated from the PCB. [3]

If recycling is considered, it is more likely that the material will be reused. According to Schmidt et al., this can be done by reusing the material for an equivalent successor product or for a substandard product. Another possibility would be thermal recycling for energy generation. [3]

According to Hartmann et al. the sustainability of headlamps should be understood as a new property of a complex system product. In addition to the product level, this should also be continuously evaluated at the component level and thus include all actors in the supply chain. Thus, the headlight would also be an opportunity to gain understanding of the redesign of complex components and to apply the findings to other components of the vehicle and to be able to meet the requirements of balancing carbon footprint, functionality and circular economy. [4]

Boehm and Hartmann predict that the headlight trend will move towards function-optimized headlights but also design-oriented headlights and very energy-efficient headlights. Thus, compromise solutions are conceivable. A μ LED system with a resolution of e.g. about 100,000 pixels would represent such a compromise between cost, energy efficiency and resolution since light is only activated where it is needed. [5]

The considerations and approaches outlined above represent important steps in increasing sustainability.

Nevertheless, the operating time of the headlight is the most relevant phase for increasing efficiency. For this reason, approaches that consider the increase in efficiency during the operating time are discussed below.

The strategy of a car manufacturer outlined by Feid focuses on the operating time and aims to reduce the energy demand of the lighting function by replacing halogen tungsten lamps with LED technology. In addition to replacing halogen tungsten lamps, vehicles with high performance headlights (Matrix, Pixel, etc.) should also comply with the limit of 0.5 g CO₂ per km. Through this strategy, exterior lighting on vehicles has already contributed to a reduction in the CO₂ footprint of 0.6 to 1.1 g per vehicle and km. [6] Furthermore, the low beam function can be identified as the lighting function with the highest potential for efficiency enhancement. [6]

A study conducted by the Technical University of Darmstadt also identified the low beam as the most relevant lighting function for efficiency enhancement. This study also looked at the reduction in CO₂ emissions by replacing halogen lamps with LEDs in the low beam, daytime running lights, rear lamps and brake lights, which would lead to a reduction in emissions up to 250,000 tons of CO₂ per year when considering all vehicles equipped with halogen tungsten lamps in Germany. [7]

These considerations are very important and valuable and should be followed up and expanded. Nevertheless, it is also important here to first consider relevant and promising use cases in terms of traffic situations in order to achieve a large-scale efficiency enhancement with minimal adjustments to the lighting components.

This is exactly where this work comes in. To determine such relevant use cases in road traffic, several traffic situations are considered and analysed. From this consideration, a relevance analysis is then made for the highest efficiency enhancement potential that does not compromise road safety.

2. Traffic situations

In this section, the analysis of traffic situations is performed using traffic statistics. The basis for the analysis is mainly derived from traffic statistics in Germany.

The starting point for all the following considerations is the total annual mileage of passenger cars in Germany, which reached 644.8 billion km in 2019 [8]. Furthermore, a night time mileage share of 20 % is assumed [9-11].

2.1 Congestion

Congestion (see Figure 1) is probably the most annoying traffic situation for most road users.

Nevertheless, it is one of the traffic situations that could have a high potential for efficiency enhancement due to the number of vehicles involved.

Thus, in 2019, there were a total of 708,500 congestions in Germany with a total length of about 1.4 million km and about 521,000 congestion hours [12].



Figure 1: Congestions offer high potential for efficiency enhancement. [13,14]

Taking into account the average length of passenger cars in Germany of 4.60 m [15] and maintaining a safety distance of 2 m, equation 1 results in approximately 215.6 million vehicles stuck in congestion in 2019. [12,15]

$$n_{\text{Vehicles}} = \frac{d_{\text{Congestion}}}{d_{\text{Vehicle}} + d_{\text{Safety}}} \quad [1]$$

In order to consider the total time spent by these vehicles in congestion, the average duration of a congestion is first calculated. For this purpose, the ratio between congestion hours (521,000 hours) and the number of congestions (708,500) is calculated. This results in an average congestion time of about 0.74 hours per vehicle.

If this average congestion duration is multiplied by the number of vehicles in congestions, the total duration is about 159.5 million hours, which is divided into 127.6 million hours during the day (80 %) and 31.9 million hours during darkness (20 %).

To address the issue of which lighting functions should be considered to increase efficiency during congestion, daytime and night time congestion situations are considered separately.

While driving in daylight, only the daytime running lights are activated in the headlights for better visibility of the vehicle. In a congestion situation, this information is not urgently needed because the relevant road users are also in the immediate vicinity in a stationary state. It would therefore be conceivable here to switch off or at least dim the daytime running light function. In the rear area, the brake light is active in congestion situations, which should not be changed

in daylight, since the brake light function, in addition to the flashing warning lights, signals the end of the congestion to the following traffic.

If the congestion situation is considered at night, both the low beam, which is responsible for the driver's visibility, and the position light of the headlight are switched on. At the same time, the low beam can no longer fulfil its actual function in a congestion situation, as it only illuminates the rear of the vehicle in front. Thus, the low beam function is obsolete in night time congestion situations and could be replaced by the daytime running light or position light.

In contrast to the daytime congestion situation, the brake light function could be dimmed in night time congestion situations, since lower contrasts would already be sufficient for the signal function to be fulfilled. Another positive effect of dimming the brake light function would be the reduction of the glare potential for the following traffic.

For the adjustment of the daytime running light during the day and the low beam during night time congestions, existing sensors such as speed and GPS sensors could be used, while for adjusting brake lights, parking sensors could be used to detect the presence of any following traffic.

2.2 Rush hour at dusk

Another traffic situation that could have a high potential for efficiency enhancement is commuter traffic during dusk and dawn (see Figure 2). In Germany, 68 % of the workforce commutes to work by car, and most commuters take between 10 and 60 minutes (72.1 % of the workforce) to get to work [16]. Consequently, the rush hours in Germany are approximately between 06:30 and 08:30 in the morning and between 15:30 and 17:30 in the afternoon [17].



Figure 2: Rush hour at dusk [18,19]

Thus, with 45.4 million in the workforce [20], there are approximately 30.9 million commuters. In order to estimate the commuting time at dusk, the sunrise and sunset in Darmstadt are taken as an example (see Figure 3) [21].

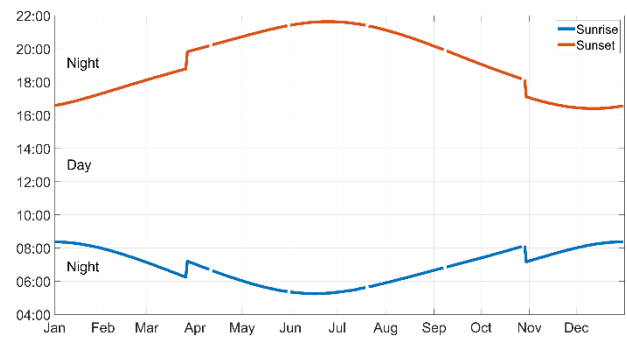


Figure 3: Course of sunrise (blue) and sunset (red) over the year in Darmstadt, Germany [21]

Looking at sunrise and sunset, it is clear that rush hour traffic occurs primarily during the winter months from November to February at dusk, which is about one-third of the year.

For the purpose of considering the total duration of rush hour traffic at dusk, the following assumptions are made based on the data shown. A commute duration of one hour in the morning and one hour in the afternoon is assumed, one third of which takes place at dusk. This results in a commute duration of 0.67 hours at dusk per day. With approximately 250 workdays per year, the dusk commute time adds up to approximately 166.67 hours per commuter. Thus, for all 30.9 million commuters, the dusk commute time is 5.15 billion hours if each worker commutes alone in his or her vehicle.

A possible modification in dusk can be made by adjusting the threshold values defined in UNECE Regulation 48 for switching between low beam and daytime running lights. Currently, the low beam must be switched on at illuminance levels below 1000 lx and switched off above 7000 lx. [22]

By identifying new suitable thresholds, daytime running lights could be used for a longer period of time and energy consumption could be reduced by switching off the low beam. The actual adjustment of the light functions can be done directly via the already existing light sensor behind the windshield.

2.3 Urban night time traffic

As mentioned at the beginning of this section, the total mileage of passenger cars in Germany was about 644.8 billion km, of which about 20 % is completed during the dark hours. If it is also taken into account that about 26 % of the mileage of passenger cars is driven in urban areas [23], the total mileage for urban traffic at night is about 33.53 billion km. With the maximum average driving speed of 27.6 km h⁻¹ for major German cities (determined in Leipzig) [24], this results in a total driving time of 1.2 billion hours in urban traffic at night. This directly demonstrates the enormous potential for efficiency enhancement in this traffic situation.

Possible adjustments would again concern the low beam. For example, the intensity of the low beam could be significantly reduced due to the street lighting that already exists in urban areas (see Figure 4). At the same time, the safety when driving a vehicle must not be compromised. For example, the low beam could be reduced to a forefield lighting in order to maintain the visibility of the vehicle and the subjective safety feeling of the vehicle occupants.



Figure 4: The urban traffic area offers great potential for increasing efficiency due to existing street lighting

The adaptation of the low beam could be realized via various already existing sensors, such as GPS, the light sensor or even cameras, which are used to control ADB systems.

2.4 Traffic lights

Standstill during traffic light red phases also offers potential for increasing efficiency. Assuming a daily operating time of passenger cars in Germany of about 0.75 hours [25] and a time loss of 10 % [26] at intersections, this results in a total stationary time of about 1.3 billion hours for the 48.5 million passenger cars [27] in Germany, which is divided into 1.1 billion hours (80 %) during the day and 265.5 million hours (20 %) during the night.

Here, as in the case of congestion at night, the brake light could be dimmed, since on the one hand the traffic light itself already signals that the traffic has to stop and on the other hand the glare potential for following traffic could be reduced. During the day, the brake light function should not be modified, as the signal function must remain clearly visible here.

3. Relevance analysis of traffic situations

In the next step, the relevance of the considered traffic situations for the efficiency enhancement is analysed, based on the following comparison parameters. This includes the total annual duration in the respective traffic situation and also the adaptable lighting functions. In addition, the power consumption of the respective lighting functions for both headlights and rear lamps is taken into account. For better comparability of the traffic situations, the maximum power consumption of standard halogen tungsten lamps for the respective lighting function is considered according to UNECE Regulation 37 [28]. In addition, the effort for the realization of the adaptation is considered [28]. Table 1 shows an overview of the traffic situation with the considered parameters.

Table 1: Traffic situations and parameters for relevance analysis in terms of efficiency enhancement

Traffic Situation	Total Duration per Year	Adaptable Light Function	P_{HAL} of Light Function	Effort for Realization
Congestion day	127.6 million hours	Daytime running light (DRL)	53 W	Sensors: already present Activation: dimming electronics
Congestion night	31.9 million hours	Low beam (LB), brake lights (BL)	116 W (LB), 53 W (BL)	Sensors: already present Activation: dimming electronics
Rush hour at dusk	5.15 billion hours	Low beam (LB)	116 W	Sensors: already present Activation: on/off switching
Urban night time traffic	1.2 billion hours	Low beam (LB)	116 W	Sensors: already present Activation: dimming electronics
Traffic lights day	1.1 billion hours	None	0 W	None
Traffic lights night	265.5 million hours	Brake lights (BL)	53 W	Sensors: already present Activation: dimming electronics

It is directly evident from Table 1 that rush hour traffic at dusk has the highest efficiency enhancement potential due to the very high total usage duration, followed by urban night time traffic. On the other hand, congestion situations and traffic light red phases are less relevant. In the case of traffic lights, the reason for this is that during the long total duration of about 1.1 billion hours during the day, it is not possible to make any meaningful adjustments to the lighting function, so that no direct increase in efficiency can be achieved here.

Thus, in the near future, studies should be conducted on the switching thresholds between low beam and daytime running lights at dusk and the necessary intensities in urban traffic areas at night in order to exploit the efficiency enhancement potential.

The fact that the effort required in all traffic situations is low allows all traffic situations to make their contribution to increasing efficiency through simple adjustments.

Finally, if the maximum possible energy savings by switching off the respective light functions in the traffic situations are considered, this results in an energy savings potential of about 6.76 GWh during the day and about 5.39 GWh at night for the congestion situation. For rush hour traffic at dusk, the potential energy savings are about 597.4 GWh. For urban night time traffic, energy savings of about 139.2 GWh would be possible. Since it was not possible to identify any useful light function for efficiency enhancement in the case of traffic light red phases during the day, only the energy savings potential at night of around 14 GWh is of interest here.

4. Conclusion

Within the scope of this work, various traffic situations were selected and analysed for their efficiency enhancement potential on the basis of traffic statistics. The selection was made for congestion situations, rush hour traffic at dusk, urban night time traffic and traffic light red phases. The analysis shows that primarily rush hour traffic at dusk and urban night time traffic should be considered for further investigation. However, since all lighting function adjustments are easy to implement in the respective traffic situations, energy savings potentials of several GWh can already be realized through small adjustments.

5. References

- [1] EN ISO 14040:2021-02: "Environmental management - Life cycle assessment - Principles and framework"
- [2] EN ISO 14044:2018-05: "Environmental management - Life cycle assessment - Requirements and guidelines"
- [3] Schmidt, C., Niedling, M., Kösters, W.: "Sustainable vehicle lights", ISAL 2021, Darmstadt, Germany, 2022
- [4] Hartmann, P., Walzek, M., Gutmensch, M., Miedler, S., Riesenhuber, M.: "Headlamps as a sustainable system product", ISAL 2021, Darmstadt, Germany, 2022
- [5] Boehm, G., Hartmann, P.: "Headlamp technologies – outlook into the future", ISAL 2021, Darmstadt, Germany, 2022
- [6] Feid, T.: "Eco-Innovation with exterior lighting – Opel/Vauxhall's contribution to CO2 savings in the EU", ISAL 2021, Darmstadt, Germany, 2022
- [7] Erkan, A., Kosmas, K., Kobbert, J., Khanh, T. Q.: "Analysis of CO2 Emissions from Light Functions", ATZ worldwide, 122, 2, Springer, 2020
- [8] Bundesanstalt für Straßenwesen (BASt): "Verkehrs- und Unfalldaten - Kurzzusammenstellung der Entwicklung in Deutschland", 2021
- [9] Wördenweber, B., Lachmayer, R., Witt, U.: "Intelligente Frontbeleuchtung", ATZ, 98, 10, 1996
- [10] Kosmas, K.: "Optimierung von adaptiven Kfz-Scheinwerfertechnologien zur Blendungsbegrenzung unter dynamischen Bedingungen", Ph.D. Thesis, Technical University of Darmstadt, Darmstadt, Germany, 2019
- [11] Stamatiadis, N.; Psarianos, B.; Apostoleris, K.; Taliouras, P.: "Nighttime versus daytime horizontal curve design consistency: Issues and concerns", J. Transp. Eng. Part A Syst., 146, 3, 2020
- [12] ADAC Staibilanz 2019, <https://presse.adac.de/regionalclubs/suedbaden/adac-staibilanz-2019---191000-kilometer-stillstand.html>, accessed on: 21.09.2022
- [13] NDR: "A1 zwischen Holdorf und Neuenkirchen-Vörden gesperrt", https://www.ndr.de/nachrichten/niedersachsen/osnabrueck_emsland/A1-zwischen-Holdorf-und-Neuenkirchen-Voerden-gesperrt,aktuellosnabrueck6616.html, accessed on: 21.09.2022
- [14] Image source: Deutsche Presse-Agentur dpa/Bernd Von Jutrczenka,
- [15] Redaktionsnetzwerk Deutschland: "Datenanalyse: Autos werden nicht erst seit dem SUV-Boom größer", <https://www.rnd.de/wirtschaft/datenanalyse-autos-werden-nicht-erst-seit-dem-suv-boom-grosser-6GTM66RRNJEC7EYHR3FQS7Y24Y.html#:~:text=Die%20Auswertung%20von%20Daten%20des,sie%20auf%204%2C60%20Meter>, accessed on: 21.09.2022
- [16] Statistisches Bundesamt (destatis): "Berufspendler", <https://www.destatis.de/DE/Themen/Arbeit/Arbeitsmarkt/Erwerbstaetigkeit/Tabellen/pendler1.html>, accessed on: 21.09.2022
- [17] TOMTOM: "Germany traffic", https://www.tomtom.com/en_gb/traffic-index/germany-country-traffic/, accessed on: 21.09.2022

- [18] Tagesspiegel: "Berufsverkehr: Pendlern fehlen Parkplätze am Berliner Stadtrand",
<https://www.tagesspiegel.de/berlin/pendlern-fehlen-parkplatze-am-berliner-stadtrand-6116299.html>,
accessed on: 21.09.2022
- [19] Image source: Deutsche Presse-Agentur dpa,
https://www.tagesspiegel.de/berlin/images/heprodimagesfotos83120161128pendlerneu335120161127154847277jpg/alternates/BASE_21_9_W1000/heprodimagesfotos83120161128pendlerneu335120161127154847277jpg.jpeg, accessed on:21.09.2022
- [20] Statistisches Bundesamt (destatis):
"Erwerbstätigkeit",
https://www.destatis.de/DE/Themen/Arbeit/Arbeitsmarkt/Erwerbstaetigkeit/_inhalt.html, accessed on:
21.09.2022
- [21] Deep Sky: "Mond- und Dämmerungskalender für Deep Sky 2017–2030 Deutschland [PDF]",
<http://deepsky.square7.ch/>, accessed on:
21.09.2022
- [22] Economic Commission for Europe of the United Nations (UNECE): "Regulation No. 48 – Uniform provisions concerning the approval of vehicles with regard to the installation of lighting and light-signalling devices", 2019
- [23] Statista: "Verteilung der Fahrleistung von Kraftfahrzeugen im Straßenverkehr in Deutschland nach Ortslage",
<https://de.statista.com/statistik/daten/studie/965022/umfrage/verteilung-der-fahrleistung-von-kraftfahrzeugen-nach-ortslage-in-deutschland/>,
accessed on: 21.09.2022
- [24] Statista: "Durchschnittliche Geschwindigkeit auf Hauptverkehrsstraßen deutscher Großstädte zur Hauptverkehrszeit im Jahr 2018",
<https://de.statista.com/statistik/daten/studie/1079302/umfrage/durchschnittliche-fahrgeschwindigkeit-zur-hauptverkehrszeit-in-deutschen-grossstaedten/>,
accessed on: 21.09.2022
- [25] Bundesministerium für Verkehr und digitale Infrastruktur (BMVI): "Ergebnisbericht: Mobilität in Deutschland – MiD", 2019
- [26] Schuman, R.: "Traffic Signals Meet Big Data",
<https://inrix.com/blog/suprising-findings-from-the-inrix-signals-scorecard/>, accessed on: 21.09.2022
- [27] Umweltbundesamt: "Verkehrsinfrastruktur und Fahrzeugbestand",
<https://www.umweltbundesamt.de/daten/verkehr/verkehrsinfrastruktur-fahrzeugbestand#lange-der-verkehrswege>, accessed on: 21.09.2022
- [28] Economic Commission for Europe of the United Nations (UNECE): "Regulation No. 37 – Uniform provisions concerning the approval of filament lamps for use in approved lamp units of power-driven vehicles and of their trailers", 2015

INNOVATIVE CONCEPTS AND COMPLEMENTARY FEATURES

Challenges for DRIVER ASSISTANCE PROJECTIONS

Philipp Roeckl

Stellantis

Tech Center Central Europe
Bahnhofsplatz 1
65423 Rüsselsheim am Main

Abstract: With new light-source technologies, which allow to project shapes and symbols on the street surface, the automotive lighting industry is facing new opportunities, but also must solve associated challenges. Beside the decision on the most efficient light source technology, the definition of useful features and the development of functional architectures, but also the impact on other vehicle systems has to be evaluated. This study shall provide an insight into the realization of driver assistance projections and its implications.

Keywords: Driver Assistance Projection, Light Source, MicroLED, Camera impact, User Experience, ADB, Front Lighting

1. Introduction

The lighting subsystem is part of a complex system which handles the environment recognition, the processing and transfer to other components. All internal and external HMI formats like Head Up Display also have to be involved into the ideation on what and how to display information to the driver

2. Main investigations

2.1 Decision on a High-Definition (HD) light source

The decision on a light source technology is a company and feature individual one. The following decision should not be taken as a general reference.

Lightsources:

- DMD
- MicroLED
- LCD

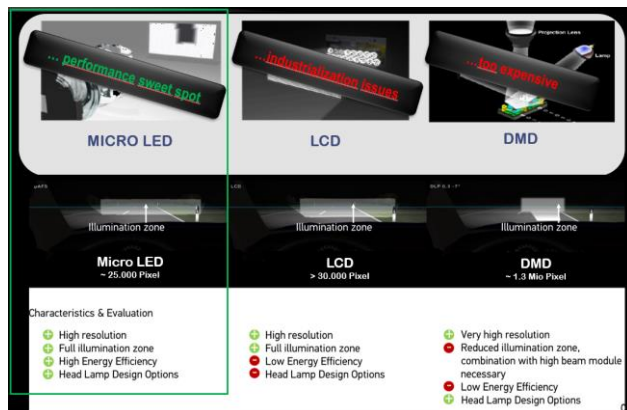


Figure 1: Decision Matrix for HD Lightsource

2.2 Driver Assistance Projection Features

Many features or use-cases can be covered by HD lighting systems. The following tables 1 and 2 list a pool of potential features:

Use case	Benefit	Example
Dynamic Guiding lines	Improve safety and comfort Reduce control corrections	
Lane keep assist	Visual support of LKA Shorter response time	
Warning Symbols	Direct warning Shorter response time compared to HuD	
Directional object detection	driver warning	
HD animation	Customer excitement	

Use-case	Benefit	example
Adaptive Distance Indication with ACC active	Avoid unwanted ACC braking, in case of overtaking event	
Maneuvering Light (Flash HD Projection)	Visual warning while parking In a noisy environment, the driver can detect a close approach through the visual projection.	
Speed indicator	Indicates "above or below" recommended Speed	
DIRECTIONAL: Bad road structured light	Predictive driver warning	
Crosswalk projection	Outboard communication	

Figure 2: Potential Features for Driver Assistance Projection

2.3 Required Resolution for Symbols

The resolution of a HD Lighting System will set the borders for executing use-cases. boundary conditions to execute the usecases. The minimum resolution for graphical content like symbols has been specified at 0.1°

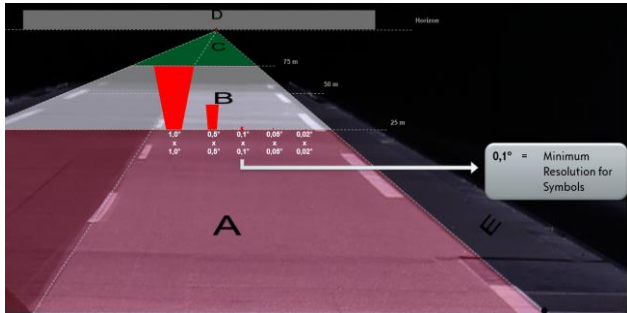


Figure 3: Pixel-Resolution on street surface

2.4 Interaction with Head Up Displays (HUD)

The information for the driver to perceive is currently limited to interior HMI systems. Driver assistance projections are the first step to visualize information outside the vehicle, but addressed only to the driver. The virtual projection plain of the HUD appears withinis at the driver's field of view outside of the vehicle and must be considered during the definition phase of where and how to visualize external content by headlights.

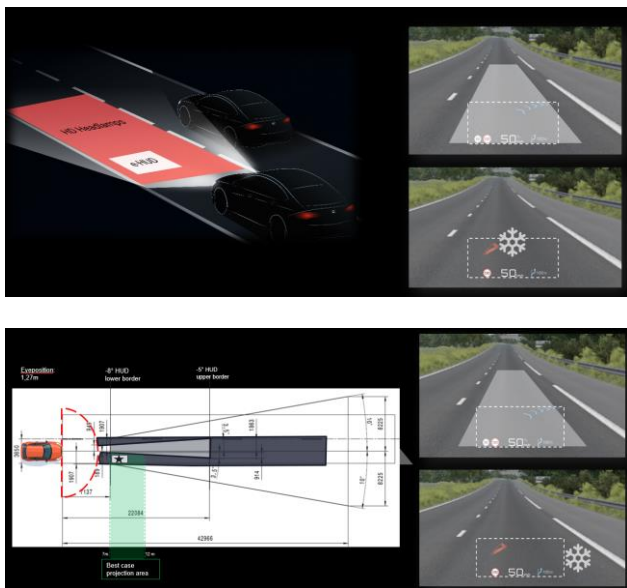


Figure 4: Area of HUD vs. area of Driver Assistance Projections

2.5 Virtual Design of shapes vs. Reality

Today all feature designs are made in a virtual environment. To handle the various shape definitions and to ease the assessment of such, the patterns to be shown to the driver were implemented into the lighting system and reviewed on real roads. The figure below shows disadvantageous optical effects which were taken into account for the shape selection:

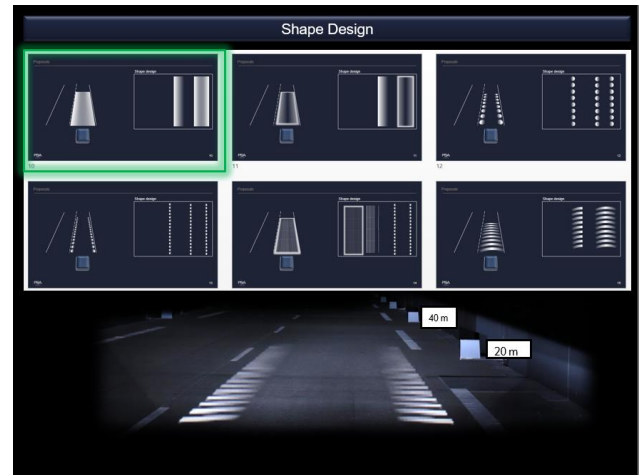


Figure 5: Optical effects in case of too complex shapes according to available resolution

2.6 Orientation of graphical content

The interaction with HUD has already be mentioned in chapter 2.4. Also the perspective orientation of symbols were reviewed during the development phase. In the figures below the different positions and different projection plains are visualized:

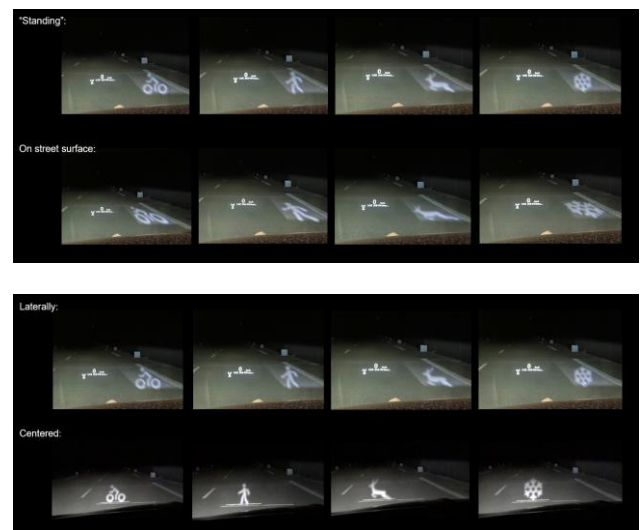


Figure 6: Position and orientation of projected symbols

2.7 Disturbance of other traffic participants

Driver Assistance Projections are intended for the driver to be seen, but every projection outside the vehicle can be recognized by other traffic participants as well. Scientific studies performed by Technical University of Darmstadt showed, that other traffic participant are not disturbed by those projections. They are visible, but not recognizable. Studies which were done during this development phase support the results of former study results.

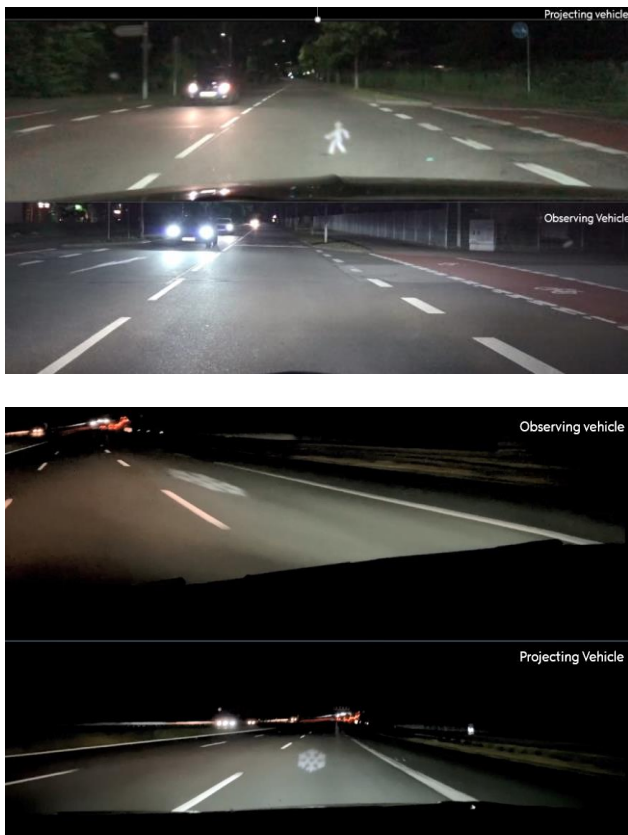


Figure 7: Visibility of Symbols by other traffic participants

2.8 Impact on Camera based ADAS features

All projections made realized with a light projection in the wavelength of, the human visible light, are also visible for the camera. In order to avoid a disturbance of any ADAS feature like lane keep assist, emergency brake, traffic sign recognition, and many more, it is necessary to develop in cooperation with industry partners a method to avoid any misinterpretation by camera-algorithms during the time of driver assistance projection. Many good technical solutions have been identified, nevertheless, this field of technology is new for standard recognition algorithms

and must algorithms have to be adapted and trained properly.



Figure 8: Camera recognized shapes of projecting headlights

3. Conclusion

Summarizing all activities during this advanced development the results of clinics show the wish of customers to equip vehicles with advanced lighting systems including Driver Assistance Projections. But with so many interactors the development must not run only at lighting systems. The complete vehicle and customer experience bandwidth has to be taken into account to create real night drive safety benefits. The regulation is proceeding and should give the car manufactures the freedom to introduce those safety features

8. Glossary

PDF: Portable Document Format

Intelligent Speed Assist for EU GSR: New cloud-based approach and key findings

A. Garnault¹, B. Bradaï¹, T. Heitzmann², F. Lejay³, S. Hannachi¹,
J. Schüttemeyer⁴, J. Landvogt⁴

1: Valeo, 6 rue Daniel Costantini 94046 Créteil Cedex - FRANCE

2: Valeo, 2121 S. El Camino Real, Building D, Suite 100, San Mateo, CA 94403 USA

3: Valeo, Max-Planck-Straße 28-32 61381 Friedrichsdorf - GERMANY

4: HERE Technologies, Invalidenstraße 116, 10115 Berlin, GERMANY

Abstract: The new General Safety Regulation “GSR2” is becoming mandatory in Europe for new vehicles. This requires a quick and affordable solution to adapt current vehicle architectures and to meet requirements for the correct determination of road speed limit. In this paper, we will present a disruptive system architecture performing a data fusion process between the camera and a map hosted in the cloud, using a telematics control unit as cellular data network access point. Results of the system evaluation after 400km real test drives as per the regulation in a variety of road conditions are analysed and key findings are presented.

Keywords: ADAS, ISA, Connected Services, Map, Regulation

1. Introduction

In the frame of the General Safety Regulation (GSR) for motor vehicles, the European Union has mandated that all new cars, vans, lorries and buses should be fitted with Intelligent Speed Assist (ISA) as standard starting in 2022.

The required Intelligent Speed Assistance system needs to provide both - explicit and implicit - speed limits and solve the “applicability problem” to display the accurate speed limit to the driver.

While cameras can detect explicit signs (with numerical value) quite well, but have limitations for implicit signs (without numerical value or strike through numerical value), and maps may face some data freshness limitations, a fusion between both will determine a more accurate speed limit.

Classically, an on-board map requires an on-board navigation system, which can be costly for an entry-level vehicle, and may not satisfy the regulatory requirements over the years as maps will age over time.

We propose a new cost-effective solution able to fulfil the requirements, with very limited impact on vehicle architectures, benefitting from the spread of connectivity in vehicles to make best use of both fresh and complementary data sources.



Figure 1: Explicit (left) and implicit (right) speed signs

GSR2 - ISA Regulation Targets :

The new General Safety Regulation “GSR2” Intelligent Speed Assist “ISA” will become mandatory on July 06, 2022 for new types of vehicles and on July-06, 2024 for all cars produced.

The system shall provide the current applicable speed limit information to the driver and either

- alert to the driver in case of overspeeding based on haptic, acoustic or visual feedback (Speed Limit Warning function) or
- connect the ISA system to the vehicle (Adaptive) Cruise Control or Speed Limiter to provide a speed limit set point for control functions (Speed Limit Control function)
- at least 15% of the test shall be performed in darkness conditions

The system’s compliance to the ISA regulation shall be tested on real world driving conditions, out of a 400 km test drive which shall consist of one consecutive route with the same start and end point, where any repeated parts of the route in the same direction shall not count towards the test distance.

The ISA regulation is requesting the system shall be able to provide correct speed limit:

- for 90% of the test distance
- for at least 80% of the distance driven on each of the three defined road types : urban roads and streets, non-urban roads, and motorways - for which each type shall account for at least 25% of the total test distance

The system shall also determine the applicable speed limit at the latest 2 seconds after the reference point the motor vehicle passes the road sign and at the latest 10 m rearward for speeds below 20 km/h.

The system's performance shall be reliable - with regards to performance targets - for 14 years after date of manufacture.
In case of usage of map data, the map shall be updated annually for at least 14 years after date of manufacture (where 7 years are free of charge).

This test drive success and Proof of conformity for all EU27 countries shall be provided for homologation of vehicles.

2. System Design

2.1 In-vehicle System

We propose a new cost effective solution able to fulfil the requirements, with very limited impact on vehicle architectures, benefitting from the spread of connectivity in vehicles to make best use of both fresh and complementary data sources.

Classically, vehicles equipped with systems determining the applicable speed limit rely on an embedded map and navigation system, which can be costly equipment for entry-level vehicles, and a front camera system.

Most new vehicles are also equipped with front camera systems for Advanced Driving Assistance Systems such as Front Collision Warning and Lane Departure Warning, becoming standard equipment.

Our solution also benefits from the spread of Telecommunication Control Units (TCU) in nowadays cars, due to the regulation introducing eCall systems in vehicles in the EU, requiring geolocalization and cellular connectivity capabilities in the vehicle.

The Front Camera system and the Telecommunication Control Unit being already widespread in vehicles, we propose to implement an Intelligent Speed Assist using only these elements, without the need for an in-vehicle navigation system and embedded map, therefore reducing the cost of the solution, and using instead the Speed Limit Online Client developed by HERE Technologies for delivering the map data information to the Fusion System “on the fly”.

This ensures compliance with the regulations with regards to performance and reliability of the solution, since the HERE Technologies maps are stored on a cloud server and being updated regularly. Therefore they are able to track long term infrastructure change in speed limit, and dynamic speed limit changes such as road works with the camera based speed sign detection system.

This evolution in the vehicle architecture is reflected from the former in Figure 2, to its connected evolution in Figure 3.

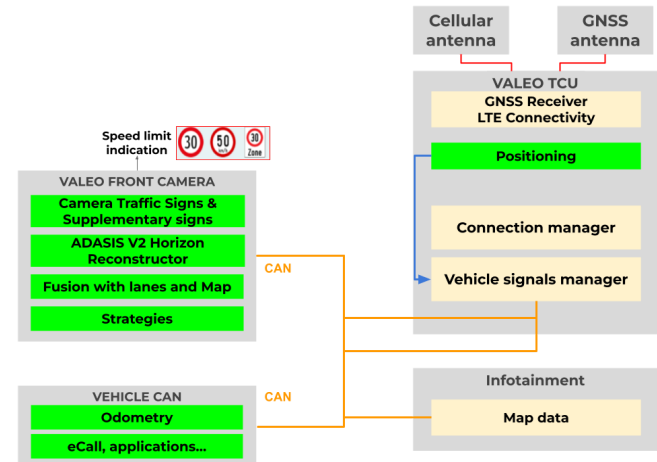


Figure 2: System with on-board map

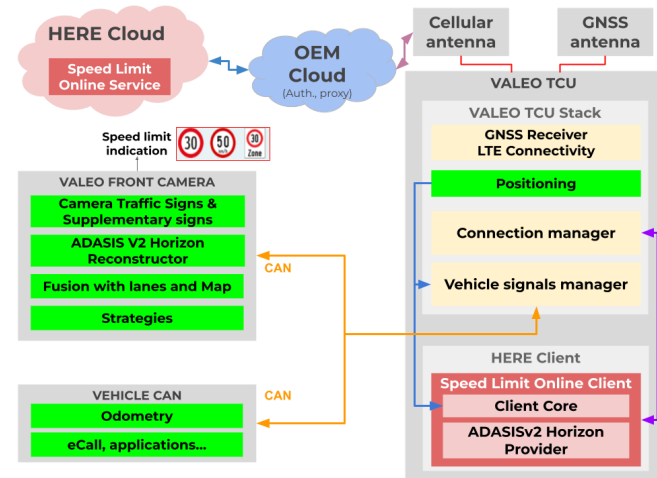


Figure 3: Targeted system with Cloud map

2.2 HERE Backend Server and Vehicle Client

The HERE Backend Server in the Cloud provides the necessary map information to the vehicles. This is mainly the geometry of the roads and attributes like Speed Limits (incl. implicit Speed Limits), side of driving, country-specific regulations etc.

The vehicle is sending its last positions to the HERE Backend Server and the server calculates a simplified map cache in front of the vehicle - individually for the received position traces. This cache has determined the most probable path and side paths, the road

geometry and assigned attributes. This cache can be seen as a simplified map – but requires a much lower data volume than a full map which is consumed for e.g. navigation use cases.

This cache is downloaded to the vehicle and cached. While the vehicle is driving, the position of the vehicle is matched against this cache – and the necessary speed limit information is provided to the ISA fusion system, residing in the vehicle. When the vehicle is approaching the end of the cache a new request to the HERE backend server refreshes the cache data.

This has multiple advantages:

1. The request intervals and packet sizes are quite low
2. Network connectivity gaps can be bridged by consuming data from the cache– if the gap is not exceeding the length of the cached track information
3. At any point in time the data fetched from the HERE Backend is the freshest data available as the HERE backend is holding the most up-to-date speed-limit data available. In contrast, a compiled map for e.g. navigation systems tends to age and can represent data which is some years old. Assuming an average change-rate of relevant speed limit data of around 10% every year, ageing of data is a substantial factor, degrading the overall ISA quality of such systems over time.

2.3 Front Camera Fusion System

Even with the freshest map data stored on the Backend, there is a risk of reality changing faster than the update process for the Backend Map Data. Thus, the information on speed limitation provided by the navigation system is relevant but does not guarantee perfect accuracy in all situations. As an example, temporary road works may affect the speed limitation on a road segment in an ad hoc fashion and leave the Backend data lagging behind reality.

Therefore, a fusion of map data with camera based evidence is imperative to cover all possible situations that might occur on the road. By combining information from vision and navigation, the system takes advantage of both local interpretation of the camera and the global information of the road segment provided by the electronic horizon from the navigation system. Many alternatives may be used for multisensor data. The most commonly used in ISA is the decision-level fusion illustrated in Figure 4.

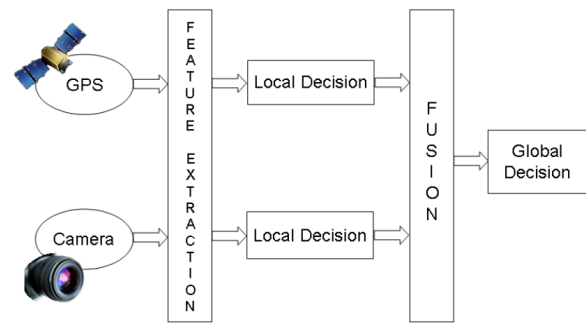


Figure 4 : Fusion system input diagram

In the initial framework, described in [1], the input data of the navigation-based system is an electronic horizon of 300 meters determined by a Most Probable Path algorithm. It is combined with the detected speed signs from the camera-based system in order to determine the most accurate speed limitation. This is achieved through the use of the Dempster-Shafer evidence theory for multi-sensor information data fusion [2][3].

This Front Camera detection and Fusion system - using an on-board map - has been in mass production since 2015, validated in 28 EU countries, more than 110 000 km cumulated.

3. System Implementation

3.1 Prototype System Architecture

The system described has been implemented in the form of a Proof of Concept, representative of the final product, demonstrating the feasibility and the performance of this system. Its architecture is depicted in Figure 5.

This system is composed of :

- HERE Technologies Cloud server
- Valeo Telecommunication Control unit, with :
 - Cellular connectivity
 - GNSS receiver
- Valeo Front Camera, embedding :
 - Sign detection system
 - Speed Limit Fusion System
- Automotive PC :
 - System supervision
 - Recording
 - HMI
 - Ground Truth annotation system
 - HERE Technologies' Speed Limit Online Client

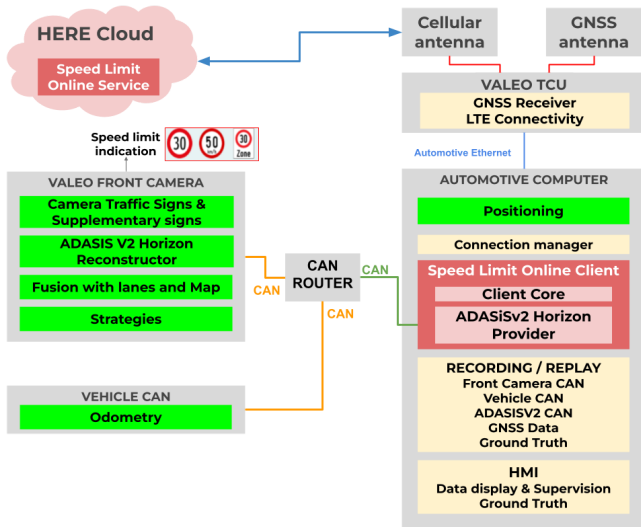


Figure 5: Proof of Concept implementation

The Speed Limit Online Client application is embedded in the Telecommunication Control Unit. It gets localization data and sends it to the HERE Cloud server, performing the map matching and returning map data to the TCU. There it gets translated into an electronic horizon in ADASISv2 CAN Bus frames data format.

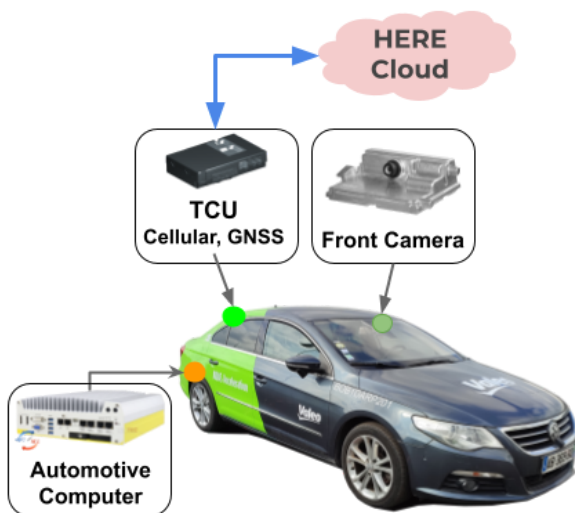


Figure 6: Test vehicle equipment

3.2 Test Drive

A test drive was performed with this system to capture data in real conditions with the vehicle and its equipment described in Figure 6, as per the test conditions given by the regulation, in this case :

- 402 km total driven distance as a loop
 - 104 km - 26.2 % - on Urban roads
 - 145 km - 36.4 % - on Non Urban roads
 - 149 km - 37.4 % - on Motorways

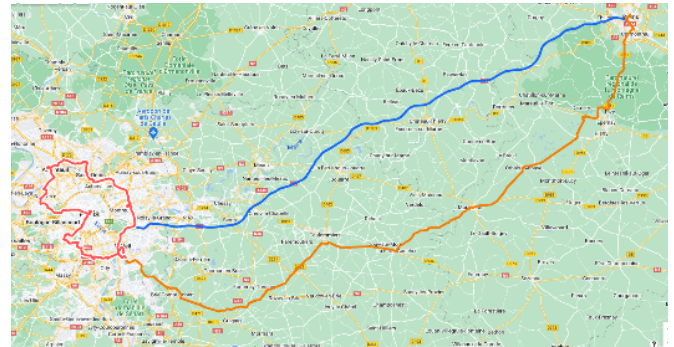


Figure 7: Greater Paris area and round trip to Reims

The above figure shows the 400 km test drive route, and the main road types :

- Red : Urban
- Orange : Non-Urban
- Blue : Motorway

The Ground Truth for the road type and the speed limit has been established manually.

All the sensor data of the system has been recorded, for detailed measurements capability, and to enable data replay to measure the impact of different system configurations.

4. Results

4.1 Connectivity

Since the system relies on downloading map data from a cloud server, handling the data and connectivity is a key aspect, considering there is no full coverage of cellular connectivity as of today.

During the test drive, the connectivity was tested with a cyclic HTTPS GET request to a remote server. This setup represents the requests and payload transmitted with the end solution. The test is considered to be failed if the system doesn't receive any answer before a defined timeout.

During this test drive, the non-connected areas, also called white zones, represented 32.6% of the total

drive. The white zones represent about 47.5% of the non-urban roads in the data collection, while they reach 28% on motorways and remain below 18% in urban areas.

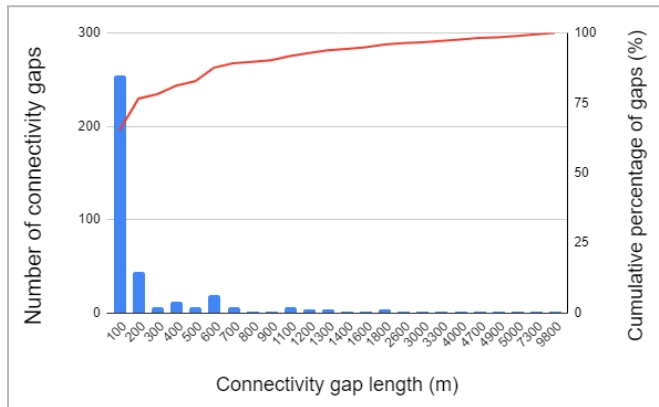


Figure 8: Connectivity gaps

These measurements show that :

- 80% of the connectivity gaps are less than 300m
- 97% of the connectivity gaps are less than 3000m

Based on these measurements, it is possible to select the minimum electronic horizon length (minimising required data transfer volume) to cover most of the connectivity gaps, without compromising the availability of map data from the server, and therefore the Intelligent Speed Assist system performance.

4.2 System performance

The performance analysis has been performed comparing the output of the Speed Limit Fusion System with the Ground Truth data.

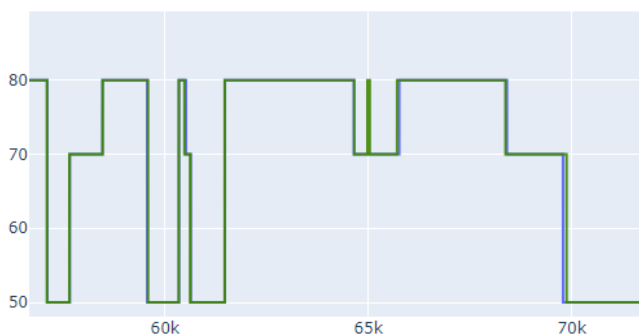


Figure 9: Detailed analysis of the ISA system performance (Green) against Ground Truth (Blue)

The figure above illustrates the detailed system performance, showing in green the ISA system speed limit determination and in blue the ground truth speed limit (y-axis : speed limit in kilometers per hour) over

the travelled distance (x-axis in meters).

A perfect overlapping of the two signals indicates that the system output matches the ground truth speed limit data.

This analysis shows this proof of concept evaluation is able to meet the regulatory requirements :

- for the total distance driven
- for the distance driven on each type of roads

According to the above connectivity analysis, the electronic horizon length has been set to 3000 meters in order to cover most of the white zones, while keeping the payload and CAN bus load acceptable.

To illustrate the need for such a length of electronic horizon length, in terms of performance, a simulation of the system showed that setting the electronic horizon length to 300 meters negatively impacts the system performance by 17%.

The system performance was evaluated providing perfect connectivity, simulating a full cellular coverage. The evaluation showed that the system performance only improved by 1.6% in these conditions.

The additional CAN bus load related to the increase of the electronic horizon length from 300 meters to 3000 meters would only add 6% of traffic for this electronic horizon data.

This confirms the assumption for using a 3000 meters length electronic horizon delivering a good performance while keeping a low bandwidth usage.

5. Conclusion

These results validate the proof of concept to meet the GSR ISA requirements, and are aligned with the expectations, especially comparing with the performance of the previously developed mass production system using an on-board map.

No regression of the system performance was observed while estimating the performance for this "snapshot" evaluation.

It is important to keep in mind that long term analysis of the speed limits change at a rate of approximately 8%-10% per year, therefore decreasing the performance of the system over time when it's not being updated.

Our solution answers this question providing fresh map data, and ensuring regulatory compliance over the years.

6. Acknowledgement

The authors would like to thank their colleagues from HERE Technologies and Valeo for their contribution to this work.

7. References

- [1] A-S. Puthon, F. Nashashibi, B. Bradai "Improvement of multisensor fusion in speed limit determination by quantifying navigation reliability", IEEE Intelligent Transportation Systems (ITSC), 2010
- [2] A. Dempster, "Upper and Lower Probabilities Induced by a Multivalued Mapping," Classic Works of the Dempster-Shafer Theory of Belief Functions, pp. 57–72, 1967.
- [3] G. Shafer, A Mathematical Theory of Evidence. Princeton university Press Princeton, NJ, 1976.

8. Glossary

GSR: General Safety Regulation

ISA: Intelligent Speed Assist

TCU: Telecommunications Control Unit

CAN: Controller Area Network

Reconstruction and mapping of the road profile from on-board sensors

R. GURIDIS^{1,2,3}, G. POINT¹, V. HERNETTE¹, G. BEL HAJ FREJ^{1,3}, X. MOREAU^{2,3}, and A. BENINE-NETO^{2,3}

¹Stellantis, Route de Gisy, Centre Technique de Vélizy, 78140 Vélizy-Villacoublay, France

²IMS, Univ. Bordeaux, CNRS, Bordeaux INP, 351 cours de la libération, 33405 Talence CEDEX, France

³OpenLab Stellantis-IMS-SANPSY "Electronics and Systems for Automotive", France

Abstract—In this paper a comparative study between two methods for road monitoring is presented. The first one describes a road monitoring technique for reconstructing the road elevation. It is exclusively based on information from on-board sensors used for the control law of the semi-active suspension installed in cars from the group Stellantis. The reconstructor is designed in the frequency domain using a model-based design method with a closed-loop structure and a loop shaping technique inspired by the second-generation CRONE control law. The second method is based on sensor fusion between a body-mounted GNSS hybrid inertial navigation system and series suspension deflection sensors mounted on each suspension arm of the car. These sensors provide the coordinates of four contact points between the car and the road in the car body frame, while the former gives the absolute precise positioning of the car body. By combining data, it becomes possible to build a georeferenced map of the road geometry. Taking advantage of the interest shown by the automotive manufacturers in connectivity, these methods can be applied to form a database that allows the concerned institutions to have real-time informations on the state of the road, thus carry out the necessary actions to maintain the good condition of road infrastructures and consequently to improve traffic safety.

Keywords: Road Monitoring, Model based, Frequency domain, Global positioning, Inertial navigation system

1. Introduction

Connectivity has become a key focus on automotive industry since a few years. It is currently common to use this system for preventive maintenance of vehicles, obtaining information on traffic status or information purposes. Moreover, sensors used for active safety and automation of certain driving tasks have also proliferated [1], as reflected in the increase in cars equipped with Advanced Driver Assistance System (ADAS).

The idea of combining the connectivity of cars with ADAS technology for road monitoring is interesting, since both technologies are featured in new cars and their implementation would not require a significant investment in equipment by manufacturers.

In this way, the information of the road condition collected by each vehicle through the ADAS systems could be available to cars equipped with active or

semi-active suspensions to improve safety and comfort. This information could also be useful for the services in charge of road maintenance to carry out preventive maintenance. Another application could be the use of a comfort criterion in trajectory calculation applications to offer less bumpy routes.

Considering the potential of road monitoring several works have been carried out on this subject. The state of the art [2] compiles the techniques developed in the last two decades for road monitoring based on proprioceptive sensors which equipped the commercialised vehicles. The road profile estimate can be understood as an unknown input estimate. According to authors the techniques used for profile estimation can be classified into three groups: derivations of the Kalman filter [3], machine learning techniques [4] and techniques in the frequency domain [5]. Other techniques also used for the estimation of unknown inputs are those related to the inversion of the model. In [6] a comparison between methods based on sliding modes and inverse model is performed.

This paper presents a comparison between two methods for estimating the profile of the road. The first uses an inverse-model approach developed in the frequency domain, through a loop-shaping technique inspired by the second-generation of the CRONE control law [7]. The second method uses suspension deflection measurements from a well-calibrated sensor, combined with measurements from a very accurate GNSS GPS sensor to create a georeferenced map of the road profile. Unlike other works [8] where GPS measurements are mainly used to determine the longitudinal and lateral position of the obstacles (potholes, speed-bumps, etc.), in the proposed work the vertical coordinate is used to determine the absolute height and thus have a reference point.

The remainder of this work is organized as follows. Section 2 presents the method for the road profile input reconstruction (RIR), including the model used and the results obtained. Section 3 describes the method for georeferenced road monitoring (GRM), the equipment used and the results obtained. Finally conclusions are given in the section 4.

2. Road input reconstructor

2.1 Model

This section shows the model used for the synthesis of the road profile reconstructor. Knowing that in the prototype car (Figure 1) used for the validation of the reconstructor, the sensors are located on the axle of the suspension column, the reconstruction of the road profile input can be carried out taking into account only the dynamics of the quarters of the car. In this way, the estimation of the road profile is achieved locally, without need of modal center variables. The key idea is that the tires act as independent probes, thus obtaining four simultaneous input reconstructions.



Fig. 1: DS Automobiles DS7 prototype car on the four-post test rig

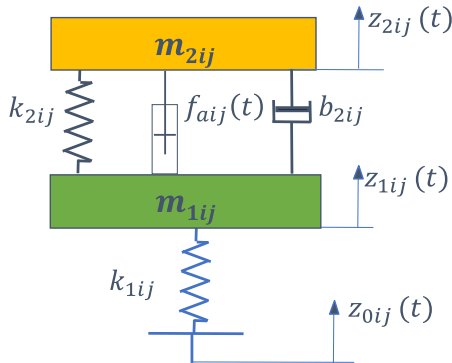


Fig. 2: Two DoF quarter car model

Figure 2 shows a schematic of the quarter-vehicle model with 2 degrees of freedom (DoF). sub-index $i \in [f, r]$ indicates front or rear axle and sub-index $j \in [l, r]$ indicates left or right side respectively. z_{2ij} and z_{1ij} are the vertical displacements of the sprung m_{2ij} and unsprung m_{1ij} masses respectively. k_{1ij} and k_{2ij} represent the stiffness of the tires and suspensions. f_{aij} is the force exerted by the semi-active suspension. The dynamics of this model are described in [9].

Since the proposed method for the reconstruction of the road profile input is carried out in the frequency domain, it is necessary to perform the Laplace transform of the model. Assuming that the model is linear and that the initial conditions are null, taking the road elevation as input and the suspension deflection ($z_{21}(t) = z_2(t) - z_1(t)$) as output the corresponding transfer function $G(s) = Z_{21}(s)/Z_0(s)$ for any suspension arm (the indexes are omitted for sake of simplicity) is:

$$G(s) = \frac{k_1 m_2 s^2}{((\frac{s}{\omega_{n1}})^2 + \frac{2\zeta_1 s}{\omega_{n1}} + 1)((\frac{s}{\omega_{n2}})^2 + \frac{2\zeta_2 s}{\omega_{n2}} + 1)}, \quad (1)$$

where:

$$\omega_2 = \frac{k_2}{b_2}, \quad \omega_{n1} = \sqrt{\frac{k_1}{m_1}}, \quad \omega_{n2} = \sqrt{\frac{k_2}{m_2}}, \quad (2)$$

$$\zeta_1 = \frac{b_2}{2\sqrt{k_1 m_1}} \text{ and } \zeta_2 = \frac{b_2}{2\sqrt{k_2 m_2}}.$$

Note that $\omega_{n1} \gg \omega_{n2}$. Numerical values of the parameters are provided in Table I

Knowing that the force of the semi-active suspension is managed by the control law, it is assumed that the semi-active suspension input is perfectly known, thus it is not taken in account as an input to be reconstructed. From the parameters in table I, figure 3 shows the frequency response of (1). Figure 3 show the frequency response of 1. The modes of the sprung and unsprung masses are clearly distinguished. The dynamics of front axle suspension columns are very similar so they will be considered identical for the rest of this section. It is the same for the rear axle.

Variable	Value	Description
ω_{2fl}	19.05 rad/s	Transitional frequency
ω_{2fr}	22.05 rad/s	
ω_{2rl}	23.64 rad/s	
ω_{2rr}	23.64 rad/s	
ω_{n1fl}	67.59 rad/s	Unsprung mass natural frequency
ω_{n1fr}	67.59 rad/s	
ω_{n1rl}	71.91 rad/s	
ω_{n1rr}	72.17 rad/s	
ω_{n2fl}	6.74 rad/s	Sprung mass natural frequency
ω_{n2fr}	6.92 rad/s	
ω_{n2rl}	8.82 rad/s	
ω_{n2rr}	8.52 rad/s	
ζ_{1fl}	0.15	Unsprung mass damping coefficient
ζ_{1fr}	0.13	
ζ_{1rl}	0.15	
ζ_{1rr}	0.15	
ζ_{2fl}	0.18	Sprung mass damping coefficient
ζ_{2fr}	0.16	
ζ_{2rl}	0.19	
ζ_{2rr}	0.18	

TABLE I: Values of $G(s)$ parameters

2.2 Reconstructor

Any road profile input reconstructor must guarantee:

- A good response speed
- A transient regime without oscillations
- A zero error in steady state

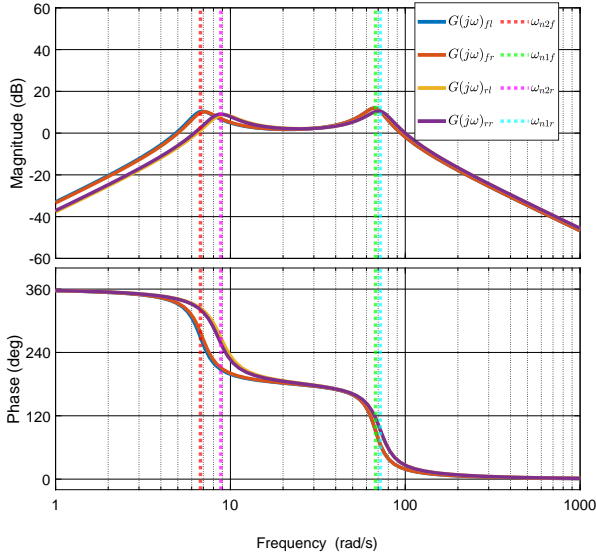


Fig. 3: Bode plot of $G(j\omega)$

- A sensitivity to noise of the sensors as low as possible

Due to the similarities in the frequency response of the front and rear axles (see Figure 3), the method presented further is developed only for the front left quart of the car and the result obtained is applied to the rest of the car suspensions. The structure of the reconstructor (Figure 4) can be divided into two parts: the measurement generator (blue part) and the measurement reconstructor (orange part). The measurement generator is used to obtain measurements from the vehicle's proprioceptive sensors. These measures are derived from the vehicle's sensors (Figure 4a) or from a simulation environment (figure 4b).

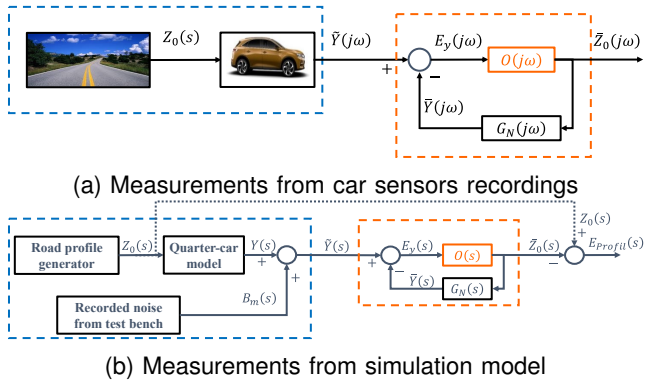


Fig. 4: Reconstructor structure. Blue dotted line: measurements generator. Orange dotted line: Road profile input reconstructor

For the design of the reconstructor, the scheme of Figure 4b is used. This allows to analyze the reconstruction quality and the influence of sensor noise independently. To analyze the reconstruction error $E(s)$ during the method development process, it has been assumed that the road elevation is known.

This assumption is reflected by the gray dashed line in Figure 4b. Taking this assumptions into account, the error expression is

$$E(s) = Z_0 - \bar{Z}_0(s). \quad (3)$$

In Figure 4b, $Y(s)$ represents the quarter-car model output, $B_m(s)$ the sensor noise, $\tilde{Y}(s)$ the model output with added noise, $\bar{Y}(s)$ the estimated reconstructor output, $E_y(s)$ the error between the model output and the reconstructor output and $\bar{Z}_0(s)$ denotes the reconstruction of the road profile input. $G_N(s)$ the transfer function of the nominal model and $O(s)$ the transfer function which allows adjustments to the reconstructor. From Figure 4b we obtain :

$$E(s) = S(s)Z_0(s) - R(s)B_m(s), \quad (4)$$

where:

$$S(s) = \frac{1}{1 + \beta(s)}, \quad R(s) = S(s)O(s) \quad (5)$$

and (5) $\beta(s)$ is the open loop transfer function defined by :

$$\beta(s) = G_N(s)O(s). \quad (6)$$

The reconstructor described in this paper is designed with a model-based frequency domain approach, applying the Loop-Shaping technique inspired from the second-generation CRONE control law [7]. To achieve the time domain specifications, the reconstructor must be sufficiently fast to ensure good tracking of road elevation ($S(s) \rightarrow 0$) and at the same time, filter the measurement generator output to reduce the error relate to the sensor noise ($R(s) \rightarrow 0$). To reach these objectives, the open-loop transfer $\beta(s)$ must be shaped such that the closed-loop transfer function between road elevation input and the reconstructed profile defined by:

$$T(s) = \frac{\bar{Z}_0(s)}{Z_0(s)} = \frac{\beta(s)}{1 + \beta(s)}, \quad (7)$$

behaves as a low-pass filter of the road profile. In order to achieve this, the transfer $\beta(s)$ should have an integrator shape, whose expression is described in [7].

To reach the time domain constraints, the loop shaping technique developed in the frequency domain [7] leads to the following expression of $\beta(j\omega)$:

$$\beta(j\omega) = \frac{\beta_0}{(j\omega/\omega_l)(1 + j\omega/\omega_h)}, \quad (8)$$

with

$$\beta_0 = \frac{\omega_u}{\omega_l} \sqrt{1 + (\omega_u/\omega_h)^2},$$

where ω_l is the low transitional frequency, ω_h the high transitional frequency and ω_u is the bandwidth of the reconstructor.

Equation (8) allows to adjust the reconstructor in terms of rapidity and stability. The rapidity can be ad-

justed through the value of ω_u , which must be chosen taking into account the trade-off between rapidity and filtering capacity. By introducing a scaling variable μ such that $\mu \gg 1$, then $\omega_u = \mu \omega_{n1}$. If the value of μ is low, the filtering capacity is improved but some of the useful information is filtered out. If μ increases, the speed and thus the accuracy of the reconstructor improves, but filtering capacity is lost. Stability is linked to the gap between ω_l and ω_h . If the gap is small, the risk of oscillations in the transient regime increases; on the other hand, if the gap becomes too large, especially if ω_l is very low, there is a risk of attenuating part of the information coming from the output of the measurement generator.

Another scaling factor a is thus introduced, such that $\omega_l = \omega_u/a$, $\omega_h = a\omega_u$ and $a \geq 10$. It can be said that the rapidity and stability can be adjusted by a convenient setting of μ and a respectively.

2.3 Frequency analysis

This subsection illustrates the frequency response of the development presented in the previous subsection. The results showed in Figure 5 are obtained by setting: $\mu = 6$ and $a = 10$ empirically.

Figure 5 shows the frequency response of the closed-loop functional equations (5) and (7). By applying the final value theorem [7] and by taking a look to the plot of $S(j\omega)$ it can be assured that in stationary regime the error linked to the dynamics of the reconstructor is null. On the other hand, the trace of $R(j\omega)$ indicates that the reconstructor is extremely sensitive to sensor noise. This suggests that the quality of the road profile input reconstruction will be highly dependent on the quality of the sensors.

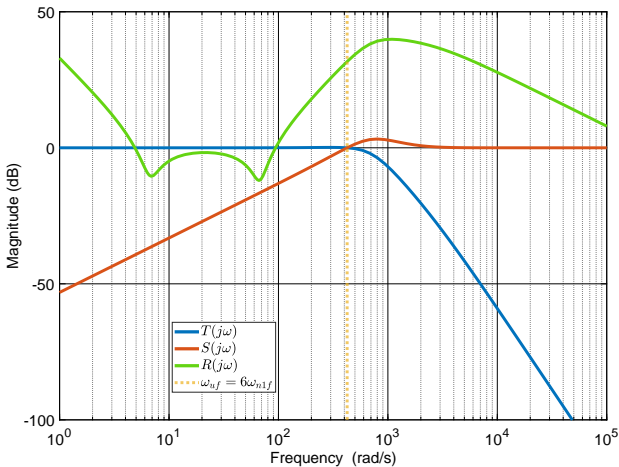


Fig. 5: Frequency response of close loop functional transfers

Finally the plot of $T(j\omega)$ shows that the dynamics of the reconstructor is similar to a low-pass filter, so that at low frequencies ($\omega \ll \omega_u$) it copies the roadway profile and at high frequencies ($\omega \gg \omega_u$) attenuates

the information. Therefore, it is possible to filter the disturbances in the high frequency without degrading the information of the signals around the interval of the frequencies of interest $[\omega_{n2} : \omega_{n1}]$.

2.4 Reconstructor results

This section shows the results of the RIR in the time domain. These results have been obtained in a simulation environment, using the structure shown in Figure 4b.

The profile shown in Figure 6 has been used as input. To show the impact of sensor noise, we have added recordings of the vehicle's sensor signal when the vehicle is on the test bench without any disturbance or perturbation.

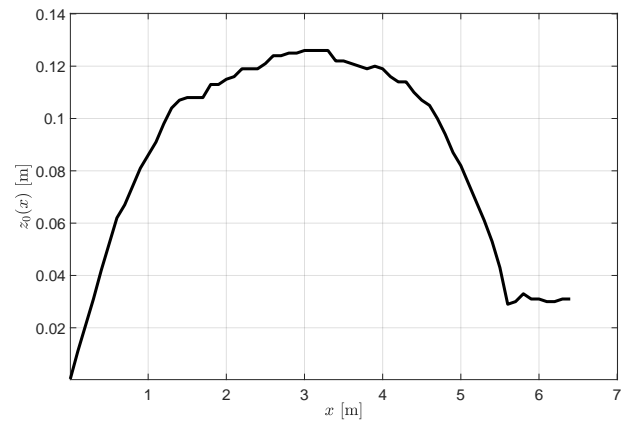


Fig. 6: Reference road profile

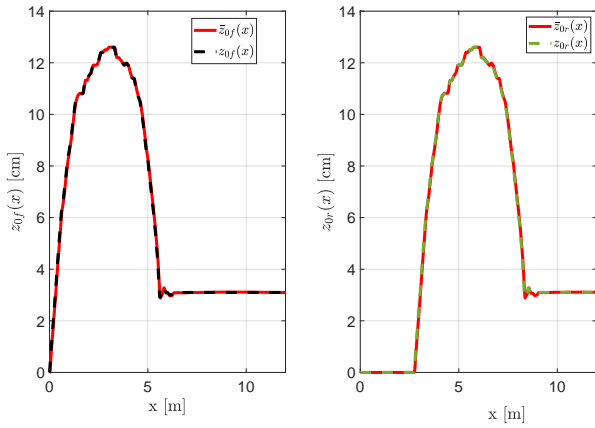
Figure 7a shows the reconstruction result (red line) without added noise superimposed on the reference profile (black dotted line). As can be seen the reconstruction result is satisfactory, the apparent error (Figure 8a) is linked to the reconstruction dynamics and comes from the delay of the reconstructor due to its similarity to a low-pass filter. To completely eliminate this error, the reconstructor bandwidth (ω_u) should be infinite, otherwise, the reconstructor would lose its filtering capacity.

Figure 7b shows the result with added sensor noise. As predicted in the frequency results, the noise at low frequencies is amplified. Despite degrading the RIR accuracy, the results obtained are still satisfactory. The reconstruction error in Figure 8b illustrates this phenomenon. In the case when the noise signal value is a non zero constant, integration drift phenomenon appears.

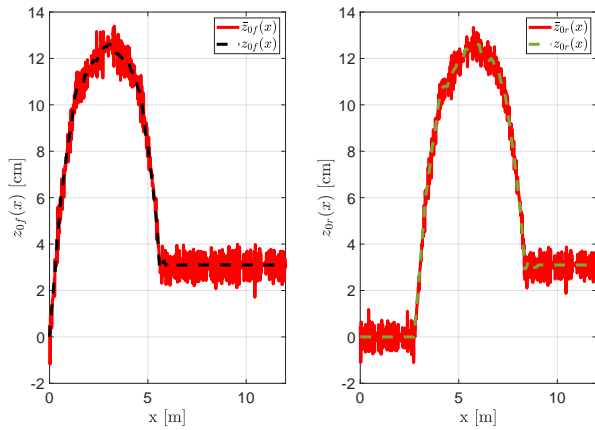
3. Georeferenced road monitoring

In order to provide a georeferenced measurement of the road surface with centimetric relative accuracy, another method based on data-fusion has been developed. Two kinds of sensors are used:

- A GNSS-hybrid inertial navigation system (INS) providing a highly accurate positioning of the vehicle body on which it is installed;



(a) Road profile reconstruction without sensor noise added



(b) Road profile input reconstruction with sensor noise added

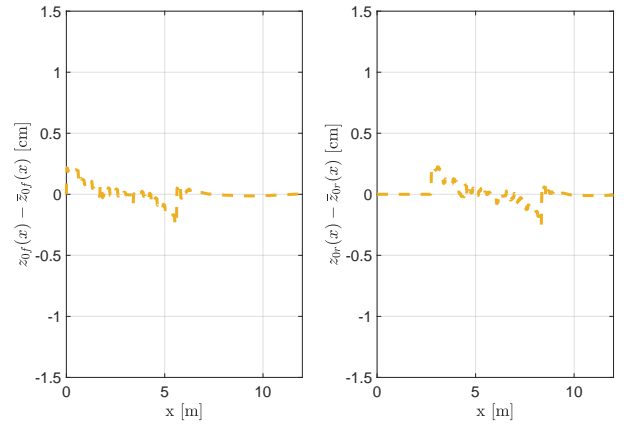
Fig. 7: Road profile input reconstruction results in time domain

- Suspension deflection sensors providing a measurement of the vertical displacement of each suspension arm of the vehicle.

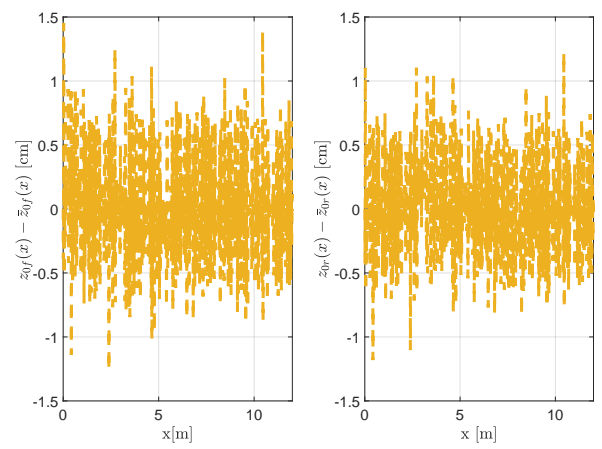
Under the assumption that all deformations in the suspension (e.g. tire flattening) are negligible, suspension height sensors, once calibrated, can then be used to get a measure of the vertical distance between a reference point on the car body and the ground below the concerned wheel. The four sensors therefore provide regular measurements of the position of four tire/ground contact points in the car body frame under each wheel. Once coupled with the localization information provided by the INS, it becomes possible to generate a georeferenced mapping of the road surface in the form of a scattered data.

3.1 Vehicle for data acquisition

The system is implemented on a labcar of the Stellantis group depicted in figure 9. This vehicle is a Peugeot 3008 II dedicated to the testing of various perception systems for the design of new ADAS/AD functionalities.



(a) Road profile reconstruction error without sensor noise added



(b) Road profile input reconstruction error with sensor noise added

Fig. 8: Road profile input reconstruction error results in time domain



Fig. 9: photograph of the labcar used in the study.

The sensors installed in the car for this specific work are:

- an OxTS RT3000v3 as the GNSS-hybrid INS;
- a set of four (instead of two for the series vehicle)

suspension height sensors like the ones used in the series vehicles. Those are rotating sensors measuring the suspension translation motion as an angular value.

The INS is receiving RTK corrections to bring the localization accuracy down to the centimeter-level in good GNSS reception conditions. It is outputting localization information with a 100 Hz refresh rate. Suspension height sensors were calibrated by putting the vehicle on a car lift and slowly raising the car body up while measuring both the actual distance from the body to the ground and the signal value from the sensors.

3.2 Relative accuracy estimation

Firstly, the best achievable relative accuracy of the proposed method is investigated. By relative accuracy we mean how precisely the system was able to reconstruct the local ground profile with respect to an arbitrary height reference. This step is crucial because no good absolute accuracy can be reached if the relative accuracy is insufficient in the first place.

To this purpose we made several acquisitions driving over a road hump, from which the profile was previously measured using a bubble level (figure 10b).

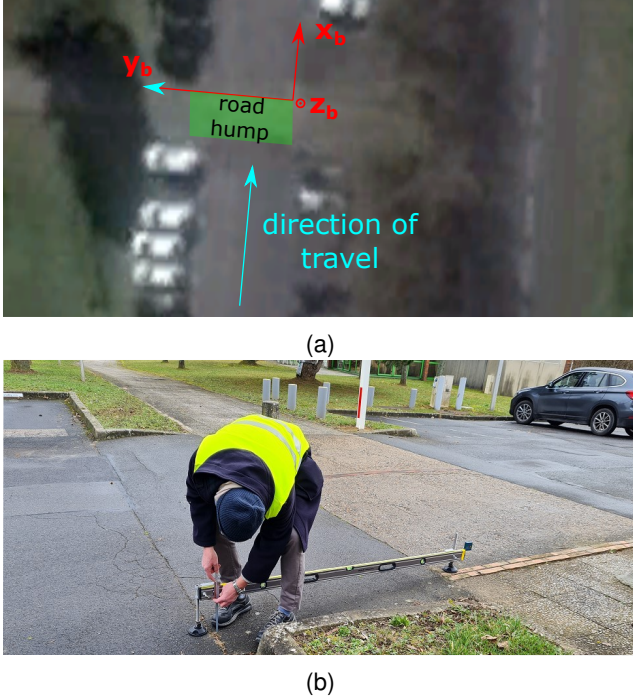


Fig. 10: (a): satellite picture of the road hump displaying the local bump Cartesian frame used in the study; (b): photograph of the hump being measured.

To provide enough statistics, 10 acquisitions were performed at a constant speed of 20 km/h , and 10 others at a constant speed of 30 km/h . Local road profiles recorded by the car were then computed of-line and compared to the measured reference profile to evaluate the relative error of the method.

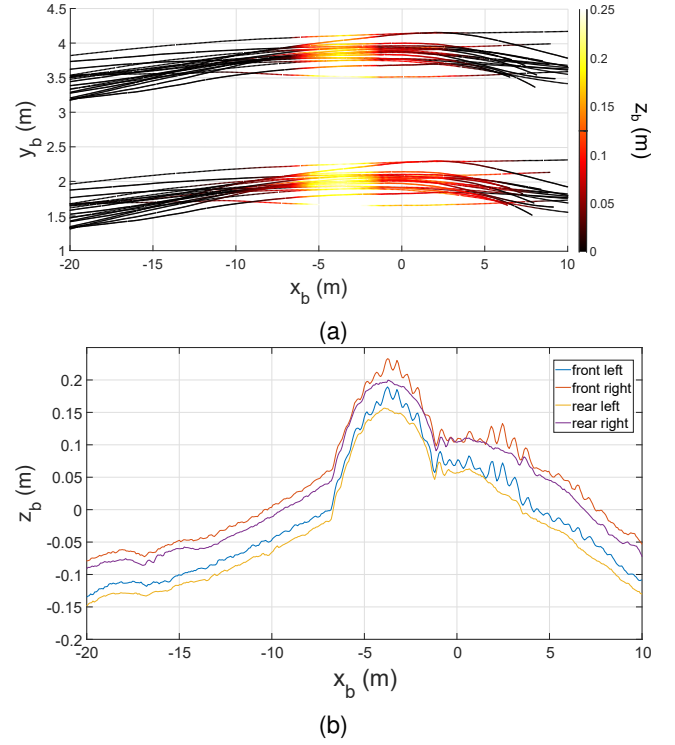


Fig. 11: (a): Scattered data of the ground surface obtained after the 20 acquisitions; (b): road profiles for each wheel of the car for a single acquisition.

Figure 11 displays the road profiles obtained from the labcar. Figure 11a shows the relatively small trajectory dispersion obtained over the 20 acquisitions and clearly highlights the hump. A single acquisition was selected and the corresponding individual road profiles for each wheel was plotted in figure 11b. We can clearly see height discrepancies between the different wheels, although the global profile appears quite similar. First, the left wheels have a noticeably lower height profile than the right wheels. This can be easily explained by the fact the road is not level but is sloping down towards the left along y_b . One can also see that there seems to be a constant offset between the front wheels and the rear wheels of about 15 mm . We explain this difference by the fact that the method used to extract the ground position for each wheel relies on the hypothesis that there is no deformation in the suspension. In reality not only is such deformation, for instance the tires experience flattening, but it can also vary between the front and the rear axle, depending on the weight repartition of the vehicle.

Taking into account that we know that the hump is sloping down towards the left, and that we only measured its actual profile at the $y_b = 0$ mark, we generate a full 3D model of the bump by considering an infinitely long volume with the same height profile as the one measured rotated by a roll angle (rotation around x_b) α . The value for α is estimated by performing a least-squares fitting of the experimental data displayed in

Figure 11a with the 3D hump model and found to be -1.40° . Now that a complete model is available, it becomes possible to compute the reference height of the road bump at an arbitrary position.

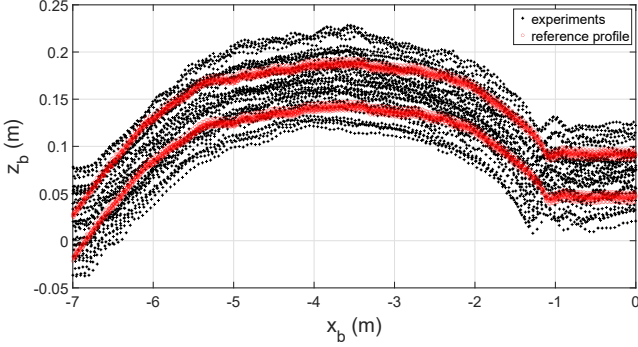


Fig. 12: superimposed road profiles recorded at 20 km/h (black) and reference profile obtained from the measurement (red).

Figure 12 shows the superimposed road profiles over the hump as a point cloud, in addition to the 3D reference profile. The upper red cluster corresponds to the reference profile for the right wheels of the car, which are higher than the left ones (lower red cluster) due to the negative roll of the hump.

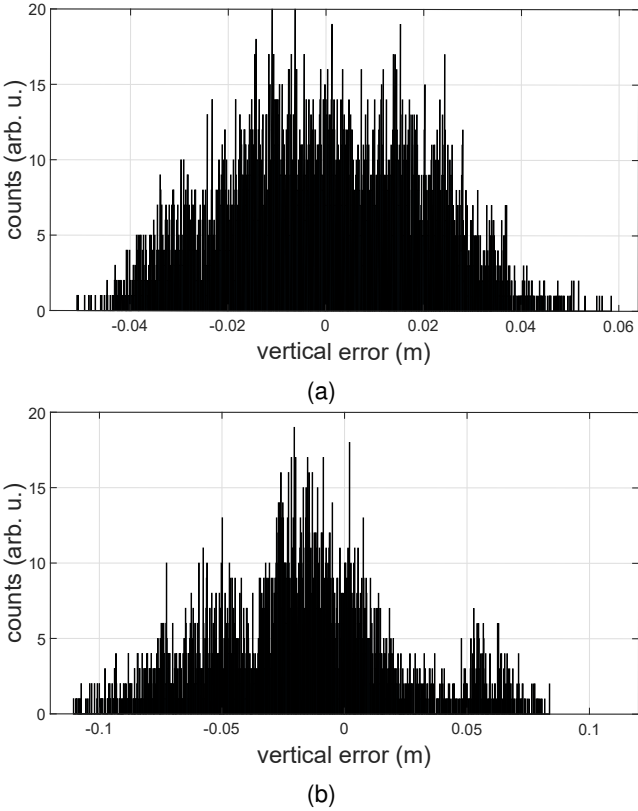


Fig. 13: vertical error histograms at 20 km/h (a) and 30 km/h (b).

Histograms for the vertical error between the measurements and the hump model are given in figure 13

for the two velocities. Both error profiles are approximately centered but the error spread is significantly larger at 20 km/h than at 30 km/h. Namely the sample standard deviations are:

$$\begin{cases} \sigma_{20} = 19.6 \text{ mm} \\ \sigma_{30} = 36.4 \text{ mm} \end{cases}$$

This finding is not surprising: as the vehicle is moving faster over the obstacle, since the sensor measurement frequency is fixed, there will be less points per unit length available, therefore decreasing the spatial resolution of the road profile measurement. Another effect can come from the increased deformation susceptibility of the suspension, which will also tend to increase the measurement noise, thereby negatively affecting the system accuracy. More important though, this proves that the method we devised is able to provide a centimeter-scale relative accuracy for the reconstruction of the road profile, which is more than enough to reconstruct obstacles such as road humps or potholes.

3.3 Absolute accuracy estimation

The absolute accuracy of the system can be estimated using the fact that the measurement noises from the absolute localization given by the GNSS-aided INS and the one from suspension height sensors are uncorrelated. In this case the total variance for the absolute road profile measurement is simply the sum of the variance from the absolute positioning measurement and the variance for the relative road profile measurement:

$$\sigma_{abs}^2 = \sigma_{INS}^2 + \sigma_{rel}^2 \quad (9)$$

This value will therefore be mainly dependent on the absolute accuracy that the GNSS-aided INS will be able to reach.

In our case, using a high-end INS and RTK GNSS corrections enables us to achieve a horizontal (North/East) absolute accuracy of less than 3 cm and a vertical absolute accuracy of less than 4 cm in the best GNSS reception conditions. This yields an absolute accuracy of a few centimeters.

Using a less precise localization solution such as a non-differential GNSS receiver would result in a far worse accuracy, making our method unreliable.

4. Conclusions

The work presented shows two techniques for road monitoring. The first follows an approach based on the inverse of the model developed in the frequency domain and the second uses measurements from well-calibrated suspension arm elevation sensors, coupled with a high-precision GNSS GPS system that allows to map the road profile elevation. Figure 14 shows the results of both techniques.

As shown in Figure 14 both methods get convenient results. GRM reconstructs the shape of the speed

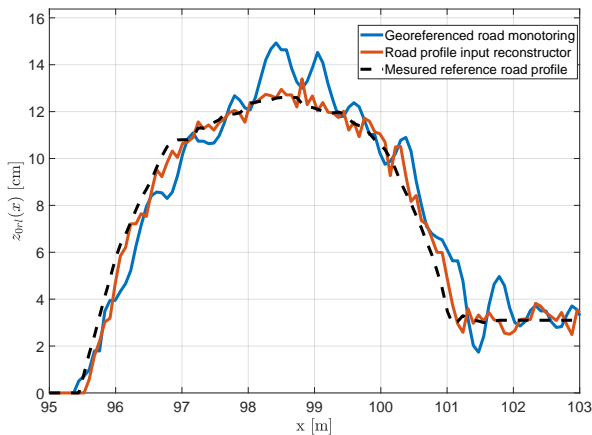


Fig. 14: Comparison of the two methods presented for road profile estimation

bump with a degree of error linked to the variation of the wheel deformation caused by a mass distribution different from that used at the time of calibration of the suspension arms displacement sensors. The result of the road profile input reconstructor method is closer to the reference profile, despite the delay induced by the RIR low pass filter dynamic. Unlike the GRM, the RIR method depends on a great knowledge of the test car model parameters, because parametric uncertainties can lead to a degradation of the performances.

Both methods have a strong dependence on the quality of the sensors. The GRM obtains the measurements directly from the sensors without any transformation of the information, therefore the sensors must be well calibrated. On the other hand, the quality of the results of the RIR depends on the quality of the sensor used, since the RIR tends to amplify the noise at low frequencies.

In future works it would be necessary to study a method to reduce the influence of sensor noise and apply the RIR taking into account the nonlinearities and uncertainties of the model used.

5. Acknowledgement

This work took place in the framework of the OpenLab 'Electronics and Systems for Automotive' combining IMS laboratory and STELLANTIS Groupe company.

References

- [1] Martina Hasenjäger and Heiko Wersing. "Personalization in advanced driver assistance systems and autonomous vehicles: A review". In: *2017 IEEE 20th International Conference on Intelligent Transportation Systems (ITSC)*. 2017, pp. 1–7.
- [2] Teron Nguyen, Bernhard Lechner, and Yiik Diew Wong. "Response-based methods to measure road surface irregularity: a state-of-the-art review". In: *European Transport Research Review*. Vol. 11. 1. Oct. 2019, p. 43.

- [3] Yechen Qin et al. "Road profile estimation for semi-active suspension using an adaptive Kalman filter and an adaptive super-twisting observer". In: *2017 American Control Conference (ACC)*. 2017, pp. 973–978.
- [4] H.M. Ngwangwa et al. "Reconstruction of road defects and road roughness classification using vehicle responses with artificial neural networks simulation". In: *Journal of Terramechanics*. Vol. 47. 2. 2010, pp. 97–111.
- [5] Qi Wang et al. "Road profile estimation of city roads using DTPS". In: *Sensors and Smart Structures Technologies for Civil, Mechanical, and Aerospace Systems 2013*. Ed. by Jerome Peter Lynch, Chung-Bang Yun, and Kon-Well Wang. Vol. 8692. International Society for Optics and Photonics. SPIE, 2013, pp. 911–918.
- [6] Mei Zhang et al. "Unknown input reconstruction: A comparison of system inversion and sliding mode observer based techniques". In: *2017 36th Chinese Control Conference (CCC)*. 2017, pp. 7172–7177.
- [7] Alain Oustaloup. *Diversity and Non-integer Differentiation for System Dynamics*. Wiley, 2014.
- [8] Shravanth SB, Abhay Bhargav KM, and Geetishree Mishra. "Sensor Based Pothole Detection System". In: *2021 IEEE International Conference on Cloud Computing in Emerging Markets (CCEM)*. 2021, pp. 15–22.
- [9] G. Bel Haj Frej et al. "A Multi-Modes Semi-Active Suspension Control Strategy for Peugeot 308 RCZ Vehicle". In: *2020 28th Mediterranean Conference on Control and Automation (MED)*. 2020, pp. 200–205.

6. Glossary

ADAS: Advanced Driver Assistance System
 CRONE: Commande Robuste Non Entiere
 GNSS: Global Navigation Satellite System
 GPS: Global Positioning System
 INS: Inertial Navigation System
 AD: Autonomous Driving
 RTK: Real Time Kinematic positioning
 GRM: Georeferenced Road Monitoring
 RIR: Road Input Reconstructor

Pave the way for a safe automated driving at level crossings

Richard DENIS¹, Virginie TAILLANDIER², Romain DEMARETS³, Brouk WEDAJO⁴, Amel BERNIER⁵, Florent MEURVILLE⁶, Samia AHIAD⁷

1. VALEO, France, richard.denis@valeo.com
2. SNCF, France, virginie.taillandier@snCF.fr
3. VALEO, France, romain.demarets@valeo.com
4. VALEO, France, brouk.wedajo@valeo.com
5. VALEO, France, amel.bernier@valeo.com
6. VALEO, France, florent.meurville@valeo.com
7. VALEO, France, samia.ahiad@valeo.com

Abstract: France has among the highest number of level crossings in Europe (more than 15 400), crossed daily by 16 millions of vehicles [1].

As increasingly intelligent, connected & automated vehicles are emerging on the roads, the SNCF (French railway operator) and VALEO (automotive equipment supplier) have joined forces to study how to enable a safe automated driving at level crossings. For this purpose, impacts on both vehicle and infrastructure sides have been investigated. In particular, a comprehensive safety methodology has been defined: functional safety, SOTIF (safety of the intended functionality) and cybersecurity analysis have been simultaneously considered, while the railway and automotive approaches were confronted. This paper presents this methodology and some results obtained with it, especially some examples of safety countermeasures proposed on both vehicle and infrastructure (level crossing) sides.

Moreover, a taxonomy of "smart level crossings" will be described, that ranks them according to the level of assistance provided to automated vehicles (via V2X communications).

Field tests results that highlight the relevance of these studies will also be discussed.

Keywords: V2X, Automated Vehicle, Smart infrastructure

1. Introduction

In France, the infrastructure managed by SNCF Réseau accounts for more than 15,400 level crossings (LC) on the operated railway lines. These LC are concerned by 100 to 150 collisions (train vs road user), leading to 25 to 30 fatalities, on average per year [1].

Compared to other types of road areas, accidents at LC have a much higher ratio of fatalities (from 30% to 50% of accidents at LC lead to death [1] vs 0,02% out of LC [2], in France). Level crossings are thus a challenging type of intersection for automated vehicles (AV), that leave little room for driving errors.

This may discourage car makers to include LC in the Operational Design Domain (ODD) of their AV.

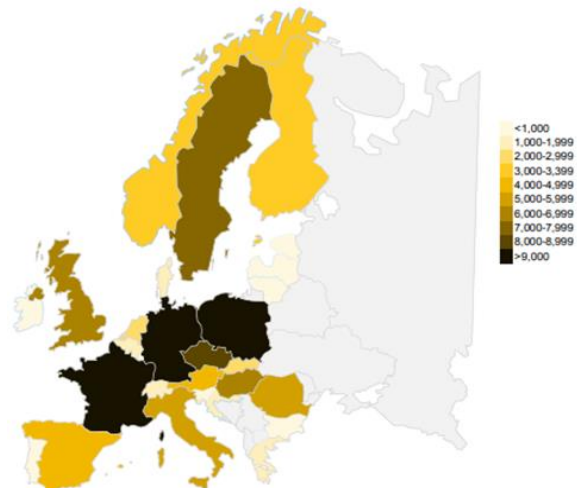
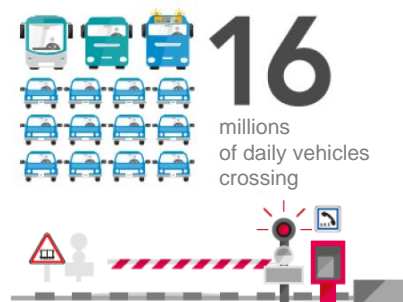


Figure 1: Total number of LC in Europe, 2014 [3]



450 000 closure cycles every day

Figure 2: Figures about LC in France, 2019 [1]

2. Assumptions of the study

2.1 Assumptions on the level crossings

In France, a ministerial decree defines 2 main categories of level crossings:

- Automatic level crossings with 2 half-barriers or 4 half-barriers

- Unguarded level crossings.

Each year, around 60% of collisions with a train occur at active/automatic LCs equipped with 2 half-barriers, where rail and road traffic is much more dense than at passive/St Andrew cross LCs. Such active LCs represent 60% of LCs.

In this project, we thus considered active level crossings in France (equipped with an automatic luminous signaling system with half-barriers).

To be noticed :

- Even if the Geneva Convention aims at ensuring a certain homogenization in terms of level crossings equipments (e.g. fixed or flashing red lights, traffic signs, etc.), there are still differences between countries regarding their physical aspects (e.g. red & white barriers in France and Germany but yellow & red in Norway and Sweden) or their modes of operation (e.g. various flashing frequency for the traffic lights, various closing time, etc.)
- The delimitation of responsibilities between the managers of road and railway infrastructures differs depending on the country. In France, the railway infrastructure manager is in charge of the level crossing facilities and its position signage, but the early signage (e.g. signs announcing a LC at 150 meters) is under the responsibility of the road infrastructure manager.

2.2 Assumptions on the automated vehicles

In this study, we considered:

- Level 3 and level 4 automated vehicles, capable to cross an active level crossing
- Level 3 automated vehicles, NOT capable to cross an active level crossing (because not designed for that purpose or because affected by a problem).

We also assumed the below preliminary technical architecture, in which the automated vehicle can interact with the infrastructure (including the level crossing) through 2 interfaces:

- IF1: interface between its exteroceptive sensors and the physical infrastructure elements (eg road signs, etc.)
- IF2: connectivity interface, through which information can be exchanged via a wireless communication.

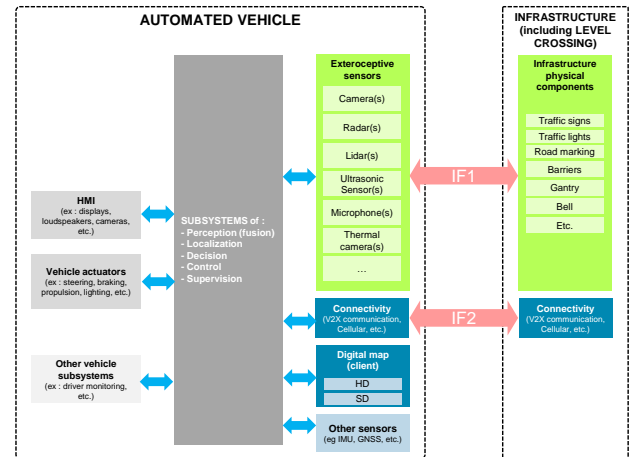


Figure 3 High-level technical architecture assumed for the Automated Driving System

3. A comprehensive safety methodology

In order to design an automated driving system (ADS) capable to navigate safely at level crossings, the below approach has been followed:

- 1) An initial "Preliminary Hazard Analysis" (PHA) has been conducted to identify all hazardous behaviors (called "undesired events") of the ADS
- 2) Then 3 different types of dependability studies have been done in parallel:

A "functional safety", a "safety of the intended functionality (SOTIF)" and a "cybersecurity" study, whose goals were to:

- Identify & evaluate risks due to hazardous behaviors of the ADS that are caused by (respectively) random hardware failures, disturbances targeting performance limitations of subsystems (especially sensors)¹, and cyber-attacks/malicious human behaviors
- Define countermeasures to reduce such risks at a "reasonable" level.

A focus has been done in this paper on dysfunctions of the ADS perception of road & level crossing.

The methodology framework used for these 3 studies has been based on (respectively) ISO 26262, ISO/PAS 21448 and ISO 21434 standards.

- 3) A conciliation phase has finally been done between these 3 types of countermeasures, to ensure that they were consistent/not contradictory/complementary between each other.

This approach has been "vehicle-centric": countermeasures have been investigated first on vehicle side, then complementary assistance from road infrastructure (especially from level crossings) has been explored. In parallel, a functional safety analysis has been done in order to protect specifically

¹ SOTIF also addresses other causes of hazardous behaviors, e.g. reasonably foreseeable misuse

the level crossing against new risks carried by the V2X connectivity.
This paper shows a non-exhaustive list of identified risks & associated countermeasures, derived from this methodology.

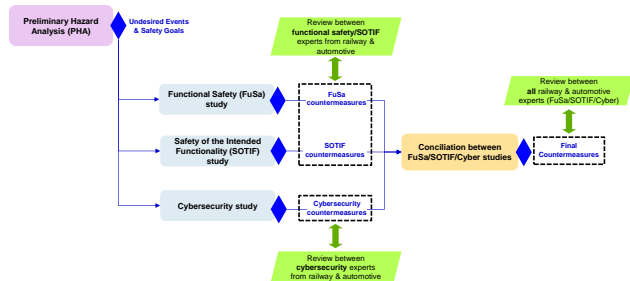


Figure 4: Comprehensive safety methodology followed to determine safety countermeasures

4. Hazardous behaviors of the automated driving system

Among all hazardous behaviors of the ADS ("undesired events") identified in the PHA, we propose in this paper to focus on the 2 below ones:

# ID	Undesired Event (at the Automated Driving System level)	Effect on vehicle level (in Level Crossing area)	ASIL ranking
UE-01	Cross the level-crossing when inappropriate (eg level-crossing is closed, exit not cleared, etc.)	Collision with train	ASIL A
UE-02	Cross the level-crossing with an inappropriate trajectory	- Run-off-road accident - Head-on collision or Side-collision with other road users	ASIL B

5. Identified Risks

The below section describes some identified hazardous scenarios (driving scenarios in which AV is exposed to particular disturbances) and threats (cyber-attacks or malicious human behaviors with harmful intent) that may trigger a hazardous behavior of the ADS, especially due to performance limitations or vulnerabilities of the ADS perception of road & level crossing.
Examples of possible associated countermeasures (both on AV and LC sides) will be described further.

5.1. Hazardous scenarios & SOTIF triggering conditions related to level crossing areas

ID	Hazardous scenarios / SOTIF triggering conditions (disturbance)	Effect (at ADS perception level)	Effect (at vehicle level)
TE_01	Crossing a level-crossing / Rail tracks with high contrast compared to road pavement	Rail tracks misinterpreted by cameras as road boundaries (due to high contrast with road pavement)	Cross the level-crossing with an inappropriate trajectory (UE-02) => Run-off-road accident or Head-on collision or Side-collision with other road users
TE_02	Crossing a level-crossing / Traffic lights specific to Level-Crossings ("R24" traffic light)	R24 traffic lights not detected by cameras (due to specific physical aspect compared to conventional traffic lights)	Cross the level-crossing while inappropriate (UE-01) => Collision with train
TE_03	Crossing a level-crossing / Phenomena masking the level crossing traffic signs, warning & protection systems	Level crossing presence not detected or Level crossing status misinterpreted (due to phenomena masking the level crossing equipments e.g. traffic lights/traffic signs/barriers/etc.)	Cross the level-crossing while inappropriate (UE-01) => Collision with train



Figures 5 to 8: Illustration of SOTIF triggering conditions in level crossing areas (from left to right) [4]: Rail tracks with high contrast compared to the pavement, R24 traffic light, Parked vehicle masking R24 traffic light & barrier, Vegetation masking the traffic sign

5.2. Threats to automated vehicles

ID	Threat
TH_01	Attack on integrity & availability of information received via V2X communication from the level crossing
TH_02	Attack on integrity & availability of information returned by the exteroceptive sensors

For illustration of the threat TH_02, McAfee managed in 2020 to spoof cameras of Tesla vehicles by using "adversarial stickers", so that a "STOP" sign was misclassified as an "ADDED LANE" sign [6]. This kind of attack is known as "adversarial attacks" and exploits vulnerabilities of machine learning/deep learning algorithms.

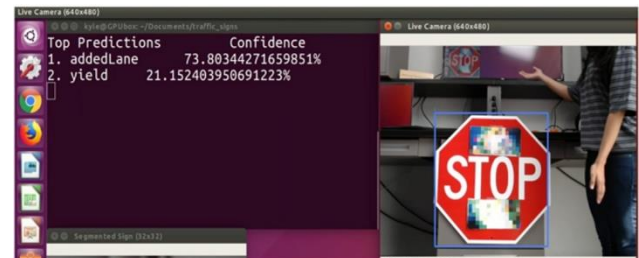


Figure 9: Illustration of an adversarial attack [6]

6. Countermeasures

6.1. Countermeasures on vehicle side

ID	Countermeasure (example)	Risk addressed		
		FuSa	SOTIF	Cyber
CMV_01	Improve capability of cameras to : - detect the road boundaries in the presence of rail tracks with high contrast compared to the road pavement - detect the level crossing (presence/status) despite phenomena masking the level crossing signs & systems (eg traffic lights/traffic signs/barriers/etc.) or despite particular physiognomies (eg R24 traffic light vs conventional tricolor traffic lights, etc.) (ex: algorithm improvement, etc.)		x	
CMV_02	Protect exteroceptive sensors against attacks on integrity & availability of information returned by the exteroceptive sensors (ex: protect cameras against machine-learning/adversarial attacks, etc.)			x
CMV_03	Protect V2X communications against attacks on integrity & authenticity of the received V2X information (ex: check signatures & certificates of V2X messages received from level-crossing, etc.)			x
CMV_04	Use redundancy for the perception of road & level crossing (ex: use multiple sensors with diverse technologies, use information provided by the level crossing via a V2X communication, use a digital map, etc.)	x	x	x
CMV_05	Detect a non-capability of the automated driving system (ADS) to cross a level crossing and : - (if the ADS not activated yet) do not allow the ADS activation when approaching a level crossing - (if the ADS is activated) request the driver "early enough" to take back control when approaching a level crossing (for a L3 system) or stop the vehicle in a safe area before the level crossing or use an itinerary circumventing level crossings (for a L4 system)	x	x	x

6.2. Countermeasures on infrastructure side

ID	Countermeasures (example)	Risk addressed		
		FuSa	SOTIF	Cyber
CMi_01	Ensure the road marking (e.g. edge lines) is present with a sufficient quality within the level crossing area		x	
CMi_02	Provide to automated vehicles : - information about presence & status (e.g. open/closed/etc.) of the level crossing - detailed description of the road within the level crossing area (ex: via V2X communication, digital map, etc.)	x	x	x
CMi_03	Protect V2X communications against attacks on integrity & authenticity of the emitted V2X information (ex: use certificates & signatures in V2X messages to be sent to automated vehicles, etc.)			x

7. Taxonomy of smart level crossings

The relevance of C-ITS services (based on V2X communications) offered by the infrastructure, and especially by the level crossing, has just been highlighted, in particular to offer redundancy to AV perception in case of disturbance or cyber-attacks/malicious human behaviors affecting the AV sensors.

The Inframix project [5] has introduced a taxonomy of intelligent road infrastructures, ranking them according to the assistance provided to automated vehicles, on a scale of 5 "ISAD" levels ("Infrastructure Support levels for Automated Driving").

We thus propose in this paper to refine this taxonomy for level crossings, as depicted in below table.

ISAD Level	Name	Digital information provided to AVs										Services provided by the level crossing infrastructure									
		Type	V2X message (E/TB/ITS)	Map	Map	Map	Map	Map	Map	Map	Map	AV perception (by providing AV the following information)	AV decision (by providing AV the following information)	AV decision (by providing AV the following information)	AV decision (by providing AV the following information)	AV decision (by providing AV the following information)	AV decision (by providing AV the following information)	AV decision (by providing AV the following information)	AV decision (by providing AV the following information)	AV decision (by providing AV the following information)	AV decision (by providing AV the following information)
Digital infrastructure	A	Cooperative driving	X	X	X	X	X	X	X	X	X	X	X	X	X	X	X	X	X	X	X
	B	Cooperative perception	X	X	X	X	X	X	X	X	X	X	X	X	X	X	X	X	X	X	X
	C	Dynamic digital information	X	X	X	X	X	X	X	X	X	X	X	X	X	X	X	X	X	X	X
	D	Static digital information / Map support	X	X	X	X	X	X	X	X	X	X	X	X	X	X	X	X	X	X	X
	E	Conventional infrastructure / No AV support	X	X	X	X	X	X	X	X	X	X	X	X	X	X	X	X	X	X	X
ISAD Levels (legacy from Inframix project)		Refinement for the smart level crossing (proposal)																			

Figure 10: ISAD taxonomy refined for level crossings

8. Demonstration

Two demonstrations were carried out in 2021 to assess the relevance of the assistance provided by a smart LC to AV.

A LC with a "ISAD C" level was then assessed.

8.1 Set up

The demonstrations took place at the LC "PN 449" in Brec'h (in Brittany, France), which is an active LC equipped with flashing red lights and two half-barriers. The LC management system was connected to a "Road Side Unit" (RSU), in charge of sending information about the LC area ("V2X messages") to the AV, via a wireless communication ("V2X communication"), standardized according to the ETSI ITS communication protocol stack [7].

The AV was also equipped with V2X connectivity, and could detect in particular the LC by using its exteroceptive sensors (e.g. camera) and a digital map in addition of such V2X link.

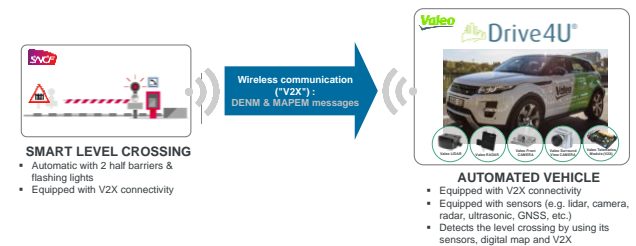
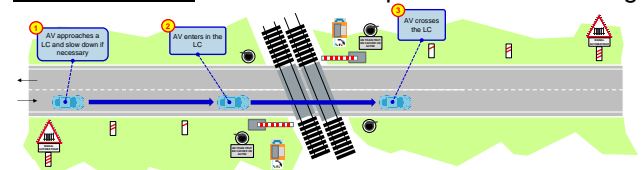


Figure 11: Demonstration set-up ("ISAD C" level crossing)

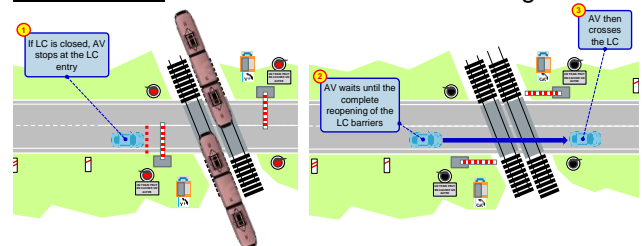
8.2 Target scenarios

A first set of scenarios were demonstrated, in which a SAE "level 3" or "level 4" automated vehicle (AV) was assumed to be capable to cross the level crossing (i.e. without any driver's intervention or even without need of a driver).

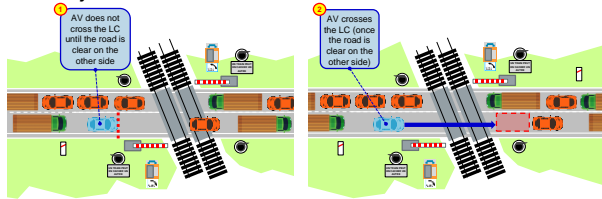
- Scenario 1: Cross an "open" level crossing



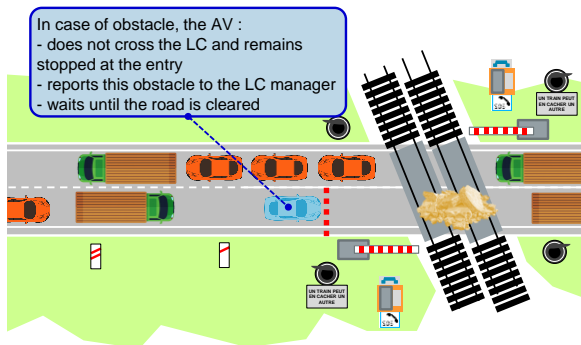
- Scenario 2: Cross a "closed" level crossing



- Scenario 3: Cross an "open" level crossing while a traffic jam



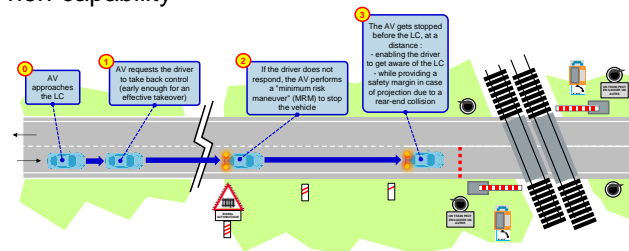
- Scenario 4: Cross an "open" level crossing with obstacles blocking the way



A second set of scenarios was also demonstrated, in which a SAE "level 3" AV was assumed NOT to be capable to cross the level crossing, either because the automated driving system:

- is not designed for such purpose (i.e. the LC is out of its operational design domain)
- or is affected by a major dysfunction, e.g. loss of a sensor (before entering in the level crossing).

- Scenario 5: Stop before the level crossing in case of non-capability



8.3 Demonstration results

The target scenarios could be fulfilled by the AV with the expected performance, in terms of functionality and safety (i.e. without hazardous behavior).

In particular, the assistance brought by the "ISAD C" LC via the V2X communication link turned out to be effectively useful to ensure the redundancy of the AV perception. Indeed, the flashing red lights ("R24 traffic lights") were not detected by one of the AV cameras during these demos.

Moreover, the use of already existing V2X standards (DENM/MAPEM), with a profile adjusted to the LC use

case, allowed to manage all target scenarios (i.e. the relevant data fields & values within the DENM/MAPEM standards were selected to fit with the LC use case).

In particular, the range of such V2X communication (>300m during the demonstrations) was sufficient to handle the minimum risk maneuver (MRM) scenarios, considering a "takeover request" duration of 10s and a deceleration at -4m/s^2 .

9. Conclusion

A comprehensive safety methodology has been defined and explored successfully, allowing to derive some possible safety countermeasures on both AV and LC sides.

In particular, this study has highlighted the relevance of C-ITS services (based on V2X communications) that may be offered by level crossings (or more generally by the infrastructure), especially to allow AV perception redundancy in case of operational disturbance or cyber-attacks/malicious human behaviors affecting the AV sensors (e.g. contrast between rail tracks and road pavement, adversarial attacks, etc.). This led us to propose a taxonomy of smart level crossings, ranking them according to the assistance provided to AV (via V2X communications). It should also be noted that the countermeasures presented in this paper must not be understood as mandatory requirements for AV nor LC, but rather as a possible basis of comparison. Indeed, the ADS technical architecture taken as input of the study (albeit voluntarily chosen to be the most generic possible) may differ depending on the AV, and therefore the necessary countermeasures may vary as well.

Possible perspectives of this study could be:

- to iterate this comprehensive safety analysis (as the technical architecture taken as input may have to be updated following this 1st round of analysis), until risk is reduced under a "reasonable" threshold
- to investigate the applicability of this study results to other countries than France. This point of attention must be taken into account especially for AV operating in border areas
- to investigate how to conciliate 2 possibly contradictory points of view:

(from infrastructure managers' perspective) providing assistance to AV without additional costs (or at least at a reasonable cost) and without exposing itself to liability risks/transfers of responsibility, and

(from AV industrials' perspective) receiving assistance from the infrastructure with a sufficient level of quality to reduce the cost of automated driving systems and ensure sufficiently safe driving operations

10. References

- [1] SNCF Réseau (railway accidentology in France, www.prevention-ferroviaire.fr)
- [2] Observatoire national interministériel de la sécurité routière ONISR (road accidentology in France, www.onisr.securite-routiere.gouv.fr)
- [3] European Railway Agency “Safety Overview 2021”
- [4] SAFER LC project, UIC, May 2017 - May 2020 (<https://safer-lc.eu/>)
- [5] Inframix project, Horizon 2020 research and innovation program, May 2017 - May 2020 (<https://www.inframix.eu>)
- [6] McAfee (2020), “*Model Hacking ADAS to Pave Safer Roads for Autonomous Vehicles*”
- [7] ETSI EN 302 665

11. Glossary

ADS	Automated Driving System
AV	Automated Vehicle
DENM	Decentralized Environmental Notification Message
IF	Interface
ISAD	Infrastructure Support levels for Automated Driving
LC	Level Crossing
ODD	Operational Design Domain
PHA	Preliminary Hazard Analysis
MAPEM	MAP Extended Message
MRM	Minimum Risk Maneuver
RSU	Road Side Unit
SAE	Society of Automotive Engineers
SOTIF	Safety Of The Intended Functionality
V2X	Vehicle to everything

ASSESSMENT FOR SAFETY IMPROVEMENT

Investigation of effectiveness and conflict of a road projection lamp for bicyclists, using a VR system

K. Murata¹, T. Kitazawa¹, H. Ishida¹

1: Koito Manufacturing Co., Ltd., 500 Kitawaki, Shimizu-ku, Shizuoka-shi, Shizuoka 424-8764, Japan

Abstract: The purpose of this study was to verify the effectiveness of a road projection lamp that helps road users to recognize approaching vehicles at intersections. In Japan, pedestrian and cyclists account for more than 50% of all fatalities. In this research we focused on cyclists due to the risk that comes from high speed and long braking distance.

We constructed a traffic scene in which vehicles turn right or left at an intersection in a virtual reality(VR) environment. The cognitive reaction time for vehicles was measured when there was a projection on the road, and when there was not. The analysis revealed a significant difference, with a reduced cognitive reaction time for the case with a projection on the road.

We also used the VR system to examine the conflict that the road projection lamp may distract attention on other vehicles. The cognitive reaction time for normal vehicles was measured when there was a projection on the road, when there was not. The cognitive reaction time did not change significantly, suggesting no significant conflict under our experimental condition.

Keywords: Road projection, Virtual Reality(VR), Effectiveness, Conflict, Test with subjects

1. Introduction

To reduce the number of traffic accidents at night, road projection lamps for motor vehicles, which project symbols and other light patterns onto the road surface, are being considered as a means of informing pedestrians, bicyclists, other drivers, and so forth of the vehicle's behavior and warnings. These lamps are a new feature, and various studies have examined their performance and effectiveness.

Preceding studies have reported that: from dusk to nighttime, approaching vehicles producing road projections of an appropriate luminance contrast make it easier for pedestrians to notice them[1]; flashing road projections help to reduce the luminance contrast necessary for pedestrians to notice them[2]; road projections help bicyclists to pull the brake levers faster[3], etc. These results showed the effectiveness of appropriate contrast and flashing of road projections.

However, these experiments were conducted under static conditions simulating actual traffic environments, and did not evaluate real-world

situations such as participants and vehicles in motion approaching each other.

In this study, therefore, we conducted experiments using VR equipment to simulate reality. VR is a generic term for a technology that immerses participants in a virtual world created by computer graphics and allows them to experience it as if it were the real world. By using VR to reproduce a traffic environment and immersing the participants in it, it is possible to safely conduct experiments that match reality. One preceding experiment using VR to evaluate the behavior of participants[4] evaluated how pedestrians visually recognized the external display of a vehicle in a parking lot in a VR environment.

On the other hand, when evaluating new functions of lamps, it is important to examine not only the positive effects of additional functions but also the negative ones (conflicts). One example of a possible conflict is a situation where a vehicle's road projection dominates the bicyclist's attention and delays their noticing another vehicle approaching, which they would otherwise have noticed much earlier, thus exposing them to danger. VR devices that can reproduce various scenes and easily change the experimental setup also seem to be effective for evaluating conflicts. One preceding study using VR for conflict evaluation of functions[5] reported on the evaluation of negative effects of using an external human-machine interface on pedestrians' behavior in checking their surroundings in a VR environment, but to the author's knowledge, no study has evaluated the conflict of lamp functions.

In this study, we constructed a system that evaluates the functions of a road projection lamp by immersing participants in a VR space that simulates traffic environments and clarified the effectiveness and conflict of road projection between when the vehicle used road projection and when it did not, based on measurements of participants' cognitive reaction times.

2. Investigation the scenes of traffic accidents

Before setting up situations for evaluating effectiveness and conflict between when the vehicle turns with road projection and when without, we surveyed the characteristics of accident situations in Japan based on past traffic accident data. For this purpose, we used an international traffic safety

database[6] and the accident survey data of the Institute for Traffic Accident Research and Data Analysis (ITARDA)[7] [8].

Figure 1 shows the percentage of fatal accidents by mode of mobility in 2019 by country. In the Japanese traffic environment, pedestrians and bicyclists accounted for a large proportion of traffic fatalities, exceeding 50%. This is presumably due to the large numbers of pedestrians and bicycles, which often intersect with two-wheeled and four-wheeled motor vehicles.

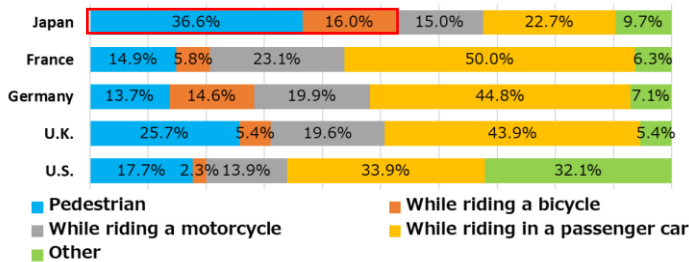


Figure 1: Comparison of composition of deaths within 30 days by road user by country(2019)[6]

Figure 2 shows the percentage of traffic fatalities by type of accident site in 2019. Forty-two percent of traffic fatalities occurred at intersections.

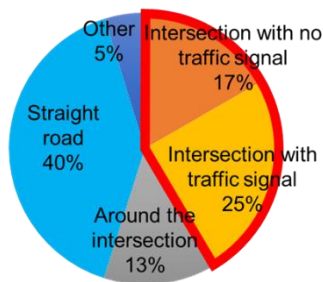


Figure 2: Composition rate of deaths in 2019 by road alignment[7]

Figure 3 shows the percentages of the causes of accidents in which the fatalities were bicyclists. It shows that a contributing factor to accidents is that the bicyclist often expects the approaching vehicle to take action first to stop. To help bicyclists avoid collision due to this expectation, it is vital to aware bicyclists of an approaching vehicle earlier.

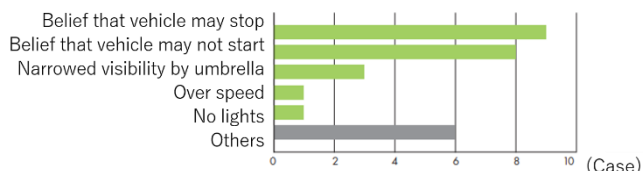


Figure 3: Human factor of accidents between automotive and bicycle in 2011[8]

Based on these results, we chose an intersection as the scene to be evaluated and assumed that a

vehicle approaching with road projection would help other traffic participants to notice it earlier, increasing their time-to-collision (TTC). The typical braking distance for a bicycle traveling at 18 km/h is known to be 1.5 m, while that for a pedestrian is 0.3 m. Accordingly, providing an early warning of approaching vehicles is likely to be more effective for reducing serious accidents among bicyclists, so we decided to study bicyclists. Further, as a case where it is difficult for the bicyclist to notice an approaching vehicle, we chose a scene where the bicycle and the approaching vehicle enter the intersection both from the same direction.

3. Experimental conditions

This study was conducted with the approval of the ethics committee of Koito Manufacturing. The participants joined the experiments of their own free will. To prevent the participants from getting “3D-sick” in the VR, the duration of the experiment was limited to 1 hour per participant.

3.1 Common conditions for the experiment

a. Road projection data

- Road projection shape: Linear
- Road projection illumination color: Amber(synchronized with turn signal lamps)
- Road projection size: As shown in Figure 4
- Position of road projection: Where the edge of the road projection is 4.7 m from the vehicle edge, at an angle of 30° to the overall length of the vehicle
- Road projection flashing frequency: 1Hz(satisfying the flashing frequency specified in UNR 148[9])

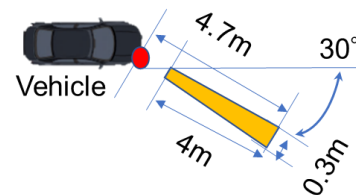


Figure 4: Shape and size of road projection

b. Conditions of road projections and ambient illumination

- Luminance contrast: 0.2(cited from reference [1])

c. Hardware

- Head Mounted Display(HMD): HTC Vive pro eye(See Figure 5)



Figure 5: VR-HMD (HTC Vive pro eye)

d. Software

- VR image generation software: Unreal Engine 4
- 3D models of vehicles, road surfaces, etc.: AUTO City by VERTEchs
- Vehicle motion control: Sirius by Misaki Design

e. Participants

Participants (healthy adults of age 26 to 59): 20 people, of which 16 were male and 4 female with an average age of 37.45 and an SD of 11.1

f. Layout of experiment devices

Figure 6 shows the layout of devices in the booth. In the booth, the participant was instructed to ride a bicycle, which was fixed on a stand to prevent them from falling over during the experiment.

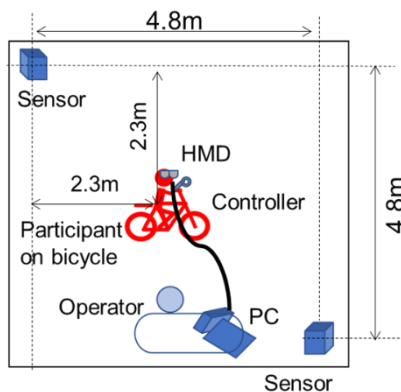


Figure 6: Layout of equipment in experimental room

g. Method for measuring the cognitive reaction time

Wearing a VR-HMD, the participant held the controller shown in Figure 7 in their hand and watched a VR image displayed on the HMD. The participant was instructed to press the button on the controller when they noticed a vehicle approaching them in the VR image.



Figure 7: Controller

3.2 Evaluating the effectiveness of road projection

a. Experimental setup

Figure 8 shows the experimental setup for the effectiveness evaluation. A bicyclist was going straight through an intersection, while a vehicle with a road projection lamp was entering it from behind the bicyclist to turn left or right, thus approaching each other. The bicyclist's cognitive reaction time to the vehicle was measured for both when the vehicle

was with road projection and without, each for when turning right and left.

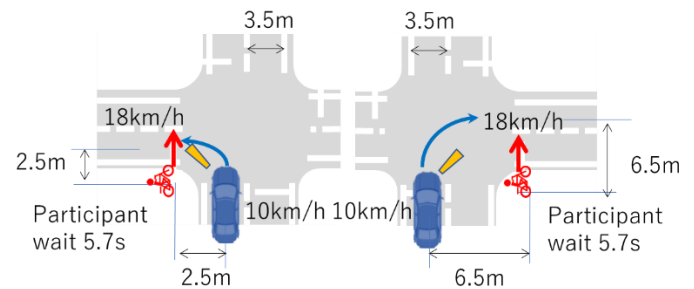


Figure 8: Layout of effectiveness investigation (Left:left turn scene, Right:right turn scene)

b. Task

To control the consciousness of the participant in the effectiveness evaluation, we assigned them a task. Figure 9 shows the image that the participant watched in the VR world.

The participant was told to watch a rectangular 3D model like a smartphone screen, on which a random number from 1 to 9 was displayed, changing every second. Every time the number changed, the participant was asked to keep a mental total of the numbers and say the last digit of the current result (Uchida - Kraepelin psycho-diagnostic test).

Right-turning vehicle Road projection



Task object (random number)

Figure 9: Participant's view

c. Number of trials

- 3 trials with road projection
- 3 trials without road projection
- 3 dummy trials(the vehicle goes straight through the intersection)

Each of the above including right turns, left turns, totaling 18 trials.

d. What the participant saw in the VR image

1. From 20 m behind the bicycle (out of the participant's sight), the vehicle starts approaching at 10 km/h..

2. At the intersection, the bicyclist stops before crossing, looks at the smartphone and starts doing the task.
 3. The vehicle approaches the bicyclist from behind and, if it is with road projection, the projected light comes into the bicyclist's sight.
 4. The bicyclist starts moving at 18 km/h while doing the task. Not controlled by the participant, the bicycle automatically moves as the scenario intends.
 5. From the left or right, the body of the vehicle enters the bicyclist's sight.
 6. The vehicle turns at the intersection and approaches the bicyclist.
- e. Experimental procedure

The experimental procedure was as follows.

1. The participant rides the bicycle and holds the controller.
2. The participant puts on the VR-HMD and calibrates it.
3. The participant watches the VR image and starts doing the task.
4. Upon noticing the vehicle, the participant presses the button.
5. The participant does 3 trials for each of the 3 conditions (the vehicle with and without road projection, and dummy), for a total of 9 trials.
6. Changing the scenario (the vehicle turning right and left), the participant does the same as in step 5, i.e. doing 18 trials in total.

Figure 10 shows the appearance of the participant during the experiment.

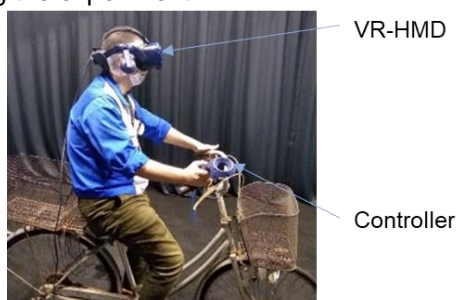


Figure 10: Participant on the bicycle

3.3 Evaluating the conflict of road projection

a. Experimental setups

Figures 11 and 12 show the experimental setup of the conflict evaluation. In this scene, it is assumed that the bicyclist's attention was distracted by the road projection of the vehicle coming from behind, which delays the bicyclist's noticing another vehicle

coming from the street perpendicular to theirs without road projection to go straight through the intersection. The bicyclist's cognitive reaction time to this second vehicle crossing the intersection was measured, when the vehicle coming from behind was with road projection and without.

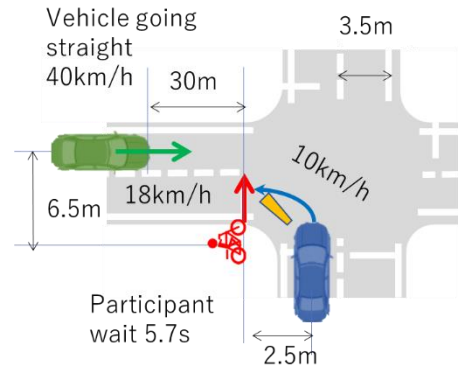


Figure 11: Layout of conflict investigation of left turn scene

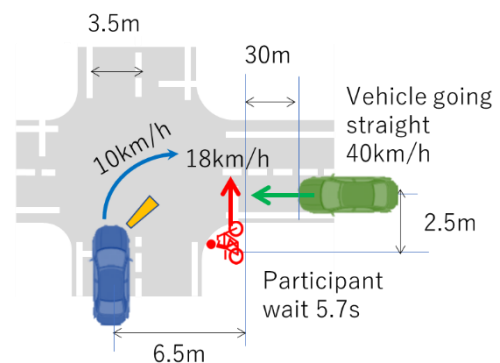


Figure 12: Layout of conflict investigation of right turn scene

b. Number of trials

- 3 trials with road projection
- 3 trials without road projection
- 3 dummy trials (no vehicle going straight through the intersection)

18 trials in total with the vehicle turning right and left

c. What the participant saw in the VR image

1. From 20 m behind the bicyclist, the vehicle with a road projection lamp starts moving at 10 km/h.
2. At 30 m to the right or left of the bicyclist, another vehicle starts approaching at 40 km/h to go straight through the intersection.
3. If the vehicle coming from behind is with road projection, the projected light enters the bicyclist's sight.
4. The bicycle starts moving at 18km/h. Not controlled by the participant, the bicycle automatically moves as the scenario intends.

5. The vehicle with road projection enters the intersection and stops after it comes into bicyclist's sight.
6. The vehicle coming from the side to cross the intersection enters the bicyclist's sight.
7. The vehicle crossing the intersection approaches the bicyclist.

d. Experimental procedure

The experimental procedure was as follows.

1. The participant rides the bicycle and holds the controller.
2. The participant puts on the VR-HMD and calibrates it.
3. The participant watches the VR image and presses the button when they decide to brake to avoid a collision with the vehicle crossing the intersection.
4. The participants does 3 trials for each of the 3 conditions of the vehicle coming from behind (with and without road projection, and dummy trial), i.e., a total of 9 trials.
5. Changing the scenario (the vehicle coming from behind turning right and left), the participant does trials under the same conditions as in step 4, i.e., a total of 18 trials.

4. Results of the experiments

4.1 Results of the effectiveness evaluation

Figure 13 shows the average cognitive reaction times for the 20 participants after repeating 3 trials under the same conditions. Comparing the average cognitive reaction times, the participants responded faster by 0.64s in the right-turn scenes and by 0.92s in the left-turn scenes when the vehicle turned with road projection.

The Shapiro-Wilk test was conducted to check normality. The results showed no normality ($p < 0.05$) in right-turn scenes when the vehicle turned with road projection, while showing normality ($p > 0.05$) when without.

Similarly, the left-turn scenes showed no normality when the vehicle turned with road projection ($p < 0.05$) and normality when without.

Accordingly, a Wilcoxon rank sum test was conducted to test for significant differences, and significant differences were found between when the vehicle turned with road projection and when without for both the right-turn and left-turn scenes ($p < 0.01$ for both).

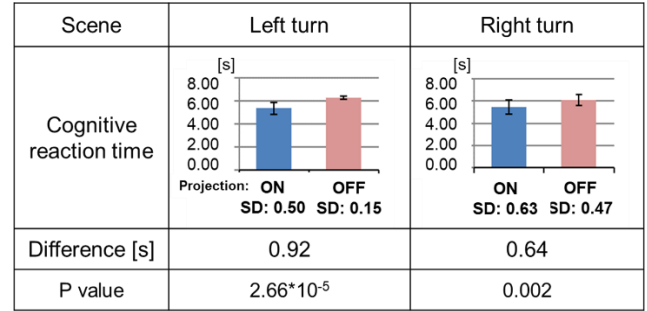


Figure 13: Comparison of average cognitive reaction time

4.2 Results of the conflict evaluation

Figure 14 shows the average cognitive reaction times for the 20 participants after repeating 3 trials under the same conditions.

Comparing the average cognitive reaction times, in right-turn scenes, there was no difference in how fast participants responded, whether the vehicle was with or without road projection, while, in left-turn scenes, they responded faster by 0.02s when the vehicle was with road projection.

The Shapiro-Wilk test was conducted to check normality. The results showed no normality with $p < 0.05$ regardless of whether the vehicle turned with road projection or without and whether it turned right or left.

Accordingly, a Wilcoxon rank sum test was conducted to test for significant differences, but no significant differences were found between when the vehicle turned with road projection and when without for both right-turn and left-turn scenes ($p > 0.05$ for both conditions).

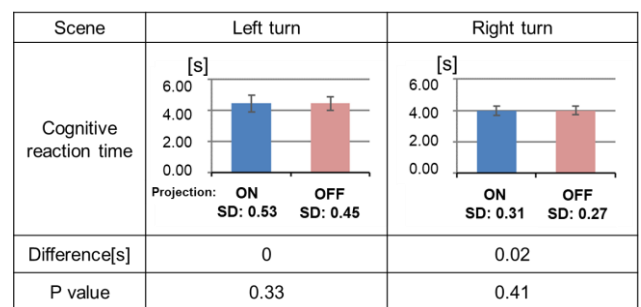


Figure 14: Comparison of average cognitive reaction time

5. Discussion

5.1 Effectiveness evaluation: Comparison of cognitive reaction times

We confirmed that the cognitive reaction time was shorter in both right-turn and left-turn scenes when

the vehicle turned with road projection and that there were significant differences in the reduction.

Comparing the right-turn and left-turn scenes, when the vehicle turned left, the absolute value of the difference in cognitive reaction time between when the vehicle was with road projection and when without was large and the p-value was small. This was presumably because, in the experimental setup of this study, the distance between the vehicle and the bicycle on the shoulder was shorter when the vehicle turned left than when it turned right. When the distance between the vehicle and the bicycle was closer, the movement of the vehicle and the road projection felt faster to the bicyclist even if the vehicle moved at the same speed, which made it more noticeable to the bicyclist.

Further, the standard deviation was smaller for both right-turn and left-turn scenes when the vehicle turned without road projection. This was presumably because the timing at which the participant noticed the vehicle with road projection was different: some noticed the approaching vehicle when the road projection lamp was on, while others noticed it when the lamp was off. On the other hand, since the timing at which the vehicle came into the sight of the bicyclist was the same for all trials, it is considered that there was little difference in the timing at which the participant noticed it. However, the standard deviation for when they noticed it when the vehicle turned with road projection was smaller than the difference in cognitive reaction times between when the vehicle turned with road projection and when without. Therefore, it is suggested that, for the participants who were slow to notice the road projection, the cognitive reaction time was shortened by road projection.

5.2 Effectiveness evaluation: Comparison of the TTC

Figures 15 and 16 show histograms of the time-to-collision (TTC), i.e., the number of seconds before the predicted time of collision, for each condition. The horizontal axis represents the time of recognition, with zero being the time of collision. The vertical axis indicates the number of people who recognized the risk of collision at that time.

The histogram shows that, in the left-turn scenes where the vehicle turned without road projection, there were no participants who noticed the risk of collision before 1.2s, while they noticed the risk when the vehicle turned with road projection, most between 1.6s and 1.8s, which indicates that road projection was highly effective in the left-turn scenes.

In the right-turn scenes, too, the peak shifts to the left as in the left-turn scenes, but the change in the number of participants who did so was less pronounced than in the left-turn scenes.

The average time for a human, after noticing an obstacle ahead, to take action to avoid a collision is said to be 0.4s. The TTC for the bicyclist when the vehicle turned right with road projection was 1.85s and 1.44s for when it turned left, both of which were longer than 0.4s.

Further, the margin of distance increased by 4 m (= $5 \text{ m/s} \times (1.44 - 0.6 \text{ s})$) (calculated from the bicycle speed in this experiment of $18 \text{ km/h} = 5 \text{ m/s}$ and the stopping time for a regular bicycle of 0.6s). This is more than twice the stopping distance of a regular bicycle (1.5 m), which means that the bicyclist and the vehicle going straight through the intersection were far away enough from each other.

From the above, it is considered that vehicles with road projection increase the TTC and margin distance, helping other road users avoid collision.

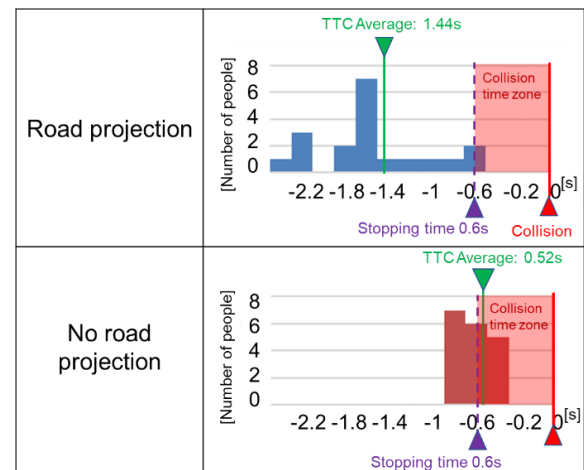


Figure 15: Comparison of TTC of left turn scene of effectiveness evaluation(Solid line:average TTC, Dotted line:braking time of 18km/h bicycle)

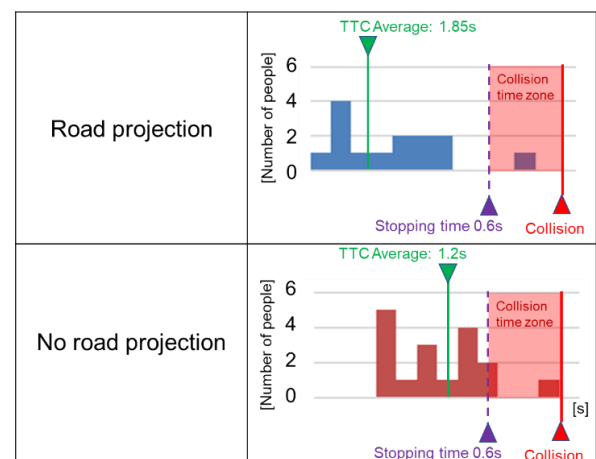


Figure 16: Comparison of TTC of right turn scene of effectiveness evaluation(Solid line:average TTC, Dotted line:braking time of 18km/h bicycle)

5.3 Conflict evaluation: Comparison of cognitive reaction time

We confirmed that there was no difference in the bicyclist's cognitive reaction time, whether the vehicle turned with or without road projection, for both right-turn and left-turn scenes, and found no significant difference.

This was presumably because the participants did not have to keep looking at the road projection of the vehicle coming from behind and were not deterred from noticing the vehicle coming from the side to cross the intersection. When setting the specifications of the road projection lamps, it is important to select a design and flashing frequency that help other road users to notice the vehicle without having to stare at it coming.

6. Conclusion

This study evaluated the effectiveness and conflict of road projection lamps using a VR system. Two types of scenes were set up in the VR environment, one in which a vehicle turned right and the other in which it turned left, and the cognitive reaction time of the participants acting as a bicyclist was measured when the vehicle turned with road projection and when without.

In the effectiveness evaluation, we measured the bicyclist's cognitive reaction time to the vehicle with a road projection lamp and confirmed that the time was significantly shorter when the vehicle turned with road projection, both in right-turning and left-turning scenes.

On the other hand, in the conflict evaluation, the cognitive reaction time of a bicyclist, who was being approached by the vehicle coming from behind, to another vehicle coming from the side to go straight through the intersection, was measured using the same method as the effectiveness evaluation. It was confirmed that there was no difference in the bicyclist's cognitive reaction time regardless of whether the vehicle coming from behind turned right or left, or whether it was with road projection or without. This proved that a VR system can be used to properly evaluate both the effectiveness and conflict of road projection lamps.

VR systems allow us to evaluate various subjects by simulating actual traffic environments without being restricted by location or time. However, the horizontal field of vision of VR-HMDs is currently about 110°, which is narrower than the average human's field of vision (about 200°), requiring us to select appropriate experimental conditions. We look forward to the development of VR-HMDs in the future.

Eventually, it will be necessary to conduct real-world experiments, but VR systems are surely efficient and safe for preliminary evaluations.

In the future, we plan to keep conducting evaluations of road projections by using VR systems in traffic environments other than intersections (such as parking lots) and scenes where multiple vehicles are involved. Building on the advantages of VR, we will continue our evaluations toward the commercialization of road projection lamps.

7. Acknowledgement

We sincerely thank all the participants who assisted this study.

8. References

- [1] Y. Shibata: "Required Luminous Intensity and Glare Inspection of Road Projection Lamp for Turn Signal Lamp", JSAE transaction, 2020, 51(6): 1068-1074.
- [2] T. Singer: "Behavior of automated vehicles in critical situations with pedestrians – Accident prevention through additional light signals", SIA VISION Congress, Paris, France, 2021.
- [3] Y. Aoki: "The Risk Evaluation of Smartphone Use while Cycling and Alert Effect by Road Projection of Turn Signal Light", JSAE review, 2021, 20216222.
- [4] T. Singer: "Investigation and comparison of pedestrian behaviour in different encounter scene with automated vehicles", Proceeding of International Symposium on Automotive Lighting (ISAL) 2019, p.557-566 (2021).
- [5] T. Daimon: "Communication between autonomous vehicles and pedestrians/traffic participants – External HMI(Human Machine Interface)", SIP-adus Workshop 2020, (2020).
- [6] International comparison of traffic accidents, ITARDA (2019).
- [7] Traffic statistics, ITARDA (2019).
- [8] ITARDA information No. 95, ITARDA (2012).
- [9] <https://unece.org/sites/default/files/2021-05/R148e.pdf>

9. Glossary

VR: Virtual Reality
HMD: Head Mounted Display
TTC: Time To Collision

Where does the driver need light?

International survey for a customer-oriented assessment of headlights

C. Hinterwälder¹, Dr. M. Hamm², Dr. J. Kobbert³, M. Braun⁴

1,2,3,4: Audi AG, Headlight Development, 85045 Ingolstadt, Germany

Abstract: This paper presents the results of a survey with more than 400 international participants to make headlight evaluation criteria more customer-oriented. Based on the survey results, the selection and weighting of benchmark criteria can be discussed and optimized within existing evaluation systems. The survey deals with the subjective assessments of the relevance of various criteria for headlamp light distributions. In particular, the personal perceptions regarding the headlight benchmark criteria, such as brightness, range, width and homogeneity, are analysed depending on different types of roads (city, highway and country road). The results provide an opportunity to adapt the objective assessment of headlights closer to the subjective perception of the drivers.

Keywords: Headlight Benchmark, Survey, Evaluation Criteria, Road Safety, Headlight assessment

1. Introduction

Headlights illuminate the road in the dark and thus make a major contribution to road safety. Due to the lighting, the driver is able to recognize the course of the road and objects at an early stage and react accordingly. Therefore, headlights must meet legal requirements for approval. Headlight rating systems use various criteria to test the performance of headlights above the criteria set by law makers. The test result is intended to provide the consumer with information and orientation. Figure 1 illustrates the rating principle of such a system compared to legal requirements that only distinguish between allowed and not allowed.

Legal requirements	Headlight rating
Fulfilled	very good
	good
	satisfying
	sufficient
	deficient
	insufficient

Figure 1: Example of a headlight evaluation

Some of the existing evaluation systems differ fundamentally in the test procedure and in the selection and weighting of the criteria used for evaluation. This can lead to very different rating results of the same headlight model, which can contribute to consumer confusion. Furthermore, the objectively determined rating does not have to correspond to the subjective impression.

Personal perception depends on many factors and is difficult to understand. With the help of a survey, this paper analyses the subjective relevance of the evaluation criteria of automotive headlights. Based on the survey results, the selection and weighting of the criteria used for the assessment can be questioned and optimized within existing systems.

2. Assessment of Headlights

Headlight rating systems try to make a statement about the performance of headlights and the resulting increase in road safety when driving at dusk and at night. However, the criteria used differ and partly contradict in different rating systems. Furthermore, the criteria that were queried in the questionnaire are presented.

2.1 Headlight Rating Systems

While some benchmark systems rely on a simulative determination of the measured values, others benchmark the headlights on defined test tracks. Even under crucial boundary conditions, such as the previous aiming of the headlights, there are discrepancies that contribute to very different rating results.

Visibility is for example assessed on the basis of the distance at which 5lx is reached and continuously maintained until the vehicle is 10m away from the sensor. The question arises whether this criterion reflects the subjective feeling of the customers or the security gain?

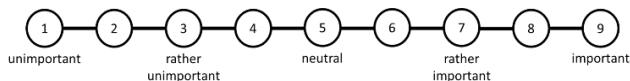
The Headlamp-Safety-Performance Rating (HSPR) evaluates the adaptive driving beam (ADB) depending on its performance. Other systems give only bonus points regardless of the ADB performance. Furthermore, no current rating system

considers the homogeneity of headlights as a plus point for customer comfort. At this point, many differences between the systems and many points that are not evaluated can be listed.

In the next step, a comparison must take place between the objective assessment of the light performance and the subjective perception.

2.2 Criteria in the Questionnaire

The criteria brightness, range, width and homogeneity of the light distribution are to be evaluated for driving on the motorway, country road and in the city. Based on the de Boer scale, respondents can assign a score of 1 to 9 [1]. As can be seen in Figure 2, the subjectively perceived relevance increases with the selected value.



Figur 2: de Boer scale used in the questionnaire

To illustrate the different traffic situations, an image of the corresponding scenario with identification of the examined criteria was inserted in the questionnaire. Furthermore, in addition to the personal data, questions about driving habits were also queried.

3. Survey

In this section, the results of the survey are presented and interpreted. First, the demographic data and the driving-related data is analyzed. This is followed by the evaluation criteria, which are considered important, divided into the driving situation city, country road and motorway.

3.1. Demographic and Driving-Related Data

The 410 fully completed questionnaires were completed by 82 women (20.0%) and 207 men (50.5%). 121 people (29.5%) did not report a gender. The average age of participants is 31.26 years with a standard deviation (s) of 12.65 years, with no participant under 18 or over 80 years of age. With 221 votes (53.9%), the majority stated that they were in the age range of 18 - 26 years. The exact distribution within the age ranges can be taken from Figure 3.

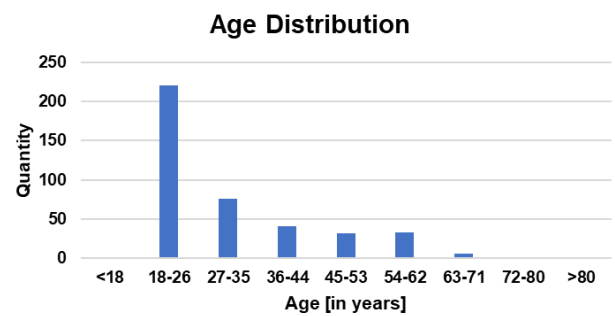


Figure 3: Age distribution of survey participants

Most of the participants' kilometers were driven in Europe with 375 votes (91.5%). Asia follows with 16 (3.9%) and North America with 11 responses (2.7%).

The most common vehicle classes are the middle class with 175 participants (42.7%) and the small car class with 134 (32.7%). When compared with Statista's statistics, mid-range vehicles with a share of 41.3% are the most frequently represented in Germany in 2021 and small cars with 18.5% [2].

A total of 56 people (13.7%) stated that they did not know or could not provide any information about the low beam technology installed in their own vehicle. The remaining votes were therefore considered 100%. 153 participants (43.2%) stated that halogen headlights are installed in their vehicle. This corresponds to a significant decrease of 29.7% compared to Zydek's evaluation in 2014 [3]. 103 participants (29.1%) reported having LED headlights on the vehicle, closely followed by 98 votes (27.7%) for xenon headlights. Compared to the survey results from 8 years ago, this represents an increase of 27.5% in LED headlights. Xenon remains at a similar level with an increase of 2.2% [3]. Figure 4 shows the distribution of the installed lighting technology.

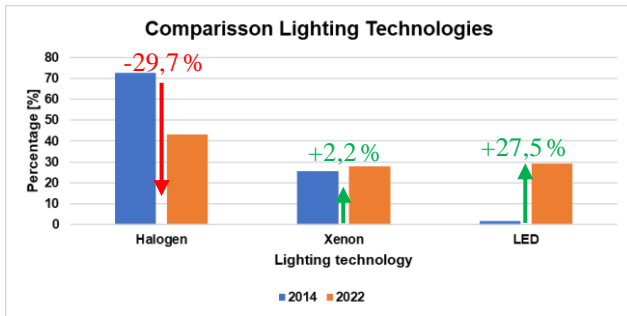


Figure 4: Distribution of lighting technologies in 2014 and 2022

When considering the lighting technologies within selected vehicle classes, only the groups small car, middle class and luxury class are used for comparison, as a price increase can be observed between them. There has been a decrease in the percentage of halogen headlights and an increase in LED headlights in vehicles of higher categories. All three halogen ($p = 1.016 \cdot 10^{-22}$) and xenon ($p = 4.584 \cdot 10^{-16}$) and LED ($p = 9.564 \cdot 10^{-13}$) show significant differences in the lighting technology components of the selected vehicle classes. The exact distribution can be found in Figure 5.

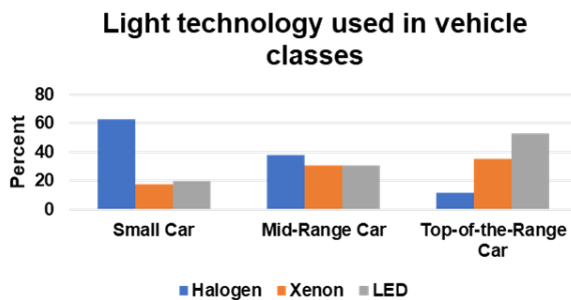


Figure 5: Built-in lighting technology in vehicle class

In the next question, the participants were asked whether they were satisfied with the performance of the headlights of their own vehicle. 17 participants did not provide any information. With the exception of these, 268 people (68.2%) are currently satisfied, 125 (31.8%) are not.

Taking into account the lighting technology, there are sometimes large significant differences ($p = 9.912 \cdot 10^{-28}$).

Halogen headlights perform worst among participants with a satisfaction rate of 36.3%. Xenon and LEDs, on the other hand, are at a similarly high level of 87.6% and 90.2% respectively, as Figure 6 illustrates.

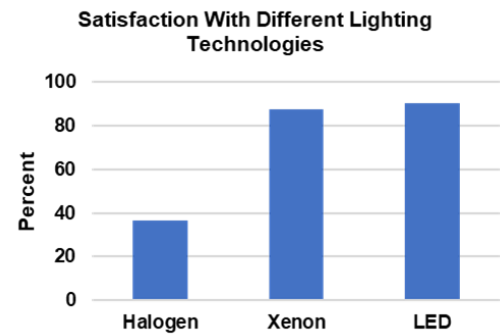


Figure 6: Satisfaction differed by lighting technology

Thus, the more modern the lighting technology, the more satisfied the respondents are with the performance of their headlights.

4.0 Relevance of the Illumination Criteria

In the following, the relevance of various criteria with regard to road illumination, which has been evaluated from the driver's point of view, is analyzed.

4.1 Relevance on Motorway

When driving on the motorway, the range of the headlights is most important to the respondents with a value of 7.79 ($s = 1.38$), followed by the brightness with 7.35 ($s = 1.52$). The width is also classified as rather important with 6.26 points ($s = 1.88$), while the homogeneity of the light distribution is rated as neutral with a value of 5.23 ($s = 2.17$). Figure 7 shows the overview of the evaluated criteria on the motorway.

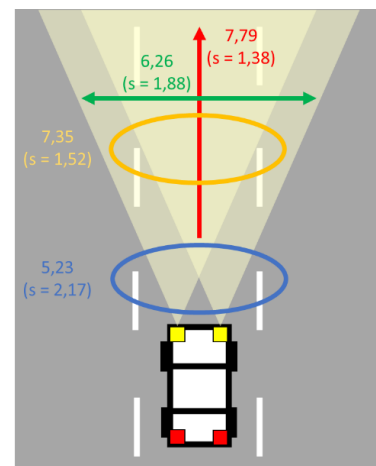


Figure 7: Importance of the criteria brightness (yellow), range (red), width (green) and homogeneity (blue) on the motorway

4.2 Relevance on Country Roads

The same order of criteria also results for the country road scenario. Range and brightness are rated as important with an average value of 8.04 ($s = 1.22$) and 7.81 ($s = 1.45$) respectively. With 7.39 points ($s = 1.73$), the test persons also find width illumination important. The relevance of homogeneity is also considered neutral in this scenario with 5.60 ($s = 2.15$). The relevance of the criteria for country road driving is shown in Figure 8.

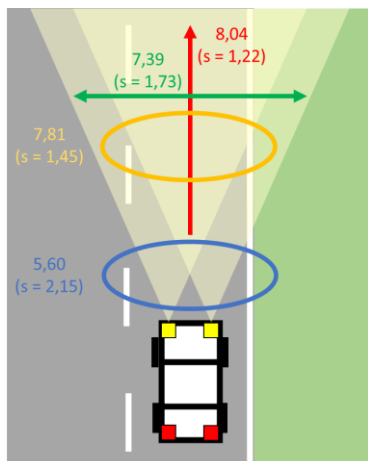


Figure 8: Importance of the criteria brightness (yellow), range (red), width (green) and homogeneity (blue) on country roads

4.3 Relevance in the City

When driving through the city, a change in the order of relevance can be observed. The width reaches a value of 6.22 ($s = 2.05$) and thus represents the most relevant criterion. The brightness is in 2nd place with 5.81 points ($s = 2.06$), the homogeneity with 5.23 ($s = 2.28$) in 3rd place. The range moves from the first to the last place compared to the motorway and country road scenario. This criterion is only rated with 5.12 points ($s = 1.94$).

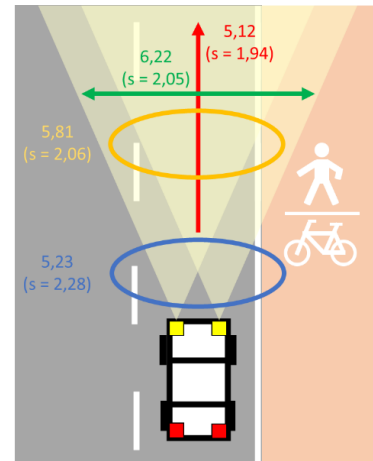


Figure 9: Importance of the criteria brightness (yellow), range (red), width (green) and homogeneity (blue) on city roads

The relevance mean values of the illumination criteria show significant deviations both on the motorway ($p = 2.911 \cdot 10^{-97}$) and on the country road ($p = 2.240 \cdot 10^{-100}$) and in the city ($p = 1.006 \cdot 10^{-15}$).

5 Summary of Criteria Across All Routes

Figure 10 shows the average of the four criteria for motorway, country road and city driving. The homogeneity is considered neutral in all scenarios, and thus overall as the least important criterion. The brightness and range of the road illumination caused by the headlights are classified as the most important factors when driving on motorways and country roads. In the city, on the other hand, the width for the detection of pedestrians and cyclists passing laterally is the most important. The relevance of the range decreases there because of the lower driving speed. The generally low relevance values of all criteria for the city scenario can be traced back by the streets, which are largely well illuminated by street lamps. The importance of the headlights decreases by driving through the city. On motorways and country roads, you are more dependent on your own vehicle headlights, which explains the average higher values in these scenarios.

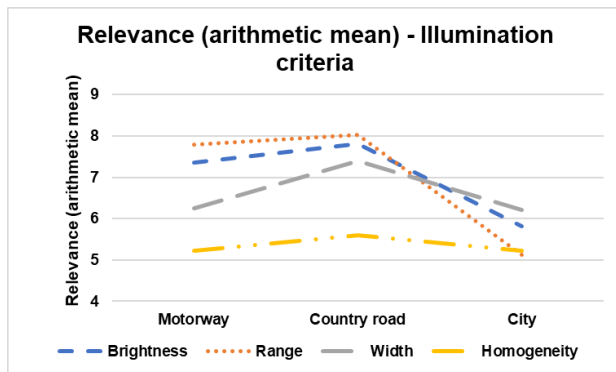


Figure 10: Overview of the 4 criteria across all road sections.

6. Conclusion

Based on a large international online survey, the paper shows how the subjective perception during night driving and the relevance of selected criteria for headlight evaluation depends on the road scenario. According to the survey's results, the lighting technology installed in the car has a strong influence on satisfaction with the headlights. In particular, the personal perceptions regarding the illumination criteria, such as brightness, range, width and homogeneity of the light distribution, were analyzed and compared depending on different road types.

The subjective relevance determination of the headlight evaluation criteria is strongly participant-dependent, but due to the high number of test participants quite meaningful.

The brightness and range of the road illumination caused by the headlights are classified as the most important factors when driving on motorways and country roads. The homogeneity of the headlamps is considered neutral in all scenarios, and thus overall the least important criterion. Nevertheless, when driving in the city, it is considered more important than the range. Homogeneity is not highly safety-relevant but in contrast, the homogeneity is not applied in a objective headlight evaluation system. Modern headlight rating systems should therefore also deal with the issue of the homogeneity of headlights.

For an evaluation of the vehicle headlights, however, it must be checked whether the criteria perceived as important by the respondents actually have a high safety relevance or only use them for comfort.

7. Acknowledgement

The authors acknowledge the contribution of their colleagues to this work and all participants of the questionnaire around the world.

8. References

- [1] De Boer, J.B., Visual Perception in Road Traffic and the Field of Vision of the Motorist (Public Lighting, 1967), 11-96.
- [2] Statista, „Verteilung der Personenkraftwagen in Deutschland nach Segmenten von 2012 bis 2021,“ 2022. [Online]. Available: <https://de.statista.com/statistik/daten/studie/316734/umfrage/pkw-bestand-in-deutschland-nach-segmenten-anteile/>. [Access on 14. September 2022].
- [3] B.W.Zydek, „Blendungsbewertung von Kraftfahrzeugscheinwerfern unter dynamischen Bedingungen,“ Technischen Universität Darmstadt, Darmstadt, 2014. [Online]. Available: <https://dnb.info/1110902026/34>.

Ambitious front lighting Ratings and latest updates of Regulations world-wide: The perfect match?

A. Austerschulte¹, S. Spatzek¹, F. Freytag¹

1: Marelli Automotive Lighting Reutlingen GmbH, Tübingerstraße 123, 72762 Reutlingen, Germany

Abstract: Several changes of influence factors for automotive lighting are gaining relevance.

This are for example regulation extensions, consolidations or updates of the FMVSS108 or the UN-ECE R149. For the GBs of China, there are already drafts available, that might come into force soon. Another set of factors is related to headlamp rating systems, with a clear focus on front lighting performance, that are receiving more consideration.

On the other hand, we notice the technical evolutions that are related to flexible software driven beam patterns. We want to highlight related aspects and therefore compare the latest of regulations, overlay them with the most respected rating systems and analyze, if latest technology of main function optics can provide optimized solutions.

Keywords: Regulations, ratings, front lighting, software, HD, ADB

1. Introduction

The basis for front lighting systems is to comply with the regulation of their target region. Some examples of regulation will be presented briefly in chapter 2, so that we could refer to them later. Within this frameset of regulations, several different solutions in terms of function and design and performance are available. In chapter 3, we want to address some platform systems from basic functionality up to high performance adaptive ones. Ratings, that we address in chapter 4, are a famous and easy way for potential car owners to inform themselves and compare options precise. Having described the actual circumstances in the previous chapters, minimizing the efforts to develop headlamp solutions for different markets at the same time is a strategic goal, but there are still some challenges within the latest versions and drafts of regulations, that we want to highlight based on a few examples, in chapter 5 together with an overview table of the best possible ratings vs. technical system and function for worldwide applications.

2. Regulations worldwide

The key off the reviewed regulations is to ensure, that all necessary lighting functions for a save driving during day and nighttime are available at all cars. In addition, the regulations are defining standards on how the individual function needs to perform so to guaranty a minimum performance on one hand and on the other hand minimize the distraction or any other unintended impact of other traffic participants. Because traffic conditions are changing and they're different for the regions of the world and the technical improvements were significant during the last decades, adaption of regulation were seen as a necessity by most regulators. We picked three regulations setting to review in this paper and mention the draft of an upcoming regulation change. We highlight the FMVSS 108, the GB and GB/T of China as well as the revised UN-ECE R149 for 2023 and refer to a draft of a new consolidating GB, that might be in force within 2024 already. These regulations were chosen because they cover a big share of today's market and reflect implicitly also a huge portion of the intention of other important regulations and adaption like the CMVSS, the KMVSS, the Indian, Japanese, and Australian. Because of the high relevance already and in forecast for future market trends, we will focus our investigations on topics related to LED systems only.

2.1 United Nations Economic Commission for Europe (UN/ECE)

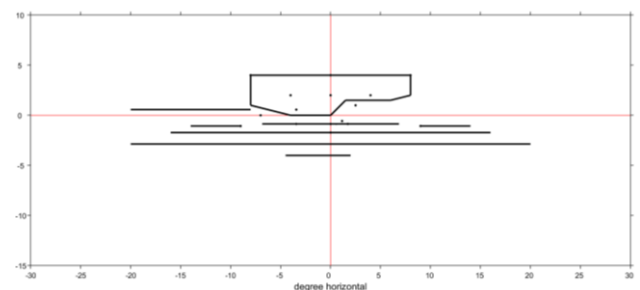


Figure 1: Sketch of the locations of selected LB class-C regulation-point, -slice and -zone definitions of the UN-ECE R149-1.

The front lighting regulations for road illumination devices (RID) of for the UN-ECE have recently been consolidated to the R149. For 2023, an update will go

into force. Whereas the R149 was intended to be a consolidation of multiple regulations in only one, without changing the content; the new amendments will target the simplification and refreshing of the rule. With this, several technical relevant changes will be introduced. Most of them target an improved minimum performance request while at the same time formulating technology independency and keeping established visibility and glare relations unchanged. But there are a few important exceptions (see figure 1). For example, the LB maximum performance won't be limited anymore for standard countryside driving, like with AFS class C and motorways of class E.

The low beam, intended for country-side driving, is still the basic light function, where HB and Adaptive Driving Beam (ADB) are in addition necessary or an option to improve visibility when possible or equipped. The intention of low beam is essentially to guarantee a good illumination in front of the car with a distinct cut-off line to the upper area above the horizon, where minimum glare is intended while still a good visibility by others and traffic sign recognition needs to be insured. Due the fundamental relevance of low beams, we present those related regulation sketches. They give an impression of today's wide variety of regulations for the markets, as can be see already when comparing with the GB's of the next paragraph.

2.2 China GB and GB/T

The front lighting regulations of China were reviewed regularly, too. For LED main functions the GB 25991-2010 must be considered (figure 2). In case of advanced functions, the GB/T 30036-2013 is ruling in addition (figure 3). This setting of regulations is relative consistent. But there are considerations ongoing and drafts available that target a consolidation of those and further GB's in one. The drafts were undergoing frequent updates during the past months. But not before 2024, a settled official update is expected, by parts of the community. A new GB might open also for assistance projection functions. The later would be a well perceived recognition of latest technology advance.

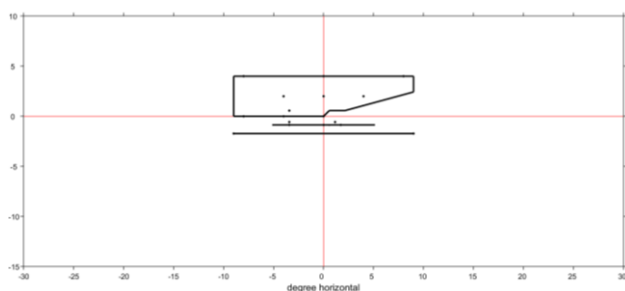


Figure 2: Sketch of the locations of selected LB regulation-point, -slice and -zone definitions of the GB 25991-2010.

Looking forward in the announcement of the official update of the China regulations, there is hope that, beside considering the special necessities of the local traffic conditions, a larger overlap with the latest UN-ECE regulation might be initiated (compare figures 1 with 2 and 3).

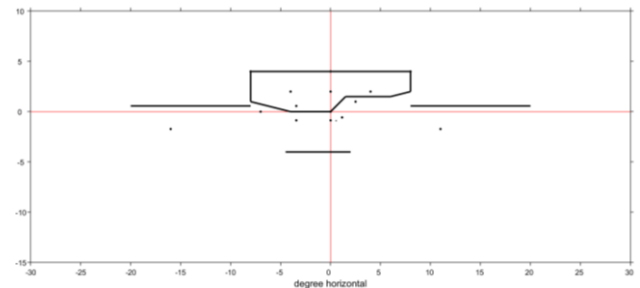


Figure 3: Sketch of the locations of selected LB class-C regulation-point, -slice and -zone definitions of the GB/T 30036-2013.

2.3 United States of America, FMVSS 108

The front lighting regulation that must be considered for the United States of America is the FMVSS 108 (see figure 4 regarding to LB). On the 22nd of February 2022 a significantly extended version was enforced.

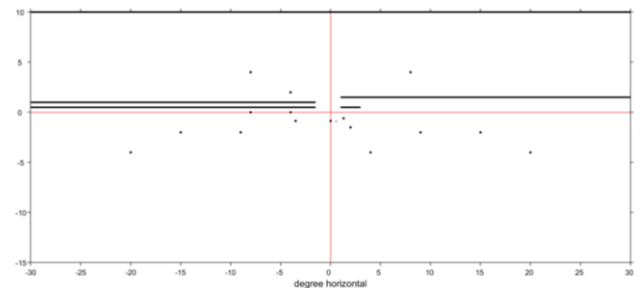


Figure 4: Sketch of the locations of selected LB regulation-point and -slice definitions of the FMVSS108.

This new version of the regulation is adding explicitly the rules for Adaptive Driving Beam for the US. The expected exceptional combination of laboratory measurements as well as test track evaluations of the whole car, adds a distinct amount of complexity to the design of adequate systems. This has been discussed in detail by authors before and it led to several expressed comments on the final rule. Nevertheless, the taste of the new rulemaking, considering implicit an expectation to further glare reductions during ADB activation, in case compared with high minimum overhead requirements of the unchanged LB formulations, can be noticed. In the sum of the aspects, a feasibility of fulfilling all laboratory measurements is possible achieve current ADB systems, but the system approach with a theoretically infinite number of different test conditions on test tracks, needs to undergo a further

interpretation alignment before statements could be given. Having LB and HB unchanged, they will be still the most important part of the regulation for the near future. Here a specialty of the FMVSS 108 LB can be seen directly at the HV point, by comparing the figures 1,2,3 and 4. And this has an impact on the worldwide applications of headlamps, as we want to discuss in the next paragraph and in chapter 5.

2.4 Adapting to the World

Today these and many more different regulations are existing in parallel. It is unlikely to happen in a short term, that a comprehensive harmonization would lead to a single light distribution that guarantees conformity to all regulations. A big difficulty, not further discussed, would be to cover RHT and LHT demands at the same time. On the other hand, adaptive software driven light distributions with different levels of precision, could provide a certain flexibility to cover several regulations. Software defined beam pattern and their plasticity are the most advanced approach and might come closest to the full flexibility in terms of regulation, with just one hardware setting. Simplification by just taking care of LB, HB and ADB function together with the performance in ratings and the chance to cover multiple different regulations will be analyzed for different technology levels in chapter 4 and 5. But before, module examples for each of the LED headlamp main function categories will be presented, to have a basic impression about up-to-date technical platform solutions.

3. Lighting solutions

3.1 LED Basic



Figure 5: Illustration of a LED Basic LB/HB projection module.

LED headlamps with basic LB and HB function are gaining a significant and vastly increasing market share compared to Halogen systems. They're the choice for good performances on an entry- or mid-level. There are two main realizations of this function. One is based on multiple LEDs in reflection systems. They're having one or more optical chambers for each function corresponding to LB and HB. These reflection type solutions were perceived as the most cost-efficient solutions for LED functions during the last years. Bi-function lens projection systems are an alternative that is expanding market share, due to

their compact geometry and off the shelf availability. Now the choice is up to the design, space and brand considerations. One examples of Marelli solutions can be seen with the new headlamp of the Buick Envista. The Buick benefits from the latest generation of LED-Bi-function projectors (figure 5). Another example is the Chrysler Pacifica. Projectors for regulations world-wide are available out of the box. As can be seen in later regarding ratings, these LB/HB projectors are capable to achieve already high scores at several ratings. Especially on those, that are not considering advanced functions like they are available with LED-ADB systems.

3.2 LED – ADB Entry

ADB Entry lighting systems are providing a big step up in performance, when compared to LED Basic systems. Here the high additional activation time of ADB segments, compared to manual or automated High Beam of Basic systems, is dominant in the impression of the driver. Already with 10 to 12 segments per headlamp, a good ADB function perception can be realized. The additional on time of selected ADB segments, when classic HB would have been switched off already, can be seen for overall night-time driving in figure 6 that was presented in [1] and is cited with the courtesy of the colleagues. With a selective look at country-side driving, it was shown already [2], that in more than 95% of the time, segments are activated. This is bringing the additional light for safety.

Average activation times	LB	HB	ADB
manually operated HB	95%	5%	-
automatically operated HB	80%	20%	-
ADB	30%	20%	50%

Figure 6: Average activation time for LB, HB and ADB. From [1]

The ADB function and their positive impact wasn't foreseen during the early research and alignment done for some of today's headlamp rating systems, that will be discussed in the following chapter 4. But here we want to mention already, that there is not always a recognition of the ADB benefits within their scope. This is for example true for the TC4-45 rating scheme as well as for the famous IIHS rating in the US. But ADB is considered for some and will be a key enabler for good HSPR ratings, as we can see later. From a regulation point of view, most markets at least consider now the application of those systems. Latest update was for example the mentioned extension of the FMVSS108. LED-ADB Entry systems are, as we see them today, fit for the laboratory measurements, of the regulation. But their limited flexibility, compared

to ADB High systems, is somehow keeping them away from being the first choice for the application in the US. But with hardware adaptations those systems could be configured to match all other markets WW.



Figure 7: Illustration of a LED-ADB Entry LB/ADB 1-row projection module

So, LED-ADB Entry systems are very strong for established ADB markets to provide drivers with the main benefits of ADB. The function is available with single or multiple lens projection systems as well as with reflectors or special style optics. For most systems seen today, single or dual lens projection systems are the major choice. Marelli's new generation of Bi-Function-ADB Modules with 12 to 16 segments in one row (see figure 7) or a set of a low beam together with a 1 row ADB module are available as platform parts. Examples of 1 row ADB applications could be found with the DS 4 and Alfa Romeo Tonale of Stellantis.

3.3 LED – ADB Mid

ADB-Mid systems are adding another level of flexibility, due to providing at least 2 rows of and up to some hundreds of pixels. The flexibility given by the additional rows of ADB is useful for additional software driven safety functions. There is the LB swiveling and some adaptations of the cut-off line. Another asset of ADB-Mid is the potential for a WW application with regulation adaption by software. With this, they are the interesting combination of intermediate effort and high value of ADB-Entry together with the flexibility of an adaption to different markets, just by software.



Figure 8: Illustration of a LED-ADB Mid projection module combination of a LB- and a 2-row ADB-projection module.

Unfortunately, for most of the ratings, these systems will be perceived comparable to LED-ADB-Entry systems as will be discussed in detail later.

With Marelli's portfolio, there are several opportunities to realize LED-ADB Mid systems with projection systems. One can be seen in figure 8. Recent applications at the Stellantis group could be found for example with the DS7, the DS9 and the Opel Grandland.

3.4 LED – ADB High

This is the open class for performance and flexibility. Beside the well-known and high performant DMD systems (figure 9), that are available since some years, we expect a typical system of the near future to be equipped with LED array pixel light source solutions. They are featuring more than 15,000 pixels in multiple rows and columns and are more efficient than the established DMD solutions. But they're suffering some limitations when it comes to the considerations of symbol projections, for example.



Figure 9: Illustration of a LED-ADB High system by a module combination of a bi-function LB/ADB 1-row and a HD-projection module

Generally, LED-ADB High systems are the most adaptable due to the software defined beam pattern [3]. Depending on the field of view, multiple regulations could be matched within the range of given flexibility and at the same time an optimization of the performance on the road is possible. This performance, particularly close to the cut-off line of the LB, as well as to the vertical Edges of ADB switching situations is key for their remarkable recognition in most of the rating evaluations. Recent examples of cars that hit the road with Marelli's HD technology are the Audi A8 as well as the Mercedes EQS.

These headlamps are challenging the rating systems in their own way. Implicitly asking for their capability to consider all the goodies for the best rating. Let's find out about some Headlamp ratings in the next chapter.

4. Headlamp ratings

4.1 Europe: TC 4-45 and HSPR

After first ideas around 2019, that a new and fair rating to evaluate also ADB-functions would be beneficial, a lot of research and investigations were done. This is where the HSPR rating was born. Certainly, it is expected to be officially settled soon. But already before, for example around 2005 to 2007, a lot of expertise was accumulated in the Low Beam and High Beam evaluation methods of the CIE 188:2010 (TC4-45) report. Consequently, HSPR is considering the still valid TC 4-45 assessments as the fundament for evaluating the Low and High Beam portion of the light distributions. Now with HSPR, the values of LB and HB will be weighted and condensed in single values for the first time and combined with the results of the new ADB evaluation and research based physiological correction factors. A complex setup but it provides, based on a solid fundament of research, the simplification and ease of use needed to be recognized. The HSPR gives an easy to catch total performance evaluation result. But the underlying algorithms are the first, that are considering the high efforts of the full adaptive HD systems. And those are expected to be necessary to reach highest evaluation scores (See [1] for reference). In a best case, this rating will be standard across the UN-ECE and well perceived by multipliers and car buyers for orientation.

4.2 China: China-NCAP and C-IASI

For China, today there are two ratings, that are catching the interest of customers. Whereas the China-NCAP rating is the most considered. The C-IASI is getting more and more attention. These ratings are individual approaches but one might find a lot of common approaches with ratings of other traffic regions. The good news is, that care is taken by both types of ratings regarding the impact of new safety functions like automated high beam or ADB. This is a very favorable consideration for the lighting community. Deep diving to the China-NCAP where a maximum of 10 points could be achieved by: An excellent LB performance is worth 6 points. 3 points could be achieved for a good High Beam. The last 1 bonus point is split and related to the availability of automatic or adaptive lighting functions. An automated HB function will be acknowledged by +0.2 points, up to 3 AFS modes by 0.1 points each and 0.5 points for ADB. All in all, a maximum of 10 points can be achieved by excellent lighting with a set of several adaptive functions. Some points are displayed, together with the basic regulation 25991 in figure 10.

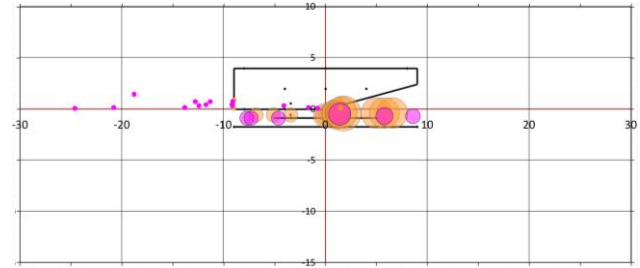


Figure 10: Sketch of GB 25991-2010 LB together with selected performance (big circles) and glare (small circles) indicators of the CN-NCAP (orange) and C-IASI (magenta) ratings. Assumed headlamp mounting height of 850 mm.

C-IASI is a rating based on measurements of light distributions. This is an efficient approach and showing, that the trade-off between illumination and glare avoidance is key for LB (15 points) and a good HB (5 points) performance is beneficial. 2 points of the score are dedicated to automated functions. These are automated light switching, auto leveling and ADB. Subsequently, a score with a maximum of 22 points is derived and part of a total rating for a car. While the lighting score is an important factor of the total car rating, it is gaining less attention than for example, when the lighting is explicitly expelled, like in the IIHS rating. The latter will be in the next paragraph.

4.3 USA: IIHS and US-NCAP

For the lighting community, the US market's today's most valued evaluations are the IIHS and US-NCAP ratings. While the former strong Consumer Report with their evaluation of light distribution is still perceived, it has a significant subjective component of the rating and a different priority in regards of performance vs. perception than most other ratings. With this it is more subjective and unpredictable regarding to the outcome.

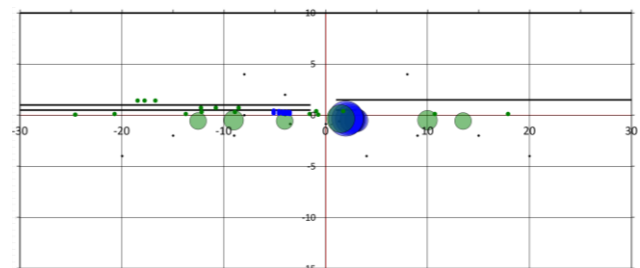


Figure 11: Sketch of FMVSS108 LB together with selected performance (big circles) and glare (small circles) indicators of the US-NCAP (blue) and IIHS (green) ratings. Assumed headlamp mounting height of 850 mm.

Despite this, it is typically leading to a soft cut-off-line for the smoothness perceptions, that is contra indicative for a good IIHS or US-NCAP rating, that are focusing on high illuminances close to the cut-off line.

Please, note figure 11 for an indication. That leads to good illumination in greater distances but with this favoring a higher gradient. IIHS is prominent, but related LB and HB only. Due to this, only swiveled light functions and automated High Beam assist are opportunities for advantages on the test result. In case they would be possible with the new regulation, the ADB function has not been considered so far. But such changes could be considered easily. Maybe, due to bonus factors like with automated high beam. More likely, an extension of the driving setup might be promoted, to gain deeper analysis of the actual functionality. This will be one of the most interesting decision upcoming, to see how first activated ADB systems on the US market might be configured and ratings might evolve to consider the new function.

5. Intersections

Having touched some of the latest topics on regulations and ratings for main traffic regions and after presenting some examples of LED main functions systems, we want to discuss now some of the implications. This is relevant, because any adaption to regions or ratings drives the cost of systems in case hardware needs to be adapted or additional software needs to be developed. We want to highlight opportunities that can improve the systematic efficiency from this point of view.

5.1 UN-ECE and SAE Low Beam exemplary differences

With the regulation as a must have and the additional expectation of achieving ambitions rating targets, there are some points that are tough to overcome. Comparing the LB regulation of the UN-ECE R149-1 with the US FMVSS108, a key area is around the HV point. Same as for the UN-ECE is true for the GBs of China, especially considering the status of the consolidating draft.

All ratings we discussed, respect the LB with high importance. The performance of LB along a straight road is crucial and effectively illuminated by the solid angle close to HV, but below the horizon. Ratings are designed on experience with actual systems and with this, they consider the technical possible within the local given regulations. Means, they are indirectly aiming relative to regulation. Now coming back to the solid angle area around the horizon the ruling is significantly different. For UN-ECE, there no limit anymore for the total maximum in several LB classes, but there is a limit of 1 lx@25m or 625 cd at the HV-point. With the R149-1 it is implicitly given by the definition of the Zone III. Also, due to the definition of the cut-off line position to be at $-0,57^\circ$, there is no significant illumination in the horizontal center below the horizon allowed. This is limiting part of the performance opportunities straight ahead. On the other hand, for a FMVSS108 VOR, one might

interpret, that there is no explicit limit defined in this area (see figure 12). Assuming VOL, the picture doesn't change, because the -0.4° cut-off line position is defined at -2° horizontally, which gives enough room for high intensities below and close to HV.

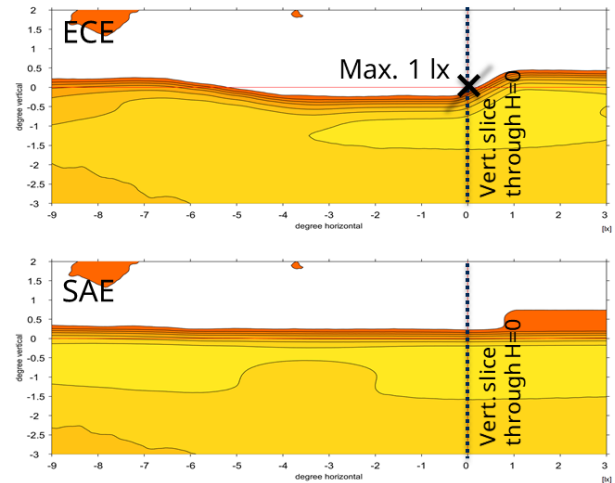


Figure 12: Exemplary ECE und SAE VOR LB light distribution adapted by software from a LED ADB High system, around the HV point.

With this difference in regulation, the basic optical layout of LED Basic and ADB Entry systems need to be adapted to the markets, to cover the expectations of rating results. This is a cost driver due to hardware adaptations in this segment. For LED ADB-High and some of the LED ADB-MID systems, the adaption is easily done by software.

Another difference between the regulation can be found in a vertical cross section through $+1^\circ$ horizontal (see figure 13).

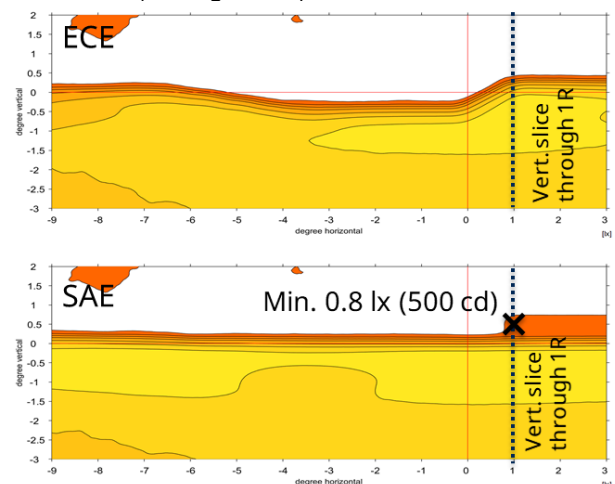


Figure 13: Exemplary ECE and SAE LB light distribution. Highlighting overhead @ 0.5° up.

Here, the main difference is the expectation of the FMVSS 108 LB regulation to guarantee a minimum of 500 cd on the line 0.5° up and at 1° to 3° on the right. The maximum at the line is defined to be 2700 cd. A precise optical layout for the FMVSS LBs is necessary

to actively bring light in this region with a solid safety margin to meet the minimum values. The UN-ECE is not asking for such a high minimum in this area. Ratings, like the IIHS during their driving test, show up also with glare sensors in this area during 150 m right curve driving. Again, different hardware for systems below LED-ADB-MID could be necessary, but not sufficient considering LED-ADB-Entry. This is because of a practical limit of the new FMVSS108 driving test for ADB systems. As stated in other publications before, during the test of ADB systems in right curves, the glare measurements in the dark zone above the horizon expect much lower values for overhead than the 2700 cd. We think that a maximum of 1000 cd might be acceptable when considering some of the additional effects during driving like reflections from the road. For sure this will lead to a different design of overhead solutions for the FMVSS with significantly reduced tolerances. But again, the use of LED ADB-High systems with their flexibility is looking maybe like a solution to overcome the ambiguity within the FMVSS108 LB/ADB easiest and due to this first.

5.2 Headlamp technology for regulations and ratings

Having now a brief picture of several aspects of regulations, ratings and headlamp technology, we want to condense these and further evaluations in a table give in figure 14. The basic efforts for LED headlamp systems increases by category. On the other hand, the flexibility of the systems increases, too. The flexibility and performance of those can be used to differentiate the regional applications in terms of regulation setup and adapt to the local ratings. It is a good development, that HSPR is one of the first ratings that is scoring the high efforts that come with HD applications. And other ratings might adapt soon, too. For now, it is possible to reach maximum ratings already with lower LED headlamp categories. We expect that the flexibility and performance is one of the future drivers for LED ADB-High headlamps.

LED category	HSPR	CNCAP	IIHS	WWV
BASIC	Excellent	> 8.5 *	Good	3
ADB ENTRY	Premium	> 9.0 **	Good	2
ADB MID	Premium	> 9.0 **	Good	1
ADB HIGH	Premium +	> 9.0 **	Good	1

Figure 14: LED headlamp category, achievable rating scores and needs for World-Wide-Versions.

6. Conclusion

This paper highlighted the latest changes and their opportunities in regulations related to front-lighting systems. Specially, the opportunities with UN-ECE-LB and the FMVSS extension to cover ADB systems were discussed. In addition to these regulations, the

according ratings were briefly mentioned. Based on a typical consideration for a car application, that must cover several regions at a time and intending to benefit from the well perceived results of rating evaluation, the opportunities to limit the hardware versions by getting full benefit of software driven light distributions was negotiated. In addition, example platform module solutions of the Marelli portfolio were given for all 4 major groups LED headlamp performance levels.

The good news is, that even if the traffic and driving in the regions seem to be significantly different, because the regulations are, they allow a fairly save driving in their region at night, for decades now. But we hope that we could emphasize, that there is room for safety improvements and efficiency left.

7. Acknowledgement

The authors would like to thank the team of Marelli Automotive Lighting Reutlingen R&D department for their engagement in finding, sharing, and implementing some of the best solutions to illuminate the roads during nighttime driving. This paper is based on the experience and work of the team.

8. References

- [1] F. Freytag, E.-O. Rosenhahn: Headlamp Safety Performance Rating (HSPR), ISAL 2021, (Darmstadt, Germany), 2022.
- [2] A. Austerschulte, B. Dreier, E.-O. Rosenhahn: "Analysis of Safety Aspects for LED Matrix High Beam Functions", ISAL 2013, (Darmstadt, Germany), 2013.
- [3] K. F. Albrecht, A. Austerschulte, E.-O. Rosenhahn: "Safety Benefit by ultra-flexible Beam Pattern in High Resolution Headlamp Technology", ISAL 2021, (Darmstadt, Germany), 2022.

9. Glossary

ADB:	Adaptive Driving Beam
C-IASI:	China Insurance Automotive Safety Index Protocol
FMVSS:	Federal Motor Vehicle Safety Standard
GB:	National Standard of the People's Republic of China
GB/T:	Recommended Standard of the People's Republic of China
HSPR:	Headlamp Safety Performance Rating
IIHS:	Insurance Institute for Highway Safety
NCAP:	New Car Assessment Program
NHTSA:	National Highway Traffic Safety Administration
UN/ECE:	United Nations Economic Commission for Europe

SIMULATION FOR ADAS DEVELOPMENT

Computer Generated Imagery to challenge physical process and mock-up

V. CALAIS, B. DESCHAMPS, J. LORENZI

Renault Group

Abstract: Renault group develops and deploys visual computer simulation solutions and methods to challenge the physical mock-up and to help shorten design loops. The different use cases cover: perceived quality, human-machine interface simulation, windshield reflection simulation, color gap, and other appearance topics. This work requires research and development in computer graphics with different partners and a HPC and GPU computing power, as well as specific display capabilities like 10 bits per component or high luminance output. Through the simulation of lighting and front camera, we will present our state of the art, needs and challenges for this type of simulation.

Keywords: Optical Simulation, Camera, interior lighting, exterior lighting, CGI, GPU computing, HPC

1. Introduction

In automotive industry, computer graphics can serve a variety of purposes, from styling to marketing, with different levels of accuracy, from a beauty shot with a possible bias in the lighting to showcase our product, to a visual simulation for validation. In recent years, the physical based rendering (PBR) approach has become more popular but has not been sufficient to challenge the physical mock-up. PBR software is not enough... How to capture material properties, how to prepare 3D data, how to capture lighting conditions and how to configure the render engine are a big part of the success. This paper presents how, within Renault group, we used computer graphics for the design and for the integration of cameras and lighting systems.

The aim of lighting simulation is to anticipate issues to deliver contractual design and to reduce the number of physical mockups during the design phase. The main challenge of our approach is that we are not only targeting to imitate some measurement like a picture or luminance map but to challenge the human perception of a real mockup. Thus, to combine objective and subjective approach. This makes the required level of accuracy and the work much harder as each human and its perception is unique and present bias that we need to deal with. Lighting

domain requests specific tools and capabilities for lighting parts rendering. First topic when function switched off is the diversity of textures and materials in a small volume where light interacts with. Another point is the management of transparent and diffusive materials with high computing cost. To find the good algorithm for off aspect is more difficult than for other parts of the car, like dashboard or car paint. When function switched on, these calculations bring an additional layer of complexity and need of computation power. In our presentation we will describe the challenges and difficulties we have overcome.

For the front camera simulation, the challenge is to replicate the physical process of validation of our supplier in early design phase to manage efficient integration of the front camera on the targeted vehicle with its parameters like orientation of the windshield, the glareshield design or the material being used for the glareshield.

2. Lighting simulation

Lighting systems are becoming increasingly complex and simulating the path of light from the emitter to the outside of the optical stack requires a great definition and knowledge of the system. Unfortunately, some of the materials being used come from a manufacturing process such as the PMMA light guide and defaults due to the manufacturing cannot be fully measured. Moreover, some other materials are not homogeneous like the diffusers.

From this observation, we have to manage a theoretical definition of the material or a partial measurement. This could be perceived as a big bias but with the physical mock-up, we have the same approach, the goal is to manage the convergence; this is why the materials or process used for prototyping are rarely the same used for final industrial production.

After a benchmark of different softwares compared to a physical mock-up the main difference was the capability to produce enough iteration without limit due to the hardware cost or time to compute necessary for that. We have increased by a scale of 1000 the number of iterations requested with a minimum of 1M needed for lighting simulation to

converge. To validate this hypothesis, we have developed a specific approach to compare a physical mock-up to a numerical simulation. The physical evaluation of this type of system reaches the limit of our human capabilities and we can give only a limited objective evaluation without details in terms of homogeneity or light leakage. We use a HDR photography approach to evaluate the physical model and manage the comparison with our simulation.



Figure 1: HDR photography approach for physical evaluation and numerical correlation

To achieve this level of quality and limit computational time, we are using a 275-nodes CPU-based HPC system and are developing a new approach that reduces the time required by at least 3 times and provides the flexibility to simulate different light environments at no additional cost. This approach is based on light path expression algorithm and the capability to combine the contribution of different light sources.

We calculate each technical light source separately and combine the result with the overall rendering of the surrounding lighting and the specific rendering configurations adapted to this type of production. With this approach, we also have the flexibility to adapt some sources by post processing. For example, if a technical light emits 1000 cd/m² in daylight conditions and only 400 cd/m² in night conditions, we have developed a tool that scales the initial result to create a specific configuration in real time.

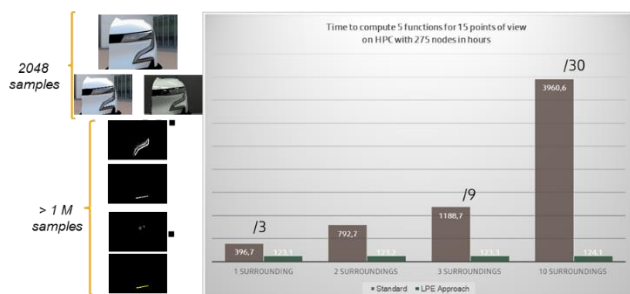


Figure 2: Light path expression (LPE) principle and impact on computing time

For technical design and convergence, we propose a false color post-processing approach to produce objective evaluation with luminance view for homogeneity check, illuminance view for light leak detection and technical evaluation.



Figure 3: Objective evaluation for homogeneity, leak of light analysis, design validation.

Beyond this objective approach, we propose subjective evaluation of our lighting simulation. The objective is to illustrate whether the design meets the specifications of the style department's requirements in the initial phase before the physical prototype or between two physical prototyping loops. The main challenge is how to reproduce in the simulation the dynamics of the physical luminance or the physiological effect due to this luminance such as glare around the sources. For this, we combine a high luminance display (1000 cd/m²) and a post-processing algorithm to emulate the glare effect.

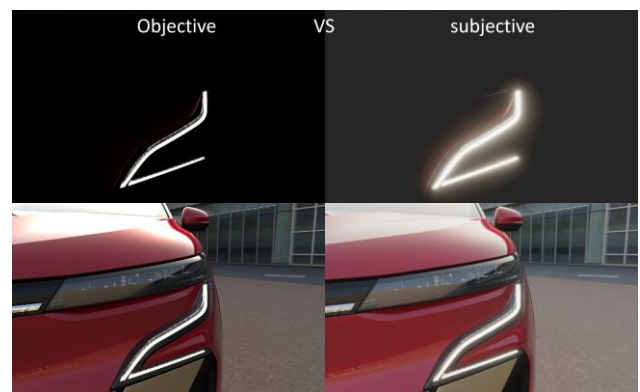


Figure 4: Objective evaluation VS subjective evaluation with eye physiology-based post processing.

As said in the introduction our approach is to give the same perception as a mockup to a human. For that we need to have higher precision and correlation on our objective evaluation than the industry state of the art. We are using less calculation approximations and we increase the precision with a definition that overpasses the physical measurement tools, as well as we realize a constant work on the whole chain of simulation to reduce the approximations that are still existing.

On the subjective evaluation, this is based on this calculation but need an extra link in the chain that is how we display the results to give the feeling of real mockup.

This combination allows us to give to styling department a realistic idea of how what they have drawn will be perceived, for example the perceived

size of a lit object at different distances and if they are still readable.

This approach allows also engineering department to be more confident in their technical choices in upstream phases.

During project development it allows us to check the mockup before the first part is manufactured and to make a technical and Perceived Quality feedback to have early corrections or deep analysis of complex optical phenomenon. This allows us to save time on the project as the problem are caught earlier and the first parts don't present issues from a late modification not fully validated. The Mockup are playing fully their roll of problem catcher.

This simulation offers also compatibility with the virtual twin so the lighting part can be seen and evaluated on the full vehicle that presents the advantage to be able to catch some problem that mockups are not able to detect.

3. Front Camera Simulation

The integration of the ADAS front camera is a delicate step between different actors: the supplier, the camera vendor and the car manufacturer, with a balance between service coverage, cost, cockpit constraint and carry-over target.

At Renault, we are responsible for the design of the glareshield part of the camera in term of geometry, and we manage with our supplier material of the glareshield, the aim is to adapt the camera to the specificity of the current studied vehicle (windshield orientation, cockpit volume, vehicle trim, ...) or limitation of our supplier's manufacturing process.

The challenge is to limit risk of a situation that would turn off or limit the safety service provided by the camera and paid by our customer.

Such situation could arise when strong light reflections hitting the glareshield are entering the lens of the camera.

Usual glareshield verification was done previously with physical part inside a car and a windshield coherent with the serial life.

By adding an optical analysis combined with a molding expertise in phase with the design of the glareshield, there is a way to anticipate the physical test, as described below.

To protect their knowledge, it is often difficult to have the technical definition of the camera that embedded all the optical stack and software of the captor necessary for optical simulation from our supplier.

Even more when the supplier integrates a technology not designed by him.

Based on this situation, we have developed a simulation that analyses the reflection on the external projection of the camera lens limited to a field of view provided by the supplier. This field of view is the result of the optical stack but also the possible software optimisation.

The main risk of the front camera is to receive secondary bounds of light due to a part of the vehicle and mainly from the glareshield.

Our approach is to digitally test several lighting conditions. One scenario is an adaptation of a supplier's physical validation and protocol to ensure that we meet their specifications.



Figure 5: Scenario close to the physical process of supplier.

The second scenario is a predictive approach that automatically detects worst-case lighting conditions and produces a simulation for all pre-calculated sun directions.

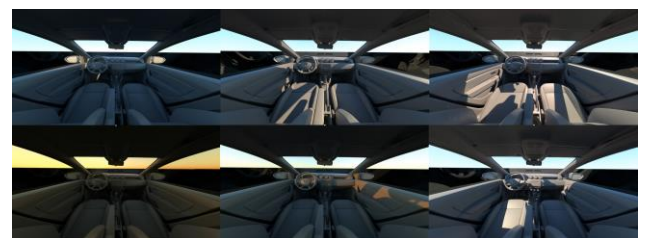


Figure 6: Physical sky simulation from automatic predictive algorithms for the second scenario.

All processing and analysis are based on image processing algorithms and are fully automated.

The material used for the glareshield is measured by our TAC7 scanner from XRite and integrated in our simulation.

We compare the simulation for different CAD and different material and produce a view of the splitted lens surfaces for the different lighting condition.

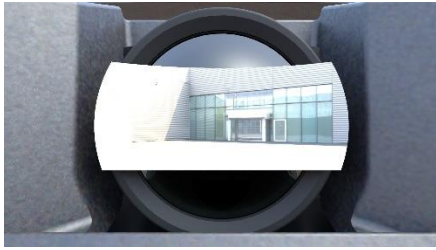


Figure 7: Example of the field of view projected from the camera lens, based on the optical stack and the working area of the embedded software.

For each result we analyse the luminance and compute the contrast ratio to automatically detect the main source, excluding the direct lighting and identifying secondary bounds.

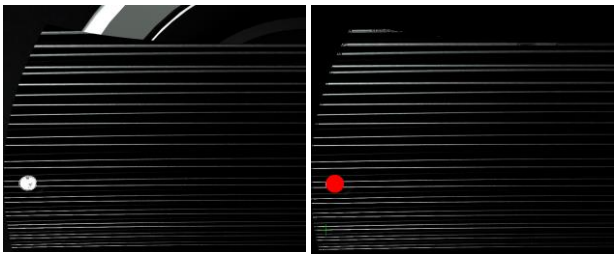


Figure 8: Example of automatic evaluation with detection of the primary source and the main secondary bounds.

We can compare all configurations and improve the availability of the ADAS system.

The main benefit of this approach based on computer graphics is to avoid risk to change the mold at the end of the process with the associated cost and delay.

We complete the process to detect if we have possible lighting condition from cockpit elements like pictogram, display or indirect lighting from reflective part. We manage that by direct visibility analysis based on pixel color detection and cartography.

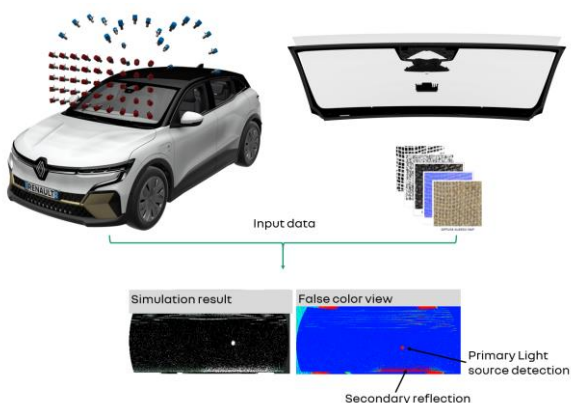


Figure 9: Numerical simulation

4. Conclusion, perspectives and stakes

On lighting simulation, we succeeded to deploy a workflow that challenges the physical mockup but that requests a good knowledge of the optical system simulated and a higher quality off the CAD used for simulation compared to some other simulation use-cases. But since few years lighting is a part of signature of Styling orientation of a brand or a vehicle, these systems embed more and more innovation and more challenges in term of material property or technical elements. Combined with the face vehicle approach we have to manage also to study on display capability to allow an evaluation in different position and the necessity to guarantee no bias by the system. One of our current challenges turns around diffusing material, way to measure it, simulate it and way to adapt from a sample measurement to a complex geometrical part.

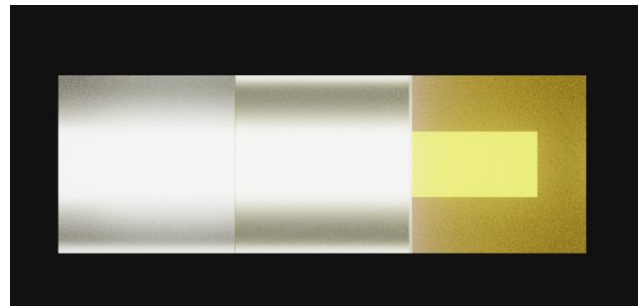


Figure 10: Example of different hypotheses studied to simulate a translucent material with variation of properties per face.

The numerical representation of the emissive element is also a topic that we must consider, conversion, in different models to fit with a coherent simulation pipeline.

The simulation of lit function is always a trade-off between introducing more details or characteristics to calculate and the power of computation/ time to result. The chromatism by material is an example of feature that we can calculate to increase accuracy but that is demanding on calculation power to obtain convergence of the result.

But the natural improvement in the HPC hardware and continuous work to improve algorithm will allow us to increase the precision or to reduce the requested time for simulations.

Based on our current results, we are very confident that we can reduce to one physical mockup for standard lighting functions.

On the subjective perception we are working on the glare topic as shown before with special algorithms to trick human perception on the display to believe the

brightness peak is higher than reality, but this approach has a lot of limits. So, we are working on the display parameters to improve this important parameter for lighting perception.

The vehicle embeds more and more ADAS system (cameras, sensors, etc.), that are regulatory. One of the main challenges will be the integration and how to guarantee that we will not have interaction between different systems, materials or elements in the cockpit. One of the next steps will be infra-red camera topics because of the interior camera responsible for monitoring driver's attention. The pre-requisite to produce simulation with the same accuracy is to deploy an ecosystem in these wavelength ranges: measurement with spatial variation approach (BRDF is not enough), render engine, lighting condition, Unfortunately, appearance material characterization tools are developed to monitor properties in the visible part of the spectrum (appearance approach). All these cross-assessments will have to be managed by considering the responsibility of the automotive company, the supplier who integrated the camera and the camera manufacturer.

CGI: Computer Generated Imagery

VMU: Visualization Mock-up

PBR: Physical based Rendering

BRDF: Bidirectional Reflectance Distribution Function

ADAS: Advanced Driver Assistance Systems

LPE: Light Path Expression

HPC: High Performance Computing

GPU: Graphics Processing Unit

5. Acknowledgement

We would like to acknowledge all the VMU team for their contribution and brainstorming on this topic. Jan Meseth from Dassault Systèmes and his team for the R&D on their render engine and support, XRite, Eizo, Nvidia.

Vehicle project teams for their challenges on these two topics.

6. References

[SIGGRAPH 97] Recovering High Dynamic Range Radiance Maps from Photographs
<http://www.pauldebevec.com/Research/HDR/debevec-siggraph97.pdf>

[DS19] Dassault Systèmes, Enterprise PBR shading model, specification version 2020x, 2019.
<https://github.com/DassaultSystemes-Technology/EnterprisePBRShadingModel>

[GTC S42367] Next Challenges in Computer Graphics for Automotive Lighting Simulation - Benoit Deschamps, Renault Group, 2022

[GTC E31274] How Renault Challenges Physical Mock-ups by Distributing Rendering on 4,000 GPUs. AWS, Renault Group, NVIDIA, Dassault Systems

7. Glossary

Crossing Road Intersections by an Autonomous Vehicle: Evaluation via Simulation

M. BOUDALI¹, J-Y. YAP², K. QUNTERO¹, M. EL-ZEENY¹, A. GARCIA GUERRA²,
J. IBANEZ-GUZMAN³, J. DAUWELS⁴, M. TLIG¹,

1: IRT SYSTEMX, France

2: Nanyang Technological University, Singapore

3: RENAULT, France

4: TU DELFT, Netherlands

Abstract:

Intersection crossing by an autonomous vehicle (AV) is a difficult task due to multiple situations that may occur in an area with convergence of multiple traffic entities. The vehicle needs to understand its situation with regards to its spatio-temporal relationship with respect to the perceived traffic agents, the context imposed by the intersection geometry, and traffic rules.

The testing and evaluation of this manoeuvre in real conditions is difficult even in proving grounds. For this purpose, simulation techniques are used. This paper presents the evaluation of this function using two open-source simulation-AV software stacks, namely Carla-AutoWare & SVL Apollo-Baidu. The purpose is to test their performance using different metrics and as a first step, in this paper the focus is in collision results.

Keywords: Autonomous driving systems, scenario-based validation, simulation, decision-making planner evaluation.

1. Introduction

The metric performance evaluation of intelligent vehicles with high levels of autonomy, that implement the sense-act-act paradigm is considered as a strategic endeavour. This can be done at component level or at system level either on proving grounds or using simulation techniques. Testing in public roads is done only after a rigorous evaluation process and approval by various stakeholders.

The results presented in this paper are the product of a joint study between industry and academia that seeks to develop evaluation methods based on simulation technologies whilst leveraging in the strong field experience of the different partners.

The evaluation of an AV can be partitioned into two phases: components and systems. Whilst ideally most of the work can be done in a proving ground under controlled scenarios, these evaluations require much resources with hazardous situations being difficult to recreate or simply forbidden. Component level evaluations imply the formulation of different assumptions and constraints in the different tests.

For the purposes of this study the decision-making and planning function has been chosen, with the use case of crossing road intersections. Choosing the decision-making & planning function implies that several assumptions need to be made in particular with regards to the perception, localisation and map functions. These assumptions will be detailed along the paper.

Road intersections have been identified as one of the most challenging scenarios within the Operational Design Domain (ODD) for autonomous vehicles. It is a part of the road network entailing the co-existence of different traffic agents with different behaviours, and different types of traffic rules. It is thus a configuration where numerous accidents occur [1], [2] and therefore these scenarios have been widely studied due to the complexity for AVs to maneuver safely and efficiently, see [3], [4] [5], [6].

In order to cross autonomously, the vehicle needs to make several decisions including adjusting its speed and direction accordingly with its situation. Simple questions such as Does it have sufficient time to cross the intersection in the presence of nearby vehicles? Does it need to stop due to the traffic signs? What will be the attitude of the upcoming vehicle who has no priority at the intersection? Or What would be the manoeuvre executed by the pedestrian close to the intersection? These questions are related to decision-making and path planning which are at the core of AV functions and control its behaviour according to the mission to accomplish and its situation within its navigation environment. Figure 1 shows a typical functional diagram of an AV.

The approach taken for the evaluation of the decision-making and path planning function as applied to the crossing of intersections is based on two major considerations: the selection of the *software stack* and the selection of the *simulators*.

The software stack implements the functions of the architecture of an AV (shown in Figure 1) and the simulators shall enable the evaluation of the system under test.

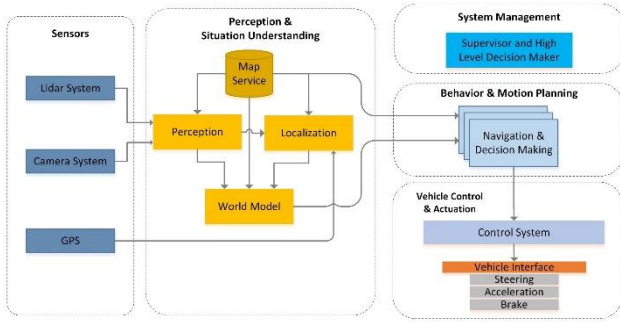


Figure 1: Functional architecture of an AV (courtesy of Renault S.A.)

A design consideration has been to use open-source software for both items. Intellectual property issues drive this consideration since the cost can be considerable both in terms of simulators as well as AVs. The goal is then to profit from the shared knowledge of the open-source community and to also contribute in the field.

The Software Stack

Among the most known open-source software stacks Autoware and Apollo baidu have been used by large companies and governmental organizations (e.g., Lincoln, Volvo, Ford, Intel, Hitachi, LG, and the US Department of Transportation). These are the autonomous driving systems considered in this work; however, the methodology is in no way restrictive and can be deployed on other platforms.

Very few studies compare the performance of these AVs pipelines (i.e. Apollo Baidu and Autoware). Among the existing work, in [7] the comparison has been made in terms of architecture and algorithms used. Another interesting work [8] has compared the two AVs in terms of the number of bugs in the software. In this study, the proposal is to compare the two AVs performance in terms of behaviour and decision making.

The latest version of Autoware can be found in [9] and for Apollo-Baidu in [10].

The Simulators

Virtual environments are often used for the development and testing of Autonomous vehicle systems (AVs) before exposing them to their actual physical deployment environments, especially when actual physical actuation is involved. Generic simulation environments are popular amongst researchers as it promotes and democratizes the development of AVs.

SVL Simulator (formerly known as LGSVL Simulator) [11] and CARLA [12] are two of the most well-known

open-sourced simulation tools. These are notable in their use of well-known gaming engines such as the Unity Engine [13] and the Unreal Engine [14] respectively. Furthermore, they provide bridges towards open-source Automated Driving System (ADS) such as AutoWare [15] or Apollo [16]. In this study, both simulators would be adopted, where Apollo would be tested in SVL Simulator while AutoWare would be tested in CARLA. Both platforms enable the researchers to develop specific scenarios to be tested and generate synthetic data which would be used to analyze and compare the AVs behavior and decision making.

Paper Structure

The remainder of the paper is structured as follows: Section 2 provides an overview on metrics for this problem type and in the larger scope of the project. Section 3 describes the approach applied to evaluate both platforms, from the experiment design to the analysis methodology and the metrics considered. Section 4 presents the results which are mainly focused on collisions, and Section 5 concludes the paper and outlines perspectives.

2. Overview on Metrics

This section aims at providing a state of the art on metrics related to the addressed problem in the larger scope of the project, however the results presented in this paper are collision-oriented.

The safety validation of AD (Autonomous Driving) Systems is still an unsolved issue. Metrics play an essential role in the validation process and must be selected and/or adapted for different applications, some examples include [17] [18]:

- Identification of safety critical test scenarios derived from recorded data, supporting the scenario-based testing approach in simulation or proving grounds. This application is interesting for both AV developers and certification bodies.
- Estimation of the safety performance of a specific AD:
 - for AV developers to improve the decision making. Live monitoring of the AV state thought appropriate metrics will allow developers to identify a safe trajectory and to execute the appropriate reactions, and
 - for certification bodies to evaluate and assess the AVs behaviour

In this research, we will focus on the last purpose using a scenario-based testing approach and a set of metrics to evaluate through simulation the driving performance of two ADS (Autonomous Driving Systems), Apollo and Autoware, on an intersection scenario.

AV stakeholders agree on the need of metrics to assess safety performance. Several ways and metrics have been put forward, but not widely adopted. It is assumed that a combination of metrics will be needed to support the evidence of safety performance.

In addition, there is a subjectivity to classify acceptable and non-acceptable situations produced by different metrics. Metrics and specific thresholds to distinguish dangerous interactions from safe interactions are strongly dependent on the scope of application and scenarios.

Driving safety metrics are classified according to distinct characteristics (e.g. data source, accessibility, applicability, among others).

- *Lagging metrics* based on the frequency of the event measured (e.g. collision frequency) versus *Leading metrics* involving assumptions and models being able to predict future outcomes (e.g. TTC and PET)
- *Black box metrics* using data that can be obtained without any access to the ADS versus *Grey and White box metrics* needing access to the ADS information.

As an overview, in the larger scope of the ASV project, a set of *Black-box- Leading* metrics has been identified as essential and are described in the internal publications [19] “*Metrics for behavioural safety validation of Automated vehicles- A literature review*” and [20] “*Definition of Metrics for Intersection Evaluation*”. These metrics are based on the safety envelope and exhibit contextually safe vehicle motion concepts [21]. Thresholds related to these metrics can and will be used namely deriving from naturalistic driving data widely used in the literature [22] [23] [24] [25] [26].

In the scope of this paper a subset of metrics is used since the purpose of the results is collision-oriented. The metrics used include classic dynamics such as speed, acceleration, relative distance and distance to the intersection for each actor. These are considered sufficient for the results presented herein and allow the early identification of interesting differences between the software stacks.

3. Evaluation Approach

The following subsections describe the process of generating the data necessary for the first building blocks of the evaluation task in the ASV project. Firstly, simulations were carried out on both frameworks: Autoware running on Carla simulator and Apollo running on SVL simulator (where the simulator offers the 3D environment and the planning module of the AD controls the ego vehicle), data

quality was then assessed in order to ensure homogeneous implementations on both frameworks (i.e. metrics, vehicles’ geometry, test plan parameters) and, once quality was satisfactory, then the evaluation phase took place.

In order to evaluate the planning module, the localization of the vehicle and the environment detection using sensors [15] are necessary information. Vehicle dynamics characteristics could also influence the planning module evaluation.

To avoid any impact on evaluation in this work, we propose to limit the influence of other modules (see Figure 1) by exploiting the ground truth signals and implementing similar vehicles on both simulators.

In addition, to ensure the consistency of the scenarios in different simulation platforms such as the map and behavior of the actors, the same map is shared between simulators and the synchronization of the actor behaviors by a distance-time based trigger are done on the same way.

The following subsections describe the definition process of the test campaign (i.e. experiment design), and the analysis methodology based on the selected metrics.

3.1 Experiment design

The planning module remains among the most complex autonomous driving tasks to perform as it determines vehicle actions and therefore safety. The evaluation of this module is carried out in the functional scenario of a cross intersection in an urban area.

In the studied intersection configuration 2 actors interact. The first actor is considered as the ego vehicle controlled by the AD while the second one is considered as the intruder controlled by the simulator.

In order to evaluate the AD and how it reacts to the traffic sign and its behaviour in the presence of other vehicles, two scenarios are proposed, see Figure 2. The first scenario, called SC_1.2, includes a stop traffic sign in the roadside of the ego vehicle. The objective of the ego vehicle is to respect the stop sign and to cross the intersection safely as shown in the figure bellow. The second scenario, called SC_1.1, includes a stop traffic sign in the roadside of the intruder vehicle but it is considered that the intruder commits a violation and ignores the stop sign to engage in the intersection. The purpose of the ego vehicle is to cross the intersection safely and to adapt its velocity given the trajectory and velocity of the intruder.

For the two proposed scenarios, several test cases are generated by varying: speed of the ego, speed of the intruder and the triggering event for the meeting

between the ego and the intruder vehicle. The triggering events are controlled by the distance between the bumper of the intruder and the intersection.

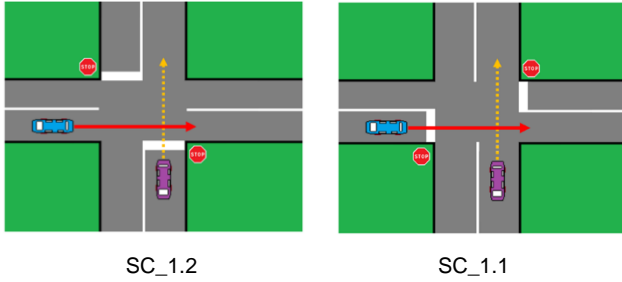


Figure 2: Simulation Scenarios

Three distances are chosen for the meeting between actors: the first one is computed between the bumper of the intruder and a point A located before the intersection, the second one is computed related to a point B in the middle of the intersection and the third one is related to a point C located after the intersection. Using these distances, the intruder vehicle should be at the selected point (A, B, or C) when the ego vehicle intends to cross the intersection, see Figure 3. This synchronization between the ego and the intruder vehicle is theoretically performed according to the time necessary by the intruder to reach the given point (A, B, or C) and the time necessary for ego to reach the intersection without considering the deceleration of the ego due to the presence of the intruder. The speed of the ego and that of the intruder vary, respectively, between 20 km/h and 30 km/h, and between 25 km/h and 40 km/h as summarized on Table 1. To reduce the impact of using two different simulators, we adopt similar configurations by using the same vehicle configuration and the same map to perform test cases.

Table 1: Test campaign

Intruder speed (Km/h)	Ego max speed (km/h)	
	30	20
40	Test 1A,1B,1C	Test 4A,4B,4C
25	Test 2A,2B,2C	Test 5A,5B,5C
35	Test 3A,3B,3C	Test 6A,6B,6C

3.2. Simulation analysis methodology

The method is used to generate the simulation dataset, perform quality assessment on the data and focus on the results of the decision-making module of

each AD stack. The global workflow is presented on Figure 4.

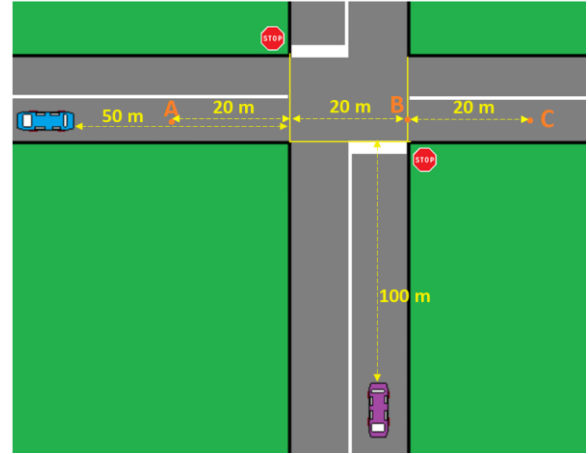


Figure 3: Overview of test case definition - Carla

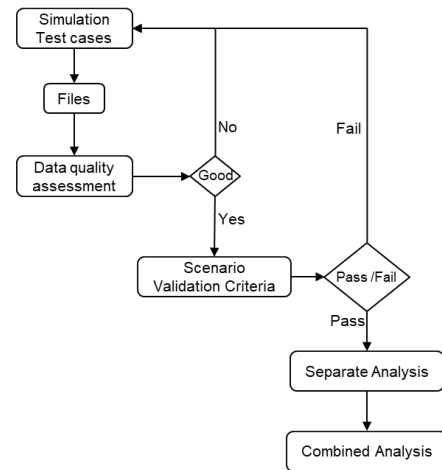


Figure 4: Analysis methodology

As the analysis is done in black-box mode, the method focuses on defining the following steps of the analysis strategy.

1. Scenario validation criteria: Automatically validate the simulation results of both AD stacks for each specific scenario, i.e. ensuring that positions and dynamics are respected. Scenario specifications are verified for the simulation campaign by Pass/Fail criteria.
2. Separate analysis: Analyze the AD stacks results separately in order to understand the behaviour of the AD system. At this stage, the focus is on the decision-making of each system in relation to the pre-defined scenario criteria.
3. Combined analysis: Compare the decision making of Autoware with the results of Apollo. Once the separate analysis is done, results can be compared between both stacks allowing to identify key differences, and the risk levels on each AD stack by means of comparison.

The first results of the application of the method are focused on collision analysis. For this purpose (i.e. collision identification and characterization of global behaviour in both platforms) only basic metrics are used, namely: speed for both actors in both scenarios, relative distance and distance to the intersection for each actor.

However, in the broader scope of the project and out of the scope of this paper, some of the metrics identified as essential include: clearance, Post Encroachment Time (PET), Proportion of Stopping Distance (PSD), and Delta Time To Collision (DTTC).

4. Results

From a general point of view, results analysis on both platforms should be done for situations in nominal conditions (no risk associated), safety critical conditions¹, and for collision situations. This work focusses specifically on the results for collision cases and lays the ground for further work aiming at the study of safety critical events and the comparison of nominal behaviour to identify prevention strategies and accepted risk levels on both AD stacks.

However, even though the focus herein will be collision-oriented, for introductory purposes, the nominal behaviour will be firstly presented in both platforms. Subsequent subsections describe the collision profile for the dataset, and then a zoom on collision in both platforms and a zoom on collisions on one framework which does not occur on the other one.

In what follows we will refer to Autoware and Apollo when presenting results for simplicity; however, it is reiterated that the two frameworks studied in this work are Autoware running on Carla's simulator and Apollo running on SVL's simulator².

4.1 Nominal Behaviour

Figure 5 and Figure 6 show the behaviour for both platforms in the absence of risk, i.e. nominal behaviour, for test case 3B, B being the riskiest configuration where the ego vehicle should encounter the intruder the closest by definition right inside the intersection. This nominal behaviour exemplifies how the ego vehicle reacts to the intruder vehicle by braking and no collision occurs. In can be seen in Figure 6 that nominal behaviour in Apollo's case implies that the ego vehicle starts braking as soon as the intruder starts moving (in all test cases studied in this work). In Autoware's case, ego braking occurs in the intersection, see Figure 5. This particular behaviour in Apollo's nominal case is observed systematically in all test cases in the dataset.

¹ Also referred to as near-misses which could result into collisions if parameters were slightly

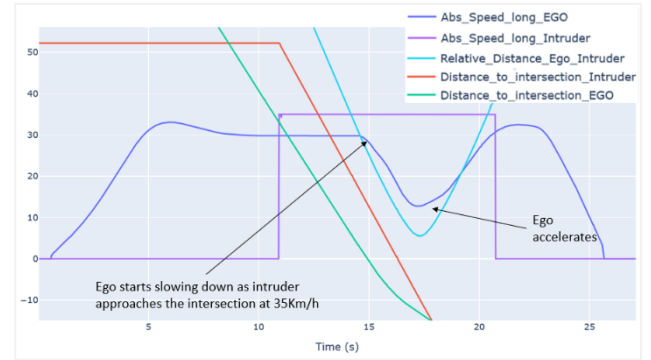


Figure 5: Nominal behaviour test case 3B - Autoware

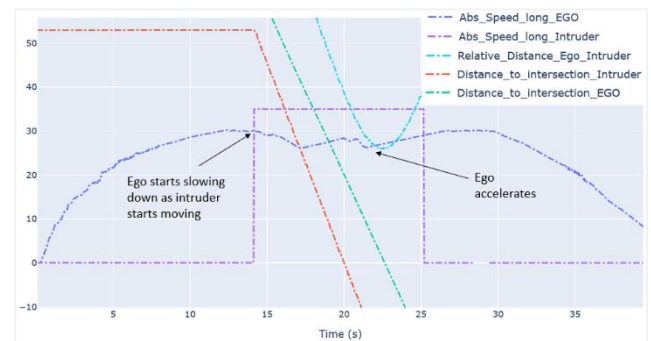


Figure 6: Nominal behaviour test case 3B - Apollo

4.2 Collisions Profile in the Dataset

Collision situations are the main focus of the results presented herein and they lay the ground for the work currently addressed in the scope of the project and out of the scope of this paper. As a reminder, a total of 36 test cases were simulated in each platform for which 18 test cases corresponded to a scenario with no stop line and the other 18 corresponded to a scenario with a stop line. The global distribution for the detected collisions is displayed on Figure 7.

Table 2 summarizes the collisions encountered in this first dataset. In general, the following points are identified:

- Collisions in the scenario with a stop line on ego's path do arise which could be unexpected since the intruder is not performing any unexpected manoeuvres and the stop line should in theory serve as a protection mechanism for ego,
- More collisions are observed in Autoware in the scenario without the stop line which is intuitive since the stop line is expected to act as a prevention measure; however, the opposite behaviour is observed in Apollo,
- Some collisions observed in Autoware correspond to the ego vehicle stopping in the

² These frameworks are in no way restrictive and can be adapted if judged useful.

middle of the intersection (i.e. speed at collision = 0 km/h in the table) as the intruder approaches. This behaviour is observed for both scenario types (i.e. with and without the stop line in ego's path).

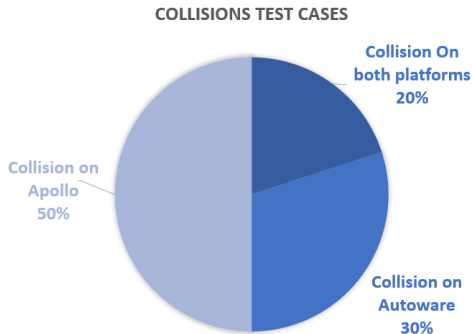


Figure 7: Detected collisions

Table 2: Collision Results

	EgoSpeed AtCollision (Km/h)	IntruderSpeed AtCollision (Km/h)
No Stop Line		
Apollo_Test3A	30.3	35
Autoware_Test4B	0	40
Autoware_Test5B	3.6	25
Autoware_Test6B	0	35
Stop Line		
Apollo_Test4A	9.7	40
Apollo_Test6A	9.7	35
Apollo_Test3A	12.3	35
Apollo_Test2A	8.7	25
Autoware_Test2A	0	25
Autoware_Test6A	0	35

4.3 Collisions on Both Frameworks

For this first dataset, two test cases proved to result in a collision both in Autoware as well as in Apollo (test cases 2A and 6A). The overall behaviour for both of these cases is presented in the following figures for case 2A for illustration purposes.

In both platforms, the behaviour is such that:

- Ego restarts after the stop line even though intruder is approaching at constant speed
- Ego slows down in the middle of the intersection and then the collision occurs. In the case of Autoware the ego comes to a full stop.

The hypotheses for these first preliminary results for the ADs are:

- Apparent lack of consideration of the intruder's dynamics.

- Apparent lack of consideration of the intruder's geometry. Ego seems to either slow down or even stop in Autoware's case aiming to avoid the collision which would have potentially happened if it were not for the size of the intruder.

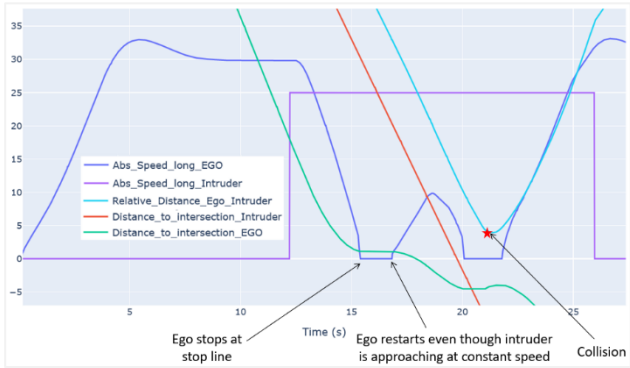


Figure 8: Test case 2A – Autoware

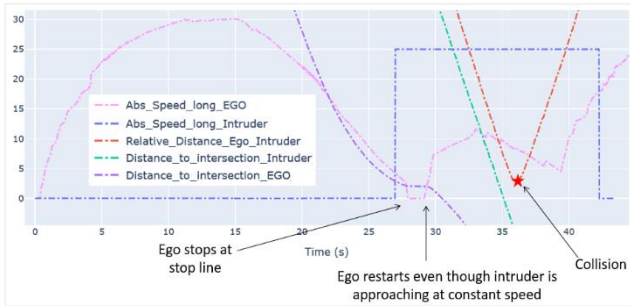


Figure 9: Test case 2A – Apollo

This will be further analyzed with an extensive test campaign in which not only patterns could emerge but also a clearer view on the robustness of the simulations. It is however interesting that for this first exploratory phase collisions are found in both platforms specifically for the scenario providing theoretically a safer context given the stop line.

4.4 Collisions on Autoware vs No Collisions in Apollo

As described in Table 2 for Autoware, collisions arise, as expected, mostly in the scenario without a stop line and specifically for case B which is the case in which the ego vehicle encounters the intruder the nearest in the intersection.

For all these cases of collision without a stop line for ego, the observed behaviour is as the one presented in Figure 10 for case 4B. This is, for all of these cases the ego vehicle slows down and stops in 2 out of the 3 cases and as a result it gets hit by the intruder. In all 3 cases the ego vehicle enters the intersection before the intruder as displayed in the figure.

Conversely, in Apollo, for these particular test cases the behaviour is as the one presented on Figure 11. Namely, since Apollo slows down a lot earlier, from the moment the intruder starts moving regardless of the distance, the ego vehicle then crosses the intersection systematically after the intruder and no collision can occur. At this stage, the absence of collision is then judged to be a consequence of the very much anticipated behaviour of the ego vehicle.

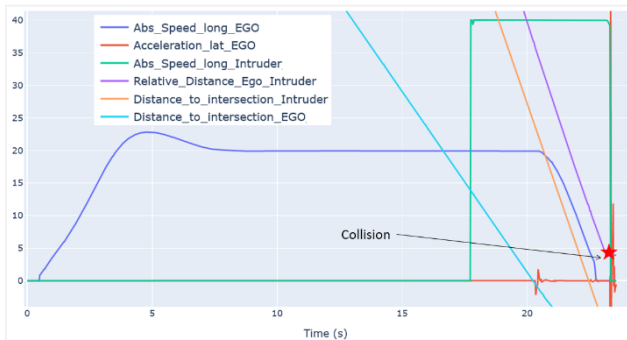


Figure 10: Test case 4B – Autoware

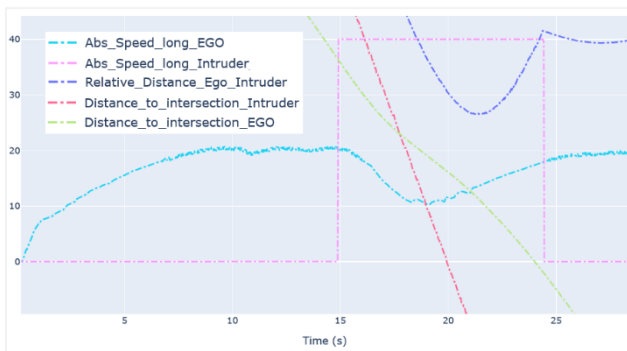


Figure 11: Test case 4B – Apollo

4.5 Collisions on Apollo vs No Collisions in Autoware

In the cases where collisions occur in Apollo and do not arise in Autoware, the behaviour is summarized by the ego vehicle systematically crossing the intersection before the intruder vehicle and starting to slow down but failing to avoid the collision if indeed this was the intention. This behaviour is illustrated

with one example for Apollo in

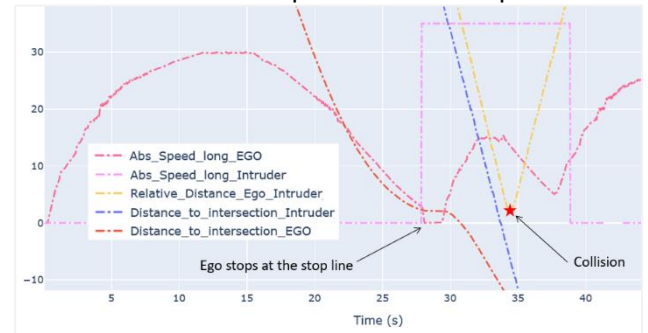


Figure 12 for the scenario with a stop line. The ego vehicle stops at the stop line, restarts, then slows down as the intruder engages in the intersection and the collision occurs.

Conversely, for Autoware, the behavior is consistent with the example provided on Figure 13. This is, ego also reaches the intersection before the intruder, stops at the stop line, restarts and stops again as the intruder vehicle engages in the intersection successfully avoiding the collision. Ego then is able to restart again.

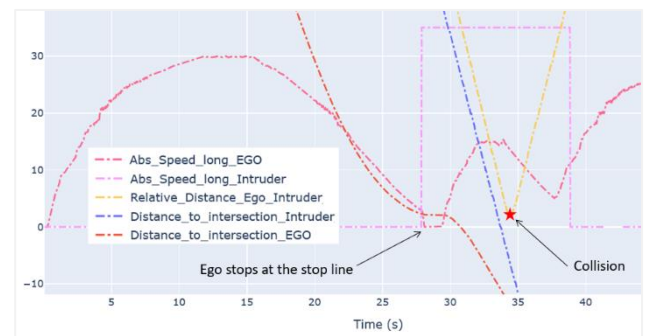


Figure 12: Apollo 3A – scenario with stop line

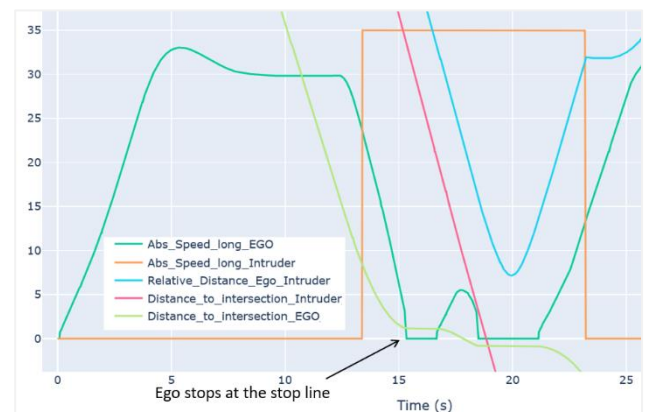


Figure 13: Autoware 3A – scenario with stop line

6. Conclusion and Perspectives

For this first phase, analysis of collision situations was performed for a scenario of a cross intersection with and without a stop line on the ego vehicle's path. This first dataset, even though restrictive in size but rich in configuration and interaction possibilities, allowed acquiring preliminary comprehension of the behavior in both AD stacks in order to better guide the following test campaigns. The following general results emerge:

- Apollo seems to react to the intruder from the moment it starts moving. In further phases the pertinence of such behavior will be evaluated with larger datasets and statistical representation.
- Autoware seems to react to the intruder as the interaction is likely to occur in the intersection as human driving would also suggest.
- Collisions do occur in scenarios with a stop line with both stacks, contrary to what could be expected. Causes cannot be stated in this paper and a subsequent repeatability study should shed a light on this subject.

More broadly it could be argued that the interactions between actors are coded differently in both ADs and that the behavior should be similar for most scenario types (other than intersections). This should be confirmed with proper testing.

The theoretical ground has been laid for the next analysis phase regarding the fundamental set of metrics to be analyzed in order to state on the prevention strategies and risk levels accepted on each AD stack.

The subject of *new metrics* more suitable to the new studied situations could arise when having to address nominal behavior and safety critical cases. At this point it is envisaged to study the PET in order to verify if evident differences can be found in terms of the risk taken when crossing the intruder in the intersection.

It is foreseen to explore the subject of *repeatability* and verify how the responses of the systems may vary and induce different outcomes and in what proportion.

New scenarios are also envisaged, namely by considering the addition of Vulnerable Road Users (VRU) and subsequently situations where the ego's mission is inherently riskier such as left turns for example.

Finally, further studies envisage the use of the same simulator for both ADs in order to homogenize the testing environments.

7. References

- [1] Li, G., et al, "Drivers' visual scanning behavior at signalized and unsignalized intersections: A naturalistic driving study in China," *Journal of Safety Research*, vol. 71, no. Elsevier, pp. 219-229, 2019.
- [2] T. Richard, "A random parameters probit model of urban and rural intersection crashes.," *Accident; Analysis and Prevention*, vol. 84, p. 49–54, 2015.
- [3] V. e. a. Astarit., "Surrogate Safety Measures from traffic Simulation Models a Comparison of different Models for Intersection Safety Evaluation," *Science Direct*, vol. 37, pp. 219-226, 2029.
- [4] S. R. e. a. Bonela, "Review of traffic safety evaluation at T-intersections using surrogate safety measures in developing countries context," *ATSS Research*, 2022.
- [5] T. B. B. Ali Pirdavani, "Evaluation of Traffic Safety at un-signalized intersections using microsimulation," *Research Gate*, 2020.
- [6] R. A. Zaid Tahir, "Intersection focussed situation Coverage-Based Verification and Validation Framework of Autonomous Vehicles Implemented in CARLA," *Digital Library*, p. 191–212, 2021.
- [7] G. Raju, "Performance of open autonomous vehicle platforms: Autoware and Apollo," in *5th International Conference for Convergence in Technology*, 2019.
- [8] Y. F. e. a. J Garcia, "A Comprehensive Study of Autonomous Vehicle Bugs," in *ACM/IEEE 42nd International Conference on Software Engineering*, Seoul South Korea, 2020.
- [9] O. SOURCE, "Github," [Online]. Available: <https://github.com/autowarefoundation/autoware>.
- [10] O. SOURCE, "Github," [Online]. Available: <https://github.com/ApolloAuto/apollo>.
- [11] G. R. e. al, "LGSVL simulator: A high fidelity simulator for autonomous driving," *CoRR*, vol. abs/2005.03778, 2020.
- [12] G. R. e. a. A. Dosovitskiy, "CARLA: An Open Urban Driving Simulator," in *in Proc. of the 1st Annual Conference on Robot Learning*, 2017.
- [13] U. Technologies, "Unity Engine," 2020. [Online]. Available: <https://unity.com>.
- [14] E. games, "Unreal Engine 4," 2020. [Online]. Available: unrealengine.com.
- [15] S. T. e. a. S. Kato, "Autoware on Board: Enabling Autonomous Vehicles with Embedded Systems," in *9th ACM/IEEE International Conference on CyberPhysical Systems, ICCPS 2018, 2018*, pp. 287–296.
- [16] "Baidu apollo," [Online]. Available: <https://apollo.auto>. [Accessed 2021-07-23].
- [17] PROJECT PEGASUS, "Requirements and conditions- Critical scenarios for human drivers-critically metric," https://www.pegasusprojekt.de/files/tmpl/Pegasus-Abschlussveranstaltung/08_Criticality_Metric.pdf, 2019.
- [18] J. G. A. v. B. a. O. B. Georg Volk, "The Worst-Time-To-Collision Metric for Situation Identification".

- [19] A. I. G. Guerra, "ASV- D1.11 - Metrics for behavioural safety validation of Automated vehicles- A literature review," Singapore, 2022.
- [20] M. E. ZEENNY, "ASV- D2.8 - Definition of Metrics for Intersection Evaluation," ASV project Document, Paris.
- [21] Automated Vehicle Safety Consortium, "AVSC Best Practices for Metrics and Methods for Assessing Safety Performance of Automated Driving Systems (ADS)," Program of SAE ITC, 2021.
- [22] *Basic theory of Driving*, Singapore , 2020.
- [23] Research_IATSS, *Application of proximal surrogate indicators for safety evaluation*, March 2017.
- [24] J._Wishart, S_Como, M._Elli and B._et_al._Russo, *Driving Safety Performance Assessment Metrics for ADS-Equipped Vehicles*, SAE Technical Paper 2020-01-1206, 2020.
- [25] *Addendum 78: UN Regulation No. 79 Revision 3*.
- [26] J._Schindler, *Validation: Metrics& KPIs for Autonomous vehicles. AutoMate Workshop*, 2018.

Virtual modeling of an ADAS radar

V.J. PALMIER¹, S. PRABAKARAN¹², F. FAUCHER¹³, A. SERVEL¹, A. PEDEN¹⁴

1 : IRT SYSTEMX, 2 Bd Thomas Gobert, 91120 Palaiseau

2 : AVSIMULATION, 1 Cr de l'Île Seguin, 92100 Boulogne-Billancourt

3 : OKTAL-SE, 11 Av. du Lac, 31320 Vigoulet-Auzil

4 : IMT ATLANTIQUE, 655 Av. du Technopôle, 29280 Plouzané

Abstract: Safety has been an increasingly important issue for the development of autonomous cars. Within the 3SA project, the team is working on a simulation platform with the vocation to solve the problems related to the safety of the autonomous car. Regarding the perception, we propose methods for modeling ADAS sensors in constrained environments. Radars are part of these sensors. By their ability to detect targets with different parameters as range, speed or even angular position over a range up to 200 meters but also by their low sensitivity to meteorological conditions, radars provide several advantages for perception. However, some environmental parameters disturb the radar and affect its accuracy and reliability. Our team, a joint collaboration between academic (IMT Atlantique - IRT SYSTEMX) and industrial (Renault, AVSimulation, OKTAL-SE, STELLANTIS) partners, is working on the development of a physics based virtual radar model and on stress patterns in synthetic scenes. This paper addresses a particular validation step: the construction of a virtual radar model based on real characterization. To obtain an accurate radar model, our method combined theoretical radar concepts together with the use of a RF reference bench. We will see how real data of characterization of canonical forms obtained by the bench and the knowledge of the analytic RCS results of these forms allow to justify the results obtained with the real radar and to build the virtual model with a better level of accuracy.

Keywords: Radar, RCS, Simulation, Physics-based, ADAS, Autonomous Driving

1. Introduction

A sensor's physically based virtual modeling requires real characterization of this sensor in order to build a consolidated model. For an autonomous vehicle, the development of a virtual simulation synthetic environment and the validation of the system behaviour should take into external disturbances. Those external disturbances are due to phenomenon that can influence the decisions making process of the vehicle and the safety of its behaviour. In order to highlight some of these phenomena, while building the virtual radar model, the conception and the validation of these models require real data

acquisition according to a specific experimental protocol.

Within the 3SA project, a joint collaboration between academic (IMT Atlantique - IRT SYSTEMX) and industrial (Renault, AVSimulation, OKTAL-SE, STELLANTIS) partners, the team attached to the radar modeling, is working on the development of a physics based virtual radar model and on disturbance patterns in synthetic environment.

Firstly, this paper presents theoretical elements regarding radars. Secondly, it exposes the works for the characterization of the sensor and some real small targets characterized at IMT Atlantique Brest. Thirdly, it explains the transfer of this study to the virtual simulation through the modeling of the 3D replicas for the small targets and their physics-based modeling. Finally, after a benchmarking study between the experimental results and the simulation outputs, we draw conclusions about the state of the method and discuss its future perspectives.

2. Radar Cross Section

2.1 Definition and usages

Usually, the RCS is used to characterize objects to measure and to define their detectability. For the scope of this study, the methodology is inverted: some references objects with their known RCS for a real radar are used to model and validate a virtual radar. Data from real experimentation will enable to build the virtual radar step by step while ensuring the robustness. This consolidation via RCS measurement requires the use of known RCS analytical measurement targets. These objects characterized by simple geometries (cubic, sphere, rectangular plate, dihedral....) are said to be canonical.

For the exploitation of real data, the radar equation enables to obtain the radar cross section [2] with the exploitation of real measurements of the parameter $|S_{21}|^2$ explained as follows [1] :

$$|S_{21}|^2 = \frac{G_{TX}G_{RX}\lambda^2\sigma}{(4\pi)^3d^4} = \frac{P_{RX}}{P_{TX}} \quad [1]$$

d=distance between the target and the radar [m];
 λ =wavelength [m]; P_{TX} =Transmitted Power [W];

P_{rx} =received power [W]; G_{tx} =transmission gain;
 G_{rx} =reception gain; σ = radar cross section [m²];
 $|S_{21}|^2$ =measured parameter

The equation [1] enables to obtain:

$$\sigma = \frac{P_{rx}}{P_{tx}} \frac{d^4 (4\pi)^3}{G_{tx} G_{rx} \lambda^2} \quad [2]$$

In this expression, the distance d must be long enough to be in the far field of the object in order to have a correct value of RCS.

When the object is far enough to the radar, the measured RCS is considered to be in agreement with the theoretical value of RCS. This far field criterion is defined by the following formula where L [m] represents the biggest dimension of the target and λ represents the wavelength.

$$d \geq 2L^2/\lambda \quad [3]$$

2.2 Interest of the RCS Measurements

Usually, the RCS is used to characterize objects to measure and to define their detectability. For the scope of this study, the methodology is inverted: some references objects with their known RCS for a real radar are used to model and validate a virtual radar. Data from real experimentation will enable to build the virtual radar step by step while ensuring the robustness. This consolidation via RCS measurement requires the use of known RCS analytical measurement targets. These objects characterized by simple geometries (cubic, sphere, rectangular plate, dihedral....) are said to be canonical.

The theoretical determination of the RCS of canonical forms is based on the assumption of an "ideal" experimental configuration:

- The sensor is mono static: the same antenna acts as transmitter and receiver
- The target is positioned in the far field
- Radiation is considered to be isotropic
- There is no power loss

3. Measurements and data acquisition

3.1 Targets and analytic RCS results

For this part of the experimentations, six small targets are used. Five of them meet the following criteria:

- Their sizes: the object is small (a few centimetres for the largest dimension) enough to allow far field measurements inside an anechoic chamber described below.

- Their geometries: with a canonical form, the comparison with analytic results provides an additional reference point for the modeling.
- Their materials: the compositions are known and described in order to have a corresponding physical-based calculation.

The sixth target was a small metallic object with a simple geometry that can be compared with a car (see Figure 8). Its interest is to verify the robustness of the method with an unknown geometrical form.

In this paper, three of the six targets are presented for the scope of this paper: a sphere of four centimetres diameter, a dihedron with six centimetres side and the Small Metallic Car (SMC).

		Sphere (Diameter of 40 mm)	Dihedron (a=60mm h=59.5mm e=10.1mm)
F(GHz)	RCS expression	πr^2	$8h^2 a^2 \frac{\pi}{\lambda}$
79	Max RCS in m ²	0.001	14.913
	Max RCS in dB	-29.008	11.736
92.5	Max RCS in m ²	0.001	21.204
	Max RCS in dB	-29.008	13.264

Table 1 - Maximum RCS for the two objects with a canonical form

3.2 IMT RF Reference Bench



Figure 1 - Details of the quasi-monostatic configuration for the antenna with the connecting elbows

Transmission Frequency	79 GHz
Bandwidth	35GHz
Range resolution	4.2mm
Gtx	23,35 dB
Grx	23,35 dB

Table 2 - Description of the bench with the parameters of calibration

3.3 Real radar

In order to evaluate the radiation patterns of the power measurement of the radar and compare them to the datasheet, the radar is placed in a far field distance, facing a horn antenna connected to a vector analyzer in the far field. The radar is activated in transmission as follows:

- Each of the 3 T_x alone
- The 3 T_x together.

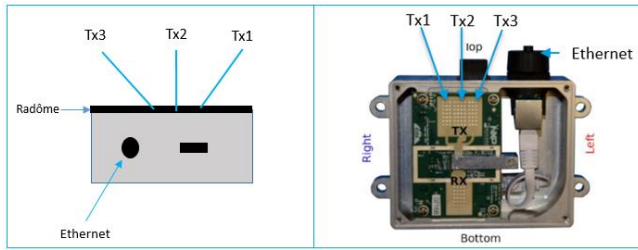


Figure 2 - RDK-S32R274 Reference Platform from NXP

The mixer located at the back of the horn induces a noise of around -20 dB. For the main lobes, the results showed a good match between the manufacturer's data and the measurements but the noise induced by the mixed and the vectorial analyzer was too important to obtain the global diagrams.

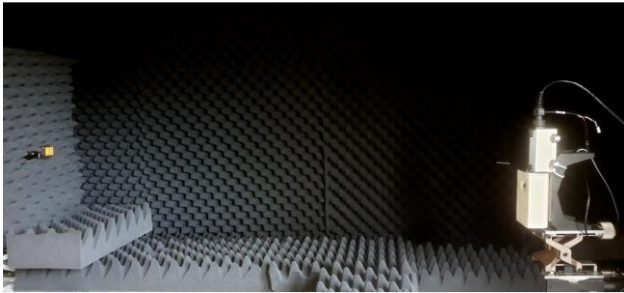


Figure 3 – Measurement protocol of antenna patterns in the azimuthal plan

Acquisitions of the RCS were made with two different configurations of activation of the transmit antenna: T_{x2} only and 3 T_x together. For both, parameters of acquisition are the same and presented in the following table.

Transmission Frequency	79 GHz
Tx activated	T_{x2} or 3 T_x together
Bandwidth	2GHz
Range resolution	75mm
Maximal range of detection	19,13m

Table 3 - Parameters

In this paper, only the results with the central antenna T_{x2} will be presented. This choice is justified by the following facts:

- It is the central antenna
- It is the only one for which the datasheet diagrams in elevation and azimuth were available
- It is the one offered greater measurement dynamics compared to the noise specific to the measurement device

3.4 Description of the experimental design scene

In order to ensure the most optimal experimental conditions possible, the measurements were carried out in an anechoic chamber, thus ensuring the elimination of parasitic reflections and the maximum reduction of environmental noise.

For the respect of the theory of the Radar Cross Section, each target is placed at a far field distance defined regarding its size.

	Far field distance (m)		
f (GHz)	Sphere	Dihedron	SMC
79	0.85	1.90	1.32
92.5	0.99	2.23	1.55

Table 4 - Minimum distance of the far field criteria for each target

The anechoic chamber is 2 meters long and after subtracting the occupied length reference bench system, there remains a distance amplitude of 1.6 meter. That means the dihedron couldn't be in far field distance inside the anechoic chamber. Thus, for the respect of the far field theory for each target, the experiment was split into 2 configurations:

- Configuration 1: Target and measurement system are both in the anechoic chamber at a distance of 1.6 meter each other. During the acquisitions, the chamber was closed.

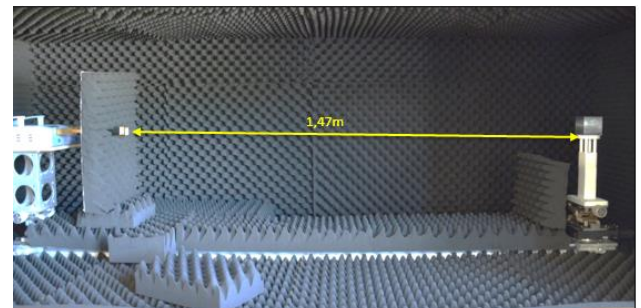


Figure 4 - Picture of the opened anechoic chamber with the installation of the reference bench. Distance between the front of the horns and a target Add approximately 13cm to the distance to take into account the connecting elbows of the horns (reference bench)

- Configuration 2: The target is in the anechoic chamber and the measurement system is outside the chamber at a distance of 3m (Figure 8). During the acquisition, the chamber was opened.

The acquisition system and the target were at the same height in both configurations validated with a LASER. The declination of the system is zero.

The acquisition system is fixed and the target is in rotation. The target is placed on a foam support of permittivity substantially equal to 1 positioned on a rotary motor with a precisely calibrated rotation pitch.

The rotation pitch is defined and chosen according to the target studied.

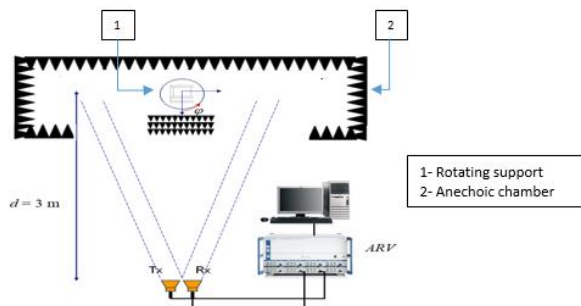


Figure 5 Measurement configuration with the bench outside the chamber

The protocol is the same for both devices. To ensure the experimental protocol, when it takes the place of the reference system, the radar is placed at 1.6m of the target to take into account the distance included by the connecting elbows of the reference one. The targets are changed between two acquisitions without moving the system {rotary motor + support}. Before changing the measurement system, all the targets are tested first.

3.4 Results and comparison of the real experimental results

At the time of writing this article, the values obtained via the radar are still being studied: so, they are not presented here.

Although the looks RCS of the 3 targets are the same for the theory, the reference bench and the real radar, some discrepancies between the theoretical values and the measurements were to be expected.

These errors come from both the point of view of the reference bench and the point of view of the radar. Indeed, at the section 2.2, we introduced the fact that the theory was built in an ideal case but in real experimentation both for the environment and for in relation to the sensor itself, the framework cannot be ideal.

The reference bench is not really mono static contrary to the theory and its radiation is not isotropic; the alignment between the center of the transmission antenna and the center of the target is not perfect. This error leads to a mean error between the specified maximum gain and the one deduced from the RCS measurements of the sphere of 1.45 dB

The real radar is not mono static and its radiation is not isotropic.

The anechoic chamber:

- In the configuration 1, the anechoic chamber has some leaks that could lead to minimal additional signal losses as well.

- In the configuration 2, the anechoic chamber is opened which create a large leak. Moreover the edge of the chamber, at the joint, has a metal coating and there are losses caused by the reflections outside the chamber.

The support, although its low permittivity, have its signature observable in the measurement.

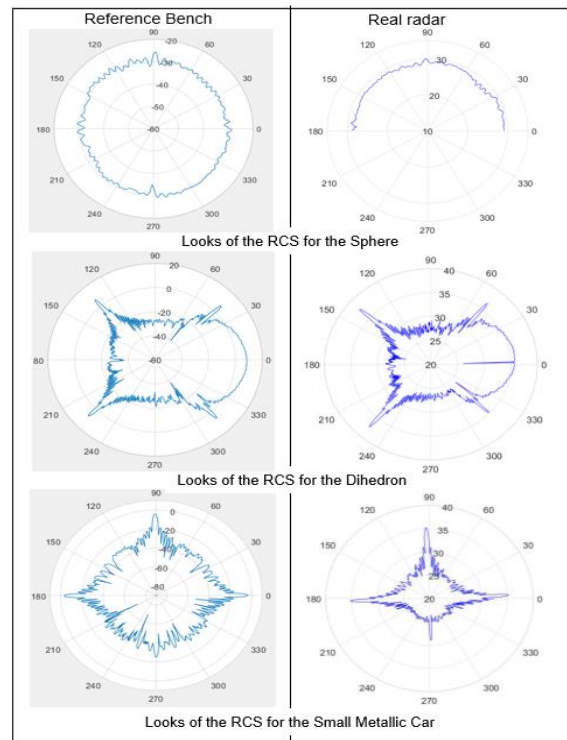


Figure 6 Looks of the RCS at 79GHz – reference bench (cf. 3.2) – real radar (cf. 3.3). The measurement for the sphere with real radar were made on 180 degrees because of the duration of the acquisitions and the sphere form looks perfectly

4. Simulation of radar data

The simulation goal is to provide data which areas realistic as the phenomenon we want to model. Generally, in the automotive field, it relies on having a description of 4 elements:

- A detailed environment which comprises the terrain
- Actors including the behaviour of the ego and all the targets surrounding it in the detection range
- A perception model characterized by the sensors and all its specifications

In this case, for RCS simulation, there is no environment or ego to describe because we focus only on radar interaction with its targets. Thus, the next parts of this paper will only deal with objects modeling, sensor description and acquisition.

4.1 Object modeling

The first step is the definition of a workflow of object modeling for physical sensor simulation. Objects are defined by their geometries (3D models) and their material descriptions (reflection, specular, rugosity, etc.). This definition can be written in a .BDD file which is the file extension of SE-WORKBENCH.

In order to obtain this file for a specified object, the applied workflow is described in the Figure 7. The objective of this workflow is to have different formats corresponding to the different software that are used in the simulation. These files are generated from the same source 3D model which is then declined in different formats. These toolchains are described in the next paragraph.

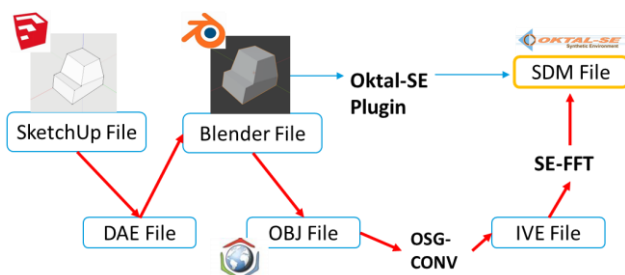


Figure 7 - Applied workflow of 3D modeling

The modeled objects are listed in the table below.

Sphere (40 mm diameter)	Dihedron (width of 60 mm)	Small Metallic Car (width of 50 mm)

Figure 8 - Calibration objects and their corresponding 3D Geometry (Blender)

4.2 Physical simulation with SE-WORKBENCH

The physical RCS simulations were performed thanks to the SE-RAY-EM software which is the EM kernel of SE-Workbench-RF product line. SE-RAY-EM solver uses asymptotic methods coupled to ray tracing in order to compute scattered electromagnetic fields at the bench and radar bandwidth. This method is relevant for the automotive domain since the size of the objects is large compared to the wavelength (a few millimetres for 79GHz). In the case of complex targets and large 3D scenes, the full wave methods are not applicable for several reasons. Where a few

GHz is a high limit for “exact” solutions used on this type of objects, it is almost a low limit in terms of physical validity for asymptotic methods. The standard computation range addressed by this method is roughly between 1 to 100 GHz on complex 3D scenes that suit to automotive scenarios. Moreover, asymptotic method coupled to ray tracing produces results that are very similar to the “exact” methods for a very much lower computation time [1]. Ray-tracing is done through the Shooting and Bouncing Rays (SBR) technique that has been further optimized to calculate efficiently the intersections between rays from the transmitter towards the 3D target and back to receiver. Figure 9 shows that rays are traced from the transmitter through a grid (pixels). The intersections of these beams are computed.

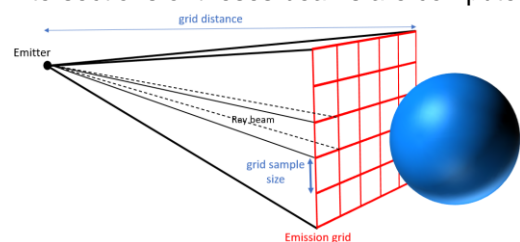


Figure 9 - Ray-tracing grid

There are two types of interactions that are based on three formulations [2]:

- Geometrical Optics (GO) when the beam is reflected by a metallic or dielectric surface.
- Physical Optics (PO) towards the reception points at each interaction.
- Equivalent Current Methods (ECM) for computing edge diffraction toward the reception points.

Since the canonical targets are metallic pieces, the Perfect Electric Conductor (PEC) material was the only model involved under the following simulations. In order to be able to properly compare the results with the measurements, the following parameters set of the simulations matches the measurements conditions:

- The longitudinal distance between the antenna and the target
- The vertical alignment of the target according to the antenna
- The distance between the phase center of the emitter and the receiver antenna
- The path of the antenna around the target
- The number of angles computed (same azimuth sampling)
- The same bandwidth

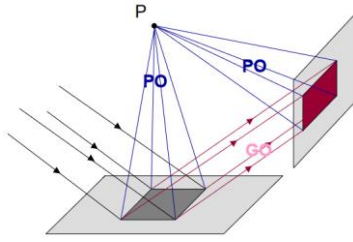


Figure 10 - Principle of beam interactions [1]

The results of the three simulations presented in this section were performed with the same set of ray-tracing parameters given on the Table 5 in the next section. Each scenario of the three simulations only comprises a single target, the source antenna and a reception point that take place within a free space environment. Hence, as soon as SE-RAY-EM has computed the complex EM field, it is simple to get the RCS value from the radar equation. This equation leads to the expression given below.

$$\sigma(\theta) = \frac{(4\pi)^2 R^4}{2 Z_0 P_t} |Er(\theta)|^2 \quad [4]$$

Where $\sigma(\theta)$ is the radar cross section (m^2) for a given azimuth angle θ ($^\circ$), $|Er(\theta)|$ is the module of the complex polarised electric field (V/m) computed by SE-RAY-EM at the reception point for a given θ , Z_0 is the free space impedance (around $120\pi \Omega$), P_t is the transmitted power of the source ($1W$) and R the source-target distance (m).

Figure 11, Figure 12 and Figure 13 respectively show the plots of the car shape target, the dihedron and the sphere. First, we can say that the curves of these plots fit the expected analytical ones. Since the simulations were performed very close to the near field limit, the value of σ_{max} diverges a little from the expected analytical values. However, as long as the radius distance increases, the σ_{max} converges very close to the theoretical value (up to 10^{-3} -for this set of parameters). These simulations have several goals, one of them is to check the maximum value computed by the kernel in order to compare it with the expected analytical value. Besides, the plots enable us to compare the profile of the computed curves with the measurements in order to check the validity of the solver for different wavelength from 79GHz to 92.5GHz.

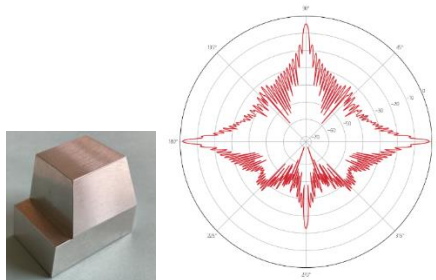


Figure 11 – RCS (θ) plot results of the car shape object

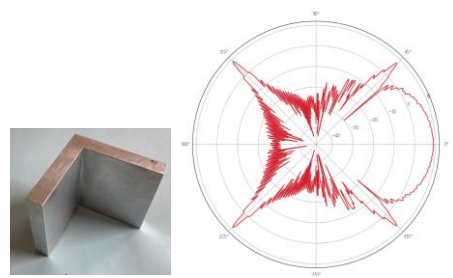


Figure 12 – RCS (θ) plot results of the dihedron

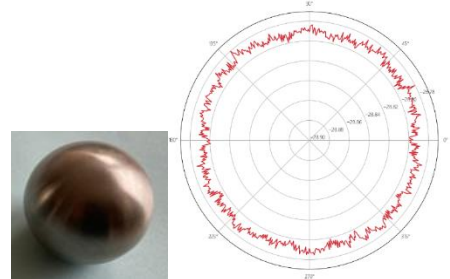


Figure 13 - RCS (θ) plot results of the sphere

Furthermore, many different measurements were performed across many different simple geometries will help us to identify the magnitude of the gap between the measurements and the simulation. This information will be ultimately used to check the validity of more complex geometries such as vehicles, traffic signs, bicycles as well as pedestrians. The ray tracing parameter set given in the figure 12 is purposely demanding for this latter reason as well. Finally, the next section will show that these simulations can be performed again in an automotive simulation context through SCANer Studio and as a validation of the software integration of SE-RAY-EM.

4.3 Applying in SCANer Studio

The previously presented tool SE-RAY-EM has been integrated in the software solution SCANer Studio from AVSimulation. The goal of such an integration is to apply the physics-based sensor modeling in the field of automotive simulation. During this study, the goal has been to use the integrated tool in SCANer Studio to reproduce the simulations that have been done with the SE-RAY-EM tool, in order to validate the fact that the theoretical value simulated by the physical-based software can be approached with another platform.

The context of the simulation is different because it is based on the scenario description of SCANer Studio. A scenario needs an ego vehicle, a terrain and the actors surrounding the ego. Here, the goal is to measure an RCS surrounding the whole object. Hence having an ego vehicle equipped with a correctly parametrized sensor. The ego has a circular trajectory around the object in order to surround every

angle of the object at the precise distance (as described in Figure 14)

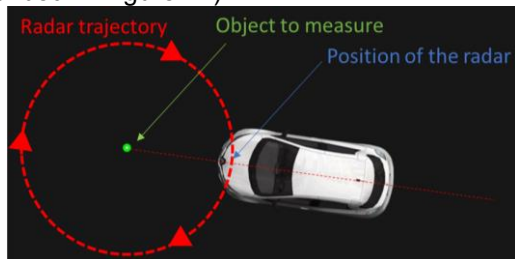


Figure 14 - SCANer Studio view of the measurement for RCS scenario

4.4 Results and comparison of the simulations

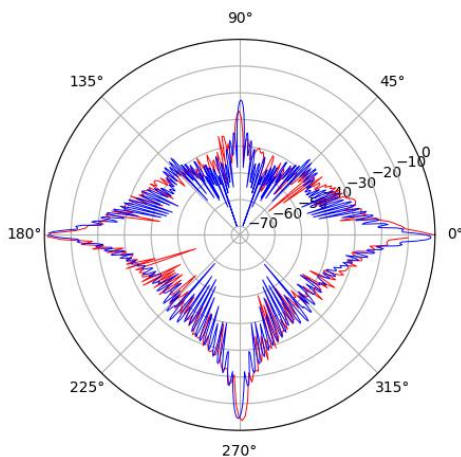


Figure 15 – Comparison of both the simulations for the small metallic car (red: SCANer and blue: SE-WORKBENCH)

When applying the simulation process to the three objects of the study, the results (an example is shown in Figure 15) obtained are similar to the simulated RCS with SE-WORKBENCH. The computation core model is the same for both tools but we can highlight some disparities due to the different context and some differences in the simulation parameters used with SCANer.

First approximation come from the scenario itself. In SCANer simulation, the ego vehicle is moving around the object applying a small velocity due to the rotation of it. This velocity can imply small dopplers. These can be avoided by stopping the car before each measurement for each angle but the impact of such dopplers is negligible.

The other approximation comes from the simulation parameters: for the integration of the SE-RAY-EM tool into SCANer Studio, some simplifications have been made to be more adequate and easier to use for an automotive use case. The table below shows the differences between SE-WORKBENCH and SCANer Studio parameters.

	SCANer	SE-WB
Grid sample size	10^{-2} m	10^{-3} m
Grid subdivision level	2^1	2^4
Curve sampling precision	1°	0.5°

Table 5 - Ray-tracing parameters set

Some parameters are less accurate in SCANer Studio because such precision is not necessary in the automotive field. In spite of this simplification, the scenario is able to get an accurate representation of the RCS even for very small objects of 4 to 5 centimetres.

5. Comparison of simulated data with real data

At this stage of development, the virtual RADAR is not finalized. However, as it appears in chapter 4 for this paper, the virtual model of the reference bench is in a good state of achievement. The discussion about the comparison of simulation data with real data will be about the real data of the benchmark.

5.1 Results

Figure 16 describes a superposition of the results of RCS obtained with OKTAL-SE, with SCANer and we compared them with the measurements that have been done at IMT Atlantique with the reference bench. The 3 results have the correct shape and the measurement shows that the model used (in SE-WORKBENCH and then in SCANer Studio) are relevant regarding the measured value in the anechoic chamber.

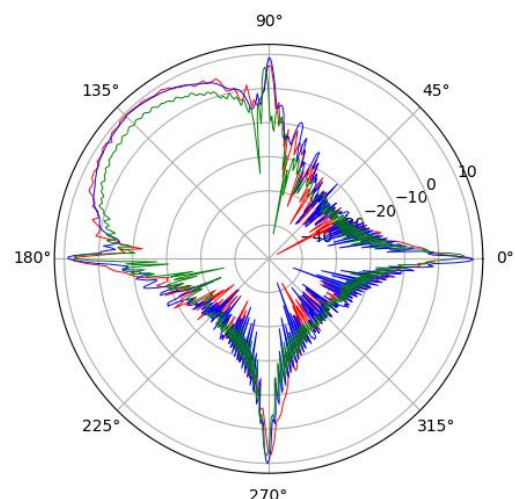


Figure 16 - Layering of the RCS of the dihedron for the 3 measurement sources (blue: OKTAL-SE, red: SCANer Studio and green: IMT)

Angle	0°	90°	135°	180°	270°
Ref Bench	7.4	6.2	6.4	7.2	7.8
SCANeR	7.7	7.7	7.5	7.7	7.7
SE-WB	7.8	7.9	8.4	7.9	10.1

Table 6 - Local max values of RCS (in dBm²) simulated and measured for remarkable angles of the dihedron

RCS max in dBm2			
	Sphere	Dihedron	SMC
Theory	-29	11,89	
Ref Bench	-30.1	8,24	-4,33
SCANeR	-27.7	11,22	-0,51
SE-WB	-28.8	10,99	-1,57

Table 7 - Results of the maximum and of the mean RCS for each object

	RCS mean error	
	Dihedron	SMC
Ref Bench/Theory	3.65 dB	
SE-WB/Theory	0.9 dB	
SCANeR/Theory	0.67 dB	
SCANeR/SE-WB	0.36 dB	0.27 dB
IMT/SCANeR	2.23 dB	2.037 dB
IMT/SE-WB	1.87 dB	2.34 dB

Table 8 - mean error (in dB) of the RCS between different data sources (only with the max RCS for the theory)

5.2 Discussion

The results are satisfying. Although, the gaps of the maximum RCS between the results of simulation and the theory are small, they are more important between the reference bench and the simulation.

These differences can be more precisely observed in Table 6 which shows local maximum values of RCS around different angles (each face of the dihedron and the center corner of it at 135°).

The identified causes can be due to:

- The causes identified in section 3.5
- In simulation (SCANeR and SE-WORBENCH), the antennas are defined as isotropic antennas unlike the real ones. This choice explains the good scores between the theory and the simulation radiation in theory is defined as isotropic (cf. section 2.2)

The first results exposed in this paper are satisfying because SE-WORKBENCH and SCANeR correctly depicts the shape of the RCS expected with the real RCS measured. The construction of virtual non isotropic antenna could enable to increase the similarity between the real and the simulations. In the same way, the simulations could deviate from the theory. This demonstrates the relevance of using two sources of reference to build the virtual model.

6. Conclusion

To conclude, this first step of the method development shows a possible and robust workflow to validate radar modeling using simulation and two sources of references (theory and experimentations). The use of RCS reference value helps verifying the correct behaviour and quantification in our sensor model in controlled use case (anechoic chamber). Furthermore, the methodology used is validated from the step of object modeling to the step of parametrization of the sensor with two different toolchains: on one side, the physics-based tool (SE-WORKBENCH) and on the other side, its integration in a software platform (SCANeR Studio) allowing us to address multiple automotive use cases.

This workflow can now be applied for more complex scenarios implying more complex objects such as real cars, pedestrians and adding an environment to the measurement (movements of the objects and actors, and surrounding infrastructures).

7. Acknowledgement

Thanks to Charaf-Eddine SOURIA for having contributed to the definition of this method.

This work has been supported by the French government under the "France 2030" program, as part of the SystemX Technological Research Institute.

References

- [1] J. Latger, T. Cathala: "Millimeter waves sensor modeling and simulation", 2015.
- [2] N. Douchin, J. Latger, T. Cathala, R. Marechal: "Simulating complex environments for the assessment of millimeter waves sensors", 2016.
- [3] N. Douchin, C. Ruiz, J. Israel, HJ. Mametsa SE-Workbench-RF: "Performant and High-Fidelity Raw Data Generation for Various Radar Applications", 2019.
- [4] IRT SystemX - Simulation for the Safety of Systems in Autonomous Vehicles (3SA Project): <https://www.irt-systemx.fr/en/projets/3sa/>.
- [5] OKTAL-SE: <https://www.oktal-se.fr/>
- [6] AV Simulation: <https://www.avsimulation.com/>

8. Glossary

RCS: Radar Cross Section

SMC: Small Metallic Car